universität wien

DISSERTATION

Titel der Dissertation

Two dimensional gel electrophoresis (2-DE) and MALDI-TOF-MS analysis of rDNA derived, therapeutic monoclonal antibodies trastuzumab and rituximab and fusion protein abatacept

angestrebter akademischer Grad

Doktor/in der Naturwissenschaften (Dr. rer.nat.)

Verfasserin / Verfasser:	Mag. pharm. Dasnor Nebija
Matrikel-Nummer:	0509665
Dissertationsgebiet (lt. Studienblatt):	Pharmazie 449
Betreuerin / Betreuer:	o.Univ.-Prof. Mag. Dipl.-Ing. Dr. Christian Noe

Wien, im 01.Dezember, 2008

Acknowledgment

This PhD Thesis work has been carried out at the Department of Medicinal and Pharmaceutical Chemistry, Faculty of Life Sciences, University of Vienna.

I would like to gratefully acknowledge my Mentor, Prof.Dr. Christian Noe for accepting me in his Research group and introducing in the field of Bioanalytics. His enthusiasm, support and professional help accompanied all the period of preparing and finishing this work.

Special gratitude for the Assessors of this work, Prof. Dr. Theo Dingermann and Prof.Dr. Hermann Wätzig for their exceptional supervision and help during the Thesis evaluation.

Cordial thanks to Dr. Bodo Lachmann and Dr. Hannelore Kopelent for invaluable advice during the scientific discussions.

My colleagues, Dr. Bettina German, Mag. Martina Stessel, Mag. Furuhashi Takeshi, and Dr. Winfrid Neuhaus deserve a distinguished acknowledgment. Our wonderful teamwork made my experience in Austria very pleasant and comfortable.

This work could not have been completed without the financial support from Büro Für internationale Beziehungen, and Dr. Tatjana Antalowsky to whom I am especially grateful for the Research Grant.

I would like to acknowledge colleagues from MarienApotheke 1160 in Vienna, as well, and particularly Mag. Pharm. Monika Alvarado-Dupuy for their exceptional support.

And finally, above all, gratitude for my family who supported me constantly during my studies, particularly to my parents to whom this work has been dedicated.

Contents

List of Figures

List of Tables

Glossary of symbols and terms

ACN	Acetonitrile
ADC	Antibody drug conjugate
ADCC	Antibody-dependent Cell-mediated Cytotoxicity
APS	Ammonium persulfate
APTS	8-aminopyrene-1,3,6-trisulfonate
BHK	Baby hamster kidney
BLA	Biologics licence application
BWFI	Bacteriostatic Water for Injection
CA-IEF	Carrier ampholyte isoelectric focusing
CD	Circular dichroism
CDC	Complement dependent cytotoxicity
cDNA	Complementary DNA
CDR	Complementarity determining region
CE	Capillary electrophoresis
CE-LID	Capillary electrophoresis-laser-induced fluorescence
CHCA	α-Cyano-4-hydroxycinnamic acid
cIEF	Capillary isoelectric focusing
CISH	Chromogenic in situ hybridization
CTLA4	Cytotoxic lymphocyte associated antigen
DC	Direct current
1-DE	One-dimensional gel electrophoresis
2-DE	Two-dimensional gel electrophoresis
DIGE	Difference gel electrophoresis
DMARD	Disease-modifying antirheumatic drug
DTT	Dithiothreitol
ECD	Extracellular domain
EGFR	Epidermal growth factor Receptor
ELISA	Enzyme-linked immunosorbent assays
EMEA	European Medicines Agency

ESI-MS	Electrospray ionisation mass spectrometry
Fab	Fragment antigen binding
Fc	Fragment crystallisable
FcγR	Fc gamma receptor
FcRn	Neonatal Fc receptor
FDA	Food and Drug Administration
FISH	Fluorescence in situ hybridization
FR	Framework region
HACA	Human anti-chimeric antibodies
HAGA	Human anti-globulin antibodies
HAHA	Human anti-human antibodies
HAMA	Human anti-mouse antibodies
HER2/neu	Human Epidermal growth factor Receptor 2
HIC	Hydrophobic interaction chromatography
HPAEC	High performance anion exchange chromatography
HPIEC	High performance ion-exchange chromatography
HPLC	High performance liquid chromatography
HP-SEC	High performance size-exclusion chromatography
IAM	Iodoacetamide
ICAT	Isotope-coded affinity tagging
IEC	Ion-exchange chromatography
IEF	Isoelectric focusing
Ig	Immunoglobulin
IHC	Immunohistochemistry
IPGs	Immobilized pH gradients
L	Linear
LIF	Laser induced fluorescence
LFA-1	Lymphocyte function-associated antigen 1
MALDI-TOF	Matrix-assisted laser desorption/ionization time-of-flight
MCB	Master Cell Bank
2-ME	2-Mercaptoethanol
MHC	Major histocompatibility complex
Mr	Relative molecular mass

MS	Mass spectrometry
NL	Non-linear
NP-HPLC	Normal phase high performance liquid chromatography
NMR	Nuclear Magnetic Resonance
PAD	Pulsed amperometric detector
PCR	Polymerase chain reaction
pI	Isoelectric point
PSD	Post-source decay
PMF	Peptide mass fingerprinting
rDNA	Recombinant DNA
rhGH	Recombinant human growth hormone
RIA	Radioimunoassay
rmAb	Recombinant monoclonal antibody
RP-HPLC	Reversed phase high performance liquid chromatography
scFv	Single-chain variable fragment
SDS	Sodium dodecyl sulfate
SDS-CGE	Sodium dodecyl sulfate-capillary gel electrophoresis
SDS-PAGE	Sodium dodecyl sulfate-polyacrylamide gel electrophoresis
SELDI	Surface-enhanced laser desorption-ionization
SLE	Systemic lupus erythematosus
SWFI	Sterile water for injection
TEMED	Tetramethylethylenediamine
TFA	Trifluoroacetic acid
TNFα	Tumor necrosis factor alfa
USAN	United States Adopted Names
UV/VIS	Ultraviolet/visible
VEGF	Vascular endothelial growth factor
WCB	Working Cell Bank

1. Introduction

1.1. Biological medicinal products

Recombinant monoclonal antibodies are currently rated as important and growing class of biological medicinal products. Many of them have been already approved and marketed, being used in different therapeutic areas such are oncology, auto-immune and inflammatory disorders, cardiovascular disorders, organ transplants, etc. and many of them are undergoing different phases of clinical studies[1, 2.]

Biological medicinal products, also known as biologics, are products for which the active substance has been made by or is derived from a living organism and often represent the cutting edge of medicinal science and research. They can be composed of sugars, nucleic acids, proteins or complex combination of these substances, or they may be living entities such as cells or tissues. In contrast to chemically synthesized small molecules, which have a well-defined structure and can be thoroughly characterized, biological products are complex in structure, and thus are usually not fully characterized[3].

Therapeutic biological products include wide range of medicinal products such as monoclonal antibodies and related substances designed as targeted therapies in cancer and other diseases, cytokines, growth factors, enzymes, immunomodulators and thrombolytics, therapeutic immunotherapies, proteins intended for therapeutic use that are extracted from animals or microorganisms, including recombinant versions of these products, allergenic extracts, blood and blood components, gene therapy products, human tissue and cellular products used in transplantation, vaccines, devices and test kits[3,4]

Often the term “biologics” is used more restrictively, referring to classes of medications that are produced by means of biological processes involving recombinant DNA technology.

In addition, to represent a class of products produced by modern biotechnological techniques in 1980s originated other term known as “biopharmaceuticals”.

Biopharmaceutical may be defined as proteins or nucleic acid based pharmaceuticals used for therapeutic or *in vivo* diagnostic purposes and produced by means other than direct extraction from a non-engineered biological source.

According this definition biopharmaceuticals comprise proteins based-products produced by genetic engineering, recombinant monoclonal antibodies, nucleic acid based drugs used in gene therapy and antisense technology. Proteins obtained by direct extraction from native sources and cell based products are excluded from this definition[5].

Biomedical research today focuses on cellular and gene-based biologics, given that they may make it possible to treat a variety of medical conditions, including diseases for which no other treatments are available. In the EU gene and somatic cell therapy medicinal products, as well as tissue engineered products, are summarized under the term *advanced therapy medicinal products*, and, as special expertise is needed for their development, EMEA will establish the Committee for Advanced Therapies to review their future marketing authorization applications[6].

Due to developments in targeted therapies, genomics and proteomics - amongst others - the recombinant therapeutic protein market has experienced great expansion. By 2003, 140 recombinant therapeutic proteins including recombinant mAbs, had gained approval for general human use in the EU and/or US with approximated global market of $30 billion, approximately double its global value in 1999[7,8]**.** However, in 2007, global prescription sales of biopharmaceuticals increased to more than $75 billion, while twenty-two rDNA derived products including targeted oncology therapies, autiomune agents antidiabetic agents and pure vaccines, generated sales exceeding $1 billion[9].

A small number of cell based products continue to gain marketing approval and one antisense based product; fromivirsen (Vitravene®, ISIS Pharmaceuticals) has been approved. In 2003 the first gene therapy product, human adenovirus engineered to contain the human *p53* tumor suppressor gene (Gendicine®), indicated for the treatment of head and neck squamos cell carcinoma, gained approval in China[10].

1.1.1. rDNA derived therapeutic proteins

Over the past quarter century, advances in molecular biology, and genetic engineering led to rapid growth in the availability of recombinant protein products. Invention of restriction endonucleases and transformation of E.coli cells with recombinant plasmid by Boyer and Cohen in 1973 represented key events for the development of recombinant DNA technology[11-13]. Shortly after that, recombinant

human insulin, the first medicinal product obtained by rDNA technology, gained marketing authorization (1982, Humulin, Eli Lilly), followed by somatropin, *rhGH,* produced by Genentech under trade name Protropin® - the first recombinant pharmaceutical product to be manufactured and marketed by a biotechnology company[14,15].

These events set an entire industry into motion, to produce not only natural proteins for treatment of deficiency-associated diseases such as insulin or hGH, but also variety of products-from hormones and enzymes to receptors, vaccines, anticoagulants, cytokines, fusion proteins and monoclonal antibodies to treat a broad range of clinical indications thought untreatable just two decades ago[16].

There are many advantages of recombinant therapeutic proteins over traditional drugs consisting primarily on their improved safety, efficacy and cost issues. Unlike most low molecular weight pharmaceuticals, these proteins are developed not because of the novelty of their structures, but because of the novelty of their actions[17]. For the replacement therapy protein recombinant protein drugs are obvious choice, while when an agonist action is needed, they are generally preferred option.

On the other hand, production of protein with identical sequence to its naturally produced counterpart reduces the possibility of complications resulting from antibody production against sequence variants resulting from species-to-species variation of molecular structure. Furthermore, innadequate preparation purity, for example of porcine or bovine insulin, can cause allergic reactions due to the presence of animal proteins. Recombinant human insulin is chemically identical to endogenous insulin and is free of pancreatic contaminants, therefore is less immunogenic than purified pork insuline[18].

Problems related to shortages and limited supplies, as well as iatrogenic Creutzfeldt-Jakob disease (CJD) acquired after the use of growth hormone (GH) obtained from pituitary glands sourced from autopsy material are avoided with the replacement of NPA growth hormone with rhGH[20]. Furthermore, concerns regarding the infectious disease risk of plasma-derived concentrates such are HIV and hepatitis B and C, can be overcome by the development of recombinant clotting factors.

Targeted bioengineering strategies are developed to improve functional activity, half life and immunogeneicity of exististing recombinant proteins, and this combined with advances in alternative recombinant protein production in transgenic animals could

result not only in improved clinical profile of these drugs, but it could yield to and affordable supply and increased availability to broader populations, as well[21].

Of the 32 new products, between 2002-2006, 12 have been re-engineered to have either an altered amino acid sequence or post-translational modification of parental structure, *i.e*. to ensure constant and prolonged release of insulin, long- acting insulin analog detemir (Levemir®) devoid of insulin B30 threonine residue and with a C_{14} fatty acid attached to B29 lysine, was designed. Substitution of 9 amino acid residues with additional pegylation in native hGH was needed, to obtain hGH analog pegvisomant (Somavert®). This analog has antagonistic effect, and is used for the treatment of acromegaly while PEG-ylation increases its serum half life[22, 23]. Reduction or elimination of antibody immunogeneicity and enhancement of human effector functions were the primary goals of the antibody structure modification and numerous marketed rmAbs resulted form this strategy[22].

rDNA therapeutic proteins are large and hydrophilic molecules and they face numerous obstacles to entering bloodstream, such are biological membranes, stomach acid and enzymes. Therefore, they are administered parenterally. In order to avoid disadvantages of parenteral administration, nonparenteral delivery of rDNA proteins is being actively studied and some products reached commercialization, *i.e*. rh-Insulin inhalation powder was the first inhalable insulin product to be marketed[24].

In Table 1.1 a list of representative recombinant therapeutic proteins has been presented.

Table 1.1. List of representative recombinant therapeutic proteins.
*Comprehensive list of recombinant monoclonal antibodies and fusion proteins is presented in Table 1.2.
CHO: Chinese hamster ovary. **FSH**: Follicle stimulating hormone. **LH**: Luteinizing hormone. **IVF**: *in vitro* fertilization. **ET**: Embryo transfer.
rh: Recombinant human. **BHK**: Baby hamster kidney. **tPA**: Tissue plasminogen activator. **APC**: Activated protein C.**HEK**: Human embryonic kidney.
HPV: Human papilloma virus

Therapeutic category	rDNA product	Trade name, Manufacturer	Expression system	Therapeutic indication
Haemopoietic Growth factors	Epoetin alfa	Epogen®/Amgen	CHO	Anemia
	Epoetin beta	NeoRecormon®/Roche	CHO	Anemia
	Darbopoetin alfa	Aranesp®/Amgen	CHO	Anemia
	Methoxy-PEG-Epoetin beta	Mircera®/ Roche	CHO	Anemia
	Filgrastim	Neupogen®/Amgen	E.coli	Chem. induced neutropenia
	Pegfilgrastim	Neulasta®/Amgen	E.coli	Chem. induced neutropenia
Human Interferons	Interferon alfa-2a	Ropheron A®/ Roche	E.coli	Cancer/Hepatitis
	Peginterferon alfa-2a	Pegasys®/Roche	E.coli	Cancer/Hepatitis
	Interferon alfa-2b	Peg-Intron®/Schering	E.coli	Cancer/Hepatitis
	Interferon beta 1-a	Avonex®/Biogen Idec	CHO	Multiple sclerosis
Interleukin related molecules	Anakinra	Kineret®/Amgen	E.coli	Rheumatoid arthritis
	Oprelvekin	Neumega®/Wyeth	E.coli	Chem. induced thrombocytopenia
rmAbs and fusion Proteins*				
	Insulin human	Actrapid®/Novo Nordisk	S.cerevisiae	Diabetes
	Insulin lispro	Humalog®/Eli Lilly	E.coli	Diabetes
	Insulin aspart	NovoRapid®/Novo Nordisk	S.cerevisiae	Diabetes
	Insulin glargine	Lantus®/Sanofi-Aventis	E.coli	Diabetes
Hormones of therapeutic	insulin detemir	Levemir® /Novo Nordisk	S.cerevisiae	Diabetes
interest	Somatropin	Omnitrope®/Sandoz	E.coli	Growth disturbance
	Follitropin alfa, r-hFSH	Gonal-F®/Serono	CHO	Anovulation, IVF
	Follitropin beta, r-hFSH	Puregon®/Organon	CHO-K1	Anovulation, IVF/ET
	Lutropin alfa, r-hLH	Luveris®/Serono	CHO	LH, FSH deficiency
Blood coagulation factors	Eptacog alfa, rFVIIa	NovoSeven®/N.Nordisk	BHK	Hemophilia
	Moroctocog alfa, rFVIII	Refacto®/Genetics Institute	CHO	Hemophilia A
	Nonacog alfa, rFIX	BeneFIX®/Wyeth	CHO	Hemophilia B
Thrombolitics and	Alteplase, r-tPA	Activase®/Genetech	CHO	Acute myocardial infarction
Anticoagulants	Tenecteplase	TNKase®/Genetech	CHO	Acute myocardial infarction
	Lepirudin	Refludan®/Pharmion	S.cerevisiae	Anticoagulation
	Drotrecogin alfa,r-h APC	Xigris®/Eli Lilly	HEK293	Severe sepsis
	Antitrombin alfa	aTryn®/LeoPharma	Transgenic goat	Venous thromboembolism
Recombinant Enzymes	Imiglucerase	Cerezyme®/Genzyme	CHO	Gaucher disease
	r-h a-galactosidase A	Fabrazyme®/Genzyme	CHO	Fabry disease
r Vaccines	r-HPV vaccine	Gardasil®/Sanofi MSD	S.cerevisiae	HPV infection prevention

1.2. Therapeutic recombinant monoclonal antibodies and related products

Among other therapeutic proteins, antibodies currently play an important role in the treatment of many diseases such are cancer, infectious diseases, allergy, autoimmune diseases, and inflammation. There are many reasons which make these molecules very attractive for commercial development. First, their action is specific, generally leading to fewer side effects. Second, in order to achieve efficient delivery to target site, and thus reduce potential side effects, antibodies can be conjugated with other therapeutic entities such are immunotoxins or chemotherapy agent. Furthermore, for specific diagnostic purposes they may be conjugated with radioisotopes. Finally, technology advancement has made complete human MAb available, which are less immunogenic[25].

1.2.1. Antibody structure and classification

Naturally occurring antibodies (immunoglobulins) are roughly Y-shaped glycoprotein molecules and comprise four polypeptide chains, two identical heavy chains and two identical light chains (Fig. 1.1).
One Fc (*fragment crystallisable*) and two identical Fab (*fragment antigen-binding*) fragments can be produced by papain proteolytic cleavage of the hinge in an intact antibody molecule. Papain cleaves IgG above the hinge region containing the disulfide bonds that join the heavy chains, but below the site of the disulfide bond between the light chain and heavy chain. This generates two separate monovalent Fab fragments and an intact Fc fragment. However, to produce an $F(ab')^2$ fragment, IgG is digested with pepsin, which cleaves the heavy chains near the hinge region. One or more of the disulfide bonds that join the heavy chains in the hinge region are preserved, so the two Fab regions of the antibody remain joined together, yielding a divalent molecule, hence the designation $F(ab')^2$. The light chains remain intact and attached to the heavy chain. The Fc fragment is digested into small peptides[26].

1.2.1.1.Classes of immunoglobulins

Based on differences in the amino acid sequences in the constant region of heavy chains (γ, μ, α, δ and ε) immunoglobulins can be divided into five different classes,

IgG, IgM, IgA, IgD and IgE, known as isotypes. Immunoglobulin isotypes differ as well in the number and localisation of disulfide bridges and in their glycosilation pattern, furthermore, no hinge region is present in IgM and IgE but they have an additional heavy chain constant region[27].

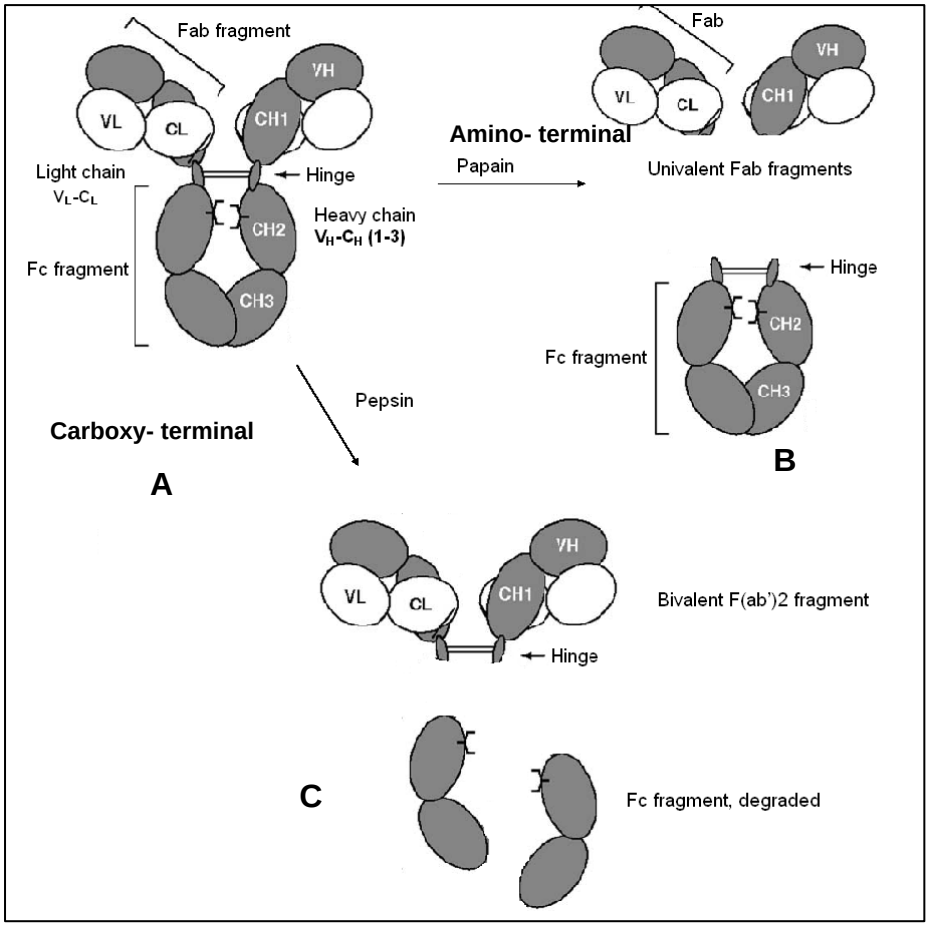

Fig. 1.1. IgG antibody structure and fragmentation. **A.** Intact IgG molecule, **B.** Papain cleaves IgG above the hinge region but below the site of the disulfide bond between the light chain and heavy chain generating two monovalent Fab fragments and an intact Fc fragment, **C.** Pepsin cleaves the heavy chains near the hinge region generating bivalent $F(ab')^2$ fragment and degraded Fc fragment. Reference [26], slightly modified.

Most immunoglobulins are monomers, but IgA and IgM are respectively, dimmers and pentamers linked by J chains. IgGs are the most abundanta and widely used for therapeutic purposes.

1.2.1.2. Immunoglobulin subclasses

IgGs are further divided into several subclasses: IgG1, IgG2, IgG3, and IgG4 (in order of relative abundance in serum plasma)[25]. The four subclasses show more than

95% homology in the amino acid sequences of the constant domains of the γ-heavy chains but show marked differences in the amino acid composition and structure of the hinge region which determines the flexibility of the molecule. Hinge-dependent Fab-Fab and Fab-Fc flexibility may be important in triggering further effector functions such as complement activation and Fc receptor binding[28]. There are two types of light chains: kappa (*κ*) and lambda (*λ*). In human immunoglobulins the average *κ* to *λ* ratio is 2:1.

IgG1 hinge region has 15 amino acids and 2 disulfide bonds while IgG2 has a shorter hinge region, with 12 amino acid residues and 4 disulfide bridges which invokes restricted the flexibility of IgG2 molecule[29]. IgG3 differs from the other subclasses by its unique extended hinge region with 11 disulfide bridges, while the hinge region of IgG4 is shorter than that of IgG1[30,31]. In addition to differences among genes encoding the IgG subclass proteins, each with different amino acid composition and derived properties, mutations within these genes have led to variations of the composition of IgG subclass proteins within the population. The latter mutations provide the basis for genetic markers (called Gm allotypes) and correspond with minor differences in primary amino acid sequence between molecules of one IgG subclass that occur throughout a species. Among individuals, different allelic forms are expressed. Subclass IgG3 is the most polymorphic, with thirteen Gm3 allotypes, IgG2 has only one allotype, whereas no allotypes have been detected on the heavy chains of IgG4[32]. In addition there are three allotypes of human *κ* light chains, Km(1), Km(2) and Km (3). There are four IgG1 allotypes located on the heavy chain: G1m (1); G1m (2); G1m (3) and G1m (17) based on amino acid residues at positions 356, 358, 431 and 214. Substitution of Lys_{214} with Arg_{214} changes allotype G1m (17) to G1m (3) and a change of Asp_{356}, Leu_{358} to Glu_{356}, Met_{358} changes the allotype G1m (1) to the isoallotype nG1m (1) which is homologous to IgG2 in this region.

There are several reasons to be concerned about immunoglobulin allotypes with regard to the engineering of antibodies for therapy, *i.e.* when a patient has a different immunoglobulin allotype from the therapeutic monoclonal antibody then there is an increased potential for an antiglobulin response, directed to both the constant region and the variable region. One approach to avoid anti globulin response is to select the most common allotype for general use[33].

1.2.2. Disulfide bonds

IgG1 molecules have four interchain disulfide bonds-two connecting the two heavy chains at the hinge region and the other two connecting the two light chains to the heavy chains. Immunoglobulins have four intrachain disulfide bonds within each domain (two Fab and one Fc, domain), therefore overall, 12 intrachain bonds: each light chain two and heavy chain 4 disulfide bridges, respectively. Native IgG mAb's, with completely formed disulfide bonds, should not bear any free sulfhydryl [34].

1.2.3. Oligosaccharides

IgG has a single N-linked biantenary complex oligosaccharide structure at Asn_{297} which is buried between the C_H2 domains, forming extensive contacts with amino acid residues within C_H2[35].

One of the most important structural features of recombinant monoclonal antibodies produced in mammalian cells is the *N*-linked oligosaccharide profile. These profiles impact recombinant therapeutics in a multitude of ways affecting distribution, efficacy, and immunogenicity[36]. Effector mechanisms mediated through FcγRI, FcγRII, and FcγRIII and C1q are severely compromised or ablated for aglycosilated or deglycosilated forms of IgG. It was documented that the interaction of effector ligands with IgG-Fc is through the protein moiety; however, generation of required IgG-Fc conformation is dependent of the oligosaccharide.[37]

Carbohydrate heterogeneity introduced during fermentation of recombinant monoclonal antibodies can include differential addition of fucose, alternative mannose branching linkages, differential presence of terminal galactose residues (termed G0, G1, G1' and G2, molecular species), and sialylation[38].

Differentially sialylated glycoprotein may display attenuated pharmacokinetics, owing to carbohydrate binding to asyalo-glycoprotein receptor and mannose receptor expressed in the liver where desialylated glycoproteins are sequestered and undergo rapid catabolism[39]. Presence of galactose residues in the non-reducing terminals of N-linked oligosaccharides affects antibody-dependent cellular cytotoxicity (ADCC) which is a major function of some therapeutic antibodies. ADCC was improved by the absence of fucose (fuc) residue at the innermost Glc-NAc of reducing end and by the presence of N-acetyl glucosamine[38]. It was demonstrated that and increased G0

oligosaccharide (lacking terminal galactose) level on the rituximab molecule is associated with a reduction in biological activity as measured by a complement dependent cytotoxicity (CDC) asay[40]. On the other hand 10-fold increase in ADCC was observed for remodeled trastuzumab and rituximab With high (>80%) bisecting GlcNAc content[41].High mannose, α-gal and other oligosaccharide species are highly immunogenic and in most cases should be minimized during antibody manufacturing[36].

1.2.4. Basic functions of antibodies

There are two functional areas in immunoglobulin G molecules: variable (V) and constant (C) regions (Fig 1.1 and 1.2). Variable regions of the two heavy and light chains, composed of two beta sheets and loops connecting the beta strands, offer two identical antigen binding sites. Regions with highest variability values in a multiple alignment of antibody sequences or complementarity determining regions (CDRs) are responsible for antigen recognition and binding[25, 42].

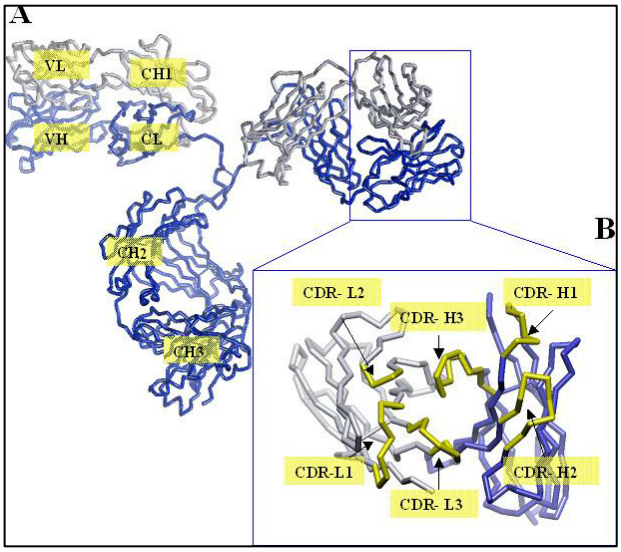

Fig. 1.2. IgG antibody structure. Acording reference [42].
A. IgG structure, showing two identical heavy (H) chains and two identical light chains (L) and their domains: V_L, C_L, V_H, C_H1, C_H2, and C_H3. The Fv fragment, indicated by a square, is the portion of the molecule that interacts with the antigen. It is composed by non-covalent pairing of VL and VH.
B. Fv fragment shown from the antigen view indicating the placement of the hypervariable loops and CDRs.

The remaining regions of V domain containing the two beta sheets and non CDR loops are referred as framework regions (FR). The CDRs in each chain are held in

close proximity by the framework regions and, with the CDRs from the other chain, contribute to the formation of the antigen binding site[43].

The constant domains are not involved directly in antigen binding, but are involved in various effector functions, which can be divided in two categories:

1. Effector functions that operate after the binding of antibody to antigen (involve participation of the complement cascade or Fc receptor (FcR)-bearing cells), and
2. Effector functions that operate independently of antigen binding (these functions confer persistence in the circulation and the ability to be transferred across cellular barriers by transcytosis)[44].

The interaction of antibodies and antibody-antigen complexes with cells of the immune system effects a variety of responses including antibody-dependent cell-mediated cytotoxicity (ADCC) and complement dependent cytotoxicity (CDC). ADCC functions are mediated by Fc receptors, which bind the Fc fregion of an antibody. Three subclasses of receptors for IgG antibodies are identified: FcγRI (CD64), FcγRII (CD32), and FcγRIII (CD16). The binding site on human antibodies for FcγR has been mapped to “lower hinge region” consisting of residues 233-239[45]. On the other hand, C1q and two serine proteases, C1r and C1s, form the complex C1, the first component of the complement dependent cytotoxicity pathway. It is suggested that the region comprising amino acid residues 318-337 might be involved in the complement fixation[46].

Another type of receptor is the neonatal Fc receptor (FcRn). This receptor, expressed in the liver, mammary gland and adult intestine plays key role in IgG homeostasis and half life. FcRn acts as salvage receptor binding and transporting pynocytosed IgGs in intact form within and across cells and rescues them from biodegradation. Furthermore, FcRn plays a role in the passive delivery of IgG from mother to young[47].

1.2.5. Polyclonal-derived antibody therapeutics

Human or animal-derived polyclonal antibody therapeutics are today are widely used in medicine for viral and toxin neutralization and for replacement therapy in patients with immunoglobulin deficiencies[48]. Human plasma-derived hyperimune immunoglobulin is used for prophylaxis or therapy against infections with hepatitis B virus (Nabi-HB®), respiratory syncytial virus (RSV) (Respigam®), cytomegalovirus

(CMV) (Cytogam®) and rabies virus (BayRab®), as well as tetanus (BayTet®), botulinum intoxication and Rhesus D (RhD) alloimmunization. The disadvantages of these products are that the limited range of infectious diseases could be treated, potential risk of infectious disease transmission and their high production cost.

In order to overcome these limitations animal-derived immunoglobulins have been used. *i.e*, Rabbit and Equine anti-thymocyte immunoglobulins, Thymoglobulin® and Lymphoglobulin®, are used as immunosuppressivs for treatment or prevention of solid organ transplant rejection.

As hyper-immunised serum contains a mixed population of antibodies, polyclonal antibody preparations are considered efficacious as they can neutralise multiple epitopes on the disease causing agents. However, due to the inherent risks associated to their use in humans such are hypersensitivity, anaphylaxis, anti-animal response and transmission of infectious pathogens including prions, their application is limited[49].

1.2.6. Development of recombinant monoclonal antibody therapeutics

Monoclonal antibodies as a highly specific naturally evolved molecules that recognise and eliminate pathogenic and disease antigens, are widely used for the treatment and prophylaxis of diseases such as infection, cancer and autoimmune disorders[50]. Today monoclonal antibody technologies allow the development of an antibody against any target of choice and provide the ability for an unlimited supply of a single antibody of reproducible affinity and specificity[49].

The discovery of hybridoma technology by Kohler and Milstein in 1975 revolutionized the development of specific antibodies for clinical use[51]. This ingenious approach involves fusing antibody producing B-cells with an immortal, non-antibody secreting plasma cell (myeloma) line resulting in a population of hybrid cells, hybridomas that are selected for secretion of an antibody specific for an antigen of interest. Non-antibody secreting plasma cell line is deficient in hypoxanthine phosphoribosyl transferase (HPRT) and when fused to B-cells and placed in medium containing hypoxanthine-aminopterin-thymidine (HAT), the aminopterine poisons the *de novo* purine synthesis pathway. Unfused cells die, and only the hybridomas survive in HAT, while the B-cell component of the hybridoma provide the purine salvage pathway and the plasma cells contribute unlimited *in vitro* proliferation[52].

Supernatants of bulk cultures of hybridomas are then screened for the presence of antibodies of interest, usually by ELISA and finally monoclonal antibody is produced either *in* vivo in the rodent ascites fluid or *in vitro* in different bioreactors[53].

1.2.6.1. Murine monoclonal antibodies

After the development of hybridoma technology, first murine monoclonal antibody, muromonab CD3 (OKT3), gained FDA approval in 1986 for clinical use in humans. Since then the number of approved antibodies, as well as mAbs in clinical trials, has steadily increased[54]. To date, three therapeutic murine mAbs have been approved by FDA or EMEA: muromonab-CD3 (Orthoclone OKT3®) used in transplant rejection therapy; antineoplastic, tositumomab-I^{131} (Bexxar®), and antineoplastic ibritumomab tiuxetan conjugated with Y^{90} or In^{111}(Zevalin®).

However, murine monoclonal antibodies have properties which limit their clinical utility:

- Murine mAbs administered to humans induce an immunogenic response, referred to as human anti-mouse antibodies (*HAMA*) or human anti-globulin antibodies (*HAGA*)
- Murine mAbs have reduced therapeutic efficacy (comparing to human mAbs), due to relatively faster clearance.
- Murine mAbs exhibit weak effector functions: *ADCC* and *CDC*

1.2.6.2. Chimeric recombinant monoclonal antibodies

In order to overcome disadvantages of murine monoclonal antibodies, i.e. reduce immunogeneicity, extend half-life and increase effector functions, chimeric mAbs, consisting of rodent variable domains fused to human constant domains are designed using recombinant DNA technology [55].

In 1997 FDA approved the first chimeric antibody against CD 20- rituximab (MabThera®) [56].

Chimeric mAbs are less immunogenic than their fully murine counterparts. This is achieved by replacing of murine antibody with about 60-70% of human antibody. However, they are still immunogenic and administered to humans can elicit human anti chimeric antibody (HACA) response. Mechanism of action of chimeric

monoclonal antibodies is very complicated. The murine variable regions including Fab portion of molecule, are responsible for antigen recognition and binding. On the other hand, activation of complement system and the recruitment of killer cells can take place as a result of human Fc fragment mediated effector functions of rmAb.
Half-lives of chimeric antibodies in humans range from about 4 to 15 days, somewhere between half-lives of human (around 24 day) and murine antibodies (1 to 4 days) [57].

1.2.6.3. Humanised recombinant monoclonal antibodies

Due to relatively short half-lives of chimeric antibodies as compared to human antibodies, the assumption is that the their mouse variable regions are still antigenic to humans. Therefore, many mouse antibodies have been “humanized” for therapeutic use in humans.
Antibody humanisation consist in grafting the complementarity-determining regions (CDRs) or hypervariable loops that can potentially interact with the target molecule from a non-human, parental antibody to a human acceptor antibody.
In this process, which is known as “antibody reshaping” as well, human antibody is genetically engineered to contain only the antigen binding site from the murine antibody of desired specificity[58]. Humanised antibody contains only the CDRs of the murine antibody, but the framework regions (as well as constant regions) of a human antibody and is considered superior to chimeric antibodies because the murine contribution (and hence the immunogeneicity) is reduced to minimum.
There is a delicate balance between specificity and humanization and in order to save the antibody specificity computer modelling is often used to overlay human amino acid sequences on mouse framework structures do determine what gene family of framework regions might least distort the CDRs[52].
Apart from CDR grafting, which is paradigm of humanisation and current standard in the field, other rational and empirical methods for antibody humanisation have been reported[42].
CDR grafting of both heavy and light chains of therapeutic antibody alemtuzumab was reported in 1988, while one year later was humanized the first FDA approved therapeutic monoclonal antibody daclizumab[59]. To date about half of approved

monoclonal antibodies in different therapeutic areas are humanized monoclonal antibodies (Table 1.2).

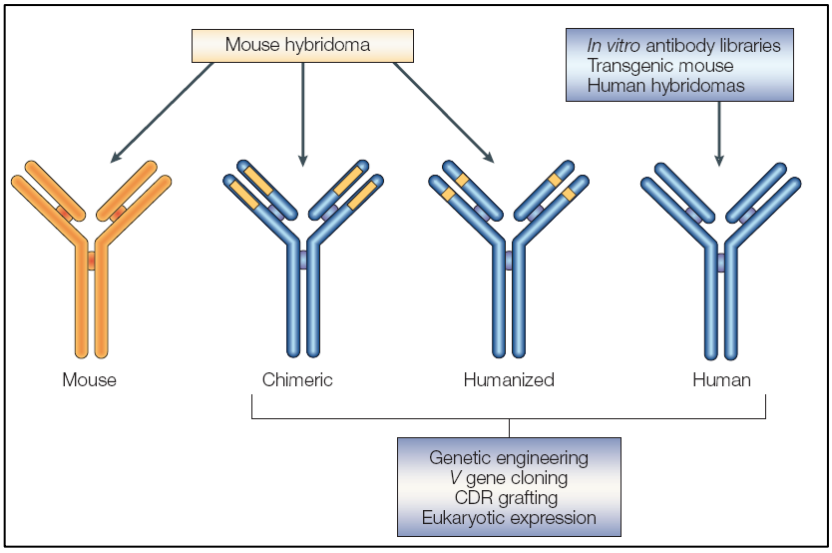

Fig. 1.3. Antibody engineering. According reference [60]
Mouse monoclonal antibodies generated by mouse hybridoma technology
Chimeric, humanised and human antibodies generated by recombinant DNA technology
Fully human antoibodies can be generated human antibody library technology, transgenic mouse technology and human hybridomas.

Although humanized monoclonal antibodies are about 95 % human, they are still immunogenic. The marketed humanized monoclonal antibodies show a range of human anti human(ised) (HAHA) antibodies from 0 to 34 % of patients.

The fact that the only currently marketed fully-human antibody, adalimumab directed against TNFα, shows significant HAHA response in patients[61], documents that even so-called 100 % human biologicals are potentially immunogenic.

1.2.6.4. Fully-human monoclonal antibodies

Adalimumab, a human antibody selected by the phage display technique against tumor necrosis factor alfa (TNFα) was the first marketed fully-human monoclonal antibody[62].

In general there are two different approaches to make fully human monoclonal antibodies: *in vivo* and *in vitro* approaches.

The *in vivo* process is based on the immunization of a transgenic mouse. Transgenic mice possess human IgG germlines instead of the normal murine germlines. The B cells harvested after immunization can be immortalized by fusion with a myeloma cell

line, as in traditional hybridoma technology and resulting hybridomas can then be screened for specific antibodies. While only one antibody derived from this technology has been already marketed (panitumumab), a large number are in the development phase[50, 54].

The *in vitro* process is based on screening the library of antibodies against an immobilized target. The nonbinding phage antibodies are washed away and the recovered antibodies are amplified by infection in *Escherichia coli.* The antibody format for screening is either Fab or single-chain Fv. The antibody fragments themselves can be used as therapeutic agents, but they can also be converted into intact immunoglobulins by the cloning of the variable genes into plasmids incorporating the constant-region genes of immunoglobulins. The genes are transfected into cell lines and therefore produce fully human immunoglobulins.

Human mAbs can also be produced from human hybroidomas or human B-lymphocyte cell lines immortalized by Epstein-Barr virus[63, 64].

1.2.6.5. Immunoconjugates

Recombinant mAbs currently approved for the treatment of malignancies exhibit varying levels of activity in several tumour types. However, efficient and prolonged intratumoral mAb uptake due to different biological and binding site barriers and antigen heterogeneity, remain problem for mAb therapeutic efficacy. In addition, even when accumulation of a mAb in the target tissue is achieved, therapeutic efficacy is often limited by the extent to which ADCC, CMC or induction of signalling events leads to cell death[65]. In order to increase therapeutic efficacy unmodified mAbs are armed with drugs, toxins and radionuclides. Already, three recombinant monoclonal antibody conjugates have been approved for cancer therapy: two radioimmunoconjugates, ibritumomab tiuxetan, Zevalin® (a CD20-specific IgG_1 κ radiolabeled with ^{90}Y) and tositumomab, Bexxar® (a CD20-specific IgG2aλ radiolabeled with ^{131}I) and one immunotoxin, gemtuzumab ozogamicin (Mylotarg®)[65]

Immunoconjugates are examples of antibodies designed to specifically deliver their toxic load directly to cancer cells. Recombinant mAbs armed with various toxins such as doxorubicin, calicheamicin and maytansines, currently are being studied[65].

1.2.6.6. Engineered antibody fragments

Advances in biomolecular engineering *i.e*. phage display technique and *in vitro* human antibody library approach, allow efficient isolation of different antibody fragments such are single chain variable (scFv) and Fab fragments, diabodies, triabodies and minibodies. These engineered smaller fragments exhibit increased affinity and specificity to almost any kind of antigen, they are less immunogenic and have superior biodistribution and blood clearance properties and have great potential to be used as diagnostic and therapeutic agents. Another advantage of these techniques is the ability to select specific antibodies against toxins, drugs, cytokines and other targets that cannot, for various reasons, be injected into an animal to raise an immune response, one of which is that the target might kill the animal or that it might not be immunogenic at all[50, 60]. Currently there are two antibody fragments approved for therapeutic use: platelet aggregation inhibitor, chimeric Fab, abciximab (ReoPro®), and antiangiogenic agent, humanized Fab ranibizumab (Lucentis®) used for the treatment of macular degeneration. Many of these prooducts are currently in the clinical and preclinical development[66].

1.2.7. Fusion proteins

Fusion proteins referred also as immunoadhesins are chimeric antibody like molecules that combine the functional domain of a binding protein, usually a receptor, ligand, or cell adhesion molecule, with immunoglobulin constant domains usually including the hinge, and Fc regions. The functional domain of protein (adhesin portion) determines target specificity and Ig- part confers IgG-like effector functions of molecule. Human fusion proteins are a novel class of biological agents and provide an alternative to human monoclonal antibodies as agents that recognize and neutralize proteins that possess pathological functions[67].

The simplest fusion protein design combines the binding region of the adhesin protein with the hinge and Fc regions of an IgG heavy chain (Fig. 1.4). Resulting protein is a homodimer, which resembles an IgG antibody, but lacks C_H1 domains and light chains. For human fusion proteins, IgG1 subclass has been used most frequently because γ1-immunoadhesins are amenable to purification by Protein A chromatography[67, 68].

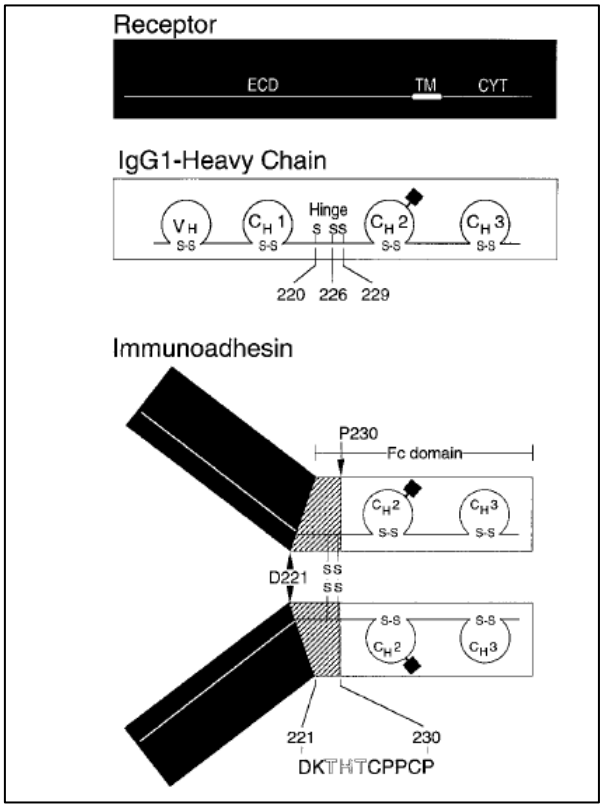

Fig. 1.4. Structure of prototype fusion protein. According reference [67].
ECD, TM, and CYT refer to the extracellular, transmembrane, and cytoplasmic domains, respectively
The N-linked carbohydrate chain at Asn-298 within the C_H2 domain is shown, as are the intrachain disulfide bonds.
Receptor- and IgG1-derived sequences are indicated by shaded and unshaded regions, respectively.
To construct the fusion protein, the receptor ECD is fused to the IgG hinge (DKTHTCPPCP sequence).
In the fusion protein abatacept, hinge region cysteines are replaced with serines, therefore intrachain disulfide bonds are located in the receptor ECD part.

On the other hand, various binding proteins that react with ligands of interest can be used as adhesion partners. Such proteins are extracellular domain of human CTLA-4, extracellular ligand-binding domain of the human TNF receptor, extracellular domain sequences of the Il-1 type 1 receptor and Il-1 receptor accessory protein, among others[69-7].

As human fusion proteins are based on human sequences of adhesin and Ig-part of molecule, there are minimally immunogenic to humans. This property is important advantage for indications that require multiple administrations. In addition, in contrast to chimeric or humanized monoclonal antibodies, construction of fusion proteins is straightforward and affinity for ligand is retained or even increased[67].

To date, four fusion proteins have gained approval for use in the different clinical settings: etanercept (Enbrel®), abatacept (Orencia®), alefacept (Amevive®) and rilonacept (Acralyst®).

1.2.8. Approved therapeutic recombinant monoclonal antibodies and fusion proteins

Currently, the US Food and Drug Administration has approved 21 monoclonal antibodies and 4 fusion proteins for targeted cancer therapy, autoimune and inflamatory diseases, antiviral prophylaxis etc. About 400 pre-approval clinical studies are ongoing, so it is to expect that the increase in approval of antibody therapeuticals will not slow down in the near future[72].

1.2.8.1. Monoclonal antibodies targeting cancers

Recombinant monoclonal antibody treatment of human malignancies today consists in two approaches: Specific or targeted antibody therapy in combination with classical chemotherapy is used for the destruction of cancer cell either by specifically targeting the tumour or the vasculature that nourishes the tumour. The most common cancer targets are HER2/ (c-erb-2) receptor, epidermial growth factor receptor (EGFR), vascular endothelial growth factor (VEGF) and CD20 and CD52. Specific and highly cytotoxic immunoconjugates on the othert hand, target CD33 and CD 20.

1.2.8.2. Anti-inflammatory monoclonal antibodies

For the treatment of auto-immune diseases specific antibodies and fusion proteins to inhibit detrimental effect of cytokines, B and T cell receptors and modulate T-cell co-stimulatory pathway, have been approved. Approved recombinant antoibodies and fusion protein for diferent therapeutic indication are presented in Table 1.2.

Table 1.2. Approved therapeutic monoclonal antibodies and fusion proteins. According references [73][74][75] [#]Orphane medicinal product designation (EMEA).
INN: International Nonproprietary Name.
Expression system: ***murine ascites;* ***[a]***murine myeloma cell line SP/20*; ***[b]***murine myeloma cell line*; ***[c]***recombinant murine plasmacytoma cell line (KD1)*;
****Chinese Hamster Ovary (CHO) cells*; ****[a]***Source*: *XenoMouse® Expression: CHO*; *****Escherichia coli*.
TNFR-IgG1: Extracellular ligand-binding portion of human tumor necrosis factor receptor (p75) fused to the Fc portion of human IgG1.
LFA-3-IgG1: First domain of the human LFA-3 protein fused to the Fc portion of human IgG1.
CTLA4-IgG1: Extracellular domain of human cytotoxic lymphocyte associated antigen 4 (CTLA-4) protein fused to the Fc portion of human IgG1.
IL-1R1 IL-1RacP-IgG1:Extracellular domains of IL-1R1 receptor and IL-1 receptor accessory protein (IL-1RacP) fused to the Fc portion of human IgG1.

Monoclonal antibody	Trade name/ Manufacturer	Approval status FDA	EMEA	Antibody type	Specificity (Target antigen)	Therapeutic indication
Muromonab CD-3	Orthoclone OKT3® (Ortho Biotech)	1992	—	Murine IgG2a*	CD3 complex on mature T-lymphocytes	Immunosuppressive therapy. Allograft rejection
Rituximab	Mabthera® (Roche)	1997	1998	Chimeric IgG1**	B-cell antigen CD20	Non-Hodgkin's Lymphoma Rheumatoid arthritis
Daclizumab	Zenapax® (Roche)	1997	1999	Humanized IgG1 anti-Tac antibody*[a]	Alfa subunit of Interleukin- 2 receptor	Prophylaxis of acute organ rejection
Basiliximab	Simulect® (Novartis)	1998	1998	Chimeric IgG1κ*[a]	Interleukin-2 receptor α-chain (CD25 antigen)	Prophylaxis of acute organ rejection
Palivizumab	Synagis® (Abott)	1998	1999	Humanized IgG1κ*[b]	Epitope of the fus. protein of res.syncytial virus RSV)	Respiratory syncytial virus (RSV) disease prevention
Infliximab	Remicade® (Centocor B.V.)	1998	1999	Chimeric IgG1κ*[a]	TNFα, soluble and transmembrane form	Rheumatoid arthritis, Crohn's disease, psoriasis
Trastuzumab	Herceptin® (Roche)	1998	2000	Humanized IgG1κ**	HER2/ (c-erb-2) receptor	Breast cancer
Gemtuzumab ozogamicin (calicheamicin derivative)	Mylotarg® (Wyeth)	2000	2004[#]	Humanized IgG4, immunoconjugate*[c]	CD33 antigen	Acute myeloid leukaemia (AML)
Alemtuzumab	MabCampath® (Genzyme)	2001	2001	Humanized IgG1κ**	Lymphocyte cell surface glycoprotein (CD52).	B-cell chronic lymphocytic leukaemia (B-CLL)
Ibritumomab tiuxetan ^{90}Y-radiolabelled	Zevalin® (IDEC)	2002	2004	Murine IgG1κ** (recombinant)	B-cell antigen CD20	CD20+ follicular B-cell non-Hodgkin's lymphoma
Adalimumab	Humira® (Abott)	2002	2003	Fully human IgG1**	Cell surface TNF receptors	Rheumatoid arthritis, Crohn's disease, psoriasis
Omalizumab	Xolair® (Novartis)	2003	2005	Humanized IgG1κ**	Immunoglobilin E	Asthma therapy
Iodine I^{131}-Tositumomab	Bexxar® (Glaxo SK)	2003	2005[#]	Murine IgG2aλ*[b]	B-cell antigen CD20	Follicular lymphoma
Efalizumab	Raptiva® (Serono)	2003	2004	Humanized IgG1κ**	CD11a subunit of LFA-1 on activated T-lymphocytes	Chronic plaque psoriasis
Abciximab	ReoPro®(Centocor)	2003	—	Chimeric Ab Fab fragment*[a]	Glycoprotein (GP) IIb/IIIa receptor of platelets	Cardiovascular disease Prevn. of cardiac ischaemia

Continued from the previuos page

Cetuximab	Erbitux® (Imclone)	2004	2004	Chimeric IgG1*[b]	Human epidermal growth factor receptor (EGFR)	Colorectal and squamous cell cancer of head and neck
Bevacizumab	Avastin® (Roche)	2004	2005	Humanized IgG1κ**	Human vascular endothelial growth factor (VEGF)	Metastatic colorectal, breast, lung and renal carcinoma
Natalizumab	Tysabri® (Biog Idec)	2004	2006	Humanized IgG4 κ*[b]	α4β1 and α4β7 integrin	Relapsing multiple sclerosis
Ranibizumab	Lucentis® (Novartis)	2006	2007	Humanized Fab fragment of IgG1***	Human vascular endothelial growth factor A (VEGF-A)	Neovascular age-related macular degeneration
Panitumumab	Vectibix® (Amgen)	2006	2007	Fully human IgG2**[a]	Human epidermal growth factor receptor (EGFR)	Metastatic carcinoma of the colon or rectum
Eculizumab	Soliris® (Alexion Eu)	2007	2007	Humanized $IgG_{2/4}$κ*[a]	Human C5 complement protein	Paroxysmal nocturnal haemoglobinuria (PNH)
Certolizumab pegol	Cimzia® (UCB Inc)	2008	—	Humanized, PEG*** conjugated Fab' frag.	TNF alfa	Crohn's disease
Fusion protein, INN	**Trade name/ Manufacturer**	**Approval status FDA**	**EMEA**	**Fusion protein type**	**Specificity (Target antigen)**	**Therapeutic indication**
Etanercept	Enbrel® (Immunex)	1998	2000	TNFR-IgG**	Human TNFα and Lymphotoxin (LTα)	Rheumatoid arthritis, Psoriasis
Alefacept	Amevive® (Astellas)	2003	—	LFA-3-IgG**	CD2 on T-lymphocytes	Moderate to severe chronic plaque psoriasis
Abatacept	Orencia® (Bristol-Mayers)	2005	2007	CTLA4-IgG**	B7 molecules (CD80 and CD86 receptors)	Rheumatoid arthritis
Rilonacept	Arcalyst® (Regeneron)	2008	2008[#]	IL-1R1IL-1RacP-IgG**	Interleukin IL-1β	Cryopirin-Associated Periodic Syndromes

1.2.9. Nomenclature of monoclonal antibodies

According the relevant guidelines for the assignment of the unique non-proprietary or generic names for medicines, the following scheme has been developed for monoclonal antibodies [76, 77]:

- General stem/suffix is used for mAbs antibodies and fragments, ***-mab***
- Sub-stems for source of product (product source identifiers): *human (-u-); rat (-a-); hamster (-e-); primate (-i-); mouse (-o-); chimeras (-xi-); humanized; (-zu-); rat/mouse (-axo-); combination of humanized and chimeric chains (-xizu-).*

These identifiers are used as infixes preceding the -*mab* suffix stem, e.g.: -**umab** (human); -**omab** (mouse); -**ximab** (chimera); -**zumab** (humanized).

- Sub-stems for disease or target class: *bacterial (-ba(c)-); cardiovascular (-ci(r)-); immunomodulator (-li(m)-); infectious lesions (-le(s)-); viral (-vi(r)-); antifungal (-fun(g)-); interleukins (-ki(n)-) etc.*

  Tumours: *colon (-co(l)-*); *melanoma (-me(l)-); testis (-go(t)-); ovary (-go(v)-*); *prostate (pr(o)-); miscellaneous (-tu(m)-*)
- Prefix should be random, e.g. the only requirement is to contribute to a euphonious and distinctive name.
- Second word: If the product is radiolabeled or conjugated to another chemical such as a toxin, identification of this conjugate is accomplished by use of a separate, second word or other acceptable chemical designation.

If a monoclonal antibody is used as a carrier for radioisotope, the latter will be listed first in the INN, e.g. Iodine I^{131}-Tositumomab.

1.2.10. Nomenclature of receptor molecules

The stem for receptor molecules (native or modified) is ***-cept*** , while a preceding infix should designate the target, *e.g.* lymphocyte function-associated antigen 3 receptors **-lefa-** (alefacept); interleukin-1 receptors ***-na-*** (rilonacept); cytotoxic lymphocyte associated antigen 4 (CTLA-4) receptors ***-ta-*** (abatacept, belatacept). On the other hand, the common stem for tumor necrosis factor antagonists is ***-nercept***. *e.g.* etanercept[78].

.

1.3. Quality of rDNA derived therapeutic proteins

Quality, safety and efficacy are key components that need to be monitored throughout the lifecycle of any medicinal product[79]. Recombinant biological medicinal products, exhibit high degree of molecular complexity and their biological manufacturing process is highly complicated, involving cloning, suitable cell line selection, fermentation, purification and formulation. Therefore, quality control of these products addresses aspects related to the final drug product (its identification and purity, impurities, potency, stability and safety assessment) and production process (production organism characterization, monitorization of fermentation, cell culture processes and recovery/purification operations)[80].

rDNA derived therapeutic proteins are large, complex and folded macromolecules and their exact conformation is critical for their therapeutic action and adverse effects. Due to the biosynthetic processes involved in their production, an inherent degree of structure heterogeneity occurs, *i.e.* glycoforms..

Current analytical methodology to ensure comprehensive product characterization and identification, including determination of physicochemical properties, biological activity, immunochemical properties, purity, impurities; and product stability, employs different physicochemical, immunological and biological methods[81, 82].

In order to identify the nature and homogeneity of the amino-and carboxyl-terminal amino acids, *N- and C-terminal amino acid sequence analysis,* is performed.

Edman degradation analysis is used to confirm the complementary DNA (cDNA)-predicted amino acid sequence and to evaluate the potential extent of proteolytic clips[80].

Peptide mapping by HPLC is a highly specific identity method, and may serve as a confirmation of a genetic stability of proteins obtained by mammalian cell culture. It is used to compare the protein structure of a specific lot of material to that of reference standard, but lot-to-lot consistency of primary structure can be confirmed as well. It can provide additional information about product, i.e.glycosilation site, N- and C-terminal peptides, and position of disulfide bonds. Therefore, this technique is particularly important in the quality control of rDNA derived proteins, especially *rmAbs*. Peptide mapping using an appropriately validated procedure is a method frequently used for the structure confirmation for lot release purposes[83, 84].

1.3.1. Post-translational modifications

Apart from the proteolytical processing, potential types of post-translational modifications are N- and O- glycosylation and acetylation, hydroxylation and gammacarboxylation. In addition, there are post-translational modifications that occur as degradation products such as deamidation and oxidation.

1.3.2. Carbohydrate determination

Glycosilation is characteristic of recombinant proteins expressed from eucariotic cell lines. Although polypeptide chain of a glycoprotein is synthesized under direct control of genetic code, oligosaccharides are not primary gene products; they are synthesized by enzymes glycosyltransferases. Glycosylation as a common co-and posttranslational modification of proteins may have profound effect on protein structure and function, including folding, trafficking and protein-protein recognition. One feature of protein glycosylation is that a single site can be occupied by any one of a number of glycan structures, and this can give rise to extremely heterogeneous glycoprotein populations, termed *glycomorfs*. The glycosylation pattern of a glycoprotein is not random but dependent on the cell-line, so glycoproteins with identical polypeptide chains made in different cell lines may have considerably different carbohydrate structures.

For glycoproteins, regulatory authorities demand the determination of carbohydrate content, the study of structure, carbohydrate chains, the oligosaccharide pattern (antennary profile) and glycosylation site(s).

The phenol-sulphuric acid method is the easiest and most reliable method for the determination of total neutral sugars, while free sialic acid content can be determined by thiobarbituric acid method after acid hydrolysis and periodate oxidation[85, 86.] On the other hand, individual sugars can be separated by high performance ion exchange chromatography (HPIEC) and quantitated as underivatized with pulsed amperometric detection (PAD). Once the glycans have been released from the glycoprotein, the glycan pool can be analyzed by MALDI-TOF mass spectrometry or, after fluorescent labeling, by either HPLC or MS, or both. This strategy can provide a “glycan profile” or a “glycosylation pattern” that is highly characteristic of the glycoprotein. The technology can be applied to compare glycan profiles of different

batches of recombinant protein products. High pH anion exchange chromatography with pulsed amperometric detector can be used with native glycans. Matrix-assisted laser desorption/ionization time-of-flight (MALDI-TOF) mass spectrometry is the most widely used MS technique. MALDI-TOF MS and NP-HPLC are used for glycane sequencing after appropriate incubation of glycan with specific glycosidases[83].

Due to advantages, as short analysis time, ability to separate and quantify isomeric species and high sensitivity, capillary electrophoresis coupled with on-column laser induced fluorescence (CE-LIF) and hyphenated CE-MS with on-line LIF detection, are used for glycan profiling of glycoproteins (*e.g.* recombinant mAbs)[87,88].

Oligosaccharide mapping and monosaccharide content are required by European Pharmacopoeia for the demonstration of molecular identity and structural integrity of *rmAbs*[89].

For characterization of biotechnology derived therapeutic proteins, different analytical techniques are required by regulatory authorities[81]. *Molecular weight or size* is determined by size exclusion chromatography (SEC), SDS-PAGE, and mass spectrometry (MS); *isoform pattern* by isoelectric focusing (IEF); *extinction coefficient* by UV/VIS spectrophotometry; *electrophoretic patterns* and data on identity, homogeneity and purity by SDS-PAGE, Western-blot and CE; *liquid chromatography pattern* and data on identity, homogeneity and purity by SEC, IEC, and affinity HPLC; *spectroscopic profiles* by the determination of UV/VIS spectra and circular dichroism (CD) and NMR spectroscopy for examination of high-order structure.

1.3.3. Determination of purity, impurities and contaminants in biotechnology derived therapeutic proteins

The determination of absolute or relative purity of a biologics and biotechnology drug substance presents considerable analytical challenges, and the results generally are method dependent[81]. In biological therapeutics obtained by recombinant cell culture expression systems, a huge variety of impurities may be present, and their origin cannot be easily predicted. They can not only affect safety of the final product but also interact with the expressed protein and, then, alter its functionality[90]. The analytical procedure of choice should allow complete separation of the desired product and product-related substances from impurities and the purity of biologics

and biotechnology drug substances is generally assessed by a combination of analytical procedures[91].

Table 1.3. Potential immpurities and Contaminants in Biotechnology-derived Products. According references [81] and [83].
LAL: Limulus amebocyte lysate; **EDA**: Edman degradation analysis; **SDS-PAGE**: Sodium dodecyl sulfate-polyacrylamis gel electrophoresis; **HPLC**: High performance liquid chromatography; **IEF**: Isoelectric focusing; **MS**: Mass spectrometry; **HP-SEC**: High performance size-exclusion chromatography; **CE**: Capillary electrophoresis; **CPE**: Cryopathic effect; **HAD**: Hemadsorption; **MAB**: Murine antibody production

Impurities or Contaminants	Detection Method
Impurities	
- Endotoxins	Bacterial endotoxin test (LAL test), Pyrogen test
- Host cell proteins	SDS-PAGE, Immunoassays
- Host cell DNA	DNA hybridization, UV spectrophotometry
- Other protein impurities (media)	SDS-PAGE, Immunoassays, HPLC
- Protein mutants	Peptide mapping, HPLC, IEF, MS
- Formyl methionine	Peptide mapping, HPLC,MS
- Oxidised methionins	Peptide mapping, HPLC, Amino acid analysis, Edman degradation analysis
- Proteolytic cleavage	IEF, SDS-PAGE (reduced), HPLC, Edman degradation analysis
- Aggregated proteins	SDS-PAGE, HP-SEC, CE
- Deamidation,isomerized, mismatched S-S linked, altered conjugated forms	IEF, MS, HPLC, CE, Circular Dichroism, Edman degradation analysis
- Monoclonal antibodies	SDS-PAGE, immunoassays
- Amino acid substitutions	Peptide mapping, MS, Amino acid analysis, Edman degradation analysis
Contaminants	
- Microbial (bacteria, yeast, fungi)	Microbial limit tests, Sterility tests
- Mycoplasma	DNA binding fluorochrome test. Other tests
- Viruses (endogenous and adventitious)	CPE and HAD test, for exogenous virus only; reverse transcriptase activity, MAB

Impurities in biotechnology derived therapeutic proteins can be of known structure, partially characterized, or unidentified, including:

- Process-related impurities, derived from manufacturing process, *i.e.* cell substrates, cell culture or downstream processing (Table 1.3)

- Product related impurities, molecular variant arising during manufacture and/or storage, which do not have properties comparable to those of the desired product with respect to activity, efficacy and safety.
- Contaminants, include all adventitiously introduced materials not intended to be part of the manufacturing process, such as chemical and biochemical materials (*e.g.*, microbial protease), and/or microbial species[81].

When different source and manufacturing methods result in different impurity profiles, different sets of analytical procedures may be needed and for impurity identification and quantification.
Choice and optimization of the analytical procedures should focus on the possibility to separate the desired product from the impurities, to identify and quantify all the possible impurities with suitable sensitivity, and to evaluate the biological activity of the product and related impurities[90, 91].

1.3.4. Biological activity testing

Often, for complex molecules, the physicochemical information may be extensive but unable to confirm the high-order structure which, however, can be inferred from the biological activity. Assessment of biological activity constitutes an equally essential step in establishing a complete characterization profile of biotechnology derived products. Potency is the quantitative measure of biological activity based on the attribute of the product which is linked to the relevant biological properties. For the potency determination suitable validated procedures should be used, including:

- animal-based biological procedures, which measure an organism's biological response to the drug substance,
- cell culture–based biological procedures, which measure biochemical and physiological response at the cellular level,
- biochemical procedures, which measure biological activities or biological responses induced by immunological interactions,
- ligand or receptor binding assays, which are based upon in vivo attribute(s) of the drug substance.

Activity-based procedures, such as enzyme assay, ligand binding, and cell culture–based procedures can be stability-indicating. ELISA procedures may or may not be stability indicating, depending upon whether the modification affects the three-dimensional structure of the antigenic epitope(s). Combining an applicable potency test procedure with a physicochemical or biological assay for the determination of content permits measurement of specific activity[81, 91].

1.3.5. Immunoassays

Immunoassays are used either as active drug substance methods to identify and quantitate the protein of interest or as impurity profile methods to detect and quantitate known host cell protein impurities. Additionally, immunoassays may serve as potency assays for monoclonal antibodies using an appropriate antigen[83]. Immunoassays, including radioimunoassays (RIAs) and enzyme-linked immunosorbent assays (ELISAs), consist of a large group of assays that depend on specific high-affinity antibody: antigen interactions.

1.3.6. Protein quantity determination

Bicinchoninic acid assay (BCA) and Bradford method are generally used for the determination of protein concentration in rDNA products[92].

1.3.7. Stability testing of biotechnology-derived therapeutic proteins

In the medicinal products obtained by *rDNA* technology, maintenance of molecular conformation and, hence of biological activity, is dependent on non-covalent as well as covalent forces. The products are particularly sensitive to environmental factors such as temperature changes, oxidation, light, ionic content, and shear. In order to ensure maintenance of biological activity and to avoid degradation, stringent conditions for their storage are necessary.

The evaluation of stability may necessitate complex analytical methodologies, and appropriate physicochemical, biochemical and immunochemical methods for the analysis of molecular entity and the quantitative detection of degradation products are needed. Assays for biological activity should be part of stability studies, as well[93].

There is no single stability-indicating assay or parameter that profiles the stability characteristics of biotechnology-derived therapeutic proteins. Consequently, a stability-indicating profile that provides assurance that changes in the identity, purity and potency of the product will be detected should be provided.

Due to the effect of deamidation, glycosylation and other heterogeneities, the absolute purity of biotechnological products is extremely difficult to determine, therefore, the purity of these products should be determined by more than one method, and the purity value derived is method dependent. For purposes of stability testing, test for purity should focus on methods for determination of degradation products. Relevant physicochemical, biochemical and immunochemical methods should permit a comprehensive characterization of the drug substance and accurate detection of degradation changes that may result from deamidation, oxidation, sulfoxidation aggregation or fragmentation during the storage.

The storage conditions for the real-time/ real-temperature stability studies may be confined to the proposed storage temperature. It is strongly suggested to conduct accelerated and stress conditions studies which may provide data for establishing the expiration date, provide stability information for future product development, assist in validation of analytical methods for stability program and elucidation of the degradation profile.

Studies under stress conditions may be useful in determining whether accidental exposures to other condition to those proposed are deleterious to the product and to evaluate which test parameters may be the best indicators for product stability. Influence of light, container/closure system and stability after reconstruction of freeze-dried products are studied, as well[93, 94].

1.3.8. Similar biological medicinal products (biosimilars)

The recent and pending patent expirations for a number of recombinant therapeutic proteins have prompted the study and development of alternative versions of biologic products, referred to as similar biological medicinal products (biosimilars)[95].

Biosimilar or similar biological medicinal products are biological medicinal products referring to existing ones which have been submitted to regulatory authorities for marketing authorization by an independent applicant after the time of protection of the data has expired for the original products. A biosimilar medicinal product can be

granted a marketing authorization provided that its similarity to a reference product is established in terms of quality, safety and efficacy (Comparability exercises).
Biosimilars (term preferred by EMEA) or “follow-on biologics” (term coined by US FDA), are new biological therapeutics that are similar but not identical to reference product. This is unlike to the case with small-molecule generics, where the active substance of a generic is identical to the reference product. Therefore, the standard generic approach, applied to chemically derived medicinal products (demonstration of bioequivalence with a reference medicinal product by appropriate bioavailability studies), is scientifically not appropriate for biotechnology- derived products[96, 97].

1.3.8.1. Recombinant therapeutic proteins versus small-molecule drugs

Biopharmaceuticals differ from low molecular weight drugs in a number of aspects (Table 1.4). While for small-molecule drugs their relatively simple structures render them easy to synthesize and produce identical molecular “copies”, therapeutic proteins, however, are much more complex in size and structure[98].

Table 1.4. Therapeutic proteins versus small-molecule drugs. According reference [98]

Therapeutic proteins versus small-molecule drugs
• Large complicated molecules
• Heterogeneity
• Produced by genetically modified living cells
• Complex mode of action mediated by large surface area
• Complicated production and purification
• Relatively unstable

For low molecular weight drugs an arsenal of physicochemical techniques is available to fully characterize the active molecule along with its impurity profiles and contaminants. However, with the present toolbox of analytical techniques including the bioassays, it is very difficult to fully characterize proteins at the end of the downstream processing procedure[95].
Unlike low molecular weight drugs, there is a strong relationship between the manufacturing processes of therapeutic proteins and the characteristics of the final

product. In this setting for therapeutic proteins one may say “the process is the product” or “process determines product”[99].

Biological manufacturing processes involve many steps from cloning the desired gene via selection of a suitable cell type, fermentation and purification to formulation of the end product. A variety of undesired chemical alterations to the drug product can occur during this time including oxidation, deamidation and the formation of protein aggregates[100]. Differences in manufacturing processes, protein source and extraction/ purification processes result in heterogeneity of the resulting therapeutic proteins. For example, the unique cellular-expression systems used in protein manufacture inherently produce a variety of isoforms. In addition, small changes in manufacturing process can produce alterations in the three-dimensional structure of the protein, folding, the quantity of charge variants and the glycosylation profile. Any change in the process can have profound effects on the biological activity and safety profile of the final product.

The expression of the same genetic construct in different host cell expression systems has a great impact on the final structure of the protein. While due to the absence of glycosylation machinery *Escherichia coli* is not able to modify proteins by glycosylation, proteins manufactured *Saccharomyces cerevisiea* cells contain high levels of mannose sugar groups, rendering them more prone to degradation and thereby decreasing their half-life. On the other hand, use of cell lines derived from chinese hamster ovary (CHO) cells, baby hamster kidney (BHK) cells and human fibrosarcoma cells, provide necessary (typically human- like) glycosylation in the production of many other therapeutically intended naturally glycosylated proteins[101,102].

Biosimilar manufacturers will not have access to the manufacturing processes of innovator products because this is proprietary knowledge. Thus, it will be impossible for biosimilar manufacturers to precisely replicate any protein product[95].

Based on the EU legistlation, European Medicines Agency (EMEA) is currently the only regulatory agency which has issued regulatory guidelines for the approval of biosimilars while guidance documents on the development of follow- on protein products and their approval might be issued by the FDA in the future[96, 97,103,104].

So far EMEA has developed three Guidelines applying to all biosimilars, and Annexes (product specific regulatory guidelines), i.e. for *rh* erythropoietin, *rh G-CSF*,

rh insulin, *rh* growth hormone. These guidelines advocate preclinical and clinical tests of biosimilars prior to marketing authorization.

Because therapeutic biologic proteins are sometimes, although infrequently, associated with serious adverse events, EMEA guidelines also require immunogenicity testing and tailored pharmacovigilance plans to monitor the efficacy and safety of biosimilar products post-approval.

The immunogenic potential of BMPs may differ between products and is influenced by several factors, such as the nature and structure of the active substance, impurities, excipients, manufacturing process, route of administration and target patient population. These differences may compromise the *in vivo* behavior of the product, resulting in undesired host immune responses to the drug that may abrogate efficacy and may give rise to potentially fatal adverse reactions, as an example the incidence of antibody mediated pure red cell aplasia (PRCA) in patients treated with epoetins, after replacing human serum albumin with polysorbate 80 as a stabilizer in erythropoietin formulations Eprex® and Erypo®[105].

Due to the aforementioned differences between biosimilars and reference products, automatic substitution based on the prescription of the international nonproprietary name (INN) of the active substance, does not appear reasonable[95, 96].

In order to facilitate clear identification, safe prescription and dispensing of biosimilars, and support their Pharmacovigilance monitoring, it is suggested that WHO assigns a different INNs for biosimilars and their reference products and since biological products cannot be identical, labels of originator and biosimilar products must be different[106, 107].

On April 2006 somatropin Omnitrope® received EMEA approval and being the first biosimilar medicinal product to granted the marketing authorization in EU. The reference medicinal product cited for Omnitrope was Pfizer's Genotropin, which was originally authorized in the EU in 1988[108,109]. Omnitrope was quickly followed by a second EU biosimilar approval, for somatropin Valtropin®. Omnitrope® has been produced in *Escherichia* coli whereas Valtropin® in *Saccharomyces cerevisiae.* Under the EMEA guidelines a number of biosimilars are admitted to the European market such as growth hormones (Valtropin®, Omnitrope®), epoetins alfa (Binocrit®, Abseamed®, Hexal®) and zeta (Retacrit®, Silapo®), filgrastim (Tevagrastim®).

Due to the structural complexity, remains uncertain whether the European rules would allow the development of a biosimilar *rmAbs* and whether current technology

would enable demonstration of their similarity. From an innovation perspective, development of new improved formats (or second-generation) of *rmAbs* replacing existing murine or chimeric antibodies is desired[110].

1.4. Two-dimensional electrophoresis (2-DE) as a straightforward method for the examination of recombinant drugs

2-D electrophoresis is a powerful and widely used method for the analysis of complex protein mixtures. This technique separates proteins according to two independent properties in two discrete steps. In the first dimension, isoelectric focusing (*IEF*), proteins are separated according to their charge (*pI*); in the second dimension sodium dodecyl sulfate-polyacrylamide gel electrophoresis (SDS-PAGE), separates proteins according to their molecular weights (*Mr*, relative molecular mass). Each spot on the resulting two-dimensional gel potentially corresponds to a single protein species in the sample and information such as the protein *pI*, the apparent molecular weight, and the amount of each protein can be obtained[111, 112].

Two-dimensional electrophoresis was first introduced by O'Farrell in 1975. In the original technique isoelectric focusing was performed in carrier-ampholyte-containing polyacrylamide gels cast in narrow tubes. However, pH gradient instability and susceptibility to cathodic drift, low resolution and intra- and inter- laboratory 2D-pattern irreproducibility were main drawbacks of this technique[113]. These problems were overcome by the introduction of immobilized pH gradients (IPGs) generated by the co-polymerization of "immobilines" with acrylamide matrix. The replacement of carrier-ampholyte-generated pH gradients with immobilized pH gradients and tube gels with gels supported by a plastic backing, brought about superior resolution and reproducibility to first-dimension IEF[114]. The basic protocol of two-dimensional electrophoresis with immobilized pH gradients in the first dimension (*IPG-DALT*) was established by in 1988[115]. IPGs allow the generation of pH gradients of any desired range (broad, narrow and ultranarrow) between pH 3 and 12. Since the sample loading capacity of IPG-IEF is also higher than CA-IEF, 2-DE with IPGs is the method of choice for micropreparative separation and spot identification.

In addition, development of new, sophisticated mass spectrometry techniques enables the identification and characterization of small quantities of proteins from 2-DE spots and the availability of powerful computers and software, makes possible

the evaluation of highly complex 2-DE patterns. 2-D Electrophoresis not only provides information on protein modifications and/or changes in their expression levels, but also permits the isolation of proteins for further structural analyses by MALDI-TOF-MS, ESI-MS or Edman microsequencing. Due to the ability of this technique to separate large number of proteins simultaneously, 2-DE is widely used in proteome analysis. Recent advances and modernization (*i.e.* introduction of fluorescent 2D difference gel electrophoresis) make 2-DE currently the most widespread technique used for performing functional and differential proteomics[116].
This technique can detect post- and co-translation modifications of proteins which can not be predicted from genome sequence.
Apart from proteome analysis, other applications of 2-D electrophoresis include, cell differentiation, detection of disease markers, monitoring therapies, drug discovery, cancer research, purity testing of biologics, and microscale protein purification[112].
Recently 2-DE has been proposed as a reliable method for the quality assurance of recombinant proteins and 2-DE electrophoresis in combination with MS for the detection of recombinant proteins in biological fluids for antidoping purposes[117, 118].

1.4.1. General principles of gel electrophoresis

Under the influence of an electrical field charged particles dissolved or dispersed in an electrolyte solution migrate in the direction of the electrode bearing the opposite polarity. In gel electrophoresis, the movements of the particles are retarded by interaction with surrounding gel matrix, which acts as a molecular sieve. The opposing interactions of the electrical force and molecular sieving result in a differential migration rates according to sizes, shapes and charges of particles. Because of their different physico-chemical properties, different macromolecules of a mixture will migrate at different speeds during electrophoresis and will thus be separated into discrete fractions. Electrophoresis separations can be conducted in system without support phases (*e.g.* free solution separation in capillary electrophoresis) and in stabilizing media such as thin-layer plates, films or gels[119].
The fundamental driving force of electrophoresis is the voltage applied to the system. The speed of a molecule is directly proportional to the surrounding voltage gradient. Two basic electrical equations are important in electrophoresis. The first is Ohm's Law (Equation 1) which relates voltage (*U*) measured in volts (*V*), current (*I*)

measured in amperes (A), and resistance (*R*) measured in ohms (Ω). The second fundamental equation in electrophoresis is the power equation, which describes the amount of heat produced in a circuit (Equation 2):

$$\boxed{I = \frac{U}{R}} \qquad \textit{(Eq.1)} \qquad\qquad \boxed{P = UI \ or \ P = I^2R \ or \ P = \frac{U^2}{R}} \qquad \textit{(Eq.2)}$$

P is power, measured in watts (W). This heat is also referred to as *Joule heat*. In the electrophoresis circuit, voltage and current are supplied by a DC power supply; the leads, electrodes, buffer, and gel all act as simple resistors.

Power supplies used for electrophoresis hold one electrical parameter (current, voltage, or power) constant. The resistance of the electrophoresis circuit, however, does not remain constant during a run. Buffer resistance declines with increasing temperature caused by *Joule heating*. Resistance also changes as discontinuous buffer ion fronts move through a gel; in the case of discontinuous denaturing *polyacrylamide gel electrophoresis (SDS-PAGE),* resistance increases as the run progresses. For discontinuous SDS-PAGE, running at constant current leads to increasing heat generation and may require active heat removal. Whenever overheating is a potential problem, a method of heat removal should be supplied (a circulating thermostated bath or cold tap water). Conventionally, protein gels are run at constant current. Most protein isoelectric focusing experiments use constant power because the resistance of the gel becomes very high as the separation nears completion[112].

1.4.2. First-dimension isoelectric focusing (IEF)

Isoelectric Focusing is an electrophoretic method that separates proteins according to their isoelectric points (*pI*). Proteins are amphoteric molecules; they carry either positive, negative, or zero net charge, depending on the pH of their surroundings. The net charge of a protein is the sum of all the negative and positive charges of its amino acid side chains and amino- and carboxyl-termini. The isoelectric point is the *pH* at which the protein has an overall net charge of zero. Proteins are positively charged at *pH* values below their *pI* and negatively charged at *pH* values above their *pI*.

The presence of a *pH* gradient is critical to the IEF technique. In a pH gradient and under the influence of an electric field, a protein will move to the position in the gradient where its net charge is zero. A protein with a net positive charge will migrate toward the cathode, becoming progressively less positively charged as it moves through the *pH* gradient until it reaches its *pI.* A protein with a net negative charge will migrate toward the anode, becoming less negatively charged until it also reaches zero net charge. If a protein should diffuse away from its *pI*, it immediately gains charge and migrates back. This is the *focusing* effect of IEF, which concentrates proteins at their *pI*s and allows proteins to be separated on the basis of very small charge differences. Because the degree of resolution is determined by *pH* gradient slope and electric field strength, IEF is performed at high voltages (typically in excess of 1 000 V) and when proteins have reached their final positions in the *pH* gradient there is very little ionic movement in the system, resulting in a very low final current (typically in the µA range) [112].

IEF performed under denaturing conditions gives the highest resolution and the sharpest results. Complete denaturation, disaggregation, unfolding and solubilization is achieved with a mixture of urea, one or more detergents, and reductant (*i.e.*), ensuring that each protein is present in only one conformation with no aggregation, therefore minimizing intermolecular interactions. Composition of sample solution and other reagents employed for the first dimension, IEF can be found in the experimental part of this work.

As mentioned above, in the original method for the first dimension a continuous *pH* gradient was achieved applying carrier-ampholytes in cylindrical polyacrylamide gels cast in glass rods or tubes[113]. When a voltage is applied across a carrier ampholyte mixture (small, soluble, amphoteric molecules with a high buffering capacity near their pI), the carrier ampholytes with the highest pI (and the most positive charge) move toward the anode; those with the lowest pI (and the most negative charge) move toward the cathode. The other carrier ampholytes align themselves between the extremes according to their *pI*s, and buffer their environment to the corresponding *pH*s. The result is a continuous *pH* gradient. As a result of limitations and problems associated with carrier ampholyte *pH* gradients, immobilized pH gradients (*IPG*) were developed[114]. An immobilized *pH* gradient is created by covalently incorporating a gradient of acidic and basic buffering groups (immobilines) into a polyacrylamide gel at the time it is cast. Immobiline buffers are a set of well-

characterized molecules, each with a single acidic or basic buffering group linked to an acrylamide monomer.

Immobilized *pH* gradients are formed using two solutions, one containing a relatively acidic mixture of acrylamido buffers and the other containing a relatively basic buffer mixture. The concentrations of the various buffers in the two solutions define the range and shape of the *pH* gradient produced. Both solutions contain acrylamide monomers and catalysts. During polymerization, the acrylamide portion of the buffers copolymerizes with the acrylamide and bisacrylamide monomers to form a polyacrylamide gel (Polyacrylamide T = 4%, C = 3%).

For reproducible performance and simplified handling different companies produce IPG gels in form of dry strips, precast onto plastic backing, supplied with protective cover foil[120, 121]. Sigma-Aldrich Co. and GE Healthcare produce trademarks *ProteoGel*^{TM} *IPG Strips* and *Immobiline*^{TM} *DryStrips,* respectively.

IEF is performed with the Immobiline DryStrip gels using a flatbed electrophoresis unit because this setting allows efficient cooling by using the aluminum oxide ceramic strip holder and allows meeting safety standards required to operate at high voltages, as well.

The advantages of Immobiline dry strip gels are higher reproducibility of the first dimension separation (no cathodic drifting), easier handling, useful *pH* range on any single immobiline dry strip gel, higher protein loading capacity and in precast gels the need to handle toxic acrylamid monomers is eliminated.

Immobiline^{TM} *DryStrips* are available in different formats of their *pH* ranges and lengths. Shorter strips, *i.e.* up to 13 cm are commended for fast screening of the most abundant proteins, provided that, the sample load is limited. On the other hand, maximal resolution and loading capacity can be achieved with longer strips *i.e.* 18 cm and 24 cm length, but require longer times in both the first- and the second-dimension separations.

Immobiline dry strip gels allow effective IEF over a wide *pH* range, from very acidic proteins at *pH* 3 to extremely basic proteins at *pH* 11. These varied pH intervals allow fine-tuning of each separation strategy to increase first dimension loading and resolve a greater number of spots from crowded areas. Both aspects will improve later protein identification and characterization. In order to achieve maximal resolution, linear (*L*) and nonlinear (*NL*) *pH* ranges are employed.

In this study, broad range pH 3–11 *NL* 18 cm strips were used to overview total protein distribution, of recombinant monoclonal antibody therapeutics, trastuzumab and rituximab and fusion protein abatacept. For more details, however, recombinant monoclonal antibodies were studied with pH 6–9 *L* strips and abatacept with 3–6 and 4–7 *L* strips, both 18 cm length.

For the first dimension, immobiline dry strip gels are rehydrated in a solution containing the necessary components including solubilizators, detergents, reductants IPG buffers and the sample proteins. IPG Buffers are ampholyte-containing buffer concentrates used to produce more uniform conductivity along dry strip gels during IEF and to eliminate potential high background staining. IEF is performed at high voltage (Rehydration solution and experimental conditions are described in detail in Experimental section). After IEF, Immobiline DryStrip gels were stored at -60 °C.

1.4.3. Second dimension: Sodium dodecyl-sulfate polyacrylamid gel electrophoresis (SDS-PAGE)

SDS-PAGE is an electrophoretic method for separating polypeptides according to their molecular weights (Mr). Denaturing polyacrylamide gel electrophoresis using sodium dodecyle sulfate (SDS-PAGE) is the most common mode of electrophoresis used in the pharmaceutical quality assessment of protein products. Typically, SDS-PAGE is carried out under conditions that ensure dissociation of the proteins into their individual peptide subunits and that minimize aggregation. The strongly anionic detergent SDS is used to dissociate the proteins before they are loaded on the gel and the intrinsic electrical charge of the sample proteins due to its presence is not a factor in the separation. SDS is an anionic detergent and in water solutions forms globular micelles composed of 70–80 molecules with the dodecyl hydrocarbon moiety in the core surrounded by a hydrophilic shell, formed by the hydrophilic and amphiphilic stretches of the polypeptide chain, and by the sulphate head groups of the detergent[122]. The denatured polypeptides bind to SDS (in a ratio of approximately 1.4 g SDS/g protein), become negatively charged and exhibit a consistent charge-to-mass ratio regardless of protein type. Because the amount of SDS bound is almost always proportional to the molecular mass of the polypeptide and is independent of its sequence, SDS-polypeptide complexes migrate through polyacrylamide gels with mobilities dependent on the size of the polypeptide. The electrophoretic mobilities of

the resultant SDS-polypeptide complexes all assume the same functional relationship to their molecular masses. Migration of SDS complexes is toward the anode in a predictable manner, with low-molecular-mass complexes migrating faster than larger ones. The molecular mass of a protein can therefore be estimated from its relative mobility in calibrated SDS-PAGE. Modifications of the polypeptide backbone, such as *N*-or *O*-linked glycosylation, however, have a significant impact on the apparent molecular mass of a protein since SDS does not bind to a carbohydrate moiety in a manner similar to a polypeptide. Thus, a consistent charge-to-mass ratio is not maintained. The apparent molecular mass of proteins having undergone post-translational modifications is not a true reflection of the mass of the polypeptide chain[119].

In 2-DE setting, second dimension (SDS-PAGE) is performed under reducing conditions. Complete denaturation and dissociation of proteins by treatment with dithiothreitol (DTT) results in the disruption of protein three-dimensional structure by reducing disulfide bonds, unfolding and subsequent complexation with SDS. In these conditions the determination of molecular mass is more straightforward.

The most popular electrophoretic method involves the discontinuous buffer system gel electrophoresis, established by Laemmli in 1970[123]. This system consists of two contiguous, but distinct gels: a resolving or separating (lower) gel and stacking (upper) gel. The two gels are cast with different porosities, *pH* and ionic strengths. The resolving gel is buffered with Tris by adjusting it to pH 8.8 with HCl. The stacking gel is also buffered with Tris but adjusted to *pH* 6.8 with HCl. In addition different mobile ions are used in the gel and electrode buffers. The buffer discontinuity acts to concentrate large volume samples in the stacking gel, resulting in improved resolution. When power is applied, a voltage drop develops across the sample solution which drives proteins into the stacking gel. Glycinate ions from the electrode buffer (glycine *pI* 5.97), follow the proteins into the stacking gel. A moving boundary region is formed with the highly mobile chloride ions in the front and the relatively slow glycinate ions in the rear. A localized high voltage gradient forms between the leading (chloride) and trailing (glycinate) ion fronts, causing the SDS-protein complexes to form into a thin zone (stack) and migrate between chloride and glycinate phases. Within broad limits, all SDS proteins condense into a very narrow region and enter the resolving gel as a well-defined, thin zone of high protein density. At the interface of stacking and resolving gel, the proteins experience a sharp

increase in retardation due to the restrictive pore size of the resolving gel. Once in the resolving gel, proteins continue to be slowed by the sieving of the matrix. The glycinate ions overtake the proteins, which then move in a space of uniform pH formed by the tris(hydroxymethyl)aminomethane and glycine. Molecular sieving causes the SDS-polypeptide complexes to separate on the basis of their molecular masses[119, 124].

1.4.4. Characteristics of polyacrylamide gels

The sieving properties of polyacrylamide gels are determined by the three-dimensional network of fibers and pores which is formed as the bifunctional NN'-methylenebisacrylamide cross-links adjacent polyacrylamide chains. Polymerization is catalyzed by a free radical-generating system composed of ammonium persulfate (APS) and tetramethylethylenediamine (TEMED). Atmospheric oxygen is a free-radical scavenger that can inhibit polymerization. For consistent results the acrylamide monomer solution must be deaerated.

The effective pore size of a gel is operationally defined by its sieving properties; that is, by the resistance it imparts to the migration of macromolecules. As pore size of gel decreases the migration rate of a protein through the gel decreases. By adjusting the pore size of a gel, through manipulating the acrylamide concentration, the resolution of the method can be optimized for a given protein sample. Thus, a given gel is characterized by its respective composition in acrylamide and bisacrylamide.

The size of the pores in a polyacrylamide gel is determined by two parameters: total solids content *(%T*) and the ratio of cross-linker to acrylamide monomer *(%C*) (Equations 3 and 4).

$$\%T = \frac{g(acrylamide + bisacrylamide)}{Volume\,(ml)} x100 \qquad \textit{(Eq.3)}$$

$$\%C = \frac{g(bisacrylamide)}{g(acrylamide + bisacrylamide)} x100 \qquad \textit{(Eq.4)}$$

The %T is the ratio of the sum of the weights of the acrylamide monomer and the cross-linker in the solution, expressed as % w/v. For example, a 20%T gel would contain 20% w/v of acrylamide plus bisacrylamide. As the %T increases, the pore size decreases. The %T ranges from 5-30 %.

The second way to adjust pore size is to vary the amount of cross-linker. The %C is the weight/weight percentage of total cross-linker weight in the sum of monomer and cross-linker weights. Thus, a 20%T, 5%C gel would have 20% w/v of acrylamide plus bisacrylamide, and the bisacrylamide would account for 5% of the total solids weight. The %C ranges from 2.5-5%.[125]

1.4.5. Detection of proteins in 2-DE gels

Protein detection techniques applied to gel electrophoresis must meet the basic requirements such are high sensitivity, wide linear dynamic range, reproducibility and low toxicity. In addition, visualization methods should be fully capable of interfacing with modern proteomic analysis tools. Since two-dimensional (2D) gel electrophoresis is increasingly being used for the separation and isolation of proteins destined for characterization by mass spectrometry, it is now expected that protein visualization methods be validated with respect to their compatibility with this technology. For the determination of total protein in 2-DE gels, general methods such as conventional colloidal Coomassie blue and silver staining are employed. Specific detection methods suitable for revealing protein post-translational modifications have been devised and are available. In addition, difference gel electrophoresis (DIGE), multiplexed proteomics (MP) and isotope-coded affinity tagging (ICAT) as principal approaches to differential display proteomics, have been developed[126].

1.4.6 General protein detection methods

1.4.6.1. Silver staining techniques

Silver staining techniques are a sensitive, non-radioactive methods based upon saturating gels with silver ions, washing the less tightly bound metal ions out of the gel matrix and reducing the protein-bound silver ions to form metallic silver. Silver ions bind to the amino acid side chains, primarily to the sulfhydril and carboxyl groups of proteins. The protein bands are visualized as spots where the reduction occurs and, as a result, the image of protein distribution within the gel is based on the difference in oxidation-reduction potential between the gel's area occupied by proteins and the free adjacent sites[127].

Silver staining methods permit detection of as little as single nanogram of protein, but the linear dynamic range of the stain is restricted to a 10-fold range. Silver staining is a complex, multi-step process that must be stopped at some arbitrary time point in order to avoid over development. Consequently gel-to-gel reproducibility is problematic and variations of 20 % in spot intensity have been reported[128].

Though the best silver stain methods use aldehyde based fixatives prior to silver impregnation, this prevents subsequent protein analysis by Edman sequencing or mass spectrometry. The utilization of glutaraldehyde for example, causes the cross-linking of two lysine residues within protein chain thus, strongly affecting two most crucial steps for the MS analysis: hampering the trypsin digestion and highly reduces the protein extraction from the gel[129]. By omitting the aldehydes in the fixatives, the method becomes compatible with mass spectrometry analysis, although at the expense of sensitivity and uniformity of background staining[130].

In addition destaining procedures aiming sensitivity enhancement for subsequent mass spectrometric identification of gel separated, silver stained proteins, have been esblished[131].

1.4.6.2. Organic dye-based methods. Coomassie staining

Although 50-fold less sensitive than silver staining, Coomassie staining is a relatively simple method and more quantitative than silver staining. The advantage of Coomassie blue dyes (R250 or G250 type) is their low cost, ease of use and compatibility with downstream characterisation methods; therefore, almost any protein that can be visualized using Coomassie will yield interpretable mass spectrometric data. Traditional Coomassie R250 or G250 dyes are used in regressive staining approach where gels are saturated with dye that has been dissolved in an aqueous solution containing methanol and acetic acid, followed by destaining in a similar solution devoid of dye. Since the proteins have a higher affinity for the dye molecules than the gel matrix a point is reached where the background staining is minimal but protein bands are well labeled.

Colloidal G250 stains (progressive staining approach) have the benefit of very low background staining and the need for little or no destaining. The limits of detection for conventional Coomassie Blue and colloidal Coomassie Blue stains are 8–10 and 30–100 ng, respectively. Both dyes provide a linear response with protein amount over a

10–30-fold range of concentration. Thus, the principal limitations associated with Coomassie Blue-based staining methods are the poor detection sensitivity and small linear dynamic range obtained with the dyes[126].

1.4.6.3. Radioactive labeling methods

Radiolabeling is commonly accomplished by *in vivo* incorporating ^{3}H, ^{14}C, ^{35}S, ^{32}P, ^{33}P, or ^{125}I into proteins. After electrophoresis signal detection may be accomplished either by autoradiography (γ-emitting isotopes) or by fluorography (β-emitting isotopes). Though sensitive detection is readily achieved (down to 200 fg of protein), radiolabeling is both hazardous and expensive[120, 126].

1.4.6.4. Reverse stain methods

A number of reverse staining methods for visualizing proteins in SDS–PAGE have been described, including methods that employ potassium chloride, copper chloride, zinc chloride, cobalt acetate nickel chloride and zinc chloride–imidazole[126].
Zinc chloride–imidazole is the most sensitive reverse stain method to date. Negative Zinc-Imidazole staining has a detection limit of approximately 15 ng protein/spot and is compatible with mass spectrometry, but is a poor quantitation technique[120, 132].

1.4.6.5. Fluorescence-based staining methods

Fluorescence-based staining methods provide significant advantages over Coomassie blue or silver staining. Fluorescent detection offers increased sensitivity, simple, robust staining protocols, and quantitative reproducibility over a broad dynamic range.
Different dyes have been for this purpose, including Nile red dye (detection sensitivity 20-100 ng), SYPRO Red, SYPRO Orange and SYPRO Tangerine dyes (detection sensitivity 4-8 ng). However the most suitable method for the modern proteomic applications employs SYPRO Ruby dye, which is a proprietary ruthenium-, based metal chelate stain. The linear dynamic range of the dye extends over three orders of magnitude thus surpassing both Coomassie and silver staining in performance[133].

1.4.7. Immobilized pH gradient/MALDI-TOF MS and surface-enhanced laser desorption-ionization MS (SELDI-MS)

In order to overcome fundamental limitations of the 2-DE method for detecting specific classes of proteins, including those of low abundance, poor solubility, very small or large size and extreme p*I* replacing of one or both gel electrophoresis dimensions in proteome projects with alternative separation methods was reported[134]. In 1999 group of scientists replaced the SDS-PAGE dimension of 2DE by scanning IEF gels directly with a MALDI–TOF mass spectrometer, thus generating a 'virtual 2D gel' image in which the protein mass is measured by mass spectrometry. Analytical data may be presented as a computer-generated image of that is similar to a classical 2D gel in appearance[135].

Surface-enhanced laser desorption-ionization MS (SELDI-MS) involves retaining proteins based on their physico-chemical characteristics on a solid phase chromatographic surface (ProteinChip Array) and direct detection of the retained proteins by time-of-flight mass spectrometry (TOF-MS).

SELDI technology has been applied in recent years to investigate a variety of biological phenomena, due to the increasing need for high-throughput technology that allows the detection, purification, and identification of proteins at high speed and with high sensitivity. The application of this approach for biomarker analysis has been reported[136].

1.4.8. Specific detection of protein posttranslational modifications

The most common posttranslational modifications include phosphorilation, glycosylation, lipidation, and proteolytic modifications. These chemical modifications of proteins are crucial to modulating their function.

Glycoproteins can be detected by autoradiography after incorporation of ^{3}H or ^{14}C sugars into cultured cells or tissues. However, nonradioactive methods using a periodic acid Shiff base chemistry are more preferred. These methods include colorimetric procedure with acid fuchsin and a fluorescent alternative of acid fuchsin dye, dansyl hydrazine that can be used for the detection of glycoproteins in polyacrylamide gels.

Other fluorescence-based method for detection of glycoproteins is sensitive green-fluorescent glycoprotein specific stain Pro-Q Emerald 300 dye. Gels labelled with this dye may be post-stained with SYPRO Ruby dye, allowing sequential two-color detection of glycosylated and nonglycosylated proteins[120.]

1.4.9 Difference gel electrophoresis (DIGE)

Although 2-DE is well-established technique for protein analysis, it is time consuming and labor-intensive. Additionally, the system variability arise due to the lack of reproducibility between gels. In order to overcome these limitations, 2D difference gel electrophoresis (DIGE) that enabled more than one sample to be separated in a single 2D polyacrylamide gel was devised. This technique involves fluorescent labeling of as many as three different complex protein samples with succinimidyl esters of the cyanine dyes, Cy2, Cy3 and Cy5, prior to mixing them together and running them simultaneously on the same 2D gel[120,137,138]. The different protein extracts labeled with different dyes can then be visualized separately by exciting the different dyes at their specific excitation wavelengths.
This technique is more sensitive than silver staining. Sensitivities are 0.075 ng, 0.025 ng, and 0.025 ng for Cy2, Cy3 and Cy5 dye, respectively. The dynamic range is above 3.6 orders of magnitude and most critically, effects of gel to gel variation on the quantitation of a protein spot on a gel is substantially reduced.

1.4.10. Isotope-coded affinity tagging (ICAT)

Isotope-coded affinity tag (ICAT) peptide labeling is predicated upon distinguishing between two populations of proteins using isotope ratios. Isotope-coded affinity tags are reagents consisting a thiolate-reactive group to enable selective labelling of cysteinyl residues, an isotopic ethylene glycol linker containing either eight hydrogen atoms (d_0, light reagent) or deuterium atoms (d_8, heavy reagent), and an a biotin affinity tag. A reduced protein mixture from one protein specimen is derivatized with the isotopically light version of the ICAT reagent, while the other reduced protein specimen is derivatized with the isotopically heavy version of the ICAT reagent. The labelled peptides are typically detected and quantified using electrospray ionization microcapillary μRP-HPLC-MS/MS. The ratio of the isotopic molecular mass that

differs by 8 Da provides a measure of the relative amounts of each protein from the original samples[139].

1.5. Matrix-assisted laser desorption ionization mass spectrometry (MALDI-TOF MS)

The incorporation of new technologies has resulted in fundamental change in the drug development paradigm. Mass spectrometry (MS) is the bioanalytical technique which provides key attributes relevant to modern pharmaceutical analysis: sensitivity, selectivity, speed, and high throughput and it is an essential component of the modern pharmaceutical laboratory as well as an important complement to traditional methods of analysis[140].

Matrix-assisted laser desorption ionization mass spectrometry (MALDI-TOF MS) was introduced in 1987-1988 by Tanaka et al[141] and Karas et al[142], reporting the UV-laser desorption of large biomolecules for the first time. This is a rapid and sensitive technique for the characterization of peptides and proteins. Used in a variety of modes, MALDI-MS provides information such as the molecular weight of an intact protein, peptide mass mapping from a tryptic digest, and peptide sequencing.

The schematic set-up of MALDI-TOF instrument is shown in Figure 1.5.

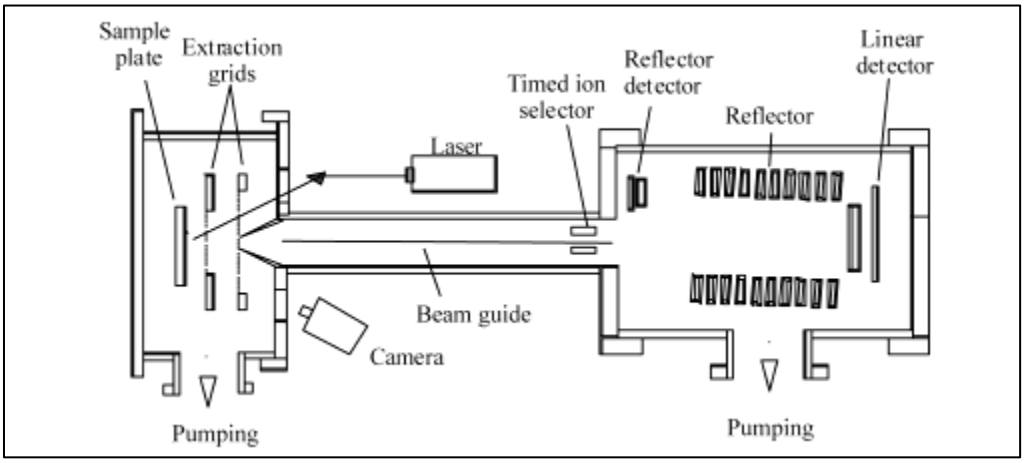

Fig. 1.5. Schematic set-up of a MALDI-TOF MS instrument. According reference [140]

MALDI-TOF MS as a “soft” ionization technique is suitable for thermolabile, non-volatile compounds, especially those of high molecular mass and is used successfully in biochemical and biotechnological areas for the analysis of therapeutic proteins, peptides, glycoproteins, complex carbohydrates and oligonucleotides. It is

relatively straightforward to use and reasonably tolerant to buffers or other additives. The lower mass limit of MALDI TOF MS is around 500 Da due to signals arising from molecular, fragment and adduct ions of the matrix. Ions generated by MALDI can be routinely mass analysed in a TOF instrument in picomole (pmol = 10^{-12} mol) down to low femtomole (fmol = 10^{-15} mol) amount with mass resolution of over 20000 (FWHM). However, attomole (amol = 10^{-18} mol) sensitivity has also been demonstrated using a MALDI TOF MS[143]. The mass accuracy depends on the type and the performance of the analyser of the mass spectrometer, but most modern instruments are capable of measuring masses with an accuracy of ± 0.01-0.05% up to 25 kDa, and ±0.05-0.3% up to 300 kDa[125].

MALDI-TOF samples are prepared with a matrix that contains a small organic molecule capable of absorbing ultraviolet light. Most commercially available MALDI mass spectrometers now have a pulsed nitrogen laser of wavelength 337 nm. A laser is used to desorb ions from the sample plate, ionized matrix molecules transfer a proton to the sample molecules in the gaseous phase, and the resulting ions are forced into the flight tube (typically 1-4 m long, maintained at a high vacuum) by application of the acceleration voltage from extraction grids.

Separation is based on mass with lighter ions traveling faster than heavier ions.

In the source of a *linear* TOF analyzer, a packet of ions is formed by a very fast (ns) ionization pulse. These ions are accelerated into the flight tube by an electric field (typically 2-25 kV) applied between the backing plate and the acceleration grid. Since all the ions are accelerated across the same distance by the same force, they have the same kinetic energy. Because velocity (*v*) is dependent upon the kinetic energy (E_{kin}) and mass (*m*) lighter ions will travel faster. E_{kin} is determined by the acceleration voltage of the instrument (*U*) and the charge of the ion (*e x z*), (*eqs 5* and *6*).

$$E_{kin} = \frac{mv^2}{2} \qquad \textit{(Eq.5)} \qquad\qquad \frac{mv^2}{2} = z \times e \times U \qquad \textit{(Eq.6)}$$

After the ions accelerate, they enter flight tube. The ions drift through this field free region at the velocity reached during acceleration. At the end of the flight tube they strike a detector, such as microchannel plate (MCP). The time delay (*t*) from the formation of the ions to the time they reach the detector dependents upon the length

of the drift region (*L*), the mass to charge ratio of the ion, and the acceleration voltage in the source (*eq. 8)*.

$$v = \frac{L}{t} \qquad \textit{(Eq.7)} \qquad \frac{1}{2} m \left(\frac{L}{t} \right)^2 = z \times e \times U \qquad \textit{(Eq.8)}$$

Eq. 8 can be inverted to *eq. 9,* which shows that that low *m/z* ions will reach the detector first.

$$t = \sqrt{\frac{m}{z}} \times \frac{L}{\sqrt{2eU}} \qquad \textit{(Eq.9)}$$

The mass spectrum is obtained by measuring the detector signal as a function of time for each pulse of ions produced in the source region. Because all the ions are detected, TOF instruments have very high transmission efficiency which increases the S/N level[144, 145].

In linear TOF mass spectrometers MALDI ions of slightly different kinetic energy are extracted from their desorption plume with an initial velocity distribution which causes ions of same mass to arrive at slightly different times at the detector. This initial velocity distribution which leads to a corresponding distribution of arrival times of ions of the same mass results in the reduction of mass resolution, and the peak broadening becomes worst for the larger ions because the energy distribution is mass dependent. In linear TOF mass spectrometers the energy distribution and its influence in the mass resolution could be reduced only increasing acceleration potential but considerations of handling very high voltages in the laboratory instruments limit this approach [125,146].

Two elegant means to improve the resolution are to use an ion mirror (a *reflectron*) and/or pulsed-ion extraction, commonly called *delayed extraction (DE)* or time-lag focusing[144]. The reflectron, located at the end of the flight tube, has an applied voltage slightly higher than the accelerating voltage at the source. It acts as an energy-focusing device correcting for small kinetic energy differences between ions of the same mass resulting in improved resolution and mass accuracy.

Second way to improve mass resolution is to use the delayed extraction (DE). In this system the ions formed by MALDI are produced in a weak electrical field, and subsequently extracted by application of a high voltage pulse after a predetermined

time delay. Decrease in energy spread of the ions and consequently increase in mass resolution is achieved by the adjustment of the field magnitude and direction during and immediately following ion production, the magnitude of the extraction field, and the time delay between the laser pulse and application of the extraction field[147].

1.5.1. MALDI sample preparation and presentation

In a typical UV-MALDI sample preparation small volumes of an analyte solution (ca 10^{-6}M) and near-saturated (ca 0.1M) solution of matrix are mixed; the solvent is then evaporated before the sample can be introduced into the vacuum of mass spectrometer.

Table 1.5. A list of commonly used MALDI matrices. According reference [146]

Matrix	*Structure*	*Wavelength*	*Major applications*
Nicotinic acid	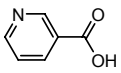	UV 266 nm	Proteins, peptides adduct formation
2.5-Dihydroxybenzoic acid (plus 10% 2-hydroxy-5-methoxybenzoic acid)	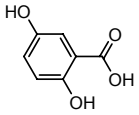	UV 337 nm 353 nm	Proteins, peptides carbohydrates synthetic polymers
Sinapinic acid	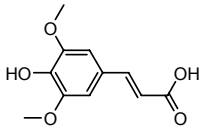	UV 337 nm 353 nm	Proteins, peptides
α-Cyano-4-hydroxycinnamic acid (CHCA)	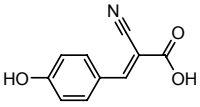	UV 337 nm 353 nm	Peprides, fragmentation
3-Hydroxy-picolinic acid	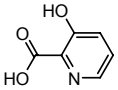	UV 337 nm 353 nm	Best for nucleic acids
6-Aza-2-thiothymine	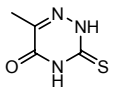	UV 337 nm 353 nm	Proteins, peptides non-covalent complexes; near-neutral pH
k,m,n-Di(tri)hydroxy-acetophenone	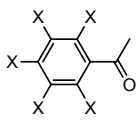	UV 337 nm 353 nm	Proteins, peptides non-covalent complexes; near-neutral pH
Succinic acid	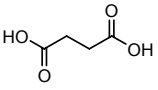	IR 2.94 μm, 2.79 μm	Proteins, peptides
Glycerol	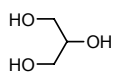	IR 2.94 μm, 2.79 μm	Proteins, peptides Liquid matrix

IR = infrared; UV = ultraviolet.

Upon solvent evaporation, the matrix co-crystallizes with analyte to form a bed of crystals of different sizes depending of on the matrix type and sample preparation details. Typical analyte: matrix molar ratio ranges from 10^{-2} to 10^{-5} depending on the analyte, matrix and solvents. There is no single MALDI matrix or sample preparation protocol which is suited to all analytes in MALDI-TOF MS. There are different matrixes of first choice for different classes of analytes. For example CHCA is used in proteomics for the peptide mass fingerprint analysis (Table 1.5).
For the determination of molecular mass of labile compounds “cold” matrices are used. They form mainly single charged ions. However, for PSD fragment ion analysis “hot” matrices, which form significant amounts of multiple charged ions, are optimal.
In this study peptides obtained from the tryptic digestion of proteins separated with 2-DE were co-crystallized with α-Cyano-4-hydroxycinnamic acid (CHCA).

1.6. Peptide-mass fingerprinting

Peptide mass fingerprinting (PMF) is the most common mass spectrometry technique used for the identification of proteins separated by two-dimensional gel electrophoresis.
After the introduction of sensitive ionization techniques, MALDI and electrospray ionization (ESI), which allowed accurate mass measurement of peptides, different groups of authors described the use of MALDI-TOF data for correlating peptide masses generated from a digestion of a protein with sequence databases. This technique allowed a rapid identification of a sample protein before committing it to protein sequence analysis[148-152]. The term “peptide mass fingerprinting” was first used in the paper of Pappin and al[148]. This technique is most simply described as a method to identify proteins already contained within a sequence database using an algorithm to match a set of peptide masses generated using specific cleavage reagents (either enzymatic or chemical) from the protein of interest, with theoretical peptide masses calculated from each sequence entry in the database if the database sequences had been cleaved with the same specificity as the reagent in the experiment[125].
There are a number of advantages of using PMF for protein identification:

- Using MALDI-TOF instruments of improved analytical performance, PMF gained speed, high specificity for protein identification and the ability to identify individual components in simple protein mixtures
- Direct correlation between the *m/z* value of the singly charged ions and mass of a peptide
- Simplicity, high mass accuracy and sensitivity, analysis of femtomolar levels of proteins
- Unlike automated Edman degradation, there is no requirement for a free amino terminus of protein
- Mass differences between the measured and predicted peptides may provide evidence for the identity of peptide modifications
- Possibility to increase the confidence of peptide mass searching through the incorporation of orthogonal approaches
- Tolerance toward contaminants
- Method is easily automated and there are available robotic workstations for high throughput operation

There are limitations to protein identification by peptide mass mapping:

- The protein sequence must be present in a database,
- Proteins that have extensive post-translational modifications may fail to yield good matches
- The individual components from mixtures of more than three or four proteins are difficult to identify
- It is not a method for protein characterization, only for identification[125, 146, and 152].

For successful peptide mass searching the possible highest molecular mass accuracy should be employed, ideally using internally calibrated monoisotopic masses. If this option is not available, when average masses are used, high mass accuracy should be achieved with an appropriate internal calibration.

In addition to the importance of mass accuracy, the specificity of cleavage is also critical.

Trypsin is the most commonly used protease for peptide mass searching. This serine protease has high cleavage specificity, efficiency and is stable under a wide

variety of conditions. Trypsin specifically cleaves at sites C-terminal to basic amino acid residues Lys or Arg (if not followed by a Pro). The distribution of Lys and Arg residues in proteins is such that trypsin digestion yields peptides of molecular weights typically within the range of 500 to 2500 Da that can be analyzed by mass spectrometry. Furthermore, basic Arg or Lys residues located at the C-terminus help to localize the positive charge of resulting ions[153]. For MS analysis trypsin of high specificity is required, because the native trypsin is subject to autolysis, it generates pseudotrypsin, which exhibits a broadened specificity. Consequently, nonspecific and/or incomplete cleavages may result. While so called missed cleavages are included as a parameter for PMF analysis in search programs, nonspecific cleavages is difficult to accommodate in search algorithms. On the other hand trypsin autolysis derived peptides can be used for the internal calibration.

In order to increase sequence coverage of studied proteins often additional enzymes are used in PMF analysis *i.e.* endoproteases AspN and LysC (cleave N-terminus of Asn and C-terminus of Lys, respectively), chymotrypsin (cleaves C-terminus of Phe, Tyr, Trp, Leu and Met), pepsin (cleaves C-terminus of Phe, Trp, Leu and Met) and *S.auresus* V8 DE and V8E (cleave C-terminus of Glu and C-terminus of Glu and Asp, respectively) [154].

Several computer programs and algorithms have been described in literature for protein identification by searching sequence databases using mass spectrometry data. A number of such programs can be found on World Wide Web and most include examples to guide their users. For PMF analysis the following programs are most commonly used.

- MS-fit (ProteinProspector, University of California, San Francisco, USA; *http://prospector.ucsf.edu/mshome.htm*)
- Aldente (ExPASy Molecular Biology server, Suiss Institute of Bioinformatics, Switzerland; *http://www.expasy.ch/tools/aldente/*)
- Profound [(Prowl), The Rockefeller University, USA; *http://prowl.rockefeller.edu/prowl-cgi/profound.exe*)]
- Mascot (Matrix Science Ltd. UK; *http://www.matrixscience.com/search_form_select.html*)

Mascot is a powerful search engine that that it integrates all of the proven methods of searching: *peptide mass fingerprint* (experimental data are peptide mass values),

Sequence query (combination of peptide mass data with amino acid sequence) and *MS/MS Ion Search* (uses MS/MS data from one or more peptides).
The sequence databases that can be searched on Mascot server are:

1. MSDB (a comprehensive, non-identical protein sequence database designed specifically for mass spectrometry applications)
2. NCBInr (a comprehensive, non-identical protein database. The entries compiled from GenBank CDS translations, PIR, SWISS-PROT, PRF, and PDB.
3. SwissProt (a high quality, protein database, uses non-redundant sequences, recommended for peptide mass fingerprint searches)
4. dbEST [contains "single-pass" cDNA sequences, or Expressed Sequence Tags (EST), from a number of organisms].

In this study peptide masses obtained by MALDI-TOF-MS after *in gel* tryptic digestion of therapeutic proteins trastuzumab, rituximab and abatacept were searched in search engines Profound (Prowl) and Mascot using open access databases MSDB, NCBInr and Swiss Prot.

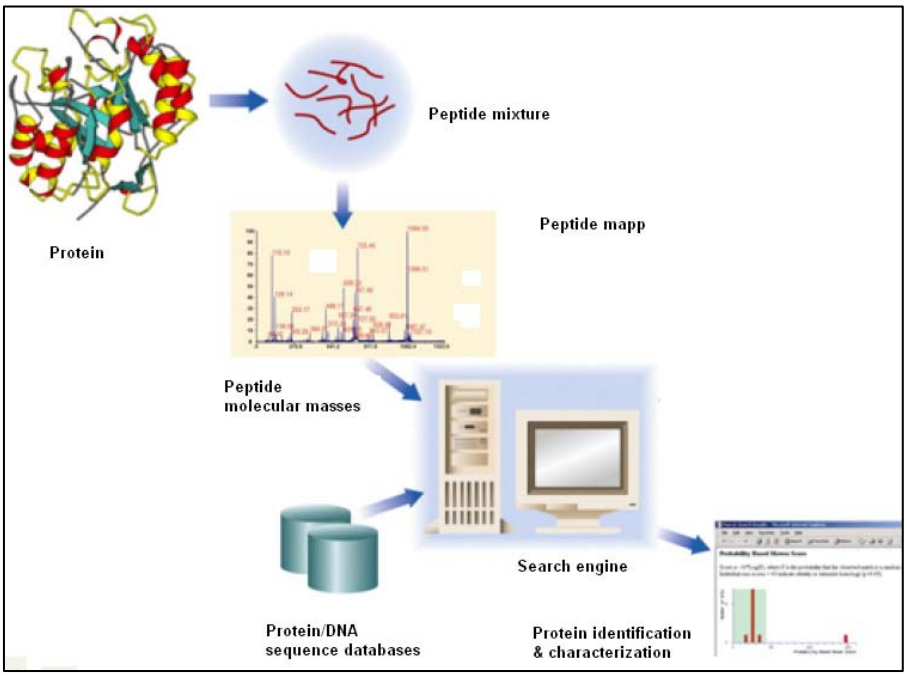

Fig. 1.6. Sheme of protein identification and characterisation using database searching. According reference [156]

Mascot incorporates a probability-based scoring with implementation of the Mowse algorithm. The fundamental approach is to calculate the probability that the observed match between the experimental data set and each sequence database entry is a chance event. The match with the lowest probability is reported as the best match and the total score is the absolute probability that the observed match is random event. However, reporting probabilities directly can be confusing because they encompass a wide range of magnitudes, and because a "high" score is a "low" probability, which can be ambiguous. Therefore, scores are reported as $-10\log_{10}(P)$, where P is the absolute probability[155]. In Fig. 1.6 a scheme of protein identification using sequence databases is presented.

1.7. Search for the new quality parameters of recombinant monoclonal antibodies and their related substances

As indicated, *rmAbs* are highly complex molecules with primary and higher order structure amenable to post-translational and chemical modifications; hence these substances and their final pharmaceutical formulations are highly heterogeneous. *rmAbs* often include subtle variations (microheterogeneity), including post-translational (different glycosilation pattern) and chemical variations (*i.e.* disulfide shuffling, deamidation, Met-oxydation, N-terminal Glu cyclization and Lys truncation). These variations can affect antibody product quality and thus its clinical efficacy and safety. Therefore, development of appropriate analytical methodologies to study the quality of these complex medicinal products remains a challenging task.

Regulatory agencies already have published guidelines concerning the production and quality control of *rmAbs*[157, 158]. In the European Pharmacopoeia two monographs related to the *production* and quality testing of *rmAbs* are available: *Monoclonal antibodies for human use* and *Products of recombinant DNA technology*[159, 160].

Principles concerning characterization of biotechnological products, discussed in Chapter 1.3 apply to *rmAbs* as well, although for this product class there are some specific requirements. For the *biochemical/physico-chemical* and *biological/immunological* characterization of *rmAbs* at least the following parameters should be determined:

- Class, subclass and light-chain composition, glycosylation pattern (G0,G1, G2 glycan structures and degree of sialilation), integrity of the molecule by analysis of the ratio heavy/light chain, microheterogeneity, molecular weight, N- and C terminal amino acid sequence, and secondary and tertiary structure of the antibody,
- The total protein content, the degree of aggregation and molecular fragmentation of the immunoglobulin,
- Especially for engineered and humanised antibodies sufficient sequence information to characterize the gene product adequately should be obtained by peptide mapping or amino acid sequencing.

A wide range of analytical techniques exploiting different physico-chemical properties of the molecule should be used *i.e.* SDS-PAGE (under reducing and non reducing conditions), IEF, IEC, CE, HPLC, peptide mapping, amino acid analysis, circular dichroism (CD) and carbohydrate mapping[94,161]. European Pharmacopoeia requires different tests, including peptide mapping, IEF, IEC, HIC, oligosaccharide mapping, monosaccharide content and mass spectrometry, to be used for the demonstration *molecular identity and structural identity* of *rmAbs*. For the *purity testing*, suitable validated methods such are SDS-PAGE or CE can be used [159].

Today very sensitive analytical methods are employed for the physico-chemical characterization of *rmAbs*, including CE-LID, MALDI-TOF MS, ESI-MS) or NMR. For the characterization of antigen-antibody interaction surface plasmon resonance has been used, whereas Circular Dichroism in near and far UV spectra makes possible the determination of antibody secondary structure[110].

On the other hand, two-dimensional gel electrophoresis (2-DE) has been widely accepted technique for the quality evaluation of *rDNA* derived medicinal products[160,162], suited for in-process, bulk and/or final product testing, *i.e. identity, purity* (testing for product related and foreign protein impurities) and *stability testing*.

Concerning planar electrophoresis methods, European Pharmacopoeia monograph *(Monoclonal antibodies for human use)*, for the demonstration of product molecular identity and structural integrity suggests isoelectric focusing whereas for purity testing one dimensional SDS-PAGE. Since 2-DE is able to efficiently separate protein mixtures in two dimensions: according protein *pI* (1st dimension, IEF) and according their molecular masses (2nd dimension, SDS-PAGE), after sensitive staining

procedure, the map of all proteins present in a sample can be detected. Thus this method which allows estimation of both *pI* and *molecular mass* of sample components provides an essential advantage versus IEF and/or SDS-PAGE performed separately. In addition, comparison of 2-DE protein spot patterns of 2-DE separated proteins with reference protein product allows the determination of product heterogeneity and isomorf pattern. Moreover, on the basis of *pI* and *molecular mass* difference of 2-DE protein spots obtained after the treatment of glycoprotein products such are monoclonal antibodies and fusion proteins, with specific glycosiades, the important information on the glycan pattern can be obtained, as well. On the other hand, 2-DE separated proteins can be downstream analyzed with complementary MS methods, especially with relatively fast, cheap and simple technique of MALDI-TOF MS analysis: whether for more detailed study of glycosylation (glycan profiling, glycosylation site) and for chemical modification (deamidation, isomerisation etc) or for the identification of resulting peptides after *in gel tryptic digestion*. Summing up, possibility for efficient separations of proteins in two dimensions, high detection sensitivity, and possibility to complement with MALDI-TOF MS analysis make 2-DE method suitable technique for the study of the quality of recombinant monoclonal antibodies not only for the in-process control, but this technique might be suitable for the testing of identity and purity of these products in Pharmacopoeia environment as well.

1.8. Basic information about the chemistry, manufacturing and mechanism of action of recombinant biological products studied in this work

1.8.1. Trastuzumab

1.8.1.1. Nomenclature

Trastuzumab [FDA, USAN INN], Herceptin [Trade name], Synonyms: huMAb 4D5-8; HER2 receptor monoclonal antibody, recombinant [BIO]; anti-p185, rhuMab HER2; c-erbB2 monoclonal antibody. Drug Bank ID: DB00072; CAS-180288-69-1

Trastuzumab is a recombinant DNA-derived humanised monoclonal antibody glycoprotein that selectively targets the extracellular domain of the human epidermal growth factor receptor 2 protein (HER2). The antibody is an IgG1 kappa that contains

human framework regions with the complementarity-determining regions (CDR) of a murine anti-p185^{HER2} antibody that binds to HER2[163, 164].

Heavy chain

```
        10         20         30         40         50         60
EVQLVESGGG LVQPGGSLRL SCAASGFNIK DTYIHWVRQA PGKGLEWVAR IYPTNGYTRY
        70         80         90        100        110        120
ADSVKGRFTI SADTSKNTAY LQMNSLRAED TAVYYCSRWG GDGFYAMDYW GQGTLVTVSS
       130        140        150        160        170        180
ASTKGPSVFP LAPSSKSTSG GTAALGCLVK DYFPEPVTVS WNSGALTSGV HTFPAVLQSS
       190        200        210        220        230        240
GLYSLSSVVT VPSSSLGTQT YICNVNHKPS NTKVDKKVEP KSCDKTHTCP PCPAPELLGG
       250        260        270        280        290        300
PSVFLFPPKP KDTLMISRTP EVTCVVVDVS HEDPEVKFNW YVDGVEVHNA KTKPREEQYN
       310        320        330        340        350        360
STYRVVSVLT VLHQDWLNGK EYKCKVSNKA LPAPIEKTIS KAKGQPREPQ VYTLPPSREE
       370        380        390        400        410        420
MTKNQVSLTC LVKGFYPSDI AVEWESNGQP ENNYKTTPPV LDSDGSFFLY SKLTVDKSRW
       430        440        450
QQGNVFSCSV MHEALHNHYT QKSLSLSPGK
```

Light chain

```
        10         20         30         40         50         60
DIQMTQSPSS LSASVGDRVT ITCRASQDVN TAVAWYQQKP GKAPKLLIYS ASFLYSGVPS
        70         80         90        100        110        120
RFSGSRSGTD FTLTISSLQP EDFATYYCQQ HYTTPPTFGQ GTKVEIKRTV AAPSVFIFPP
       130        140        150        160        170        180
SDEQLKSGTA SVVCLLNNFY PREAKVQWKV DNALQSGNSQ ESVTEQDSKD STYSLSSTLT
       190        200        210
LSKADYEKHK VYACEVTHQG LSSPVTKSFN RGEC
```

Fig. 1.7. Primary sequences of trastuzumab heavy and light chain. Complementarity determining regions are highlighted. The heavy chain N_{300} glycosilation site is indicated by underlined boldface. According references [165] and [166].

The active substance trastuzumab is produced in recombinant Chinese Hamster Ovary cells using a serum free medium. Primary sequences and complementarity determining regions of trastuzumab heavy and light chains are presented in Fig. 1.7[165,166].

Trastuzumab (rhumAb4D5-8) has been engineered by grafting the CDRs of the parental murine antibody mumAb4D5 into the consensus framework of a human IgG_1[167]. Parental murine mumAb4D5 directed against the ECD of human epidermal growth factor receptor (p185^{HER2}), specifically inhibited the growth of tumour cell lines overexpressing p185^{HER2}. However, antigeneicity and lack of effector functions limited its efficacy. Therefore, aiming to reduce anti globulin response and increase

the effector functions (ADCC and CMC) with retention of high affinity for antigen, humanised antibody version (humAb4D5) was constructed. In the humanised version only complementarity determining regions (antigen binding loops) have murine origin. The rest of molecule, including IgG1 constant domains and variable region framework residues, is human [167-169]. Trastuzumab was generated by the immunization of *Balb/c* mice with cells expressing HER-2 on their surface and partially purified membranes containing $p185^{HER2}$ according to standard hybridoma techniques. Hybridomas were either screened by an ELISA or a nude mice breast cancer xenograph model, resulting in muMAb 4D5.

Humanisation of muMAb 4D5 was performed using “gene conversion mutagenesis”. The mumAb4D5 $V_L$and V_H gene segments were first cloned by PCR and sequenced There were 24 simultaneous amino acid changes required to humanize mumAb4D5 V_L and 32 amino acid change mumAb4D5 V_H, respectively. In this way humAb4D5-5 was encoded. Additional humanized variants were constructed by site directed mutagenesis of humAb4D5-5[167]. In general, framework region residues were chosen from consensus human sequence and CDR residues from mumAb4D5. The most potent humanised variant designed by molecular modeling, *humAb4D5-8,* contains five FR residues from mumAb4D5 (the most murine variant).

This antibody binds $p185^{HER2}$ ECD three fold more tightly than does mumAb4D5 itself. In addition it has potency comparable to the murine antibody in blocking SK-BR-3 cell proliferation and is more efficient in supporting ADCC against SK-BR-3 cells. In contrast, humAb4D5-1 is the most humanised but least potent variant, binds $p185^{HER2}$ 80 fold less tightly and has no detectable antiproliferative activity (Table 1.6.).

Table 1.6. mAb4D5 variants designed by molecular modeling. According reference [167]. Human and murine residues are shown in one-letter and three-letter amino acid codes. Bold face: the most potent variant **humAb4D5-8** (trastuzumab)

	V_H residue					V_L residue			
mAb4D5 variant	72 (FR3)	74 (FR3)	79 (FR3)	97 (FR3)	109 (CDR3	55 (CDR2)	66 (FR3)	K_d nM	Relative cell proliferation
humAb4D5-1	R	D	L	A	V	E	G	25	102
humAb4D5-2	Ala	D	L	A	V	E	G	4.7	101
humAb4D5-3	Ala	Thr	Ala	Ser	V	E	G	4.4	66
humAb4D5-4	Ala	Thr	L	Ser	V	E	Arg	0.82	56
humAb4D5-5	Ala	Thr	Ala	Ser	V	E	Arg	1.1	48
humAb4D5-6	Ala	Thr	Ala	Ser	V	Tyr	Arg	0.22	51
humAb4D5-7	Ala	Thr	Ala	Ser	Tyr	E	Arg	0.62	53
humAb4D5-8	**Ala**	**Thr**	**Ala**	**Ser**	**Tyr**	**Tyr**	**Arg**	**0.1**	**54**
mumAb4D5	Ala	Thr	Ala	Ser	Tyr	Tyr	Arg	0.3	37

The resulting constructs were designed to express the human Fc γ1 (IgG1) isotype to maximally support CDC and ADCC[167, 171].

The human IgG1 heavy chain constant regions are identical with those reported in literature expect for mutations in C_H3 domain of heavy chain: E359D and M361L which were installed to convert the antibody from the naturally rare A allotype to the much more common non-A allotype (Fig 1.7, $^{...359}$EEM$^{361...}$ Gm(non-1) variant). In contrast, this mutation is not installed in the molecules of abatacept and rituximab therefore their sequence at corresponding amino acid positions is ...DEL.... and not ... EEM. Therefore, abatacept and rituximab heavy chains belong to IgG1 Gm variants[172, 173].

1.8.1.2. Chemical information

Trastuzumab (rhumAb4D5-8) is a recombinant monoclonal antibody of IgG class. It is composed of 1,328 amino acids and has a molecular weight of ~148 kDa[164]. Like all immunoglobulins of class IgG, it contains two identical heavy and two identical light chains linked via disulfide bonds. Each heavy chain contains 450 amino acids, with theoretical molecular mass calculated from the amino acid sequence derived from of cDNA 49284.65 Da and *pI* 8.49. Each light chain contains 214 amino acids with theoretical molecular mass of 23443.1 Da and *pI* 7.76. Therefore theoretical molecular mass of nonglycosilated trastuzumab is 145455.5 Da[173].

The apparent molecular mass of tratuzumab is higher ~148 kDa, due to the presence of N-linked oligosaccharides[174]. Based on the length of the hinge region and the number and location of interchain disulfide bonds trastuzumab belongs to immunoglobulin IgG1 subtype with γ1 heavy chain. The light chain is of κ subtype[167].

Heavy chain variable region (V_H) covers the first 120 amino acids and variable region of light chain (V_L) covers the first 107 amino acids, respectively. Variable regions V_H + V_L together with respective C_H1(^{121}A-^{218}V) and C_L (^{108}R-^{214}C) domains form the antigen-binding (Fab) regions, whereas the remaining sequences of heavy chain, C_H2 (^{231}P-^{343}K) and C_H3 (^{344}G-^{450}K) linked with hinge region (^{219}E-^{230}P) form Fc (fragment crystallizable) regions responsible for effector recognition and binding[175].

Heavy chains are linked via two interchain disulfide bonds at the flexible hinge region (C229 -229' and C232-232'). Heavy and light chains are linked with disulfide bridge involving heavy chain C223 and light chain C214.

Intrachain disulfide bonds reside in each domain of the H and L chain, stabilizing these domains[174]. In heavy chain there are four intrachain disulfide bonds: VH: ^{22}C-^{96}C; C_H1: ^{147}C-^{203}C; C_H2: ^{264}C-^{324}C; C_H3: ^{370}C-^{428}C. In light chain, however, there are only two intrachain disulfide bonds: ^{23}C-^{88}C and ^{134}C-^{194}C. In correctly folded immunoglobulin molecule all cysteine (C) residues are involved in disulfide bond formation, therefore no free sulfhydril groups should be present[176].
Like other IgG1 molecules trastuzumab has one N-linked biantennary oligosaccharide on the conserved asparagine ^{300}N, buried between the C_H2 domains (Fig 1.7).

1.8.1.3. Clinical formulation

Trastuzumab (Herceptin®, Roche) is a sterile, white to pale yellow, preservative-free lyophilized powder for intravenous (IV) infusion.
In EU is marketed as single-dose formulation, each vial contains 150 mg trastuzumab with excipients histidine hydrochloride, histidine, α,α-trehalose dihydrate and polysorbate 20. Reconstitution with 7.2 mL of *sterile water for injection (SWFI)* yields 7.4 mL of a single-dose solution containing approximately 21 mg/mL trastuzumab, at a pH of approximately 6.0. The reconstituted solution is physically and chemically stable for 48 hours at 2°C – 8°C.
On the other hand, in USA trastuzumab is approved as multi-dose formulation, each multi-use vial of Herceptin® contains 440 mg trastuzumab. Reconstitution with 20 mL of the *appropriate diluent (BWFI or SWFI)* yields a solution containing 21 mg/mL trastuzumab. Herceptin® reconstituted with *Bacteriostatic Water for Injection (BWFI)*, containing 1.1% benzyl alcohol is stable for 28 days after reconstitution when stored refrigerated at 2−8°C. As the use of preservative benzyl alcohol is contrary to the European Pharmacopoeia requirements, in EU countries only single dose formulation has been merketed[171].

1.8.1.4. Therapeutic indications

A paradigm shift in the management of metastatic cancer has occurred with the development of targeted therapies[177]. As the first targeted therapy approved for the treatment of metastatic breast cancer, trastuzumab has revolutionized the

management of this disease due to its clear efficacy, limited toxicity as a single agent and synergistic antitumour activity in combination with other chemotherapeutic drugs[177, 178.]

Trastuzumab is most effective when combined with cytotoxics such as the taxanes and vinorelbine, provided that, other combinations such are those with other HER2 signalling pathways modulators are being investigated. This includes combination with HER2 dimerization inhibitor, pertuzumab; HER1 (EGFR) inhibitor, cetuximab and tyrosine kinase inhibitors, gefitinib, orlitinib and lapatinib[179, 180].

Numerous clinical trials are ongoing to test the safety and effectiveness of trastuzumab for breast and other types of cancer. The ***A**djuvant **L**apatinib And/Or **T**rastuzumab **T**reatment **O**ptimisation study, (**ALTTO**),* is an international, phase III clinical trial of two targeted therapies for HER2-positive breast cancer, trastuzumab and lapatinib. It will enrol 8000 participants, in 50 countries, on six continents[181].

Targeting multiple signalling pathways in breast cancer with angiogenesis inhibitor bevacizumab is under study, as well. This approach is used to overcome primary or acquired resistance to trastuzumab in breast cancer. Additionally, antibody drug conjugate (ADC), trastuzumab-DM1 (T-DM1) is being investigated for this purpose. This investigational ADC has a proposed dual mechanism of action: anti HER2 activity and targeted intracellular delivery of DM1, a maytansine derivative that is a potent antimicrotubule agent. By targeting HER2 expression on cancer cells, trastuzumab-DM1 is designed to deliver chemotherapy to tumour cells in a precise manner[177, 182].

Currently, trastuzumab has been approved for the treatment of metastatic and adjuvant breast cancer as a single agent or as a combination therapy [183,184].

In adjuvant setting, trastuzumab has been approved as combination therapy with other antineoplastic agents:

- doxorubicin, cyclophosphamide, and paclitaxel
- doxorubicin, cyclophosphamide, and docetaxel
- docetaxel and carboplatin

For the treatment of metastatic breast cancer trastuzumab can be used as single agent (monotherapy) in patients who have received one or more chemotherapy regimens for metastatic disease and in combination with paclitaxel, docetaxel or an aromatase inhibitor[183, 185]. Herceptin is indicated for the treatment of patients with

HER2 positive early breast cancer following surgery, chemotherapy (neoadjuvant or adjuvant) and radiotherapy.
Trastuzumab is well-tolerated but associated cardiotoxicity makes use with anthracyclines and in patients with cardiac dysfunction problematic. A further adverse observation is that the rate of development of cerebral metastases is 2.8-times higher in patients who have received trastuzumab as part of their treatment regimens[182].

1.8.1.5. Determination of HER2 status and patient selection

Trastuzumab should only be used in patients whose tumors have HER2 overexpression or HER2 gene amplification. HER2 overexpression should be detected using an immunohistochemistry (IHC)-based assessment of fixed tumor blocks. HER2 gene amplification should be detected using fluorescence in situ hybridization (FISH) and chromogenic in situ hybridization (CISH). Trastuzumab treatment is only appropriate if there is strong HER2 overexpression, as described by a 3+ score by IHC or a positive ISH result. For patients with an intensity score of 2+ on IHC, confirmation of HER2 positive status by ISH is mandatory. It is also recommended for patients with 3+ staining by IHC
Over the last decade, the (HER2) became established not only as a prognostic marker but also as a predictive factor for early-stage and metastatic breast cancer. Its clinical utility as a predictive marker to identify candidates for therapy with trastuzumab, assumes the availability of high-quality testing and accurate determination of HER2 status. Appropriate selection of patients is quite important when one considers the potential cardiotoxicity of trastuzumab, and its high cost[186].

1.8.1.6. Mechanism of trastuzumab action

As indicated above, humanised recombinant monoclonal antibody trastuzumab is directed against the extracellular domain of the tyrosine kinase receptor HER2. HER2 or erbB2 is a member of the ErbB protein family, more commonly known as the epidermal growth factor receptor family[163].
The HER2 (or c-erbB2) proto-oncogene encodes for a single transmembrane spanning, receptor-like protein of 185 kDa, which is structurally related to the epidermal growth factor receptor. Overexpression of HER2 is found in 20–30% of

human breast cancers, and correlates with more aggressive tumours shortened disease-free survival and a poorer prognosis [164,187]. When epidermal growth factor and its relatives bind the ErbB family of receptors, they trigger a rich network of signaling pathways, culminating in responses ranging from cell division to death, motility to adhesion. The network is often dysregulated in cancer and lends credence to the mantra that molecular understanding yields clinical benefit: over 420,000 patients have been treated with trastuzumab since its FDA approval over a decade ago[187, 188].

A unique feature of human epidermal growth factor receptor 2 (HER2), is the absence of a known ligand. Its activity is subsequent to homo- or heterodimerisation with the other family members. HER2 levels strongly correlate with carcinogenesis, and HER2 overeexpression is an adverse prognostic factor in patients with breast cancer. Furthermore, the level of HER2 in human cancer cells is much higher than in normal tissues which invoke potentially less sensitivity of latter to the toxicity of HER2-targeting drugs. In addition, HER2 overexpression is found in both, primary tumor and metastatic sites indicating that anti-HER2 therapy may be effective at all disease sites. These features make HER2 ideal target for breast cancer treatment[189].

The proposed mechanisms of action of trastuzumab includes down regulation and enhancement of HER2 degradation, inhibition of angiogenesis, inhibition of cell cycle progression via inhibition of the mitogen-activated protein kinase pathway, and suppression of the antiapoptotic phosphatidylinositol 3-kinase and Akt (PI3K-AKT) resulting in apoptosis promotion and the arrest of proliferation. In addition, there is evidence supporting a role for trastuzumab in mediating antibody dependent cellular cytotoxicity (ADCC) mainly due to the activation of natural killer cells (NK), expressing the Fc gamma receptor, which can be bound by the Fc domain of trastuzumab [189,190].

1.8.2. Rituximab

1.8.2.1. Nomenclature

Rituximab [FDA USAN INN], Rituxan; MabThera [Trade names]; Synonyms: CD20 Mab, rDNA; anti-CD20 monoclonal antibody; IDEC-C2B8; CD20 monoclonal antibody, recombinant; DrugBank ID: DB00073; CAS : 174722-31-7.

Rituximab is genetically engineered chimeric mouse/human monoclonal antibody that is produced in mammalian cell culture using Chinese Hamster Ovary (CHO) cells. This IgG1-κ antibody contains murine light and heavy chain variable regions, and human gamma 1 heavy chain and kappa light chain constant regions[1]. Rituximab binds specifically to the antigen CD20 (human B-lymphocyte restricted differentiation antigen Bp35)1 which is found on the surface of normal and malignant B-lymphocytes[191, 192]

Light chain

```
        10          20          30          40          50          60
QIVLSQSPAI LSASPGEKVT MTCRASSSVS YIHWFQQKPG SSPKPWIYAT SNLASGVPVR
        70          80          90          100         110         120
FSGSGSGTSY SLTISRVEAE DAATYYCQQW TSNPPTFGGG TKLEIKRTVA APSVFIFPPS
       130         140         150         160         170         180
DEQLKSGTAS VVCLLNNFYP REAKVQWKVD NALQSGNSQE SVTEQDSKDS TYSLSSTLTL
       190         200         210
SKADYEKHKV YACEVTHQGL SSPVTKSFNR GEC
```

Heavy chain

```
        10          20          30          40          50          60
QVQLQQPGAE LVKPGASVKM SCKASGYTFT SYNMHWVKQT PGRGLEWIGA IYPGNGDTSY
        70          80          90          100         110         120
NQKFKGKATL TADKSSSTAY MQLSSLTSED SAVYYCARST YYGGDWYFNV WGAGTTVTVS
       130         140         150         160         170         180
AASTKGPSVF PLAPSSKSTS GGTAALGCLV KDYFPEPVTV SWNSGALTSG VHTFPAVLQS
       190         200         210         220         230         240
SGLYSLSSVV TVPSSSLGTQ TYICNVNHKP SNTKVDKKAE PKSCDKTHTC PPCPAPELLG
       250         260         270         280         290         300
GPSVFLFPPK PKDTLMISRT PEVTCVVVDV SHEDPEVKFN WYVDGVEVHN AKTKPREEQY
       310         320         330         340         350         360
NSTYRVVSVL TVLHQDWLNG KEYKCKVSNK ALPAPIEKTI SKAKGQPREP QVYTLPPSRD
       370         380         390         400         410         420
ELTKNQVSLT CLVKGFYPSD IAVEWESNGQ PENNYKTTPP VLDSDGSFFL YSKLTVDKSR
       430         440         450
WQQGNVFSCS VMHEALHNHY TQKSLSLSPG K
```

Fig. 1.8. Sequence of rituximab light (up) and heavy (down) chains. Murine variable domain highlighted. Complementarity determining regions underlined in italicized face. The heavy chain N_{301} glycosilation site is indicated by underlined boldface. According reference [193].

As all antibodies of IgG1 class, rituximab contains four polypeptides linked via disulfide bonds: two light and two heavy chains. Each light chain consists of 213 amino acids and heavy chain of 451 amino acids, respectively[194, 195]. Amino acid sequences of rituximab light and heavy chain are presented in Fig.1.8.

1.8.2.2. Clinical Formulation

Rituximab is a sterile, clear, colourless, preservative-free liquid concentrate for intravenous (IV) administration. Rituximab is supplied at a concentration of 10 mg/ml in either 100 mg (10 ml) or 500 mg (50 ml) single-use vials. The product is formulated for intravenous administration in 9.0 mg/ml sodium chloride, 7.35 mg/ml sodium citrate dihydrate, 0.7 mg/ml polysorbate 80, and Sterile Water for Injection. The pH is adjusted to 6.5[196].

It was recognized that murine *2B8* antibody specifically bound to CD20 receptor of B lymphocytes, however its immunogeneicity, lack of effector functions and short half-life limited its clinical application. Therefore a reduction of immunogeneicity and production of human anti murine antibodies (HAMA) was needed. Additional aim was to increase antibody effector functions and half- life, while retaining the binding capacity and specificity of CD20 receptor recognition. In this way, chimeric recombinant monoclonal antibody rituximab (C2B8) was obtained by the chimerization of parent murine antibody *2B8*. During the chimerization process murine variable domain of heavy and light chain was cloned into the human IgG1 immunoglobulin framework[190]. In the chimerised version only variable domains have murine origin (around 30 %). The rest of molecule is human (around 70 %).

1.8.2.3. Construction and expression of C2B8

After amplification by the polymerase chain reaction ,he light- and heavy-chain variable regions of murine 2B8 were cloned into a cDNA expression vector that contained human lgG_1 heavy chain and human kappa-light chain constant regions. Transfection into CHO cells is performed with electroporation, and the chimeric anti CD20 antibody was purified with protein A chromatography. High-level expression of chimeric-2B8 antibody (C2B8) was obtained in Chinese hamster ovary cells[191].

Rituximab is produced in cell suspension culture by a CHO transfectoma containing the *TCAE 8* expression vector in a nutrient medium containing antibiotic gentamicin, added to the culture as a final prophylactic measure against mycoplasma contamination. Following production of the formulated bulk drug substance is aseptically filled into 100 mg and 500 mg glass vials[196].

1.8.2.4. Chemical information

Recombinant chimeric monoclonal antibody rituximab (IDEC-C2B8) contains 1328 amino acids. Molecular weight calculated from the primary sequence of the reduced, non- glycosylated form of this antibody is 144.544 kDa.

As all immunoglobulins of class IgG1, it contains two identical heavy and two identical light chains linked via disulfide bridges. Each heavy chain contains 451 amino acids, with theoretical average molecular mass calculated from the amino acid sequence derived from of cDNA 49214.50 Da and *pI* 8.67. Each light chain contains 213 amino acids with theoretical molecular mass of 23056.69 Da and *pI* 8.26[197].The apparent molecular mass of rituximab is higher kDa, due to the presence of N-linked oligosaccharides[174].

Heavy chain variable region (V_H) includes the first 121 amino acid residues while light chain (V_L) first 106 residues, respectively. Variable regions of both chains comprise complementarity determining regions (CDR1-3), therefore are responsible for antigen recognition and binding. On the other hand human Fc γ1 (IgG1) fragment is responsible for ADCC and CDC. The human IgG1 heavy chain constant region belongs to IgG1 Gm allotype variant[172].

Rituximab heavy chains are linked via two interchain disulfide bonds at the flexible hinge region while heavy and light chains are linked with disulfide bridge involving heavy chain C-224 and light chain terminal C-214. Intrachain disulfide bonds reside in each domain of the H and L chain. In heavy chain there are four intrachain disulfide bonds while in light chain there are only two of them. In correctly folded immunoglobulin molecule all cysteine (C) residues are involved in disulfide bond formation, therefore no free sulfhydril groups should be present[176]. Like other IgG1 molecules, rituximab contains only one N-glycosylation site at conserved asparagine ^{301}N where neutral biantennary oligosaccharides are attached.

1.8.2.5. Therapeutic indications

Rituximab is the first approved targeted biologic therapy for the treatment of haematological malignancies and it took very short time from its first description until the approval and clinical application. On the other hand, this recombinant antibody is a valuable therapeutical option not only for the treatment of blood neoplasms but the rheumatic arthritis, as well. Moreover, further clinical studies are being conducted for

the treatment of several other indications. Approved clinical indications of rituximab include:

Non-Hodgkin's Lymphoma

For the treatment of patients with stage III-IV follicular lymphoma rituximab is used as monotherapy (second line therapy for chemoresistant patients) and combination therapy with CVP* chemotherapy (first line therapy). In addition, in combination with CHOP** chemotherapy rituximab is indicated for the treatment of patients with CD20 positive diffuse large B cell non- Hodgkin's Lymphoma. In EU and other countries (excluding USA), rituximab maintenance therapy has been approved, as well[195, 198].

*cyclophosphamide, vincristine, and prednisolone,

**cyclophosphamide, doxorubicin (hydroxydaunorubicin), vincristine, and prednisone

For the treatment of Non-Hodgkin's lymphoma rituximab is often combined with radioimunoconjugate *ibritumomab tiuxetan* (Zevalin). Zevalin (IDEC Y2B8) is an immunoconjugate in which the murine IgG1 kappa mAb ibritumomab is covalently bound to tiuxetan, linker-chelator for the radioisotopes Yttrium-90 (Y-90) or Indium-111 (In-111). The antibody moiety of Zevalin is directed against the CD20 antigen. The tiuxetan chelator provides a stable linkage between the antibody and the radioisotope, permitting radiation to be directed against antigen-positive cells. The beta emission from Y-90 induces cellular damage by the formation of free radicals in the target and neighboring cells[199].

Rheumatoid Arthritis

Rituximab in combination with methotrexate is indicated for the treatment of adult patients with severe active rheumatoid arthritis who have had an inadequate response or intolerance to other disease modifying anti-rheumatic drugs including one or more tumour necrosis factor (TNF) inhibitor therapies[198].

The efficacy and safety profile of rituximab has been studied in numerous clinical trials for other haematological malignancies (chronic lymphocytic leukaemia, Mantle cell lymphoma, multiple myeloma etc), non-malignant haematological disorders (idiopathic thrombocytopenia purpura, autoimmune haemolytic anaemia, factor VIII deficiency etc.), posttransplant lymphoproliferative disorder and other indications[200].

Since its approval in 1997, numerous off-label uses of rituximab have evolved in different therapeutic areas, mostly in the treatment of autoimmune diseases including systemic lupus erythematosus, autoimmune thrombocytopenia and haemolytic anaemia, dermatologic diseases including coetaneous B-cell lymphoma, dermatomyositis. Graft–versus-host disease (GVHD) and Wegener's granulomatosis have been treated with rituximab as well[201, 202].

1.8.2.6. Rituximab targeted cancer therapy

Rituximab binds specifically to the antigen CD20 with binding affinity of 8 nM[191]. CD 20 antigen, a nonglycosilated hydrophobic transmembrane phosphoprotein with a molecular weight approximately 35 kD located on pre-B and mature B-lymphocytes, regulates early steps in the activation process for cell cycle initiation and differentiation, and possibly it forms or regulates voltage-independent calcium channel[198].

B-cells are believed to play a role in the pathogenesis of rheumatoid arthritis (RA) and associated chronic synovitis. In this context, B-cells may be acting at multiple sites in the autoimmune inflammatory process, including through production of the Rheumatoid factor (RF) and other autoantibodies; antigen presentation, T cell activation, and/or pro-inflammatory cytokine production.

On the other hand, CD20 molecule expressed on neoplastic B cells provides a promising target for therapy of B-cell lymphomas and leukemia. This antigen is especially suitable as a target for antibody mediated therapy because the CD antigen:

a. is expressed on more then 90 % of B-cell- non-Hodgkin's lymphomas but not found on hematopoietic stem cells, pro-B-cells, normal plasma cells or other normal tissues
b. is not normally shed from the cell surface, and there are no detectable serum levels of soluble CD20, which might block targeting of antibody to lymphomas
c. it remains on the cell surface without substantial internalization after cross-linking with antibodies

d. is not expressed in non-haematopoietic tissues, where it could interfere with antibody therapy

Moreover of hematopoietic tumors are accessible and sensitive to lyses by way of immuneeffector mechanisms recruited by human Fc domain of this chimeric antibody[191, 199, 202].

1.8.2.7. Mechanism of Action

The Fab domain of rituximab binds to the CD20 antigen on B lymphocytes, and the Fc domain recruits immune effector functions to mediate B-cell lysis *in vitro*. Possible mechanisms of cell lysis include complement-dependent cytotoxicity (CDC) and antibody-dependent cell mediated cytotoxicity (ADCC). Furthermore, rituximab is able to induce the death of CD20+ cells in the absence of complement or effector cells with number of other pathways, including apoptosis[203-205].

Rituximab is an CD20 depleting agent, therefore during its clinical application it can produce numerous adverse reactions. Due to its immunosupressive effect, during anthireumatoid therapy serious infections can occur. Infusion reactions wich may be related to cytokine release must be reduced with appropriate premedication. These reactions could be worsened in the presence of human antichimeric antibodies (HACA). In the NHL patients with high tumor burden severe cytokine release syndrom can occur. This syndrome which may be associated with some features of tumor lysis syndrom can have fatal outcome.

Following off-label use of MabThera for the treatment of certain autoimmune diseases, cases of fatal Progressive Multifocal Leukoencephalopathy have been reported[206].

1.8.2.8. Second generation anti CD20

The efficacy and success of Rituximab has led to a few other anti CD20 monoclonal antibodies being developed. Currently a humanized version of rituximab, 2H7 ocrelizumab, is being developed by Genentech Inc., F. Hoffmann-La Roche and Biogen Idec Inc. Its evaluation for rheumatoid arthritis and lupus nephritis is under Phase III Clinical trials and a Phase II clinical trial for relapsing remitting multiple sclerosis is ongoing[207]. A fully human anti CD20 rmAb, ofatumumab (HuMax-CD20)

is being developed by Genmab A/S in cooperation with Medarex. Phase III clinical trials are ongoing evaluating ofatumumab for Non-Hodgkin's lymphoma and Refractory Chronic lymphocytic leukaemia (CLL). Drug candidate, modified antibody, DXL625 (CD20), for the prospective treatment of non-Hodgkin's lymphoma is being developed by InNexus Biotechnology Inc. DXL625 a humanized anti-CD20 monoclonal antibody enhanced with Dynamic Cross Linking (DXL™) technology may afford greater potency and binding affinity then parent antibody[208-210].

1.8.3. Abatacept

1.8.3.1. Nomenclature

CTLA4-Ig, rDNA [BIO]; Orencia [TR]; Abatacept [TR USAN INN]; cytototoxic T-lymphocyte-associated antigen-Immunoglobulin G1 fragment fusion protein, recombinant; 1-25-Oncostatin M (human precursor) fusion protein with CTLA4 (antigen)(human) fusion protein with immunoglobulin G1 (human heavy chain fragment), bimolecular (146→146')-disulfide [CAS]; 332348-12-6-[CAS RN]; BMS-188667 [SY].

Abatacept is a fusion protein produced by recombinant DNA technology in Chinese hamster ovary (CHO) cells[211]. It is soluble homodimer consisting of two identical subunits covalently linked by one disulphide bond. Each subunit consists of the modified amino acid sequences of:

1. the extracellular domain of human cytotoxic lymphocyte associated antigen 4 (CTLA-4),
2. modified sequence of the human IgG1 Fc region. The human IgG1 sequence is derived from hinge, CH2 and CH3 domain (Fig. 1.9.)

```
  1 MHVAQPAVVL ASSRGIASFV CEYASPGKAT EVRVTVLRQA DSQVTEVCAA
 51 TYMMGNELTF LDDSICTGTS SGNQVNLTIQ GLRAMDTGLY ICKVELMYPP
101 PYYLGIGNGT QIYVIDPEPC PDSDQEPKSS DKTHTSPPSP APELLGGSSV
151 FLFPPKPKDT LMISRTPEVT CVVVDVSHED PEVKFNWYVD GVEVHNAKTK
201 PREEQYNSTY RVVSVLTVLH QDWLNGKEYK CKVSNKALPA PIEKTISKAK
251 GQPREPQVYT LPPSRDELTK NQVSLTCLVK GFYPSDIAVE WESNGQPENN
301 YKTTPPVLDS DGSFFLYSKL TVDKSRWQQG NVFSCSVMHE ALHNHYTQKS
351 LSLSPGK
```

Fig.1.9. Amino acid sequence of abatacept. ECD of human CTLA-4 is indicated by boldface, modified sequence of the human IgG1 Fc region is highlighted, and hinge region underlined.

Two cysteine residues in the hinge region and one cysteine residue in the C_H2 region were substituted with serines by mutation of the human IgG1 gene sequence (C→S, at positions 130, 136 and 139). Furthermore, amino acid glutamine (Q) was

introduced between aspartic acid (D) from the ECD of CTLA-4 and glutamic acid (E) from the hinge region of the immunoglobulin heavy chain. There is one interchain disulphide bridge between the subunits in the CTLA-4 derived regions (Cysteine at position 120) and four intrachain bridges within each chain of abatacept (Cysteines at positions: 21, 93 and 48, 66 respectively). In addition, one proline (P) was unintentionally substituted by serine (S) in the C_H2 region (P→S, position 148, Fig. 1). For secretion into the medium, abatacept is expressed with an upstream signal sequence that is cleaved as the protein is secreted (oncostatin). In the Fig. 1.10 a scheme of construction and expression of CTLA4-IG has been presented.

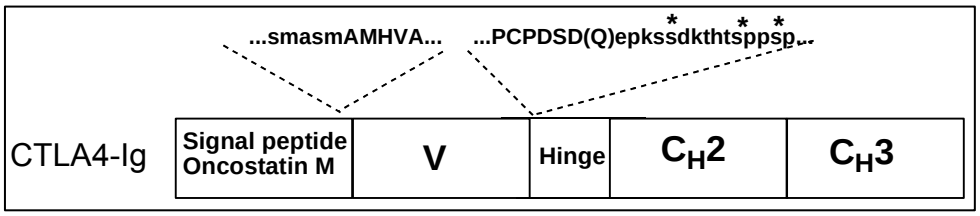

Fig.1.10 Construction and expression of CTLA4-Ig. A cDNA construct encoding Signal peptide (SP), CTLA-4 (V), and human IgCγ1 (Hinge, C_H2 and C_H3). The Amino acid glutamine (D) in parentheses was introduced during construction. Asterisks denote C→S mutations. Junctions between CTLA-4 (capital letters) and the SP of oncostatin M, and the hinge region are presented as well, Reference [217].

Modifications to the original sequences were introduced to avoid unintended disulphide bridge formation and to reduce constant region-mediated biological effector functions and complement activation[212]. The binding of the immunoglobulin to Fcγ receptor and C1q involves residues in the hinge-C_H2 region (…^{141}APELLGGS^{148}…) and C_H2 domains (^{228}E,^{230}K,^{232}K) respectivly[213, 214.] These functions should be avoided since abatacept is not intended to have T-cell depleting function.

Extracellular domain (ECD) of CTLA-4, amino acid sequence from +1-1 to 125 of CTLA4-Ig (Fig 1.9) is responsible for interaction with CD80 and CD86 (B7) receptors of T-lymphocyte. CTLA-4 is a member of immunoglobulin (Ig) superfamily. The ECD of CTLA4 shares homology with immunoglobulins and this part corresponds to the variable domain[215- 217].

Crystallographic data have shown that binding surfaces of CTLA-4 and CD80 exhibit high degree of shape similarity. The interaction is dominated by hydrophobic sequence ^{97}MYPPPYY^{103} and all residues of this motif except P^{99} are in direct contact with CD80. Amino acid changes in this domain reduce ore abolish binding[218].

On the other hand, IgG1 portion (hinge, C_H2 and C_H3) endows prolonged circulating half life of abatacept molecule[219]. In addition, abatacept comprises an Fc region, and it is therefore amenable to purification by protein A chromatography during the downstream processing[220].

Abatacept is produced by fermentation in a transfected genetically engineered CHO cell line. For secretion into the medium, abatacept is expressed with an upstream signal sequence that is cleaved as the protein is secreted (oncostatin). The fusion protein gene contains the coding sequence for the CTLA-4 prepared from the H38 cell line and the Fc-region (C_H2 and C_H3 domains) gene derived from a murine myeloma cell line producing mouse-human chimeric L6 antibody[212].

1.8.3.2 Mechanism of action

Abatacept is the first representative of a new class of drugs known as selective T-cell co-stimulation modulators. It selectively modulates a key co-stimulatory signal required for full activation of T lymphocytes expressing CD28. Full activation of T lymphocytes requires two signals provided by antigen presenting cells (macrophages or dentritic cells): recognition of a specific antigen (MHC complex found on antigen-presenting cells) by a T cell receptor (antigen-specific, signal 1), and a second, antigene-indipendent, costimulatory signal. A major costimulatory pathway involves the binding of CD80 and CD86 molecules (B7 molecules) on the surface of antigen presenting cells to the CD28 receptor on T lymphocytes (antigene-indipendent signal 2). The antigen-specific signal is not sufficient to generate a full response, and in the absence of a second signal may lead to clonal inactivation or anergy, T-cells may be poorly responsive to stimuli and apoptosis may occur. Abatacept selectively inhibits the costimulatory pathway by specifically binding to CD80 and CD86, resulting in immunosupression and decrease in T-cell activation.

Studies demonstrate that abatacept modulates T lymphocyte-dependent antibody responses and inflammation. Abatacept attenuates human T lymphocyte activation (decreased proliferation and cytokine production) and decreases antigen specific TNFα, interferon-γ, and interleukin-2 production by T lymphocytes[211, 217].

In the case of abatacept molecule, the binding specificity is achieved using entirely human components (human ECD of CTLA-4 and human hinge and Fc fragment),

hence it is expected minimal immunogeneicity to the patient and safety for chronic use.

1.8.3.3. Clinical formulation

Abatacept (Orencia®, Britol-Myers Squibb) is supplied as a sterile, white, preservative-free, lyophilized powder for parenteral administration. Each single-use vial of ORENCIA provides 250 mg abatacept, 500 mg maltose, 17.2 mg monobasic sodium phosphate, and 14.6 mg sodium chloride. Following reconstitution with 10 mL of *Sterile Water for Injection (SWFI),* the solution of Orencia® (25 mg/ml) is clear, colorless to pale yellow, with a pH range of 7.0 to 8.0[211,212].

1.8.3.4. Therapeutic indications

Abatacept (Orencia® Bristol-Myer-Squibb) in combination with methotrexate is indicated for the treatment of moderate to severe active rheumatoid arthritis (RA) in adult patients who have had an insufficient response or intolerance to other disease-modifying anti-rheumatic drugs including at least one tumor necrosis factor (TNF) inhibitor[211].

In USA and Canada abatacept is approved for the treatment of moderate to severe RA in patients with an inadequate response to methotrexate and/or TNF-antagonist therapy. Therefore, abatacept may be used as monotherapy or concomitantly with DMARDs other than TNF antagonists[221, 222].

On August, 2007 FDA accepted for filing a supplement BLA for Orencia for the treatment of paediatric patients with juvenile idiopathic arthritis[223], and for this indication it was approved on the July, 2008[224].

The studies of the use of abatacept for the treatment of psoriasis and solid organ transplant Graft-versus-host disease (GvHD) are in the phase I of clinical tryal[225]. Furthermore, abatacept is being investigated for the treatment of lupus (SLE), Crohn's disease, ulcerative colitis, and multiple sclerosis[223].

Adverse events related to abatacept include hypersensitivity reactions and infections and the use of use of abatacept with concomitant biologic RA therapy, i.e., TNF blockers, etanercept-Enbrel®, infliximab-Remicade®, adalimumab®; IL-1-blocker anakinra-Kineret® may be associated with a greater incidence of infections[212].

1.8.3.5. Chemical information

Abatacept is comprised of two homologous glycosylated polypeptide chains of 357 amino acids each forming a covalent homodimer (referred as abatacept “monomer”) linked through disulfide bond (120, 120’). The apparent molecular weight of abatacept is 92.300 kDa (determined by MALDI/TOF mass spectrometry) of which 15 % (13.500 kDa) is composed of carbohydrates. The measured molecular weight is greater than the theoretical value predicted by the cDNA-derived amino acid sequence (39.448 kDa, average mass in reduced form), owing to post-translational glycosylation.

Abatacept is produced in the CHO cells, and therefore as all other proteinic molecules it is a complex molecule containing many variants and forms which arise during the cell culture. They can be posttranslational modifications and/or modifications resulting from subsequent degradation of the molecule. Through the recombinant production process various forms of CTLA4-Ig can be produced, i.e. glycoforms, conformational isomers, and primary sequence variants[226].

1.9. Analytical methodology used for the quality assessment of recombinant biological products, trastuzumab, rituximab and abatacept

1.9.1 Trastuzumab analysis

Chemical-physical and biological parameters of trastuzumab have been characterized by a number of modern analytical techniques and multiple complementary assays have been used for the evaluation of its identity, potency, strength and stability.

Antibody dependent cellular cytotoxicity (ADCC) of trastuzumab was determined by 51-Cr release, using interleukin-2 activated peripheral blood mononuclear cells as effectors and either WI-38 or Her2(+) (SKBR-3) target cells. However this assay is not appropriate for potency release testing since it requires fresh donor cells. Therefore, antiproliferation activity potency test, able to indicate loss of biological activity under conditions of thermal, mechanical, light exposure, oxidative and pH stress is used instead[167, 227].

For quantitative analysis of trastuzumab, capillary isoelectric focusing (cIEF) and SDS-capillary gel electrophoresis (SDS-cGE) have been evaluated, demonstrating adequate sensitivity, precision and linearity for the use in a quality control environment. cIEF and IEF of trastuzumab showed five charge isomorphs (estimated *pI* 8.6-9.1). With both, SDS-CGE and SDS-PAGE the nonreduced trastuzumab migrated as a single major peak (band) with six minor peaks (bands) in the aggregate and clip regions. After reduction, the electropherogram and the slab gel showed the expected heavy chain and light chain fragments with minor peaks (bands) in the aggregate, clip regions. When using SDS-CGE for analysis of antibody molecules, the method appeared to be precise and compares favorably to analysis by Coomassie blue stained SDS-PAGE but was less sensitive than silver stain[228].

Glycosylation and protein modifications are important not only for drug stability and efficacy, but also may have consequences for the patient, for example incorrect modifications including aggregation may lead to an immune response to therapeutic monoclonal antibody[229].

Deamidation of asparagine residue to form aspartic acid and iso-aspartic acid is a cause for protein degradation, particularly during long term storage. Most of deamidated asparagine forms iso-aspartate, which is not a natural amino acid and can potentially be immunogenic. Seven deamidated forms of trastuzumab were resolved by cation-exchange chromatography, validated method used for the release of trastuzumab production lots.

Structure differences were assigned by trypsin and endopeptidase Asp-N peptide mapping and hydrophobic interaction chromatography (HIC) after papain digestion, isoelectric focusing in polyacrylamide gels and Edman degradation. MALDI-TOF analysis and Edman degradation were used for the assignment of peptide fractions.

Deamidation reactions occurred at the light chain (LC) Asn_{30}, and heavy chain (HC) Asp_{102} and Asn_{55}, including: deamidation of LC Asn_{30} to aspartate (Asp_{30}) in one or both LCs, responsible for 2 acidic forms; isomerisation of HC Asp_{102} to isoaspartate, responsible for low potency form, Asp succinimide was also detected; forms with both LC Asn_{30} deamidation and HC Asp_{102} isomerization modification and deamidation of HC Asn_{55} to isoaspartate[165].

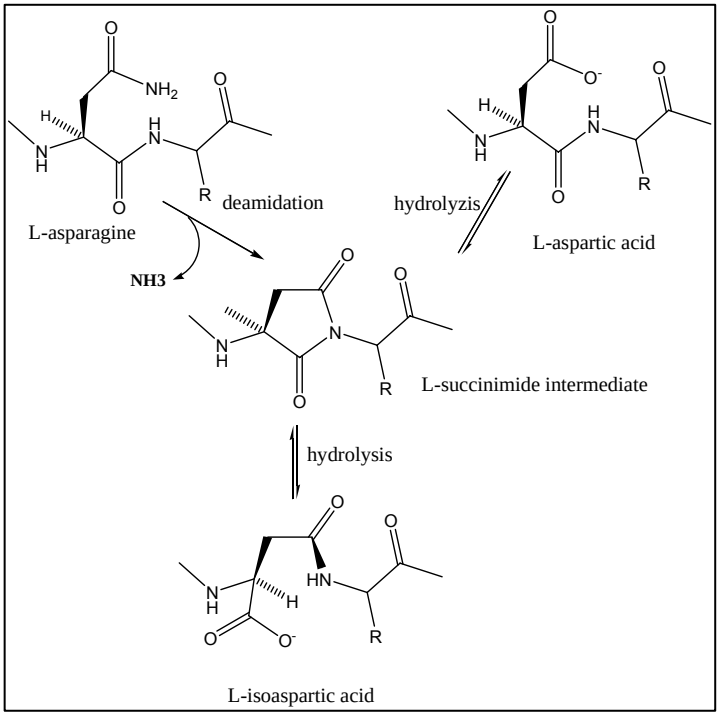

Fig. 1.11. Non-enzymatic damidation of asparagine to aspartic acid (the minor product) and iso-aspartic acid (the major product). According reference [229].

Deamidation process of peptides and proteins proceeds via a succinimide intermediate, followed by partial hydrolysis of succinimide ring to produce isoaspartate (the major product) and aspartate (the minor product), Fig . 1.11. The sole conversion of Asn_{30} to aspartate (not isoaspartate) in trastuzumab molecule, suggests that the deamidation mechanism in cell culture may be different from that during storage[229, 165.] The form with one deamidated light chain was slightly reduced in potency; whereas the form with isoAsp102 in one heavy chain CDR is greatly affected (activity of the isomerized species is only 9–21%of the major species).

All modifications were found in complementarity determining regions) of heavy and light chain suggesting that for trastuzumab surface accessibility and flexibility, both of which are relatively high in the CDR regions, is more predictive of polypeptide degradation sites than the primary sequence[165].

In the trastuzumab terminal lysine processing study, cyanogenbromid (CNBr) cleavage after Met_{431} liberated C-terminal peptides that were isolated by RP-HPLC and characterised[230].

Major product was *des-Lys*^{450} peptide (residues 432-449: HEALHNHYT QKSLSLSPG) and expected C-terminal peptide (residues 432-450: HEALHNHYT QKSLSLSPGK) was the minor product.

Charge variants resulted due to the trastuzumab incomplete terminal lysine removal were resolved with cation-exchange chromatography. Trastuzumab showed five charge species: major product had no Lys_{450} residue, two more basic species had one or two Lys_{450}(1) residues, respectively. Two more acidic species were deamidated variants at Asn_{30} in one light chain. One of them had no terminal Lys_{450} residue, whereas the other had the terminal lysine residue Lys_{450}.

Published data suggest that the absence of the C-terminal lysine residues appears to be due to the action of carboxipeptidases and plasma-derived antibodies typically lack the terminal Lys residues. Therefore the absence C-terminal residues (Lys or Arg) is not usually a regulatory concern, as plasma-derived proteins are similarly processed[230].

Although oxidation is not as prevalent as deamidation and isomerization in antibodies, it can easily occur during their storage[175]. Trastuzumab methionin oxidation was studied by cleaving the *Fab* and *Fc* fragments by papain digestion and detection of oxidized *Fc* fragment by hydrophobic interaction chromatography. In liquid formulations, trastuzumab underwent oxidation when exposed to intense light and elevated temperatures (30-40°C). The rate of oxidation was formulation dependent. Trastuzumab single and multiple dose formulation thermo- and photostability studies revealed that heavy chain Met_{255} was the primary site of oxidation. Met_{431}, on the other hand, could be as well oxidized, but only under extreme conditions[231].

Profiling analysis of oligosaccharides in recombinant antibodies trastuzumab (and rituximab) was performed by CE-LIF[174,232]. For the derivatisation of PNGaseF released N-linked oligosaccharides, derivatization reagent 2-aminobenzoic (2-AA) acid was used. CE-LIF analysis of 2-AA labeled oligosaccharides showed that apart from typical asialo-biantennary complex type oligosaccharides (major oligosaccharide component), sialo-biantennary complex type and high mannose type oligosaccharides, in minor amounts were detected, as well. Their structure was assigned by HPLC and MALDI-TOF-MS.

Asialo-biantennary complex type oligosaccharides, major oligosaccharide component, are typical core fucosilated oligosaccharides of mAbs (*G0, G1, G1'* and

G2). *G0* refers to agalacto structure, *G1, G1'* monogalactosylated and *G2* digalactosylated structure. The isomeric oligosaccharides *G1* and *G1'* have one galactose residue attached to either of the branches (Fig. 1.12.).

Sialo-biantennary complex type and high mannose type oligosaccharides were present less than 3 % of the total oligosaccharide amount. Monosialidated, disialidated and sialohybrid type of minor sialo-oligosaccharides were efficiently resolved with CE-LIF. In addition complex profile of high mannose type oligosaccharides in minor amounts was detected, as well.

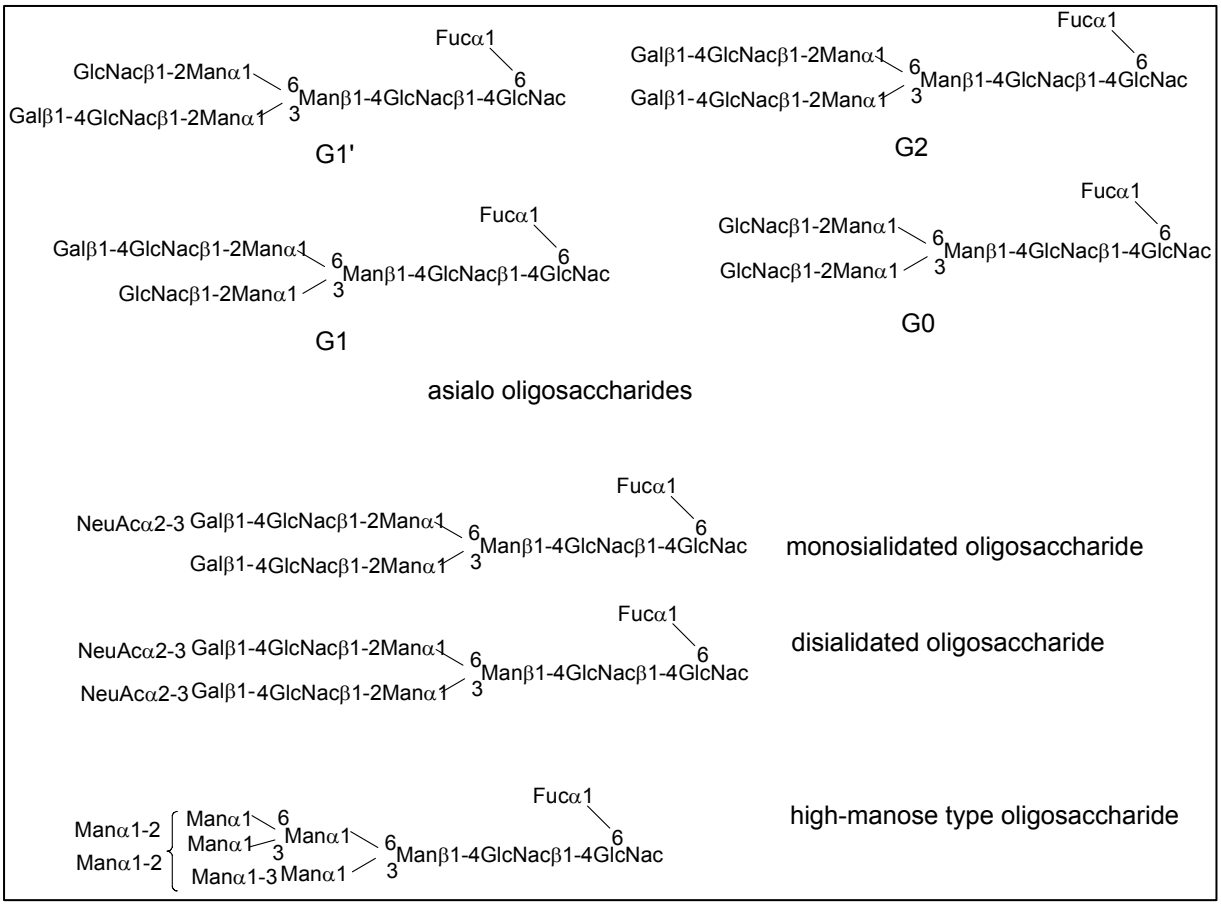

Fig. 1.12. Trastuzumab N-linked oligosaccharide profile. According reference [174].

Peptide mapping was used to assess genetic heterogeneity of recombinant cell lines. Detailed structural characterization of trastuzumab revealed heavy chain heterogeneity by recovery of two forms of tryptic peptide, with either glutamine (Q) or the expected tyrosine (Y) (see Fig 1) at residue 376. Peptide mapping experiments indicated that low-level Y376Q variant developed during transfection of the antibody heavy and light chain genes into CHO cells[233].

The impact of lyoprotectants, sucrose, and trehalose, alone or in combination with mannitol on the stability of trastuzumab at 40°C was assessed[234].
Molar ratios of sugar to protein were used, and the stability of the resulting lyophylised formulations was determined by measuring aggregation, deamidation, and oxidation of the reconstituted trastuzumab and by infrared (IR) spectroscopy (secondary structure) of the dried trastuzumab. Size exclusion chromatography (SEC) was used to determine distribution of intact antibody and soluble aggregate and/or fragments of trastuzumab. Cation-exchange chromatography was used to determine deamidation cyclic imid (Asp succinimid) product. Hydrophobic interaction chromatography (HIC) of Fab and Fc fragments of trastuzumab obtained after carboxypeptidase and papain treatment was used to detect trastuzumab oxidized species. IR spectroscopy and differential scanning calorimetry were used for the study of secondary structure of antibody in solution and lyophilized formulations. Same study demonstrated that lyophilization of trastuzumab, in the absence of sugars, led to a slight increase in aggregate (less than 1.2%). However, at accelerated conditions the extent trastuzumab aggregation increased from about 1% to >10% after 3 months at 40°C[234].

1.9.2. Rituximab analysis

The main source of the antibody heterogeneity results from differences in protein glycosylation which is one of the most common post-translational modifications of proteins in eukaryotic cells provided that, primary structure variations, deamination, deamidation, lysine truncation, methionine oxidation, sulfation and phosphorilation create additional IgG variants[235].
Glycosylation of IgG has no effect on antigen binding; however it is critical for effector functions including complement fixation, Fc receptor binding on macrophages and ADCC. Moreover, rapid elimination of IgG-antigen complexes from circulation is strongly influenced by IgG glycosylation and increase in G0 glycan level is associated with reduction in biological activity as measured by a complement dependent cytotoxicity (CDC) assay[236]. Glycosylation of hybridoma produced IgG varies with culture age, medium pH or proliferation state[237].
Predominantly, N-linked oligosaccharides present in rituximab belong to asialo, *neutral* complex biantennary oligosaccharide type, with zero (G0), one (G1 and G1')

and two (G2) terminal galactose residues, as determined CE-LIF, after the PNGase F release and derivatization with 2-aminobenzoic acid. With this method minor amounts of terminal sialylated oligosaccharides have been detected as well[174, 232]. Manufacturer of pharmaceutical product MabThera® (rituximab) as primary assay for characterization and lot release of N-linked glycans on glycoprotein products employs CE-LIF based assay wherein PNGase F release glycans are labeled with 8-aminopyrene-1,3,6-trisulfonate (APTS) fluorogenic reagent. Additionally, a method for direct characterization of major and minor glycan species using capillary electrophoresis with on-line LIF detection coupled with mass spectrometry (CE-LIF-MS), has been reported, as well. Apart from major glycan components this method allowed accurate identification of minor glycan such are asialo (0.045 mol of sialylated oligosaccharide /mol of protein) and afucosylated species. Since the fucosilation affects ADCC and sialylation affects the clearance of therapeutic proteins, the identification of these species is of particular importance to the overall characterization of rmAbs [88].

Analysis of rituximab and trastuzumab glycosylation by RP-LC coupled to ESI-MS and porous grafit carbon, PGC-LC -MS was reported, demonstrating that neutral and sialylated N-glycans of rituximab and trastuzumab could be simultaneously measured by LC-ESI-MS. Tryptic glycopeptides were used for the N-glycan profiling by RP-LC-MS, while porous grafit carbon, PGC-LC -MS of free oligosaccharides delivered qualitative structural assignment of antibody glycosilation[238].

A simple and rapid method for the determination of relative amounts of rituximab glycoforms differing in terminal galactose was reported. Samples taken from recombinant antibody cell culture process were reduced and injected directly into the HPLC system for the separation of heavy and light chain antibody fragments, and host-cell protein contaminants. Most abundant ions corresponding to the glycoforms found on the rituximab heavy chain were monitored by mass selective detection in the selected-ion monitoring (SIM) mode[40]. Charged variants of recombinant monoclonal antibodies can be studied with different methods such as Ion-exchange chromatography, isoelectric focusing, capillary zone electrophoresis etc[235, 239].

From the amino acid sequence of rituximab molecule is seen that, in both, heavy and light chain the first amino acid N-terminal residue is glutamine (Q), for example, the first nine residues of heavy and light chains are: ^{1}Q V Q L Q Q P G A… (HCn) and ^{1}Q I V L S Q S P A…(LC). Lysine K_{451} and cysteine C_{213} are the C-terminal residues of

heavy and light chain, respectively. After papain cleavage, two types of IDEC-C2B8 (rituximab) charge variants have been identified.

1. Inherent charge variants arising during cell culture from the enzymatic removal of the C-terminal lysine from one or both heavy chains to reveal a C-terminal glycine (Fc-0Lys; Fc-1Lys, and Fc-2 Lys) collectively known as Fc-Lys variants.
2. Additional charge variants which arise from the sequential cyclization of basic amino N-terminal glutamine (Q) of both the heavy and light chains to produce neutral pyroglutamate, a deamination reaction: Fab-pEpE -pyroglutamate at both N-termini; Fab-pEQ-pyroglutamate at heavy chain N-terminus and the glutamine at the light chain N-terminus; Fab-QpE- glutamine at the heavy chain N-terminus and the pyroglutamate at the light chain N-terminus and Fab-QQ-glutamine at both N-termini. These variants are collectively termed Fab pE/Q variants. At the lower temperatures predominant are cyclized species and at the higher partially cyclized species. Since the exposure of elevated temperatures decreases the activity of rmAb, product quality could be controlled by monitoring of the ratio of Fab pE/Q variants.

These charge variants can occur in a random combination at the four N-termini and the two heavy chain C-termini of the antibody leading to a possibility of 15 different species[240].

Extensive stability data were provided by manufacturer of rituximab. Numerous stability parameters including pH, color and appearance, SDS-PAGE, UV spectroscopy, Size exclusion chromatography (SEC), Ion exchange chromatography (IEC), rabbit cellular mediated cytotoxicity (CMC), were examined. Short term exposure (24 hours) of the product to intense light showed no effect on the product stability. However, increased fragmentation and loss of biological activity was caused upon to long-term exposure (3 days). The characterization of the rituximab is extensive and requires a large battery of different techniques as amino acid analysis, amino-terminal sequence analysis, peptide mapping, and analysis of oligosaccharides, ion-exchange chromatography, cIEF, SDS-PAGE, and Circular Dichroism. The oligosaccharide structure was investigated by capillary zone electrophoresis (CE) and MALDI-TOF after isolation from HPAEC-PAD[241].

Immunoreactivity of rituximab was tested by radiolabeling antibody with ^{125}I or with fluorescein isothiocyanate (FITC). They were tested by direct binding to $CD20^{+}$ target cells and detected either by gamma counter or by flow cytometry using a FACScan analyzer. Binding of human complement *C1q* and CDC was determined by fluorescein conjugation[191]. For the determination of rituximab serum levels flow cytometry and ELISA-based assays have been described[242, 243].

Rituximab lot release testing included physicochemical and biological methods such are: color and appearance, SDS-PAGE, peptide mapping, fragment IEC-HPLC, SEC-HPLC, Glycan content, cIEF, complement dependent cytotoxicity CDC, UV- VIS spectroscopy scan, sterility, endotoxin testing, osmolality and polisorbat 80 concentration. Validated human CDC assay was used for the determination of potency. Galactose content on the heavy chain oligosaccharide is found to be critical parameter for biological activity, therefore another release test for glycan content was developed (CE-LIF). It was demonstrated that while galactose content did not influence rituximab binding it influenced biological activity measured with CDC assay.

Validated UV-VIS spectroscopy is used as protein concentration release test. cIEF was used to positively identify rituximab from other recombinant monoclonal antibodies made by the Manufacturer[244].

1.9.3. Abatacept analysis

Multiple charged isoforms in the native abatacept drug substance ranging from *pI* 4.5 - 5.5 are detected using isoelectric focusing (*IEF*) [224]. Literature data revealed that the drug substance is a mixture of different iso- and glycoforms of the protein and in addition to heterogeneity derived from different glycoforms, there is N-terminal and C-terminal heterogeneity[245]. Abatacept contains N-linked and O-linked oligosaccharides in each chain.Three N-linked glycosylation sites are confirmed by peptide mapping to occur at Asn_{76}, Asn_{108} (both at CTLA4 region) and Asn_{207} (Fc region) and two O-linked glycosylation sites have been identified at Ser_{129} and Ser_{139}[245].

Glycosilation differences have been shown to impact the pharmacokinetics and the clearance of product and terminal sialic acids of the carbohydrate moieties are said to be important for pharmacokinetics of the protein[246]. Published data have documented the presence of N-land O-linked oligosaccharides in the CTLA4-Ig molecule. It was shown that N-linked oligosaccharides are neutral asialo biantennary complex type,

while O-linked oligosaccharides have different degree of sialidation: monosialidated and disialidated being the predominant type. CHO derived CTLA4-Ig has α2,3-linked sialic acids and the terminal sialic acids are important for its in vivo activity[247, 248]. Underivatised oligosaccharide mixture of CTLA4-Ig (abatacept) has been examined by CE and HPAEC-PAD under normal and thermally stressed conditions. Both methods indicated CTLA4-Ig derived oligosaccharides being predominantly neutral, disialidated (one specie) and monosialidated species (three species) [249] (Fig. 1.13). Oligosaccharide composition of different lots of CTLA4-Ig has been examined by electrophoresis of fluorophore-conjugated carbohydrates. It was indicated that CTLA4-Ig oligosaccharides are predominantly of N-linked biantennary complex-type[247] and in vivo clearance profiles of CTLA4-Ig showed that the clearance rate is inversely proportional to the oligosaccharide N-acethylneuraminic content.

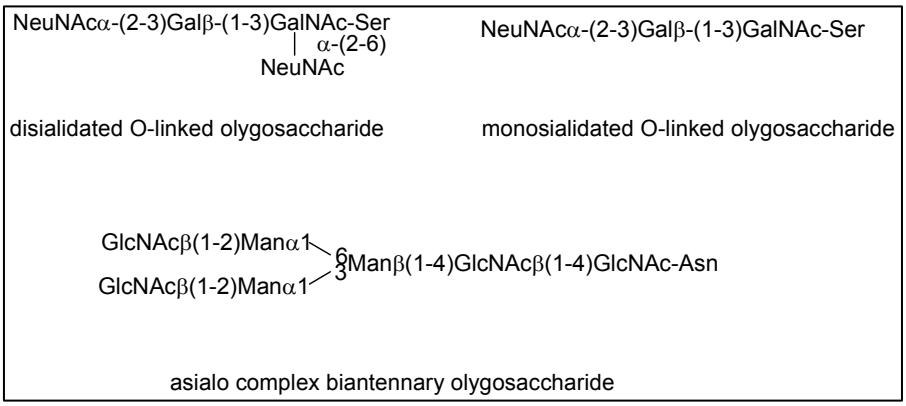

Fig.1.13. Oligosaccharide profile of abatacept. According reference [247]

For the demonstration of abatacept quality, numerous release testing have been provided by the Manufacturer of this biological drug substance: peptide mapping (which can be used as stability indicating assay, as well), to demonstrate molecular identity of abatacept, capillary electrophoresis, to discriminate abatacept from related molecule belatacept, isoelectric focusing to show the distribution of different glycoforms, IEX HPLC, monosaccharide analysis, to show the consistency of glycosylation. Bioassay has been used for the release and stability testing[245].

2. The aims of study

1. Evaluation of a reliable 2-DE method for identification and purity assessment of therapeutically relevant *rDNA* derived biological medicinal products: humanized monoclonal antibody trastuzumab, chimeric monoclonal antibody rituximab and fusion protein abatacept. 2-DE method should be able to assess product charge heterogeneity, isomorf pattern and posttranslational modifications. This method should allow demonstration of product identity and structural integrity comparing 2-DE patterns of the product and reference preparation.

2. Development and optimization of a 2-DE method for the separation of *rDNA* medicinal products complemented with MALDI-TOF MS analysis of resulting peptides generated after *in gel* tryptic digestion aiming the product identity confirmation. The suitability of *peptide mass fingerprinting* analysis as a routine technique for the rapid detection of these products should be investigated. Method should allow rapid identification of heavy and light chains of antibodies and both fusion partners of fusion proteins, therefore specific discrimination of antibodies of different origin, *i.e.* chimeric, humanized and antibody related substances *i.e.* fusion proteins should be achieved.

   The suitabilities of aforementioned analytical methodologies as official pharmacopoeia methods of quality testing of recombinant biological medicinal products should be assessed as well.

3. Forced degradation study of recombinant monoclonal antibody trastuzumab and the assessment of the stability indicating power of 2-DE method.

3. Working objectives

This work focuses on the evaluation of new analytical methodology for quality study and the exploring of new quality parameters of rDNA derived biological medicinal products.

1. Planar electrophoresis techniques, SDS-PAGE and IEF have been widely used for the quality control of rDNA derived medicinal products such are recombinant monoclonal antibodies (rmAbs):

- Purity and structural integrity characterization
- Stability characterization: due to their stability indicating power, these techniques are used to detect antibody fragmentation and aggregation under accelerated conditions and the appearance of extra bands is criterion of purity and stability.

However, SDS-PAGE and IEF performed separately provide limited information related to the rmAbs heterogeneity. Since charge and other variants define the quality of these products, establishment of suitable methods to monitor their heterogeneity would be of great importance for their overall quality assessment. Logically, as 2-DE combines separation in two dimensions, according molecular weight (SDS-PAGE) and isoelectric point, more comprehensive information related to the heterogeneity of *rmAbs* products can be obtained.

2. MALDI-TOF MS analysis has been used for the quality assessment of recombinant biological medicinal products. MALDI-TOF MS analysis of peptides obtained after *in gel* tryptic digestion of proteins separated by SDS-PAGE and 2-DE and *peptide mass fingerprint analysis* has been used in proteomic studies for the identification of proteins from SDS-PAGE and 2-DE gels, therefore, fast and simple identification of therapeutic *rmAbs* and their related pharmaceutical products using *peptide mass fingerprinting* could be achieved.

In order to achieve objectives of this work, three therapeutically relevant medicinal products obtained by *rDNA* technology will be studied:

1. Humanized monoclonal antibody (*rmAb)*, *trastuzumab* (Herceptin®, Roche)
2. Chimeric monoclonal antibody, *rituximab* (MabThera®, Roche), and
3. Fusion protein, *abatacept* (Orencia®, Bristol-Mayers)

In order to develop a suitable gel electrophoresis method complemented with MALDI-TOF MS analysis for the assessment of quality of *rDNA* derived biological medicinal products, performances of the following analytical techniques will be investigated:

1-D electrophoresis analysis under reducing and non-reducing conditions

- Molecular weight estimation
- Purity assessment
- Deglycosilation monitorization and optimization
- Forced degradation testing of trastuzumab
- Optimization of staining procedure: linearity, sensitivity of staining, reproducibility. Coomassie and Silver staining procedures will be performed.

2-D electrophoresis analysis

- Estimation of molecular weight and *pI*
- Charge heterogeneity and isomorph pattern study (2-DE patterns)
- The study of posttranslational glycosylation. N-glycosidase F, sialidase and O-glycosidase will be used to remove N-linked glycans, terminal sialic acids and O-linked glycans, respectively. Reduction of sample complexity for subsequent MALDI-TOF MS analysis will be attempted as well
- The study of lysine truncation using carboxypeptidase B
- In order to assess the effects of severe conditions on the stability of reconstituted solutions and to validate the stability indicating power of 2-DE, forced degradation testing of trastuzumab will be undertaken. The rate of chemical degradation will be increased by subjecting the reconstituted pharmaceutical formulation, Herceptin® to exaggerated conditions. Forced degradation, including *thermal stability study* (4-8°C, room temperature, 37, and 50°C), *oxidation (hydrogen peroxide solution 1 and 3 %)*, *low pH influence (trifluoroacetic acid 1 %)*, and *shear stress testing* will be performed. Testing frequency: weekly, 2 months and daily, 1 week.

- For 2-DE method development the following parameters and procedures will be optimized: sample dialysis, optimization of IEF procedure, application of different IPG strips (3-11 NL, 6-9 L, 4-7 L, and 3-6 L); optimization of gel concentration, application of gradient gels. For the visualization of gel spots, Silver and Coomassie staining procedures will be optimized.
- Optimization of electric parameters: voltage and current intensity, during the first (IEF) and the second dimension (SDS PAGE).

In gel tryptic digestion

In gel tryptic digestion of sample proteins form selected 2-DE gel positions and the extraction procedure of resulting peptides will be optimized.

MALDI-TOF-MS sample preparation and presentation

Optimization of sample preparation and deposition, selection of appropriate concentrations of matrix and sample for optimal cocrystalization will be tested as well.

Peptide mass fingerprinting analysis

For the identification purpose, experimental peptide masses will be compared with peptide masses obtained by *in-silico* trypsin digestion using different search engines and databases.

4. Material and Methods

4.1. Materials and reagents

1. *Acetonitrile*, use tested for MALDI-MS (Sigma -Aldrich Chemie GmbH, Steinheim, Germany)
2. *Acetic acid, conc. 99-100%,* HPLC grade (Merck KGaA, Darmstadt, Germany)
3. *Acrylamide 2X*, research grade (Serva Electrophoresis GmbH, Heidelberg, Germany)
4. *Agarose SERVA Standard low EEO*, research grade (Serva Electrophoresis GmbH, Heidelberg, Germany)
5. *Ammonium hydrogen carbonate*, purum, p.a. (Fluka Chemie GmbH, Buchs Switzerland)
6. *Ammonium persulfate*, analytical grade (Serva Electrophoresis GmbH, Heidelberg, Germany)
7. *Angiotensin II* Mass Spec. Standard (Sigma -Aldrich Chemie GmbH, Steinheim, Germany)
8. *Aqua bidestillata* (Mayrhofer Pharmazeutika GmbH & Co KG, Leonding, Austria
9. *Aqua purificata PhEur* (Elisabeth Schubert Ges.m.b.H, Vienna Austria)
10. *Bradykinin fragment 1-7*, Mass Spec. Standard (Sigma -Aldrich Chemie GmbH, Steinheim, Germany)
11. *Bromphenol Blue, Na-salt*, research grade (Serva Electrophoresis GmbH, Heidelberg, Germany)
12. *1-Butanol* zur Synthese, (Marck Schuchardt, Hohenbrunn, Germany)
13. *Carboxypeptidase B*, from pig pancreas, (Roche Diagneostics GmbH, Mannheim, Germany).
14. *CHAPS*, research grade (Serva Electrophoresis GmbH, Heidelberg, Germany)
15. *Chorhydric acid*, p.a. (Donauchem GmbH, Vienna Austria)
16. *Coomassie Brilliant Blue G 250*, pure (Serva Electrophoresis GmbH, Heidelberg, Germany)
17. *α-Cyano-4-hydroxy- cinnamic acid*, desiccate (Sigma -Aldrich Chemie GmbH, Steinheim, Germany)

18. *Dithiothreitol*, research grade (Serva Electrophoresis GmbH, Heidelberg, Germany)
19. *DryStrip Cover Fluid* (Amersham Biosciences AB, Uppsala, Sweden)
20. *Ethanol 96 %*, HPLC grade (Merck KGaA, Darmstadt, Germany)
21. *Formic acid 99%* pure (Acros Organics, Geel, Belgium)
22. *Formaldehyde sol. 37 %,* puriss, p.a. (Fluka Chemie GmbH, Buchs Switzerland)
23. *Glycerol*, plant (Serva Electrophoresis GmbH, Heidelberg, Germany)
24. *Glycine*, analytical grade (Serva Electrophoresis GmbH, Heidelberg, Germany)
25. *Hydrogen peroxide*, *35 % v/v* (Merck KGaA, Darmstadt, Germany)
26. *Immobiline™ DryStrip pH 3-6 L; 6-9 L, 4-7 L, 3-11 NL* (GE Healthcare Bio-Sciences AB Uppsala, Sweden)
27. *Insulin oxidized beta chain* Mass Spec. Standard (Sigma -Aldrich Chemie GmbH, Steinheim, Germany)
28. *Iodoacetamide*, research grade (Serva Electrophoresis GmbH, Heidelberg, Germany)
29. *IPG Buffers (pH 4-7; 6-11; 3-11),* (GE Healthcare Bio-Sciences AB Uppsala, Sweden)
30. *Methanol*, HPLC grade (Fisher Scientific UK Ltd. Loughborough, UK)
31. *MilliQ Water*, Resistivity 18.2 MΩcm at 25 °C (Millipore, Bedford, USA)
32. *Neuraminidase (Sialidase)*, from Arthrobacter ureafaciens, (Roche Diagneostics GmbH, Mannheim, Germany)
33. *N-Glycosiadase F (PNGase F)* from Flavobacterium meningosepticum, recombinant-E.coli , (Roche Diagneostics GmbH, Mannheim, Germany)
34. *N,N,N',N'-Tetramethylene diamine*, research grade (Serva Electrophoresis GmbH, Heidelberg, Germany)
35. *N,N'-Methylenebisacrylamide 2X*, research grade (Serva Electrophoresis GmbH, Heidelberg, Germany)
36. *O-glycosidase* from Diplococcus pneumoniae (Roche Diagneostics GmbH, Mannheim, Germany)
37. *Precision Plus Unstained Protein™ Standards*, (Bio-Rad Laboratories, USA)
38. *Silver nitrate* analytical grade (Serva Electrophoresis GmbH, Heidelberg, Germany)

39. *Sodium carbonate anhydrous*, pro analysi (Riedel de Haën, Seelze, Germany)
40. *Sodium dihydrogen phosphate monohydrate 99%* (Sigma -Aldrich Chemie GmbH, Steinheim, Germany)
41. *Sodium dodecylsulfate* for biochemical application (Serva Electrophoresis GmbH, Heidelberg, Germany)
42. *Sodium hydroxide*, *2 M* (Merck KGaA, Darmstadt, Germany)
43. *Sodium thiosulfate anhydrous*, purum p.a. (Fluka Chemie GmbH, Buchs Switzerland)
44. *2-Propanol* "baker analysed" (J.T. Baker B.V., Deventer Holland)
45. *Potassium hexacyanoferrate III*, (Neuber GmbH, Austria)
46. *Trifluoroacetic acid 1 %,* for MALDI MS (Sigma -Aldrich Chemie GmbH, Steinheim, Germany)
47. *Tris(hydroxymethyl)aminomethane*, research grade (Serva Electrophoresis GmbH, Heidelberg, Germany)
48. *Triton X-100* pure (Serva Electrophoresis GmbH, Heidelberg, Germany)
49. *Trypsin*, sequencing grade (Roche Diagnostics GmbH, Mannheim, Germany)
50. *Urea*, analytical grade (Serva Electrophoresis GmbH, Heidelberg, Germany)

Pharmaceutical formulations of recombinant monoclonal antibodies (*rmAbs)* trastuzumab (Herceptin®) and rituximab (MabThera®) were kindly provide from Rudolfstiftung Hospital in Vienna, and recombinant fusion protein abatacept (Orencia®) was bought in a Pharmacy Shop.

4.2. Apparatus

Kompact Seq, Kratos Analytical, Manchester UK. (MALDI-TOF MS)
Hoefer® SE1200 Easy Breeze™ Gel Dryer, Cat Nr: 80-6290-71, (Amersham Biosciences Inc).
Freeze Dryer Christ Alpha 2-4 LSC, Cat Nr: 102042; **Rotations-Vakuum-Konzentrator RVC2-18,** Cat Nr: 100218. (Martin Christ Gefriertrockungsanlagen GmbH, Osterode am Harz, Germany)
Heraeus Biofuge Stratos Cat Nr: 282026 (Kendro Laboratory Products, Osterode am Kalkberg, Germany)

Mini-PROTEAN® 3 Cell, Cat Nr: 165-3301. Components: Spacer Plate [10.1 cm (W), 8.3 cm (H)]; Short Plate [10.1 cm (W), 7.3 cm (H)], Gel size [8 cm (W), 7.3 cm (H)]; Casting Frame; Combs; Buffer Dam; Electrode Assembly; Clamping Frame; Mini Tank and Lid (Bio-Rad Laboratories, USA).

PROTEAN® II Xi Cell for vertical electrophoresis. Components: Lower Buffer Chamber, Central Cooling Core, Lid with electrical leads, Casting Stand, Sandwich Clamps, Casting Stand, Long plates (20 X 20 cm), Short plates (22.3 X 20 cm), Spacers (22.3 cm X 1 mm) (Bio-Rad Laboratories, USA)

Hoefer SG 500 Gradient Maker Catalogue Number: 11238-2/28/89 (Hoefer Pharmacia Biotech, San Francisco, USA)

IPGPhor™ Isoelectric focusing system, Catalogue Nr: 80-6415-35 (Ge Healthcare, Biosciences AB, formerly Amersham Pharmacia Biotech, Uppsala, Sweden)

PowerPac 1000 (Power Supply), Catalogue Nr: 165-5055 (Bio-Rad Laboratories, USA)

MultiTemp III Thermostatic circulator, Product code: 18-1120-77, (GE Healthcare Biosciences AB, Uppsala, Sweden)

Cellulose dialysis tube Φ21.4 mm X 33.3 mm X 25 m Cut off: 12000-14000, (AS ONE, Japan Medical Science, Japan)

Thermomixer comfort, Catalogue Number: 5355 000.011(Eppendorf AG, Hamburg, Germany)

Ultrasonic bath

Applied Software

PDQuest 6.2.1. (Bio-Rad Laboratories, USA)

Kompact MALDI Software Version 1.2.2 Kratos Analytical, Manchester UK.

4.3. Isoelectric focusing

For 2-DE electrophoresis analysis in the first dimension the Immobiline DryStrip gels (length 18 cm ±2 mm) of following pH intervals have been used:

- 3-6 L (abatacept)
- 4-7 L (abatacept)
- 6-9 L (trastuzumab, rituximab and abatacept)

- 3-11 NL (trastuzumab, rituximab and abatacept)

4.3.1. Sample preparation

In 1 ml aliquot of *Rehydration solution (A1*), 5 mg/ml *DTT* and 5 µl/ml *IPG Buffer* were added just prior to use. The *pH* of *IPG Buffer* was selected according the *pH* interval of Immobiline DryStrip gels:

- IPG Strips 3-11 NL, IPG Buffer 3-11 NL
- IPG Strips 6-9 L, IPG Buffer 6-11 L
- IPG Strips 3-6 L and 4-7 L, IPG Buffer 4-7 L

The given amount of sample was mixed with *Prepared rehydration solution A2* (*A1* plus DTT and IPG Buffer) and shortly vortexed. 10 µl (1 µg/µl) of sample solution were pipetted into 340 µl *Prepared rehydration solution A2*, for 2-DE electrophoresis optimization and Deglycosylation experiments, while for MALDI-TOF analysis of 2-D gel electrophoresis separated proteins 10 µl (5 µg/µl) sample were pipetted into 340 µl *Prepared rehydration solution A2*. For 18 cm long strips total volume of 350 µl mixture is obtained. The mixture was allowed to stay 1 hour at room temperature with occasional vortexing (3 X 2 s) followed by centrifugation (15 000 g, 5 min) to remove eventual insoluble components.

4.3.2. Rehydration and Isoelectric focusing

Required number of Strip Holders was put onto cooling plate/electrode contact area of IPGphor strip holder platform.
350 µl of sample-containing rehydration solution was carefully pipetted into the Strip Holder base. The solution was evenly distributed over the channel length. The cover foil was carefully removed from the Immobiline dry strip, starting from the anodic (+ end), and using forceps the strip was slowly placed onto rehydration solution, gel side-down. Trapping air bubbles under the Immobiline dry strip gel should be avoided.
To ensure that the rehydrated IPG strip gels do not dry out during rehydration and the focusing process they are overlaid with 1-1.5 ml Cover Fluid and covered with

plastic closure. Finally, after closing the IPGphor cover, the selection of instrument program and entering desired run parameters the run was started. Temperature was set at 20°C and current limited to 50 µA per IPG strip. After the IPG strips have been rehydrated (11-13 hours), IEF started according the programmed parameters (Table 4.7).

Table 4.7. IPGphor running conditions

Temperature	20°C		
Current limit	50 µA per IPG strip		
Sample volume	350µl (18cm long and 3mm wide strips)		
Step	**Voltage**	**Mode**	**Time**
Rehydration	0 V		11-13 hours
IEF S1	1000 V	Gradient	1 hour
IEF S2	2000 V	Gradient	0.5 hours
IEF S3	4000 V	Gradient	0.5 hours
IEF S4	8000 V	Gradient	0.5 hours
IEF S5	8000 V	Step-n-hold	72000 Vhrs
IEF S6 (optional)	2000 V	Step-n-hold	0-3 hours

The IPGphor can handle up to 12 Strip Holders (length, 7, 11, 13 or 18 cm). For the rehydration and IEF the program was set to allow loading of Strip Holders with sample dissolved in rehydration buffer in the afternoon, followed by automatic start of IEF during the night so that IEF was finished the next day.After IEF process, IPGstrips are taken from Strip Holders and using a clean paper towel residual cover fluid is carefully removed from the IPG strips. In this point, there are two possibilities: IPG strips can be used immediately for the second dimension or, they can be kept at lower temperature. In this work, for reproducibility purposes, IPG strips are stored between two sheets of plastic film at -80°C.

4.3.3. Preparation and cleaning of Strip Holders

In order to remove residual proteins after each first dimension IEF-run, Strip Holders have been cleaned with a neutral pH detergent (Strip Holder Cleaning Solution®) using a toothbrush for vigorous agitation, and rinsed with deionised water.

For the efficient protein removal Strip Holders were baked at 250°C for 2.5 hours.
In order to prevent contamination of clean Strip Holders they are always handled with gloves.

4.4. Second dimension. SDS-PAGE

After the IEF, the second-dimension SDS-polyacrylamide gel electrophoresis (SDS-PAGE) has been performed on vertical system, consisting on four steps:

1. Casting of discontinuous vertical SDS gels
2. Equilibration of the IPG gel strips
3. Placing of the equilibrated IPG gel strip on top of the SDS gel
4. Electrophoresis

Discontinuous gels consist of a resolving or separating (lower) gel and a stacking (upper gel).

4.4.1. Preparation of resolving gel

Gels are cast into assembled glass plate sandwiches in a casting stand.
Single percentage resolving gels (%T 10%, 12.5 % and 15 %) are made combining all reagents presented in Table 4.8 leaving out ammonium persulfate and TEMED. The monomer solution obtained is degassed 5 minutes in Ultrasonic Bath. TEMED and ammonium persulphate are added after degassing and the flask is gently swirled, being careful not to generate bubbles. After mixing, the monomer solution is poured down the spacer into each sandwich to a level about 4 cm from the top of the shorter plate. For this purpose a 25 ml pipette was used. Immediately after pouring each monomer solution was overlaid with a layer of water-saturated 1-butanol (1.0 ml) to minimize gel exposure to oxygen and to create a flat gel surface. After ca 10-20 min a sharp liquid gel interface was visible. After allowing a minimum of 1 h for polymerization, water-saturated 1-butanol overlay was removed and the gel surface was rinsed with deionized water.

Table 4.8. Single-percentage gel recipes for discontinous SDS gels

	Resolving gel			**Stacking gel**
Final gel conc. (% Acrylamide)	10 %	12.5 %	15 %	4 %
Acrylamide Stock Solution (Sol B1)	32.47 ml	40.58 ml	48.70 ml	0.65 ml
Resolving gel buffer (Sol B2)	25 ml	25 ml	25 ml	-
Stacking gel buffer (Sol B3)	-	-	-	1.25 ml
MilliQ water	42 ml	33.88 ml	25.77 ml	3.05 ml
APS (Sol B4)	62.50 µl	62.50 µl	62.50 µl	5 µl
TEMED	468.75 µl	468.75 µl	468.75 µl	50 µl
Total volume	100 ml	100 ml	100 ml	5 ml

4.4.2. Preparation of stacking gel

In this work, stacking gels were cast just before use. Volume and concentration of monomer solution of stacking gels is lower than of resolving gels (Table 4.8). All reagents needed for the preparation of stacking gel except APS and TEMED were mixed and degassed 5 min in Ultrasonic Bath. TEMED and ammonium persulphate were added after degassing and the flask is gently swirled, being careful not to generate bubbles. Before pouring the Stacking gel the area above separating gel was completely dried with the use of filter paper. Using a 5 ml pipette tip the stacking gel was poured into each sandwich to a level about 1 cm from the top of shorter plate and immediately overlaid with the layer of water-saturated 1-butanol. After allowing a minimum of 1.5 h for polymerization, water-saturated 1-butanol overlay was removed, gel surface was rinsed with deionized water and area above the stacking gel was dried with the use of filter paper. In order to prevent contamination of glasses and other working surface with hand and due to acrylamide neurotoxicity, plastic glows were used in all phases of electrophoresis analysis.

4.4.3. Equilibration of the IPG gel strips

The second-dimension gels were prepared and ready to accept the Immobiline DryStrip gel before beginning the equilibration protocol.

4.4.3.1. Preparatory steps

- 10 ml DTT Equilibration solution (1 %) was prepared dissolving 100 mg DTT in 10 ml *SDS Equilibration Buffer*, *Sol C1.*
- 10 ml Iodoacetamide (IAM) Equilibration solution (2.5 %) was prepared dissolving 250 mg IAM in 10 ml *SDS Equilibration Buffer*, *Sol C1.*

The volume of 10 ml for each solution was necessary for equilibration of 2 strips (18 cm long). This amount was divided in two parts of 5 ml for the equilibration of each strip.

4.4.3.2. Equilibration step

Focused IPG strips were removed from the plastic foil from -80 °C freezer and allowed to warm to room temperature for 1-2 min. The IPG strips were equilibrated twice, each time for 15 min. The first equilibration step is performed in DTT Equilibration solution followed by the second equilibration in IAM Equilibration solution. IPG strips (gel side-up) were equilibrated in equilibration tray by gently shaking on a rocker.

During the first step, DTT preserves fully reduced state of denatured proteins, while IAM in the second step, alkylates thiol groups on proteins and residual DTT. Unwanted reactions of Cys residues for subsequent MALDI-TOF MS analysis are minimized as well.

4.4.3.3. Placing of the equilibrated IPG gel strip on top of the SDS gel

.

Molecular weight standards (1 µl for silver stained gels and 4 µl for Coomassie stained gels) were applied to a section of filter paper and placed at the anodic end the SDS-PAGE gel.

Already equilibrated IPG strips were lubricated immersing them in the *Diluted cathode buffer* for few seconds. For easier application on the stacking gel IPG strips were cut in both ends (about 5 mm each side) and using forceps positioned between the plates on the second-dimension gel surface with the plastic backing against shorter glass plate. With a thin spatula, the IPG strip was gently pushed down to achieve complete contact with the top surface of the stacking gel ensuring no trapping of air bubbles. After that IPG strips (and molecular weight standards) were overlaid with about 1.5 ml of *Agarose sealing solution, Sol C2* cooled to 40-50°C.

Agarose sealing solution, Sol A7 was always prepared during the IPG strip equilibration because of the time needed for agarose melting (about 10 min in 100 °C heat block) and cooling it to 40-50°C. After allowing a 2-3 min for agarose to solidify, gel cassette was inserted in the electrophoresis unit. Temperature controller was switched on and temperature adjusted to 15 °C.

Into the tank of electrophoresis unit are poured 3 l of *diluted anode (lower) buffer* whereas 500 ml *diluted cathode (upper) buffer* are pored into the upper buffer chamber. Diluted anode and cathode buffers are obtained diluting *10 X Anode Buffer, Sol C3* and *10 X Cathode Buffer, Sol C4,* respectively, with deionised water.

4.5. Electrophoresis

Second dimension electrophoresis run (gels 10, 12.5 and 15 % T, homogenous, 2.6 % C; 200 X 200 X 1mm^3) was performed under constant current of 45 mA per gel, electrophoresis time about 3.5 hours. The run was terminated when the Bromophenol Blue dye has migrated off the lower end of the gel.

4.6. One-dimensional, SDS-PAGE gels

The preparation of gels for the one dimensional electrophoresis is essentially same as for the two dimensional electrophoresis analysis. Since this setting precludes the first dimension (isoelectric focusing) there are some differences in the casting of stacking gel and sample loading.

In mini-gel system [(8 cm (W), 7.3 cm (H)] the stacking gel solution was pipetted into sandwich (on the top of resolving gel) until the top of the short plate and 10 well comb was inserted between the plates taking care not to trap air bubbles below the teeth of the comb. The stacking gel was allowed to polymerize (about 1 hour). After gel polymerization the comb was gently removed and the wells were rinsed and filled with *diluted cathode buffer*. The samples were placed briefly on ice until ready for use. Samples are dissolved in *Laemmli buffer* C5 in which just prior to use are added 6.2 mg/ml DTT. The reduction/ denaturation of sample is performed by heating the sample and DTT-containing *Laemmli buffer C5* solution in termocycler, 10 min at 95°C.

Using Hamilton ™ syringe 15 µl of denatured/reduced sample solution were gently loaded beneath the buffer in specified well. No adjacent well was left empty, if the well was not needed; it was loaded with *Laemmli buffer* containing no sample. In this work 1 or 2 wells were loaded with the mixture of protein standards (1 µl for silver stained gels). After the filling the lower and upper buffer chambers with the same buffers as those used in 2-DE, and assembling electrophoresis unit, electrophoresis run was started and performed under constant voltage 125 V, for about 1 hour.
Gels were run at room temperature and the run was terminated when the tracking dye reached the bottom of the gel.

4.7. Gel fixing

After termination of electrophoresis run, 1-DE and 2-DE gels were carefully removed from plates, the stacking gel was cut out and discarded and the gels were immersed on *Fixing solution B1* with gentle shaking overnight.

4.8. Silver staining protocol according of Blum et al.[250]

Silver staining procedure was performed by gently shaking gels immersed in about 400 ml of needed reagent (volume for two gels, 20 X 20 cm), always using reagent grade chemicals. The conductivity of deionised water was less than 2 µS and to prevent the contamination, powder free latex glows were always used.
Silver staining protocol employed in this work has been presented in Table 4.9.

Table 4.9. Silver staining protocol.

Step	Reagent	Duration
Fixing	*Fixing reagent D1*	> 1hour, overnight
Washing	*Wash-solution D2*	2 X 20 min
Washing	Deionised water	20 min
Sensitizer	*Thiosulfate reagent D3*	1 min
Washing	Deionised water	3 X 20 sec
Silver	*Silver nitrate reagent D4*	20 min
Washing	Deionised water	3 X 20 sec
Development	*Developer reagent D5*	2-5 min
Washing	Deionised water	1X 20 sec
Stop	*Glycine stop reagent D6*	5 min
Washing	Deionised water	3X 10 min

4.9. Coomassie staining

Coomassie staining procedure, compatible with subsequent MALDI-TOF analysis, included gel fixing, staining and destaining steps. It was performed according Table 4.10.

Table 4.10. Mass spectrometry compatible Coomassie staining protocol.

Step	Reagent	Duration
Fixing	*Fixing reagent E1*	1 hour
Washing	Deionised water	2 X 1 min
Staining	*Coomassie staining reagent E2*	until spot/band is visible
Destaining I	*Destaining reagent I, E3*	30 min
Destaining II	*Destaining reagent II, E4*	change solution until clear background

4.10. Gel scanning

After the gel staining procedure, gels were placed on the scanner plate of Biorad Densitometer GS 710. Each gel was placed at the same position on the scanner plate and all gels were scanned using the same orientation. Gel analysis was done using PDQuest 6.2.1. (Bio-Rad Laboratories, USA).

4.11. Gel drying

For permanent storage gels were dried in the air gel-drying system. The inner part of the Gel Frame was placed on the loading platform; a wetted cellophane sheet was laid down, then the gel, and finally another cellophane sheet. The outer frame was set down and locked with quarter turns of the knobs. Finally the Gel Frames were placed into the open air drying oven, and dried 2-3 hours.

4.12. In-gel digestion of excised protein spots of silver-stained gels.

In this work for the tryptic digestion of proteins from a silver-stained spots, procedure based on the method developed by Gharahdaghi et al. was emplyed[131].

In order to reduce the background interferences and improve detectability for MALDI-TOF MS analysis, gel spots were destained prior to enzymatic digestion.

Washing /destaining

a. Gel slab was washed with Milli-Q water 2 X 15 min
b. Using a clean scalpel the spots of interest were excised from the gel (as close to the spot as possible to minimize the amount of background gel), cut into roughly 1 mm cubes and placed in an clean 500 µl Eppeddorf tube in approximately 50-100 µl Milli-Q. A gel piece of roughly the same size was excised from a gel region which does not carry any protein (control).
c. Stained gel pieces are destained in approximately 100 µl mixture of 1:1 30 mM *Potassium ferricyanide solution F1* and 100 mM *Sodium thiosulfate solution F2* for 5-10 min (until silver stain disappears). After destaining gels were rinsed with Milli-Q water until yellow color disappears (3-4 X 15 min). The solution was pulled off and discarded and the gel pieces were washed with acetonitrile 50 % (v/v) 2 X 15 min. Solvent volumes used in the washing step were roughly same as the gel volume.
d. The liquid was removed and gel particles were covered with acetonitrile (*dehydration*). After the gel pieces have shrunk (they become milky and stick together, after 2-3 min) acetonitrile was removed and gel pieces were rehydrated with 50-100 µl, 50 mM *Ammonium bicarbonate buffer solution F3* for 5 min followed by the addition of an equal volume (50-100 µl) of acetonitrile and incubation for 15 min. Solution was pulled off and discarded, and gel particles were dried in vacuum centrifuge.

Reduction and alkylation

a. Samples were removed from the speed vacuum and let cool.
b. For the reduction of protein disulfide bonds gel particles were swollen in 50µl freshly prepared 10 mM DTT in 50 mM A*mmonium bicarbonate buffer solution F3* and incubated at 56 °C in thermocycler for 45 min. Tubes were removed, chilled to room temperature and excess liquid was removed.

c. For alkylation, 50 µl of freshly prepared solution of 55 mM IAM in 50 mM A*mmonium bicarbonate buffer solution F3* were immediately added and incubated at room temperature for 30 min in the dark.
d. IAM solution was removed and gel particles were washed with 50 µl 50 mM *Ammonium bicarbonate buffer solution F3* and incubated at room temperature for 5 min. After incubation, 50 µl of acetonitrile are added to make 1:1 solution of acetonitrile: 50 mM *Ammonium bicarbonate buffer solution F3*, then incubated at room temperature for 15 min. Solution was pulled off and discarded, and gel particles were dried in vacuum centrifuge.

Tryptic digestion

a. Gel particles were rehydrated by adding *Digestion buffer F4*. 50 µl or enough *digestion buffer* was added to completely cover gel pieces and incubated at 4°C for 45 min. If gel pieces absorbed all the liquid more solution was added taking care to avoid formation of air bubbles. After that, the excess of liquid was removed, and 50 µl (or enough to cover gel pieces) of same buffer without trypsin were added and incubated at 37°C for 16 hours (overnight).

Extraction

a. The digestion mixture was briefly centrifuged (2 min, 15 000g) to gather evaporated liquid, condensed on the side and/or on the lid of tube. Supernatant is recovered in the new tube and saved at 4°C. Extraction was repeated two times with 20-30 µl solution *5 % Formic acid Sol F5: Acetonitril* 1:1 with 15 min incubation each.
b. All digestion extracts are pooled and completely dried in vacuum centrifuge.

Sample redissolution and MALDI-TOF sample presentation

Dry pellets of digestion extracts were resuspended in 5 µl of solution of 0.1 % *Trifluoroacetic acid Sol F6.*

Application of sample onto MALDI target is performed according the method which eliminates the mixing of sample with matrix prior to application to the Maldi target[159.] 0.5 µl of *Saturated matrix solution F7* (8mg *α-Cyano- 4-hydroxycinnamic acid*

dissolved in 1 ml mixture of 70 % *Acetonitrile* and 30% of the 0.1% *Trifluoroacetic acid Sol F6*) were applied onto the well of the Maldi target. After 1-2 seconds excess matrix was removed and target surface allowed to dry. After drying, 0.5 µl of sample solution was applied to the sample deposit area. While sample deposit was still wet, further 0.5µl of *Saturated matrix solution* were added and allowed to dry passively. In the same way were applied solutions of molecular mass standards.
All mass spectra were acquired on Compaq SEQ, Kratos Analytical, Manchester, UK MS instrument operated in positive reflectron mode, peptides were observed as $[M+H]^+$ ions.
For external calibration were used bradykinin fragment 1-7, angiotensin II, ACTH fragment 18-39 and insulin oxidized beta chain.

4.13. Deglycosylation experiments

The solutions of pharmaceutical preparations (23.8µl trastuzumab (Herceptin®), 150 mg/7.2 ml; 50 µl rituximab (Rituxan®),150 mg/10 ml and 20 µl abatacept (Orencia®) 250 mg/10 ml) were dialyzed against MilliQ-water for 3 days at 4 °C using cellulose membrane tubing (cut off value 12000-14000). Water was changed several times. After dialysis, solutions were freeze dried and lyophilised samples of pharmaceutical preparations (0.5 mg each) were dissolved in 49 µl of *Phosphate buffer pH 7.5* (*Sol. G1*) to obtain final concentration 500 µg/50 µl. In this study four methods of enzymatic deglycosilations were evaluated:

1. *Deglycosylation under reduced and denaturating conditions (Method 1)*
   For the reduction of proteins, prior to enzymatic digestion, 10 µl of sample solution (100 µg of each pharmaceutical substance), were mixed with 69 µl of the solution of 25 mM *Phosphate buffer pH 7.5* containing 0.1 % SDS, 1 µl 2-ME was added and mixture was boiled at 97 °C for 5 min. After reduction/denaturation step 10 µl *10% CHAPS in 0.1 % SDS (Solution G2)* and 10 µl (10 units) enzyme *PNGase F* were added and the mixture (total 100 µl) was incubated at 37 °C for 24 or 48 hours (see discussion section).

2. *Deglycosylation under nonreducing conditions employing nonionic surfactant (Method 2)*

   In this method immunoglobulin was not subjected to reduction with 2-ME neither it was boiled. Therefore in this case no denaturation has taken place. In order to increase deglycosylation efficiency non-ionic surfactant *0.5 % Triton X-100 (Solution G3)* was added.
   15 µl of sample solution (150 µg of each pharmaceutical substance) were mixed with S*olution G3* and the required volume of enzyme(s) (PNGaseF, Sialidase, O-Glycosidase) (Table. 4.11) and the mixture was incubated at room temperature for 24 hours.

3. *Deglycosylation under reducing conditions, with no surfactants and no previous boiling (Method 3)*

   15 µl of sample solution (150 µg of each pharmaceutical substance) were mixed with 1µl 2-ME, the required volume of enzyme(s) (PNGaseF, Sialidase, O-Glycosidase) and *Phosphate buffer pH 7.5* (*Solution G1*) to obtain total volume of 100 µl and the mixture was incubated at room temperature for 24 hours.

4. *Deglycosylation under non-reducing conditions, no surfactants added and no denaturation (Method 4).*

   15 µl of sample solution (150 µg of each pharmaceutical substance) were mixed with the required volume of enzyme(s) (PNGaseF, Sialidase, O-Glycosidase) and *Phosphate buffer pH 7.5* (*Sol. G1*) to obtain total volume of 100 µl and the mixture was incubated at room temperature for 24 hours.

Table 4.11. Deeglycosilation of dialysed pharmaceutical formulations of trastuzumab, rituximab, and abatacept.
Digestion buffer: *0.5 % Triton X-100 (Solution G3)*(Method 2)
Phosphate buffer pH 7.5 (*Solution G1)*(Methods 3 and 4)
For Method 3, the volume of Digestion buffer was for 1µl lower (as much was the volume of added 2-ME). Volumes of enzymes and samples are the same.
*__Trastuzumab__: enzymatic deglycosilation study (PNGase-F and Sialidase) and lysin truncation study (Carboxypeptidase B). **Rituximab**: enzymatic deglycosilation study (PNGase-F) and lysin truncation study (Carboxypeptidase B). **Abatacept**: enzymatic deglycosilation study (PNGase-F, Sialidase, O-Glycosidase) and lysin truncation study (Carboxypeptidase B).

Sample Nr.	*Enzyme treatment*	*Sample (µl)**	*Enz 1 (µl)*	*Enz 2 (µl)*	*Enz 3 (µl)*	*Digestion buffer (µl)*	*Total (µl)*
1	PNGase-F	15 µl	15 µl			70 µl	100 µl
2	Sialidase	15 µl		3 µl		82 µl	100 µl
3	Sialidase O-Glycosidase	15 µl		3 µl	9 µl	73 µl	100 µl
4	PNGase-F Sialidase	15 µl	15 µl	3 µl		67 µl	100 µl
5	PNGase-F Sialidase O-Glycosidase	15 µl	15 µl	3 µl	9 µl	58 µl	100 µl

Enzyme 1. N-Glycosidase F

PNgase F of *Flavobacterium meningosepticum, rec.* from *E. coli*, lyophilizate, 100 U. Cat. Nr. 113 651 85. Content dissolved in 100 µl MilliQ water results in a concentration of 100 mM sodium phosphate buffer, 25 mM EDTA, pH 7.2 and N-Glycosidase F 100 U/100 µl.

Enzyme 2. Neuraminidase (Sialidase)

Cat Nr. 10 269 611 from *Arthrobacter ureafaciens* 1 U (100 µl).

Enzyme 3.O-Glycosidase

O-Glycan peptide hydrolase (Cat.No. 11 347 101 from *Diplococcus pneuminiae* 25 mU (50 µl).
After finishing the digestion samples were stored at - 80 °C.

4.13.1. Carboxypeptidase B treatment

For the study of lysine truncation **Carboxypeptidase B**, 5 mg/ml (specific activity: 150 U/mg) from pig pancreas Cat. Nr 101 032 33, was used.
15 µl of sample solution (150 µg of each pharmaceutical substance) were mixed with 1 µl Carboxypeptidase B and 84 µl *Phosphate buffer pH 7.5* (*Sol. G1*) to obtain total volume of 100 µl and the mixture was incubated at 37 °C for 24 hours.
Simultaneous treatment including Carboxypeptidase B and deglycosilation enzymes (Table 10) was carried out adding 1 µl Carboxypeptidase B, required volumes of other enzymes and digestion buffer to adjust total volume to 100 µl.

4.13.2. N-Linked oligosaccharide release and storage

For the release of N-linked oligosaccharides slightly modified methods described by Kamoda et al[174, 272] were used.

1. A freeze dried samples of studied recombinant therapeutic proteins (1 mg), were dissolved in 100 µl of *Phosphate buffer pH 7.5* (*Solution G1*) followed by addition of PNGase F (10 U, 10 µl). After the incubation at 37°C overnight, the digestion mixture was boiled for 5 min and centrifuged (15000 *X g* for 15 min) and the supernatant containing released N-linked oligosaccharides was dried in centrifugal vacuum evaporator.
2. A freeze dried samples of studied recombinant therapeutic proteins (0.5 mg), were dissolved in 50 µl of *Phosphate buffer pH 7.5* (*Solution G1*) followed by addition of 1 µl 2-ME and PNGase F (10 U, 10 µl). After the incubation at 37°C overnight, 150 µl ethanol were added into the digestion mixture. After centrifugation (15000 *X g* for 15 min) the supernatant containing released N-linked oligosaccharides was dried in centrifugal vacuum evaporator.

Lyophilised samples containing released N-linked oligosaccharides were stored at -80°C. N-deglycosilated trastuzumab and rituximab, precipitated after 5 min boiling (Method 1) and addition of 150 µl ethanol (Method 2). However precipitation of N-deglycosilated abatacept was achieved only when Method 2 was employed.

5. Results and discussion

5.1. Gel electrophoresis analysis of trastuzumab

One-dimensional gel electrophoresis (1D-SDS-PAGE) under reducing and non-reducing conditions, and two-dimensional gel electrophoresis (2-DE) are used for the examination of quality related aspects of recombinant monoclonal antibody, trastuzumab (Herceptin®).

This study involved the examination of different factors influencing electrophoretic behavior of this complex molecule. 1-DE and 2-DE experiments run under different conditions were used not only to estimate its molecular weight and isoelectric point, but they served to study its isomorf and charge heterogeneity pattern. In addition, stability study involving stressed degradation and long-term conditions has been addressed, as well. The aim was to assess the capability of planar electrophoresis methods to detect the changes which arise upon different storage conditions of the drug product, and to assess its degradation profile.

For assessment of the influence of glycosylation in trastuzumab charge heterogeneity pattern, and preparation of sample for subsequent MALDI-TOF analysis, enzymatic deglycosilation study has been performed in 1- and 2-De setting involving the use of different enzymes.

5.1.1. One dimensional (1D-SDS-PAGE) gel electrophoresis analysis of trastuzumab

5. 1.1.1. Molecular weight estimation and sensitivity of staining

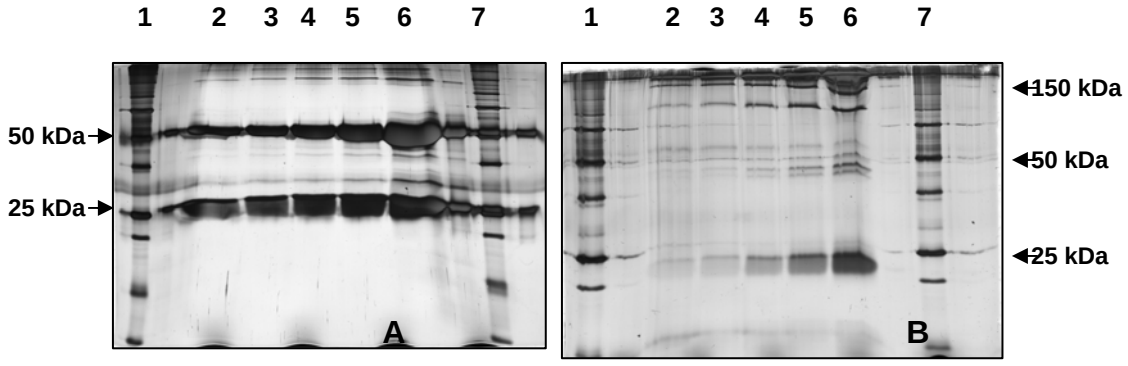

Fig. 5.14 A) 1-DE analysis of trastuzumab under reducing conditions. Acrylamid 12.5 %, %C 2.6%. Silver staining. Lanes **2-6**: Trastuzumab 1.3-20.5 µg., Lanes **1**, **7** MW standards. B). 1-DE analysis of trastuzumab under non-reducing conditions.Lanes **2-6**: Trastuzumab, 1.3-20.5 µg Lanes **1**, **7** MW standards

SDS-PAGE gels of trastuzumab under reducing and nonreducing conditions are presented in Fig. 5.14.

Under reducing conditions (Fig 5.14.A) trastuzumab is resolved in two distinct molecular weight species which migrated in two bands, upper band at about 50 kDa and lower band at about 23 kDa, confirming the migration behavior typical for IgG antibodies which are composed of two identical subunits each composed by two polypeptide chains, two heavy and two light chains, linked via disulfide bonds. Trastuzumab is an antibody molecule and therefore its basic monomer structure upon reducing conditions is cleaved in 4 polypeptide chains. Its heavy chains contain 450 amino acids and in SDS-PGE gel migrated at about 50 kDa. Light chains contain 214 amino acids and as seen in Fig 20 migrate at about 23 kDa.

This migration behavior matches with the molecular weights of trastuzumab heavy and light chains, calculated from their corresponding cDNA derived amino acid sequences (49.285 kDa and 23.443 kDa, respectively). The apparent molecular weight of the heavy chain is about 50 kDa and this difference is due to the co translational attachment of N-linked glycans which contribute in the increase of its molecular weight for about 3-5 %[174].

Under non-reducing conditions, migration behavior of trastuzumab monomer was different. It migrated at molecular weight about 150 kDa, and in contrast with reducing conditions, the band sharpness was reduced (Fig 5.14.B). The molecular weight of ~150 kDa is the sum of 2 heavy chains, each ~50 kDa and two light chains each ~23.5 kDa.

From Fig. 5.14.A is seen that band intensity was proportional to sample amount, provided that lower sample concentrations generated sharper bands.

To assess the sensitivity of silver and Coomassie staining procedures lower concentration of trastuzumab were subjected to 1-D electrophoresis under reducing conditions.

As shown in the Fig 5.15.A bands of heavy and light chains are detected even at very low sample amount, 0.005 μg trastuzumab (Fig 5.15.A, lane 6). Comparing with silver staining Coomassie staining resulted to be less sensitive. As seen in Fig 5.15.B and 5.15.C, trastuzumab light and heavy chain bands were detected in both gels. However, for trastuzumab amount 0.01 μg, bands of both chains are detected only in silver stained gels (Fig 5.15.B, lane 1) and not in the Coomassie stained gel (Fig 5.15.C, lane 1).

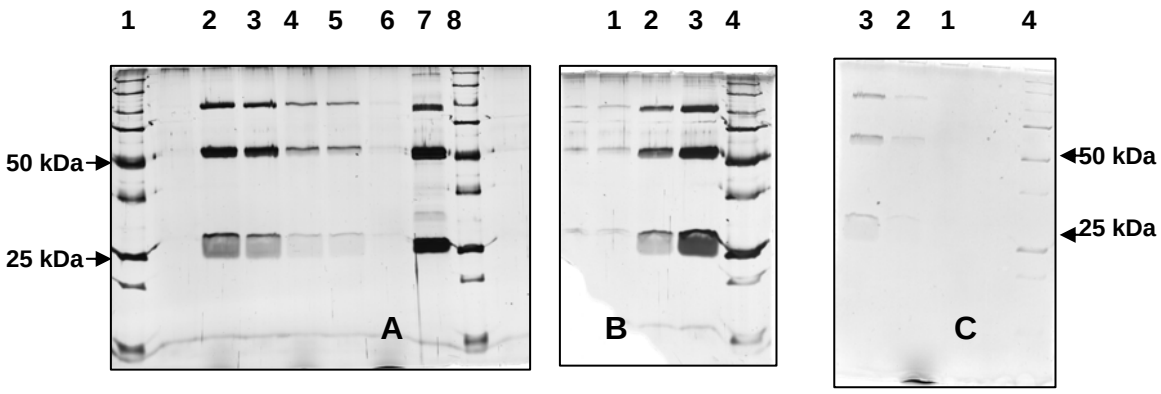

Fig 5.15 A) 1-DE analysis of trastuzumab under reducing conditions. *Silver staining*. Lanes **2-6**: Trastuzumab 0.52; 0.26; 0.1; 0.05; 0.005 µg. Lane **7**: 2 µg. Lanes **1**, **8**: MW standards. B). 1-DE analysis of trastuzumab under reducing conditions *Silver staining*. Lanes **1-3**: Trastuzumab, 0.01; 0.2; 1 µg. Lane **4**: MW standards. C). 1-DE analysis of trastuzumab under reducing conditions. *Coomassie staining*. Lanes **1-3**: Trastuzumab, 0.01; 0.2; 1 µg. Lane **4**: MW standards.

5.1.1.2. 1-DE. Deglycosilation optimisation study

N-glycosidase F was used for the removal of N-linked glycans from the trastuzumab molecule. In order to optimise the deglycosilation conditions, the influence of various factors such are reduction of sample, temperature, amount of enzyme, digestion time, and the use of different surfactants have been studied.

1. Deglycosilation under reducing and denaturating conditions (2ME, 97°C, SDS 0.1%, CHAPS 10 %

2. Deglycosilation under nonreducing conditions. Nonionic surfactant, Triton X-100, 0.5 %

3. Deglycosilation under reducing conditions, 2-ME, with no surfactants and no previous boiling

4. Deglycosilation under non-reducing conditions, no surfactants and no previous boiling

*In all studied methods phosphate buffer pH 7.2 was used. For the detailed information see experimental section (4.13. Deglycosylation experiments, page 102) Deglycosilation efficiency was monitored by comparison of deglycosilated and glycosilated (native) samples separated with 1-DE and 2-DE.

5.1.1.3. Preliminary deglycosilation experiments

In Fig. 5.16. 1-DE gels of trastuzumab treated with N-glycosidase F under different conditions are presented.

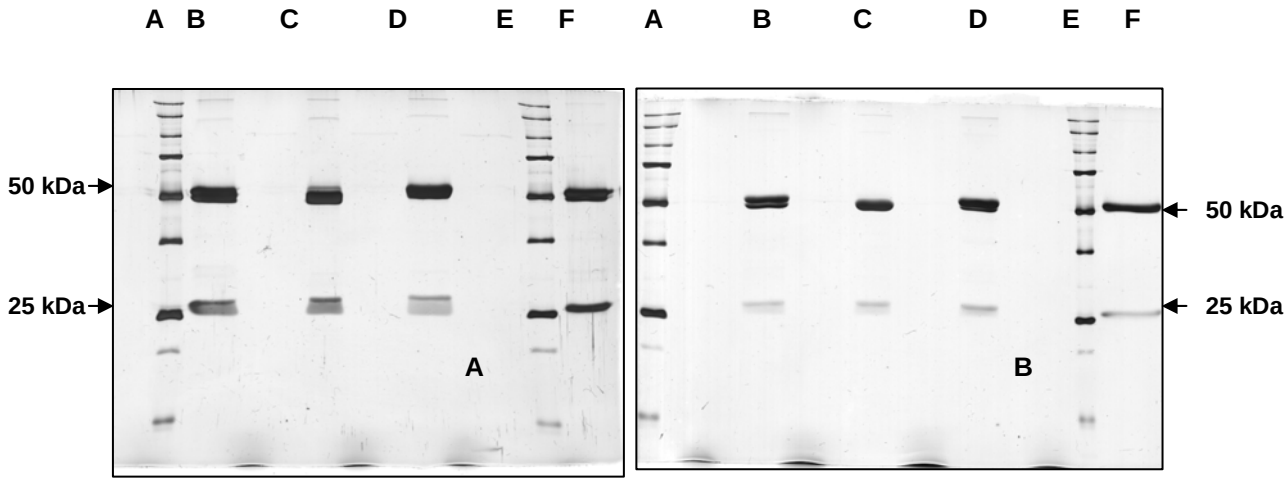

Fig 5.16. Deglycosilation monotorization. Trastuzumab 2 µg. Silver staining
A) Digestion time 24 h. Lanes **A** and **E** Molecular weght standards. Lane **B** and **F**: Method 1, 10 I.U.and 20 I.U. NGF, respectively. Lane **C**. Method 2, 10 I.U NGF. Lane **D**. Glycosilated sample/control.
B) Digestion time 48 h. Lanes **A** and **E** Molecular weght standards. Lane **B** and **D**: Method 1, 10 I.U.and 20 I.U. NGF, respectively. Lane **C**. Method 2, 10 I.U NGF. Lane **F**. Glycosilated sample/control.

Gels bands from Fig. 5.16 show that deglycosilation performed under condition of Method 1 (2-ME, with the denaturation of the sample 97 °C/10 min), brought about only partial deglycosilation. Splitting of heavy chain bands are split indicating non-efficient deglycosilation process (lanes B and F, Fig 5.16.A and B and D, Fig 5.16B, respectively).

On the other hand, lane C in both gels showed no splitting, with additional increase of the migration of heavy chain to lower molecular weight, comparing to glycosilated sample (lanes D, Fig 5.16.A and F, Fig 5.16.B, respectively). On the basis of these observations it is evident that the second deglycosilation method, which employs surfactant Triton X-100, without reduction and denaturation, is more efficient than the first method. The role of the surfactant is to increase the deglycosilation efficiency.

Actually, in native conformation the immunoglobulin G molecules are water soluble, provided that some interior regions of the molecule are highly hydrophobic. The possible cause for only partial deglycosilation in cases when 2-ME and boiling where employed is that upon denaturation, heavy chains of trastuzumab/and rituximab become insoluble. Hence, complete deglycosilation of glycans N-linked to amino acid asparagine N_{300} (trastuzumab) and N_{301} (rituximab) is difficult under denaturing conditions.

According the results from Fig. 5.16.A and B digestion time (24 and 48 hours) did not influence significantly the deglycosilation efficiency.

Monitorisation of deglycosilation efficiency for Methods 3 and 4 is depicted in the Fig. 5.17. The comparison of heavy chain bands of glycosilated trastuzumab (lane B) with the lines of heavy chains of deglycosilated trastuzumab according Methods 3 and 4 (lanes C and D, respectively) reveals that the molecular weights of both deglycosilated samples are substantially lower. Furthermore 1-DE data from Fig. 5.16 and Fig. 5.17 indicate that deglycosilation Methods 3 and 4 result as more efficient than Method 2. The first method, results the one with the lowest deglycosilation efficiency. These observations confirm that reduction and denaturation of immunoglobulins has negative impact in the deglycosilation efficiency which is in accordance with the literature data[251].

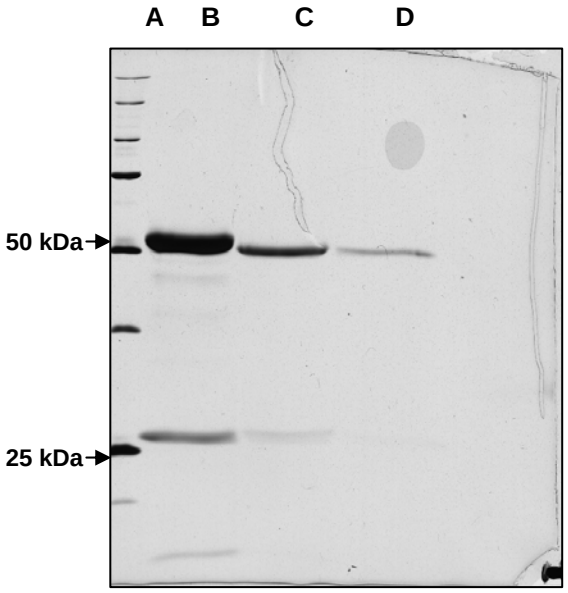

Fig 5.17. Deglycosilation monitorization. Trastuzumab 2 µg. Silver staining. Digestion time 24 h. 10 I.U. NGF. Lane **A**: Molecular weight standards. Lane **B**: Nondeglycosilated sample/control, Lane **C**: deglycosilated, Method 3, Lane **D**: Deglycosilated, Method 4

On the basis of deglycosilation optimization experiments, for both monoclonal antibodies trastuzumab and rituximab, Methods 3 and 4 resulted as optimal. However, in the case of abatacept, all deglycosilation methods, except the Method 1 were of similar efficiency. This could be explained taking into consideration solubilities of recombinant monoclonal antibodies (trastuzumab and rituximab) heavy chains and abatacept. The solubility of latter is better.

5.1.2. Two-dimensional (2-DE) gel electrophoresis analysis of trastuzumab

Preliminary two-dimensional gel electrophoresis 2-DE experiments are performed using immobiline gradients of *pH 3-11 NL* and *pH 6-9 L*. The study of trastuzumab charge heterogeneity, deglycosilation optimization and stability has been carried out employing different 2-DE conditions. For the optimization purpose different factors such are concentration of sample, immobiline pH gradient, gel concentration and staining procedure were evaluated.

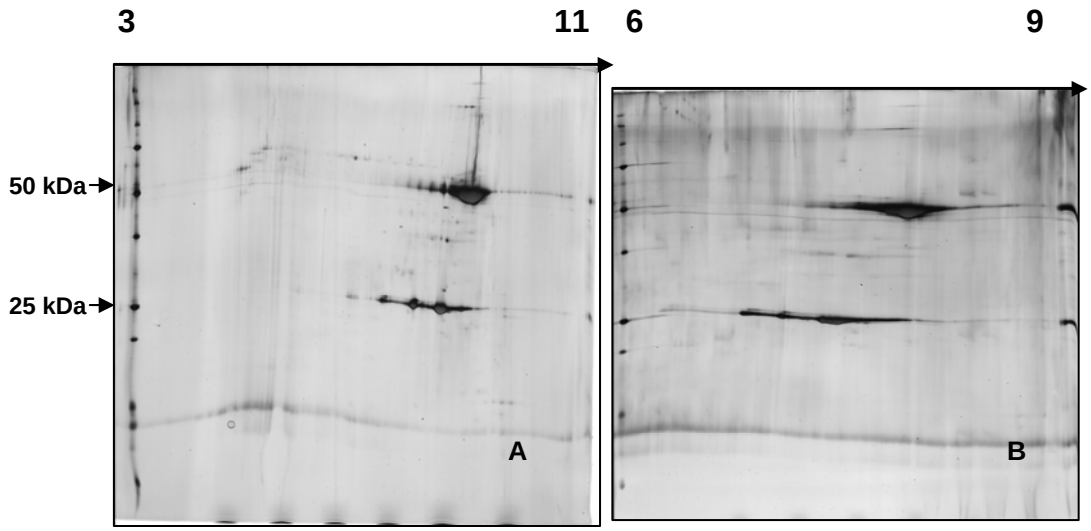

Fig. 5.18. 2-DE analysis of trastuzumab, 10 µg, Silver staining. A) *IPG* 3-11 NL, B**)** 6-9 L

On the bases of 2 DE experiments (Fig 5.18), results that after reduction of disulfide bonds trastuzumab subjected to 2-DE, demonstrated typical complex spot pattern of recombinant monoclonal antibodies. Its heavy chains in 2 DE gel migrated at molecular weight ~ 50 kD with the *pI* value between 6.5 and 8.7. The theoretical *pI* value of the trastuzumab heavy chain is 8.49 and its theoretical molecular weight

49.285 kDa. Trastuzumab light chain migrated at molecular weight ~23 kDa and *pI* ranged 5.7 to 8.1. Theoretic *pI* derived from its cDNA sequence is 7.76[252].

Trastuzumab spot pattern shows high degree of complexity which is typical for electrophoretic behavior of all antibody molecules. Like rituximab, another rmAbs studied in this work, the spot pattern of trastuzumab consists on numerous poorly resolved and overlapped spots tending to spread as bands. The degree of heavy chain complexity is apparently higher than of the light chain suggesting the contribution of the heavy chain glycosylation in the additional complexity.

As noted in Fig. 5.18., for the same sample concentration, the resolution of heavy and light chain spots is higher when immobilized *pH* gradient *3-11 NL* is employed. The superior resolution comparing to the immobilized *pH* gradient *6-9 L* was observed in all trastuzumab (and rituximab) studied gels.

Another factor which affected the spot resolution was the amount of applied sample. In the gels studied so far, independently from the type of *immobilized pI* gradient, reduction of sample concentration generally brought about improvement in the spot resolution, (Fig. 5.19.).

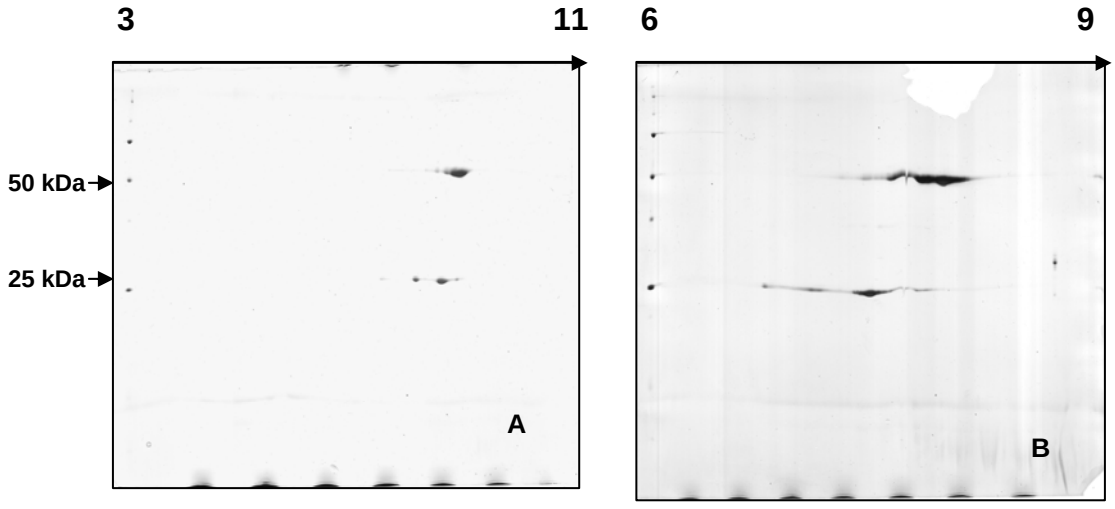

Fig 5.19. 2-DE analysis of trastuzumab, 10 µg, Silver staining. A) *IPG* 3-11 NL, 5.2µg, B**)** 6-9 L, 5.2 µg.

2 DE of trastuzumab at the acrylamide concentration of 10 %, 12.5 % and 15 % has been studied, as well.

As expected, the mobility of both chains in more concentrated gels was lower than in the more diluted gels (Fig. 5.20). The intermediate gel concentration of 12.5 % was selected as optimal and all analysis were performed at this acrylamide concentration hereof.

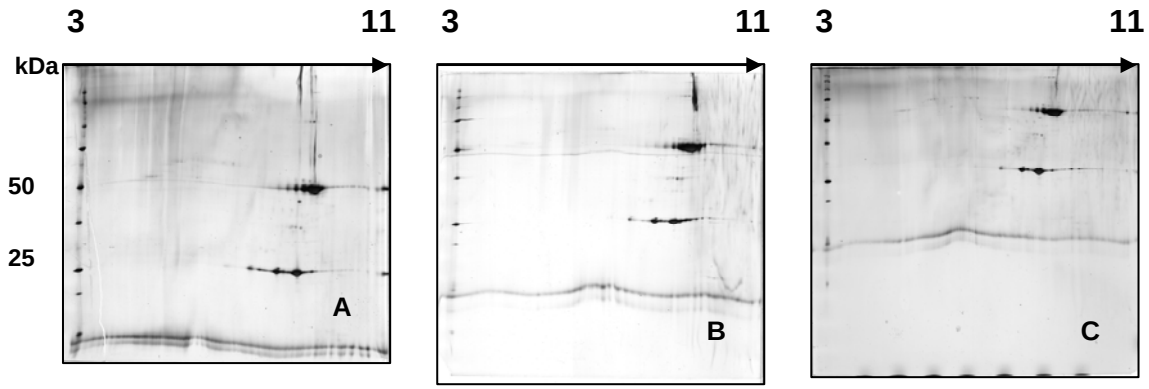

Fig. 5.20 2-DE analysis of trastuzumab, 10 µg, Silver staining. A) 10 %; B) 12.5 %; C) 15 %

5.1.2.1. 2-DE. Deglycosilation optimization study

N-Glycosidase F treatment of trastuzumab employing Method 1 provided 2-DE results similar with 1-DE experiments: trastuzumab heavy chain split in two parts, the lower part tending toward the lower pI values (Fig. 5.21.).

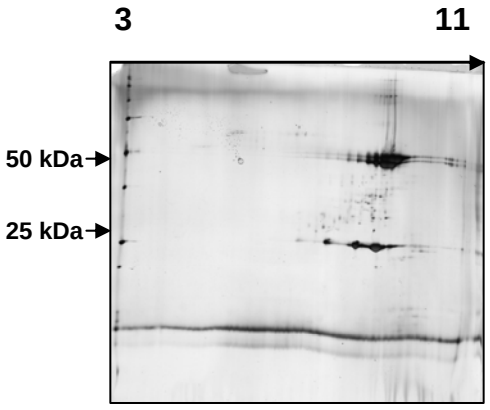

Fig. 5.21. Deglycosilation monitorization. Trastuzumab 10 µg. Silver staining. Method 1

On the other hand, 2-DE gels offered no possibility to assess the molecular weight difference between glycosylated and deglycosilated trastuzumab heavy chains according Methods 2,3 and 4 (Fig. 5.22).

In Fig. 5.22 (A and B) 2-DE gels obtained from deglycosilated trastuzumab are presented. For the N-glycan release Method 2 employing nonionic surfactant, Triton X-100 was employed.

As mentioned above, the difference between molecular weight of trastuzumab heavy chain in glycosilated and its native form is only about 3-5 % therefore this small difference is difficult to notice in 2-DE gels

In the first dimension immobiline pH gradients 6-9 L and 3-11 NL were used.

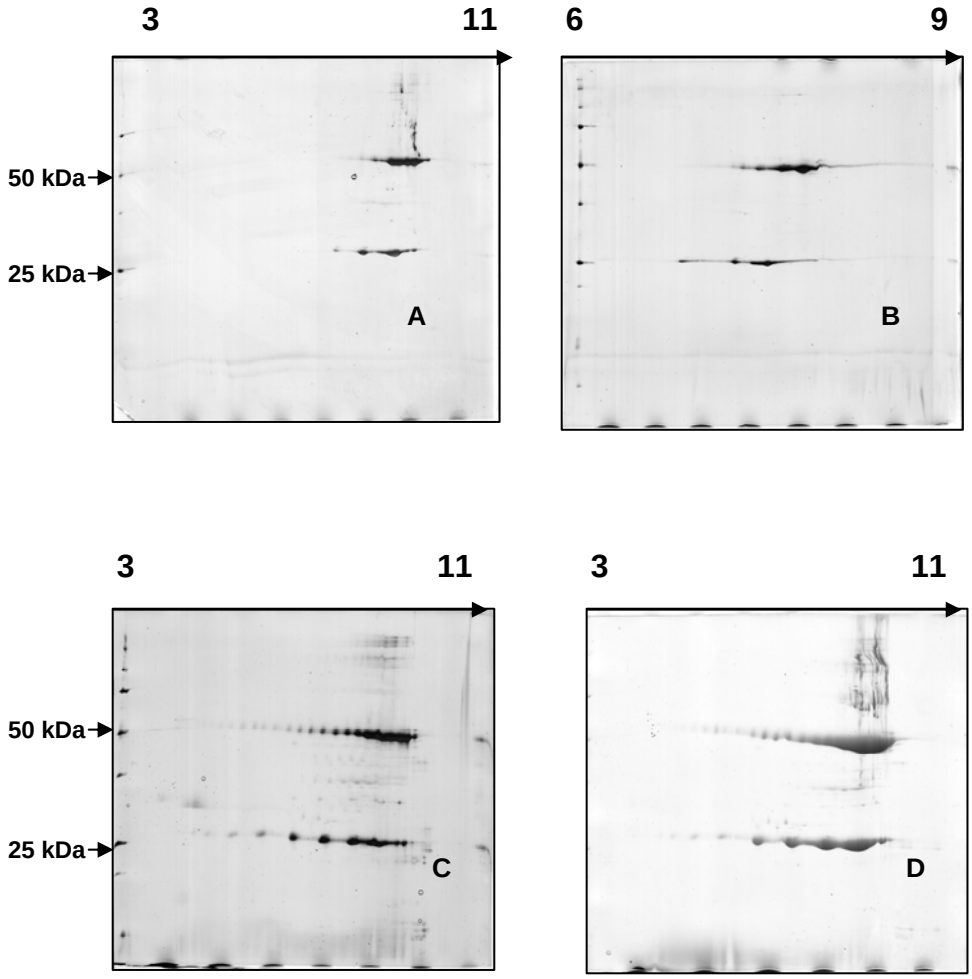

Fig 5.22. Deglycosilation monitorization. Trastuzumab 8.3 µg. Silver staining. Method 2. Non-reduced, Triton X-100, 10 I.U. NGF **A**) 3-11 NL, **B)** 6-9 L, **C)** Trastuzumab 100 µg, Method 4. **D)** Trastuzumab 100 µg, Method 4, Coomassie staining.

There were two principal reasons why Methods 3 and 4 were used for the deglycosilation of recombinant antibodies trastuzumab and rituximab, which after 2-DE separation and in gel tryptic digestion were subjected to MALDI-TOF analysis: first, because 1-DE data confirmed their superior efficiency in comparison with Methods 1 and 2, and second, the detergent absence facilitates subsequent MALDI-

TOF analysis. Literature data report that many detergents have negative impact on the MALDI-TOF process [251]. In Fig. 5.22. silver and Coomassie stained 2-DE gels of deglycosilated trastuzumab employing deglycosilation Method 4 are presented.
2-DE experiments showed no significant difference in the charge heterogeneity between deglycosilated and glycosilated trastuzumab samples.
As a consequence of N-glycosidase F action asparagine N_{300} on the trastuzumab molecule is converted to aspartic acid D_{300}, and the polypeptide chain remains intact. The conversion of N to D adds a negative charge to proteins. For small proteins which are highly glycosilated and have large charge differences between glycosilated and deglycosilated forms (i.e. abatacept, EPO etc) the process of deglycosilation may be monitored on 1-DE and 2-DE gels, respectively[117]. For recombinant monoclonal antibodies like trastuzumab and rituximab, however, 2-DE results are equivocal. This is due to the fact that the mass of glycans in trastuzumab and rituximab heavy chains counts only 3-5 % of total polypeptide molecular mass. In addition, pI difference between deglycosilated and glycosilated forms of trastuzumab and rituximab heavy chains is very low (theoretically calculated about 0.13)[253] and this is obviously difficult to be assessed with 2-DE gels.

5.1.2.2. Charge heterogeneity study of trastuzumab

In order to study the contribution of N-linked glycans and the C-terminal terminal lysine truncation in the spot complexity of *rmAb* pharmaceutical trastuzumab, three selected enzymes have been employed: N-glycosidase F; sialidase and carboxypeptidase B.
Since published data indicate that IgG molecules (trastuzumab and rituximab) contain only N-glycans, O-deglycosilation study has been omitted[253].
For the first dimension, *IEF*, immobiline *pH* gradients 3-11 *NL* and 6-9 *L* have been employed. Deglycosilation efficiency was monitored with 1-DE.

5.1.2.3. Trastuzumab charge heterogeneity IPG 3-11 NL

2-DE experiments provided similar charge heterogeneity patterns for both recombinant monoclonal antibodies addressed in this study, trastuzumab and

rituximab. Numerous poorly resolved spots were observed in both chains, particularly in heavy chain.

Since the glycan composition of these two antibodies is similar[174], it was expected that enzymatic deglycosilation experiments would provide similar results in terms of their molecular weight, pI and spot complexity. After comparison of the 2-DE experimental data both studied rmAbs, this assumption resulted to be correct.

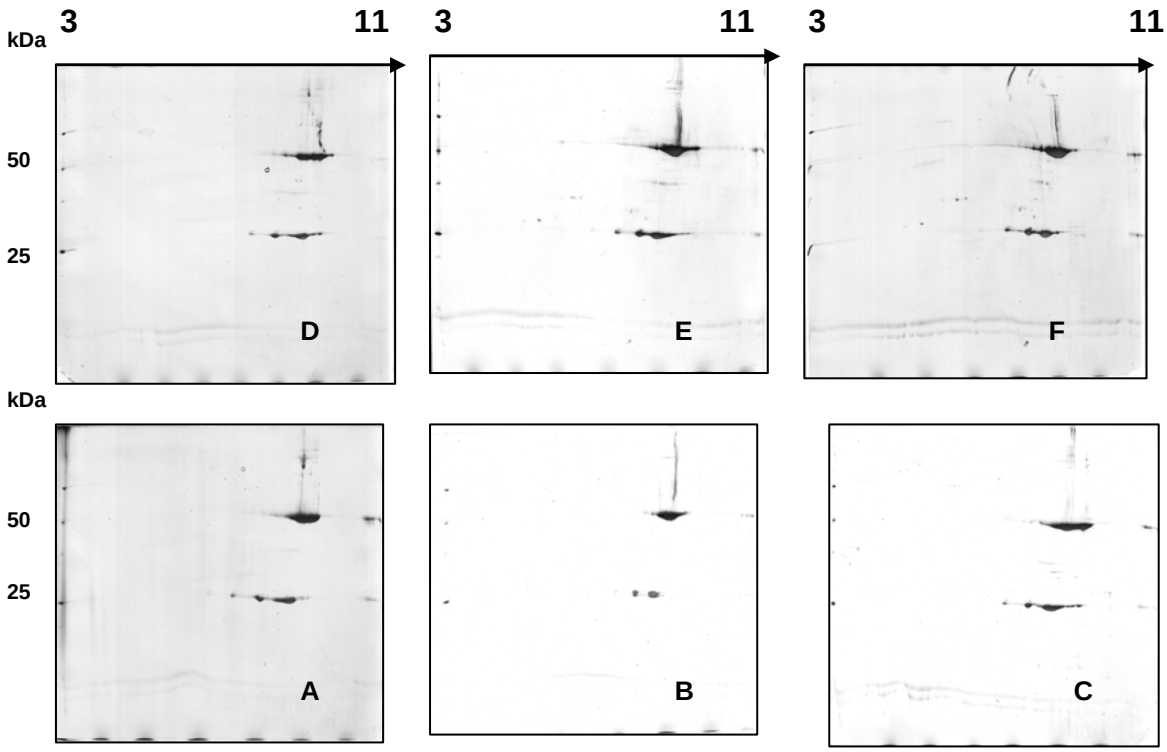

Fig. 5.23. Trastuzumab, 2-DE, 3-11 NL, 10 µg. Silver staining.
A. Control; **B.** Sialidase; **C.** Carboxypeptidase B, Sialidase, N-Glycosidase F;
D. N-Glycosidase F; **E.** Carboxypeptidase B; **F.** Carboxypeptidase B, Sialidase

As in other IgG_1 isotype antibodies, in trastuzumab molecule oligosaccharides are attached at asparagine N_{300}. 1-DE experiments comparing native and N-glycosidase F treated trastuzumab prove the presence of N-linked glycan molecules, however for the charge difference assessment 2-DE was needed.

After N-linked glycan release for each molecule of trastuzumab only one carboxylic acid of asparagic acid is released, therefore a low change in the *pI* is expected. Calculated from cDNA derived sequence this difference should be only 0.13 (ΔpI= pINg-pID= 8.49-8.36= 0.13).

As shown in Fig. 5.23, *pI* and MW difference between the control, native sample (gel 29A) and gels obtained from the N-deglycosilated, desialinated and Carboxypeptidase B treated samples is very low. The high value of gel to gel variation in the spot intensity, does not allow detecting this small changes. After sialidase treatment no change has been observed, suggesting that the N-linked sugars of trastuzumab pertain to complex biantennary type but without terminal sialic acid residues which is in accordance with the literature data[174, 232].
On the other hand, heavy chain terminal lysine truncation can be a source of charge heterogeneity. Again, comparing calculated theoretical *pI* values of trastuzumab and its truncated variant with no lysine at the position 450, the difference in *pI* is very low (ΔpI=0.13) to be detected with this method.

5.1.2.4. Trastuzumab charge heterogeneity IPG 6-9 L

In order to more accurately assess trastuzumab heavy chain *pI* changes, after its deglycosilation, narrower *immobiline pI gradient* was used in the first (IEF) dimension. However, experimental data showed that no *pI* differences between control and digested samples could be noticed (Fig 5.24, 5.25.).
In Fig. 5.25, 2-DE gels of controlled sample (A) and with different enzymes treated trastuzumab are shown. The sample amount of sample was increased to 50 µg.

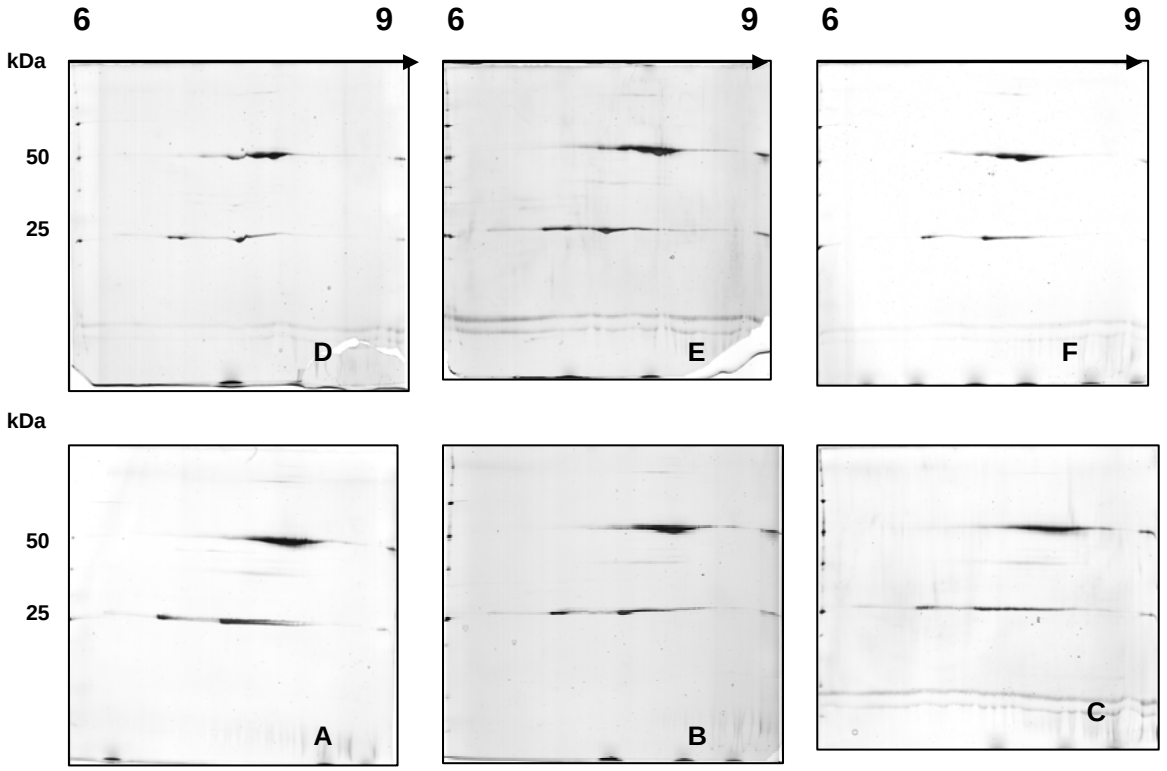

Fig. 5.24. Trastuzumab, 2-DE, 6-9 L. Silver staining.; **A.** Control; **B.** Carboxypeptidase B; **C.** Sialidase; **D.** N-glycosidase F, Carboxypeptidase B Sialidase; **E.** Sialidase, Carboxypeptidase B; **F.** N-Glycosidase F. Gels: **ABCF**, 25 µg trastuzumab. Gels: DE, 10 µg trastuzumab.

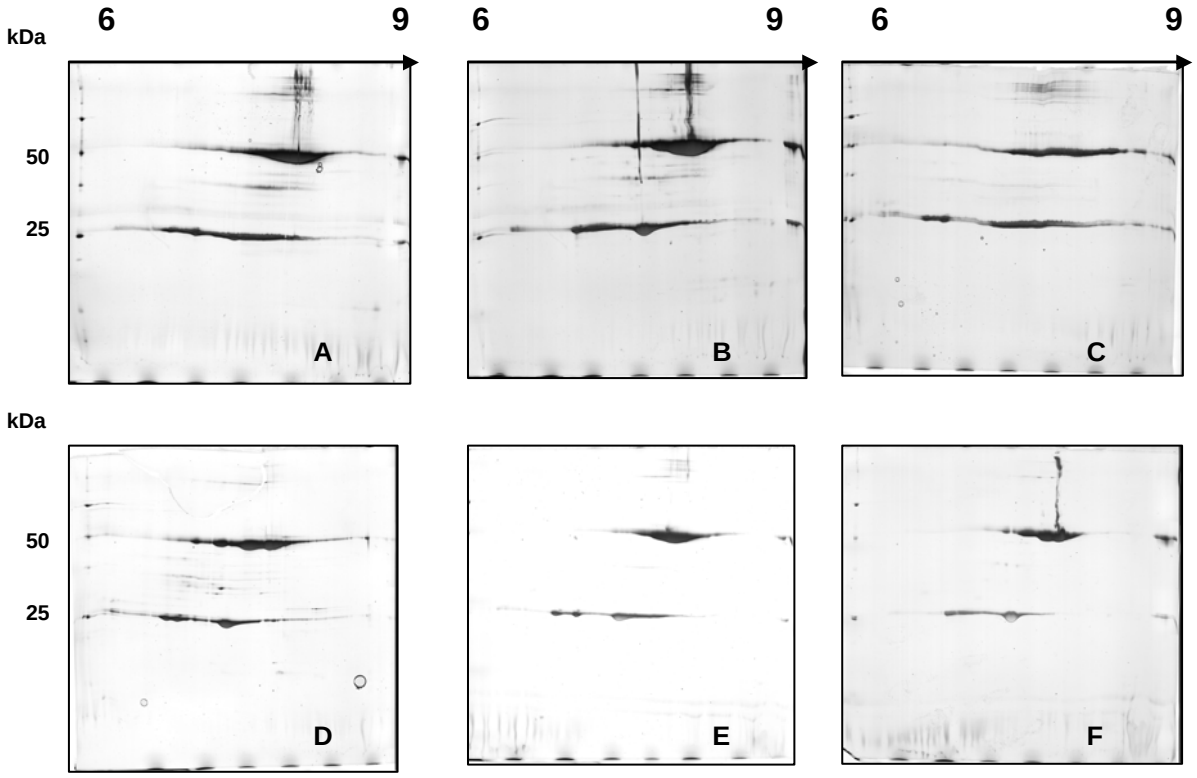

Fig. 5.25. Trastuzumab, 2-DE, 6-9 L, 50 µg. Silver staining. **A**: Control; **B**: Sialidase; **C**: N-Glycosidase F; **D**: Carboxypeptidase B, Sialidase, N-Glycosidase F; **E**: Carboxypeptidase B; **F**: Carboxypeptidase B, Sialidase

5.2. Stability study of trastuzumab

Recombinant monoclonal antibodies are biological products produced by the r DNA technology, therefore, like other protein pharmaceuticals; they also require extensive and stringent characterization of purity, structural integrity and stability[158]. A major obstacle in the development of protein drug formulations is the need to maintain the native, active protein structure both during the formulation process and upon long time storage[254].

Antibodies like other proteins are prone to a variety of physical and chemical degradation pathways. These products are particularly sensitive to environmental factors such as temperature changes, oxidation, light, ionic content and shear. All these factor can affect their potency, purity and quality[255].

Two major pathways of physical instability are denaturation and degradation. Precipitation and surface adsorption occur as well. Chemical degradation pathways include cross linking, deamidation, isomerisation, oxidation, and fragmentation[25]. Additionally, the glycosylation state of an antibody can significantly affect its degradation rate[256].

This study addressed thermal degradation of trastuzumab under accelerated storage conditions. 1-DE and 2-DE analyses were evaluated for their ability to monitor possible changes in electrophoretic pattern of trastuzumab upon forced degradation conditions, detect possible degradation products and assess the effect of other severe conditions (oxidation, low pH and shearing in the stability of this drug product.

The rate of chemical degradation was increased employing exaggerated conditions: higher temperature (room temperature, 40ºC); oxidation: H_2O_2 1 and 3 %, TFA in different concentrations and shearing.

5.2.1. Termo-degradation study

Freshly prepared reconstituted formulations of the drug substance were stored at the different conditions (room temperature, 4-8°C, 37°C, and 50°C) and after storage up to given time were analyzed with 1-DE and 2-DE. In Fig. 5.26, termodegradation study of trastuzumab solution stored at different temperatures is presented.

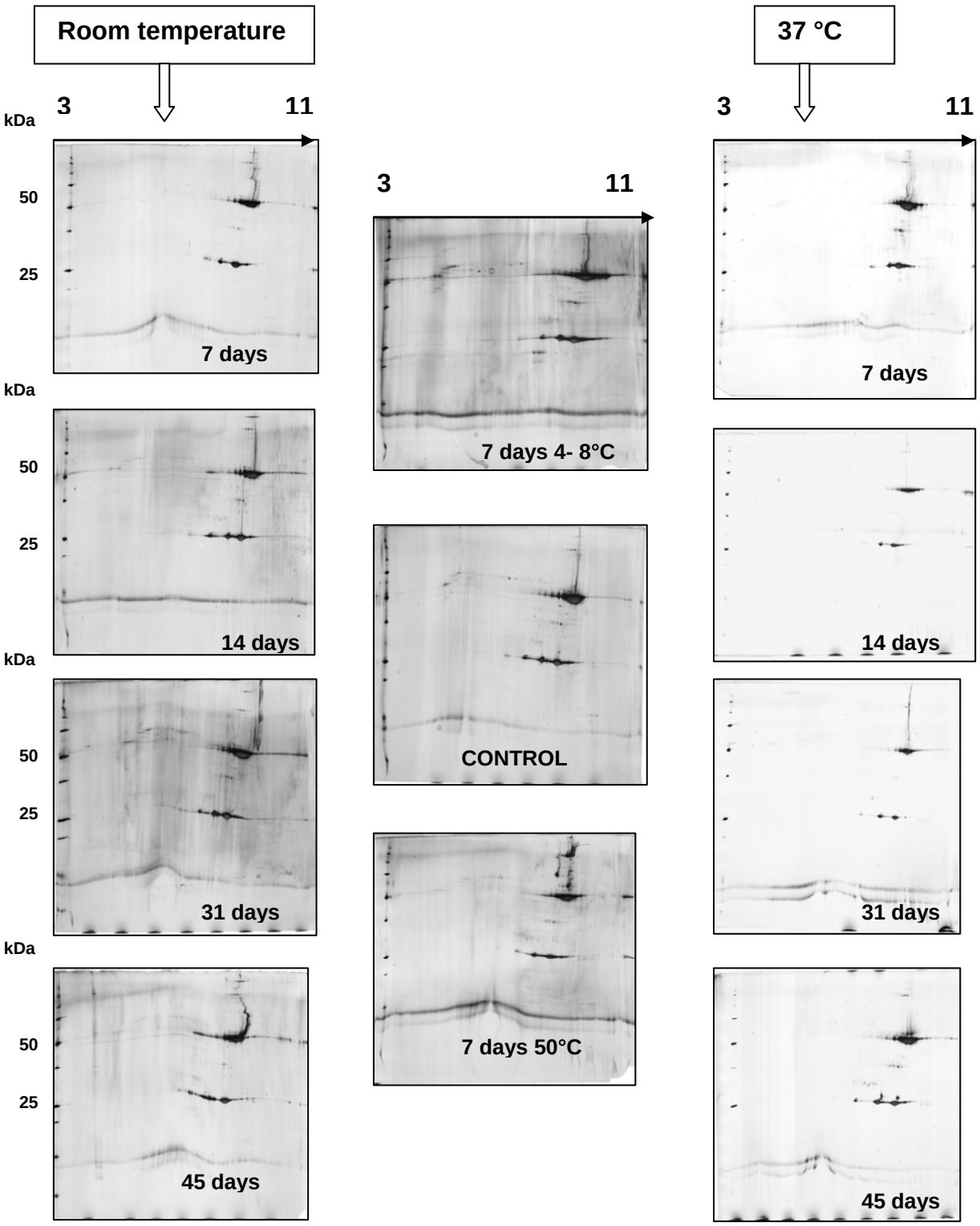

Fig. 5.26. Trastuzumab. 3-11 NL. Forced Degradation study. 3-11 NL. Silver staining

In order to assess long term stability of trastuzumab, its reconstituted solution was stored up to 90 days at the room temperature. For this analysis sample of different production series, has been used (Fig. 5.27)

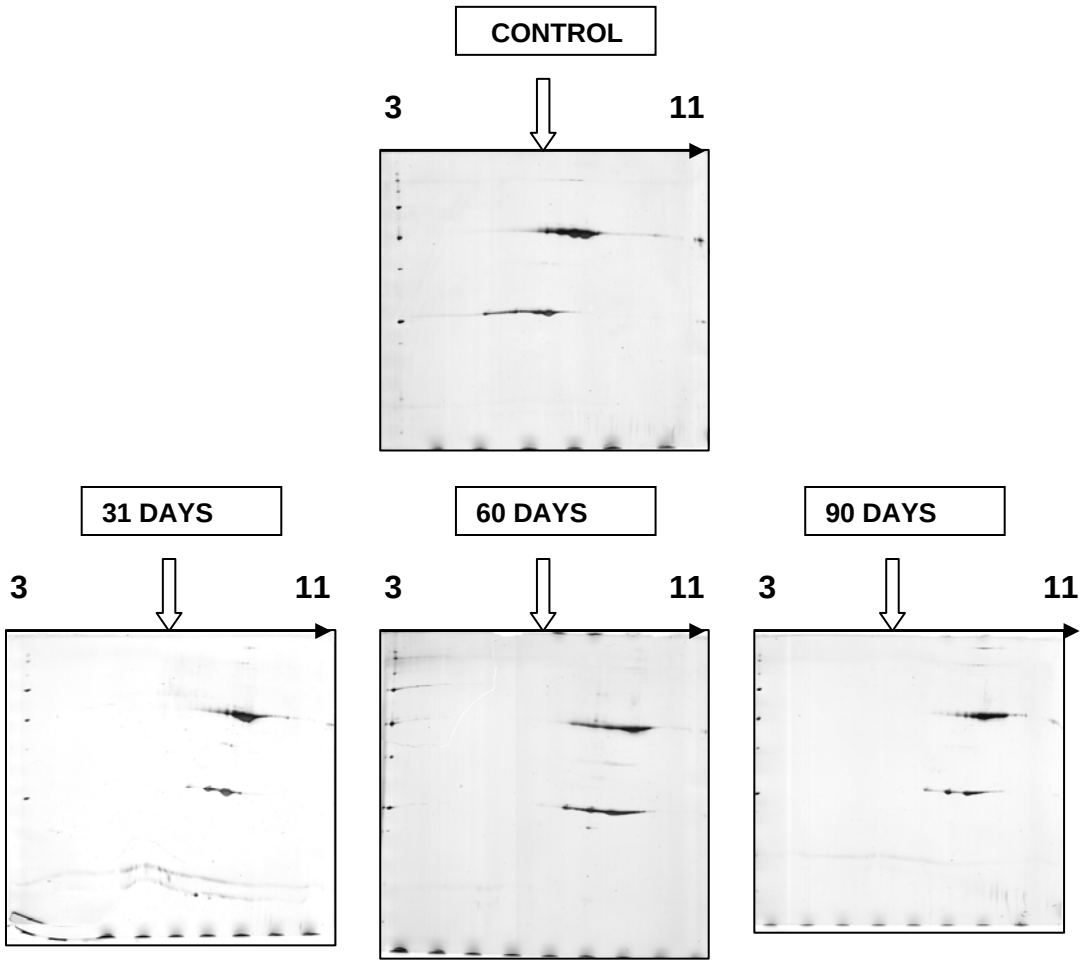

Fig. 5.27. Trastuzumab. Forced Degradation study.
Room temperature. 3-11 NL. Silver staining

Immobilized pH gradient strips *pI 6-9 L* were used for the first dimension in the following stability monitoring experiment (Fig. 5.28.).

However, experimental data revealed similar results with 2-DE with immobilized pH gradient 3 -11 NL.

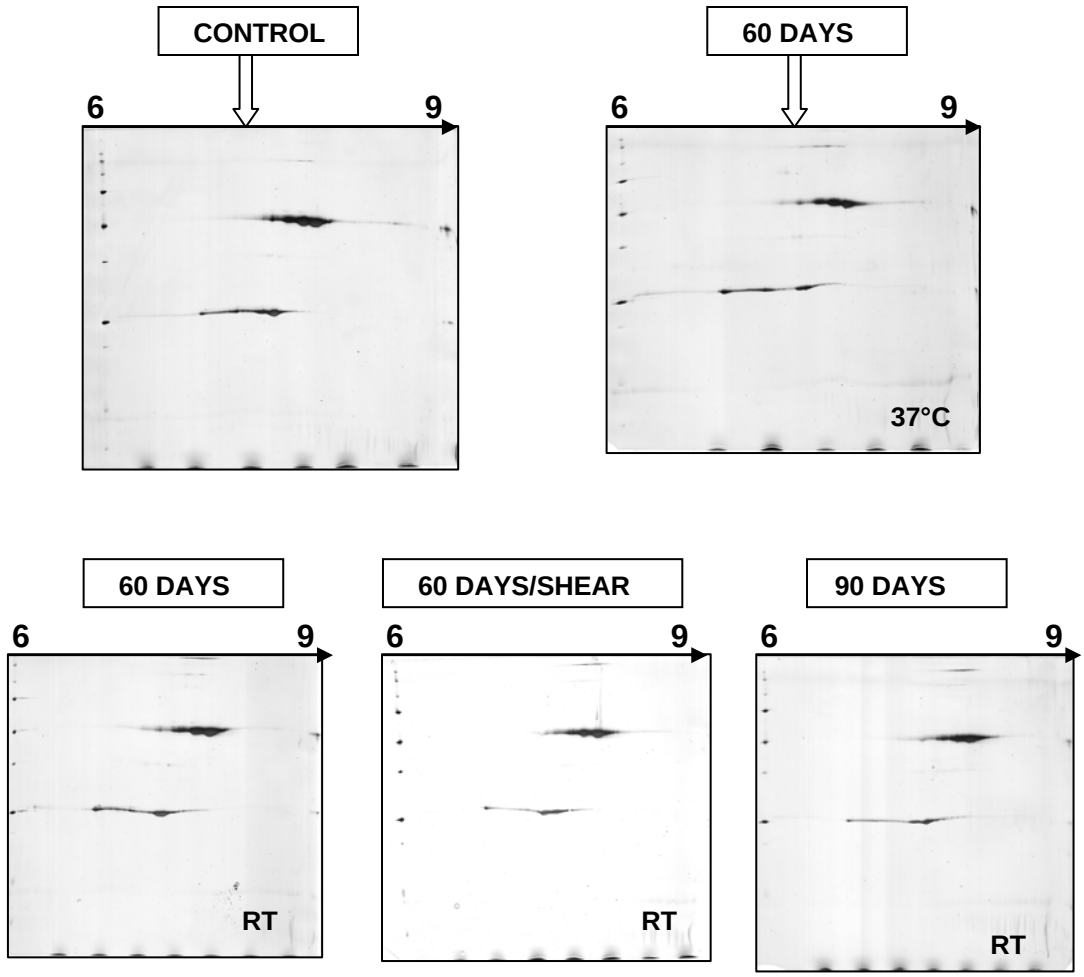

Fig. 5.28. Trastuzumab. Forced Degradation study.
Different temperatures/Shearing. 6-9 L. Silver staining

As seen from Figures 5.26, 5.27 and 5.28, 2-DE gels obtained from trastuzumab subjected to elevated temperatures (RT, 37°C and 50°C) could not reveal specific change (s) in the pI and MW of resulting spots even for aged samples (to 90 days).
The situation was different upon sample exposure to oxidation and lower pH values (Figures 5.29 and 5.30).
Significant differences in pI and MW of trastuzumab 2-DE spots are observed upon 7 day sample storage in the solution of 1 % trifluoroacetic acid, at room temperature, provided that elevated temperatures substantially accelerated degradation eventually leading to completely degradation and denaturation of sample (Fig. 5.29).

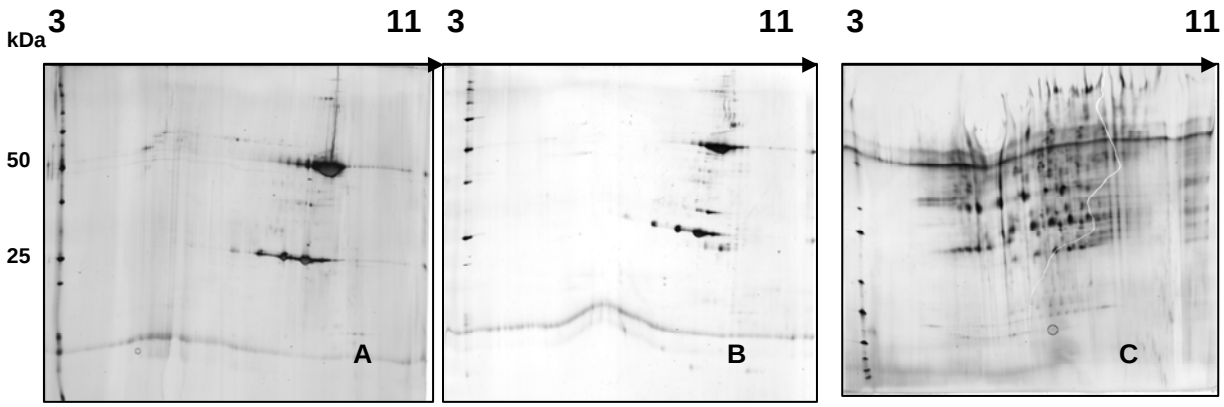

Fig. 5.29. Trastuzumab. 3-11 NL. Forced degradation study.Acidic conditions
A) Control, B) TFA 1 %, Room temperature, 7 days; C) TFA 1 % 50°C, 7 days

In Fig. 5.30., 2-DE gels of trastuzumab subjected to 1 and 3 % hydrogen peroxide solution are presented. After 7 day storage under these conditions, significant changes are observed, both in pI and MW of resulting spots. In Fig 5.30 B and 5.30 C numerous spots at pI 6-7 and around 30 kDa are noted in both gels.

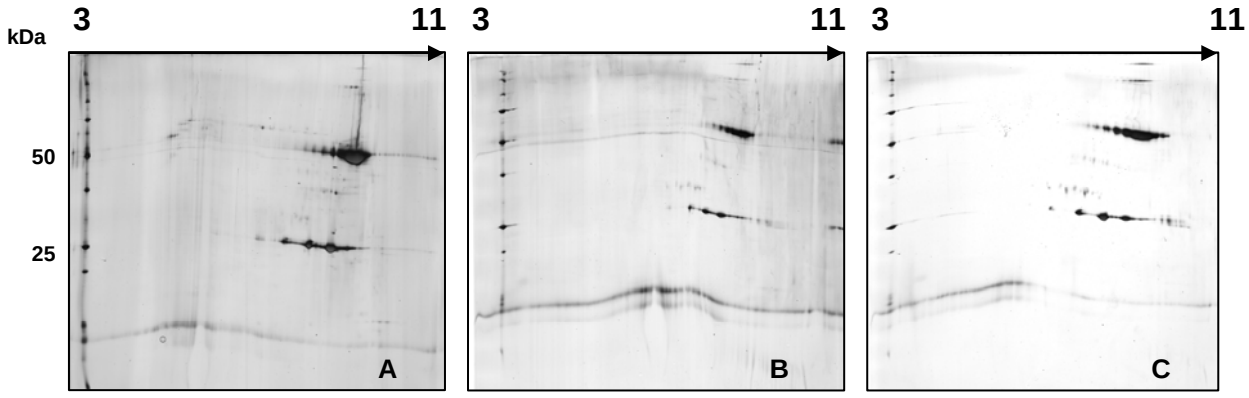

Fig. 5.30. Trastuzumab. 3-11 NL. Forced Degradation study. H_2O_2 A) Control,
B) H_2O_2 1 %, Room temperature, 7 days; C) H_2O_2 3 % Room temperature 7 days

An opened vial of trastuzumab was stored at room temperature, for 7, 14 and 30 days, respectively. Resulting 2-DE gels showed an interesting pattern of degraded sample, heavy chain spot size progressively reduced its size and new spots emerged

at about 30 kDa and pI around 6-7. A drastic change in shape of light chain spots was observed as well (Fig 5.31).

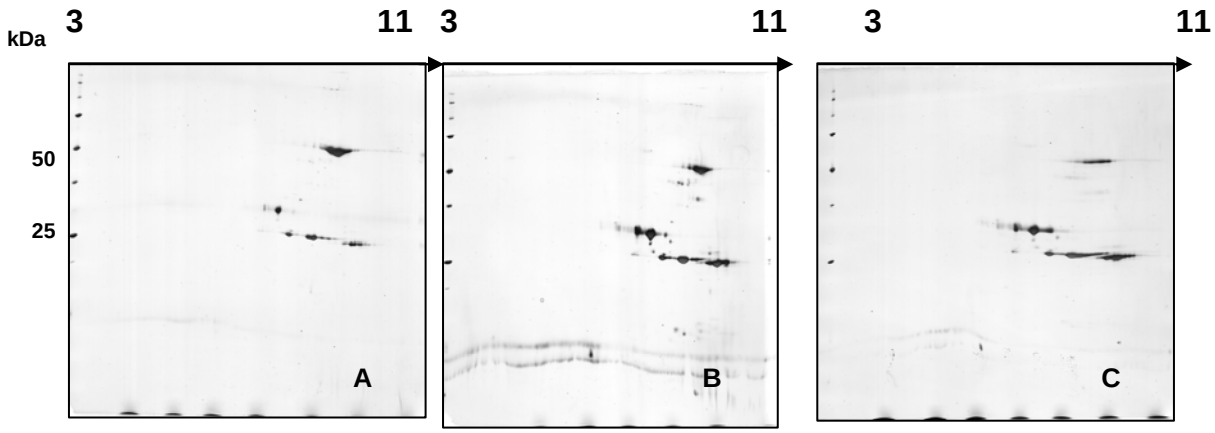

Fig. 5.31. Trastuzumab. 3-11 NL. Forced Degradation study. Room temperature. Opened vial A) 7 days B) 14 days; C) 30 days

2-DE analysis of termodegradated trastuzumab employing immobiline pH gradient 3-11 NL showed that the elevated temperatures influenced the spot pattern of the antibody. This influence is remarkable upon longer time storage. Storage for 30 and 45 days at room temperature resulted in change of the shape of both heavy and light chain spot pattern. In samples stored 45 days at 37°C new spots located above light and heavy chain are noted and in those stored 7 days at 50 °C new spots can be seen at pI 7.5-8 at molecular weights about 55, 75 and 100 kDa, suggesting possible aggregation of antibody molecule (Fig. 5.27).

On the other hand, no significant difference in spot pattern has been noted in gels stored shorter time even at 37 °C. Neither MW nor pI of spots changed significantly and consistently. This suggests that, degradation pathway of trastuzumab involves chemical reactions such are asparagine deamidation, asparagine and aspartate isomerisation and methionine oxidation, which does not cause bigger differences in molecular weight and isoelectric points of resulting species, to be detected with 2-DE.

5.2.2. 1-DE. Accelerated degradation study of trastuzumab

Although from SDS-PAGE gels no information regarding pI can be obtained, molecular weight changes of trastuzumab under different storage conditions in these

gels are evident. Samples stored at room temperature for period of 1 month, provided gels with additional bands at higher molecular masses (Fig. 5.32, Gels B, C and D). In contrast to control sample (Fig. 5.32, Gel A), in gel D, trastuzumab sample stored 1 month at room temperature, there is a sharp band at molecular weight 100 kDa which has almost same intensity with heavy chain band (50 kDa). Additional bands are present at molecular weights 150 and 200 kDa, respectively.

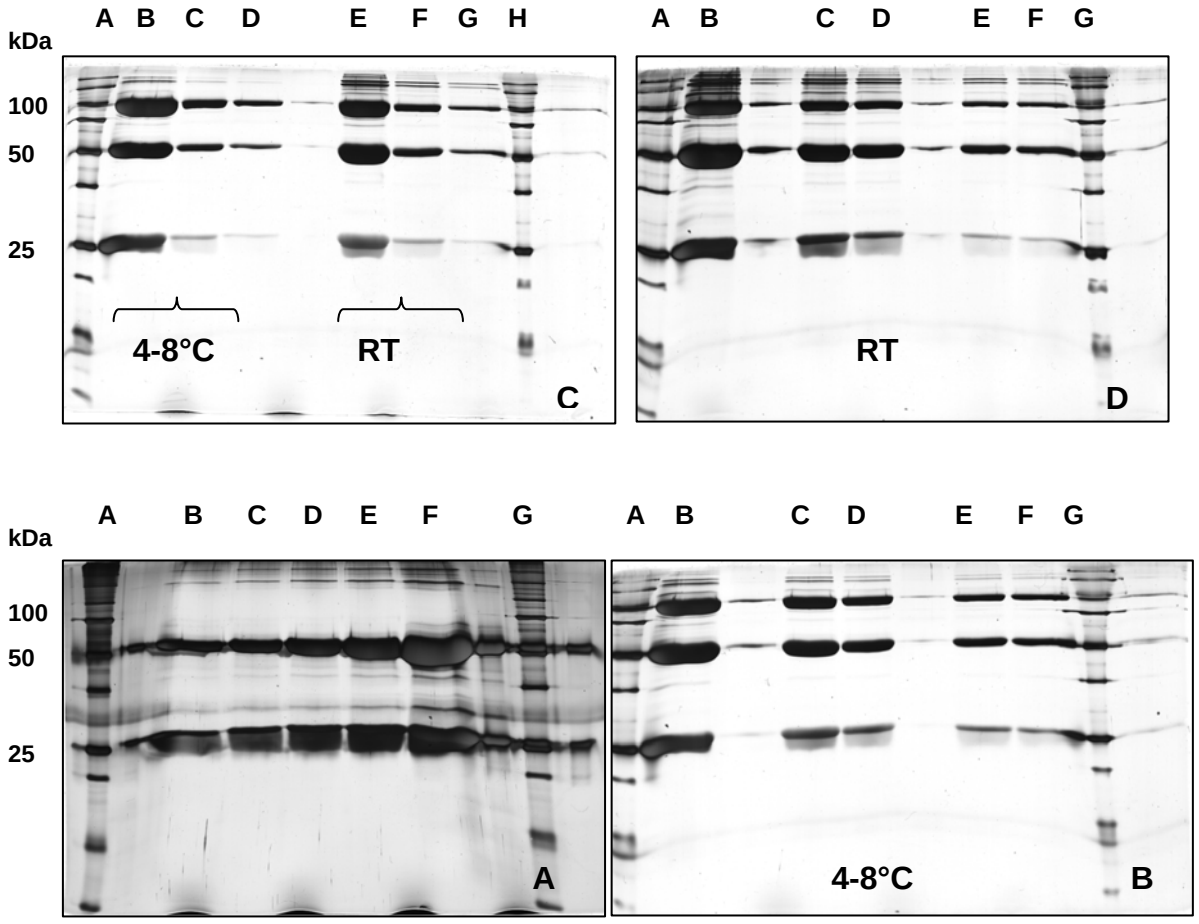

Fig. 5.32.Trastuzumab. 1-DE Forced degradation study. Silver staining.
A) Control gel. Lanes A, G: MW standards. Lanes B-F: trastuzumab, 1.3-20.5µg.
B) 31 days, 4-8°C. Lanes A, G: MW standards. Lanes B-F: trastuzumab, 20.5-1.3 µg
C) 31 days. Lanes A, H: MW standards. Lanes B-D: 4-8°C. Lanes E-G: Room temperature. Trastuzumab: 20.5-1.3 µg
D) 31 days, Room temperature.Lanes A, G: MW standards. Lanes B-F: trastuzumab, 20.5-1.3 µg

These additional bands are observed in trastuzumab samples stored 1 month at 4-8°C, as well. (Gel A).

Different lot of trastuzumab sample was loaded onto Gel C. Left part of this gel, (lanes B, C and D, trastuzumab stored at 4-8°C, 1 month) show the same molecular weight pattern as gel B. The same holds for lanes E, F, G and gel D (room temperature, 1 month). Fig. 5.32. shows that bigger number of protein bands is observed when samples were stored at room temperature (Gel D and Gel C, lanes E, F and G) comparing to samples stored at 4-8°C (Gel B and Gel C, lanes B, C and D). This observation may suggest trastuzumab aggregation as physical degradation pathway.

SDS-PAGE gels of trastuzumab stored under oxidation and acidic conditions are presented in Fig. 5.33.

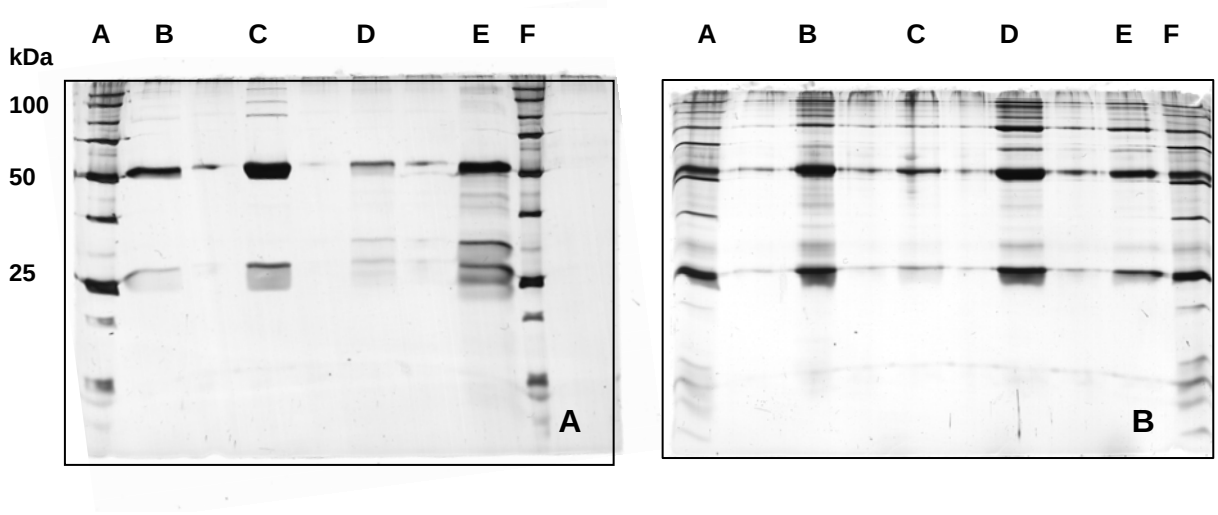

Fig. 5.33. Forced degradation study. Trastuzumab 0.2 and 0.8 µg, 19 days. Silver staining.
Gel A. Lanes A, F: MW standards, Lanes B, C: 37°C, Lanes D, E: TFA 1 % , RT
Gel B: Lanes A, F: MW standards, Lanes B, C H_2O_2 3 %, RT, Lanes D, E: H_2O_2 1 %, RT

As noted in Fig 5.33, severe storage conditions, employing TFA 1 % (Gel A lanes D and E) and H_2O_2 1 and 3 %, 19 days, (Gel B, lanes D, E and B, C, respectively) brought about a significant change in the protein band pattern comparing to control gel (Fig. 5.32A). Interestingly, additional protein bands above and below 50 kDa have been observed in H_2O_2 exposed samples. However, samples stored in the solution of TFA 1 % provided additional bands predominantly below 50 kDa (Gel A, lanes d and E). On the other hand, sample stored 19 days at 37°C, provided additional bands above 50 kDa, similarly as in Fig 5.32. (Gel D).

5.3. Matrix assisted laser desorption ionization time of flight mass spectrometric (MALDI-TOF MS) analysis of trastuzumab

5.3.1. Primary sequence confirmation. Peptide mass fingerprinting

MALDI-TOF spectrum of generated peptides from deglycosilated and in-gel tryptic digested trastuzumab heavy chain is presented in the Fig. 5.34.
As discussed above, recombinant monoclonal antibody trastuzumab contains two heavy and two light chains linked via disulfide bridges. It is composed of 1,328 amino acids: heavy chain contains 450 and light chain 214, amino acids, respectively (Fig 1.7.).

Trastuzumab is humanised antibody obtained by grafting murine complementarity determining regions (CDR regions) into the human framework. CDR regions are located in the antigen binding domains of the antibody, which comprise variable domains of both chains, C_H1 domain of heavy and constant domain of light chain, respectively. Trastuzumab Fab domains therefore have human and murine nature. On the other hand, heavy chain hinge region, C_H2 and C_H3 domains are fully human.
On the basis of peptide mass fingerprint data it was possible to identify both heavy and light chains of trastuzumab, to confirm their humanised origin, and to confirm mutations in C_H3 domain of heavy chain: E359D and M361L which were installed to convert the antibody from the naturally rare A allotype to much more common non-A allotype. MALDI-TOF peptide mass 1905.97 (1922.38) specific for the $^{...359}$EEM$^{361...}$ sequence, was not observed in the MALDI-TOF spectra of abatacept and rituximab heavy chain, since their corresponding positions have (¨ DEL¨) sequence (non-A allotype) instead.

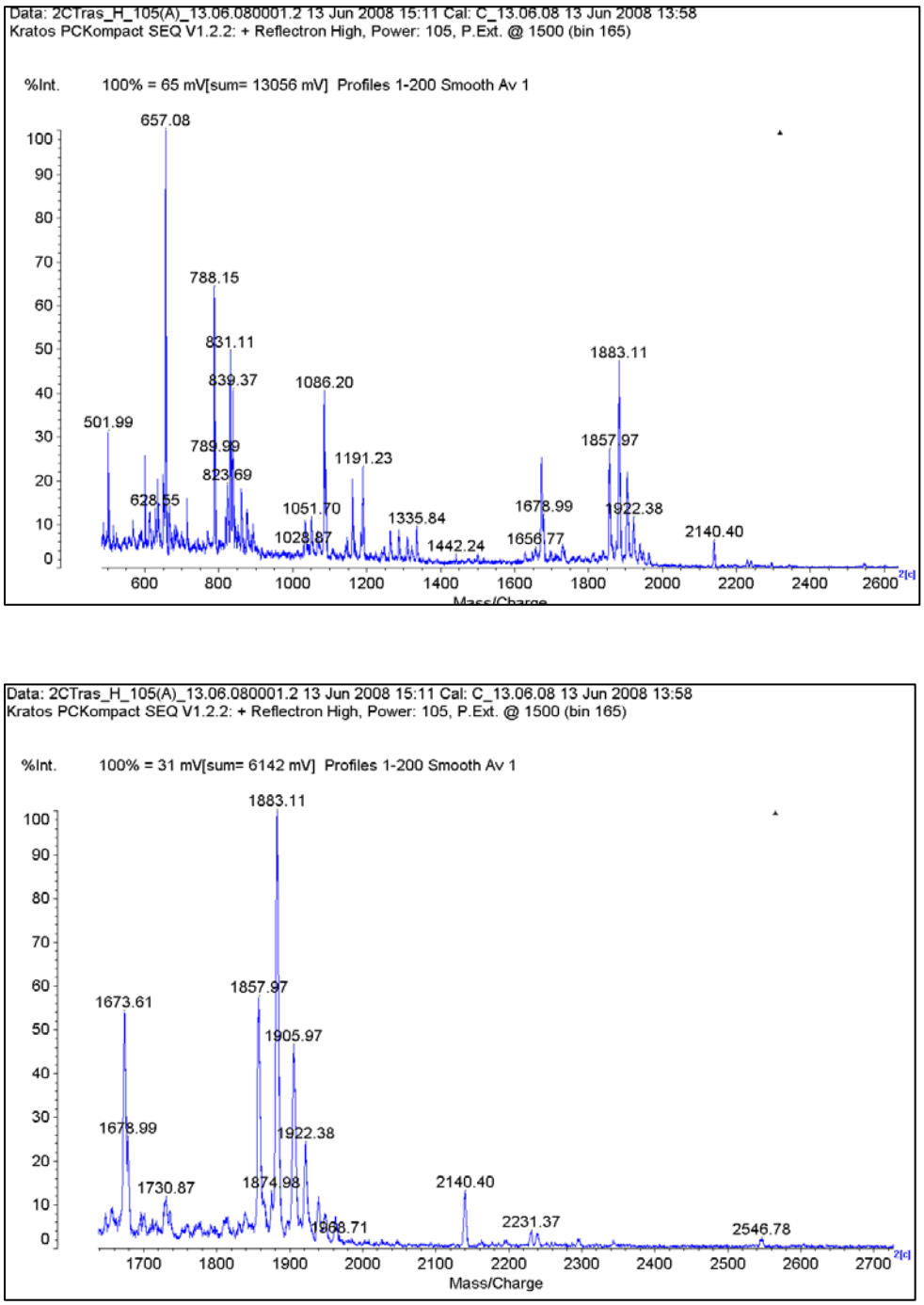

Fig. 5.34. MALDI-TOF spectrum of deglycosilated heavy chain of trastuzumab. Up: Entire spectrum, Down: Section of spectrum

5.3.1.1. Identification of heavy chain

For primary sequence confirmation and identification of the trastuzumab heavy chain, the list of 29 peptide masses (Fig. 5.35.) generated by MALDI-TOF MS of peptides obtained from corresponding positions of silver and Coomassie stained gels (Fig.

5.22 Gels C and D), were searched with MASCOT and PROFOUND (Prowl) search engines using three sequence databases: MSDB, NCBInr and SwissProt.

501.99; 600.99; 657.08; 682.80; 788.15; 818.85; 831.11; 836.12; 839.37; 1086.20; 1090.53; 1162.60; 1184.12; 1187.35; 1191.23; 1268.17; 1287.61; 1311.28; 1322.68; 1335.84; 1673.61; 1678.99; 1874.98; 1883.11; 1905.97; 2140.40; 2231.37; 2239.55; 2546.78.

Fig. 5.35. Trastuzumab heavy chain. List of entered peptide masses

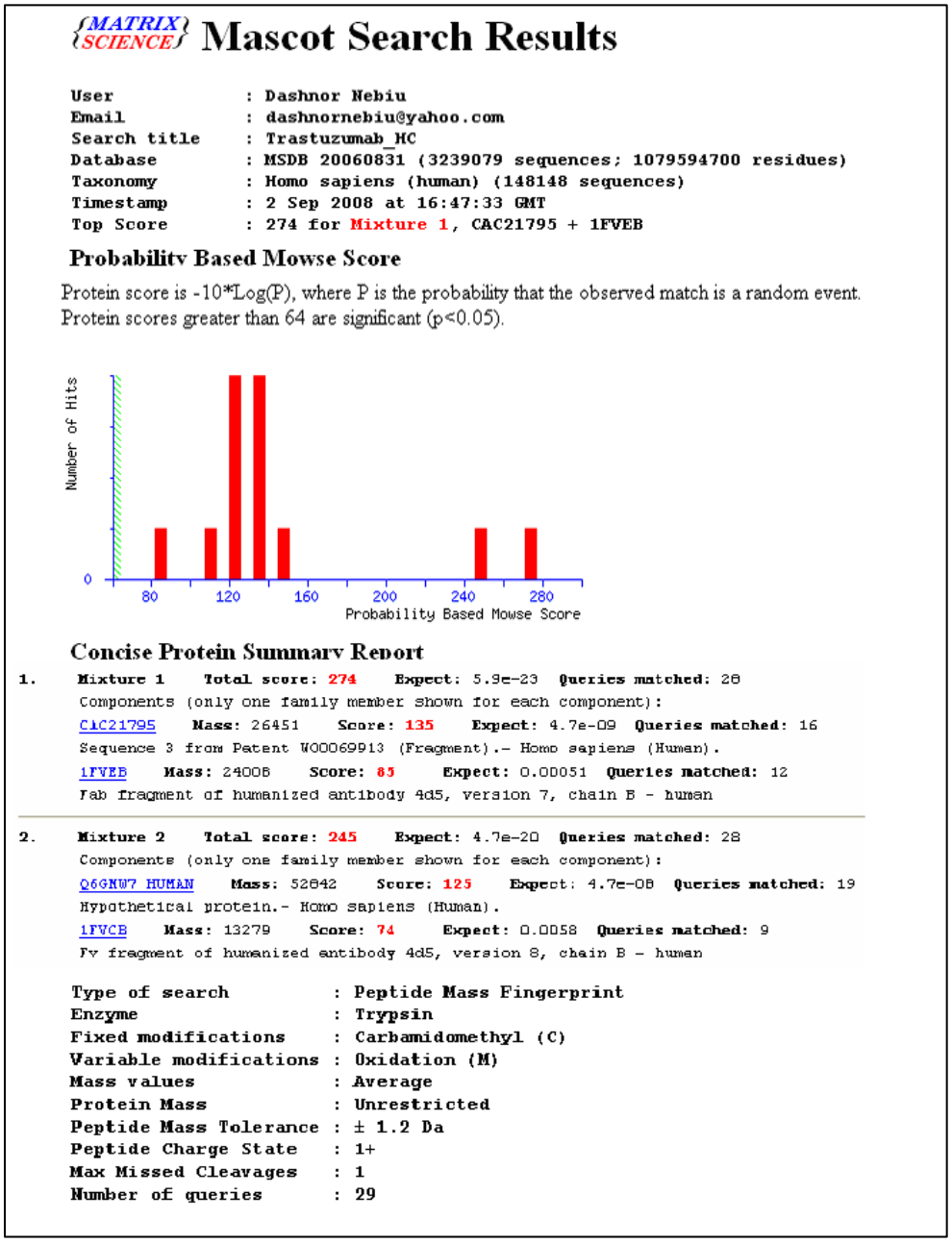

MATRIX SCIENCE

Mascot Search Results

User : Dashnor Nebiu
Email : dashnornebiu@yahoo.com
Search title : Trastuzumab_HC
Database : MSDB 20060831 (3239079 sequences; 1079594700 residues)
Taxonomy : Homo sapiens (human) (148148 sequences)
Timestamp : 2 Sep 2008 at 16:47:33 GMT
Top Score : 274 for Mixture 1, CAC21795 + 1FVEB

Probability Based Mowse Score

Protein score is -10*Log(P), where P is the probability that the observed match is a random event.
Protein scores greater than 64 are significant (p<0.05).

Concise Protein Summary Report

1. Mixture 1 Total score: 274 Expect: 5.9e-23 Queries matched: 28
Components (only one family member shown for each component):
CAC21795 Mass: 26451 Score: 135 Expect: 4.7e-09 Queries matched: 16
Sequence 3 from Patent WO0069913 (Fragment).- Homo sapiens (Human).
1FVEB Mass: 24008 Score: 85 Expect: 0.00051 Queries matched: 12
Fab fragment of humanized antibody 4d5, version 7, chain B - human

2. Mixture 2 Total score: 245 Expect: 4.7e-20 Queries matched: 28
Components (only one family member shown for each component):
Q6GNW7_HUMAN Mass: 52842 Score: 125 Expect: 4.7e-08 Queries matched: 19
Hypothetical protein.- Homo sapiens (Human).
1FVCB Mass: 13279 Score: 74 Expect: 0.0058 Queries matched: 9
Fv fragment of humanized antibody 4d5, version 8, chain B - human

Type of search : Peptide Mass Fingerprint
Enzyme : Trypsin
Fixed modifications : Carbamidomethyl (C)
Variable modifications : Oxidation (M)
Mass values : Average
Protein Mass : Unrestricted
Peptide Mass Tolerance : ± 1.2 Da
Peptide Charge State : 1+
Max Missed Cleavages : 1
Number of queries : 29

Fig. 5.36. Trastuzumab, heavy chain. Mascot search results. Primary sequence database: MSDB. Mas tolerance was set to ± 1.2 Da

During Database searching, taxonomy was restricted to *Homo sapiens*, selected enzyme was trypsin. Other search parameters were set to allow up to 1 missed cleavage, methionins in oxidized form (variable modification), cysteins in carbamidomethylated form (fixed modification), average mass, peptide ions in protonated $[M+H]^+$ form, mass tolerance was set ±1, ±1.2 and ±1.5 Da. Protein molecular mass was not specified.
All databases searched in this study generated similar results concerning the identified protein and significance of obtained data.

5.3.1.2. MASCOT/MSDB sequence database

List of searched peptides in this search engine (MSDB primary sequence database), generated the top total score 274 for mixture of two peptides at MT±2:

- **CAC21795** (Sequence 3 from Patent WO0069913 (Fragment). - Homo sapiens (Human).
- **1FVEB** (Fab fragment of humanized antibody 4d5, version 7, chain B - human), (Fig. 5.36)

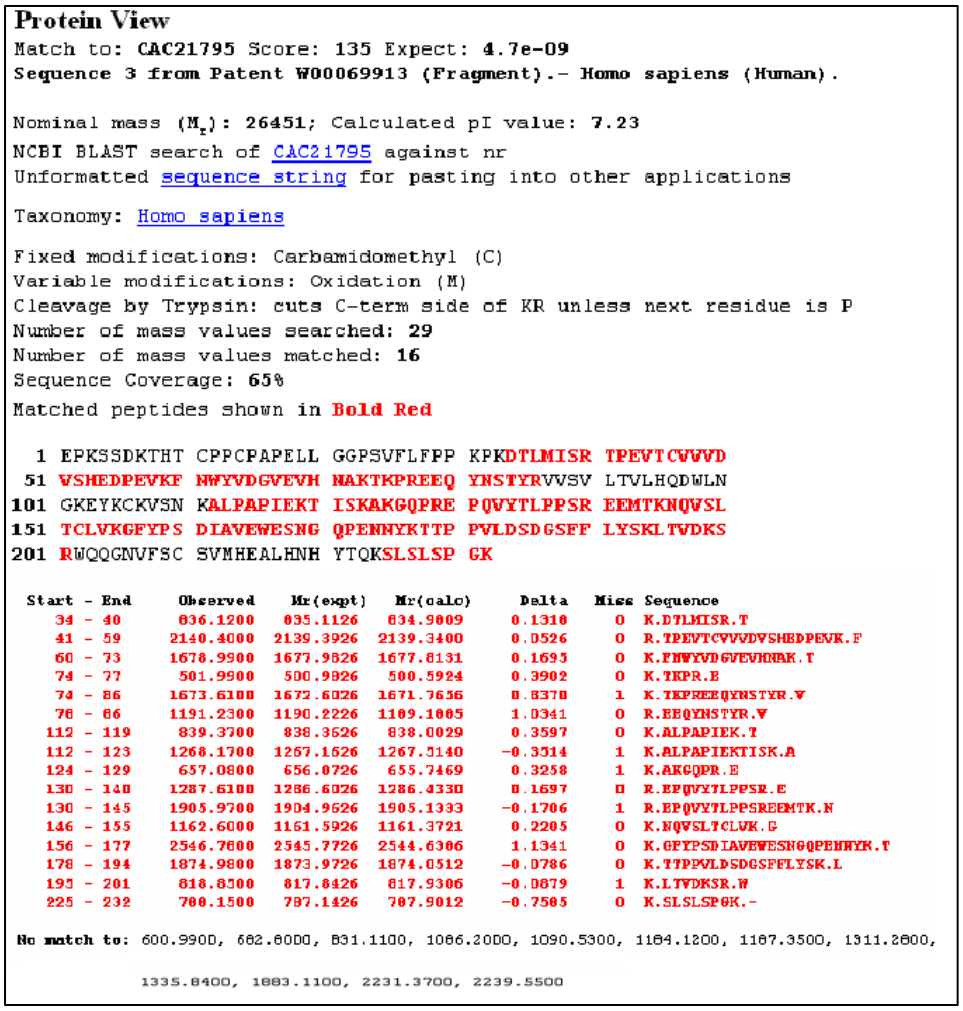

Protein View

Match to: **CAC21795** Score: **135** Expect: **4.7e-09**
Sequence 3 from Patent W00069913 (Fragment).- Homo sapiens (Human).

Nominal mass (M_r): **26451**; Calculated pI value: **7.23**
NCBI BLAST search of CAC21795 against nr
Unformatted sequence string for pasting into other applications

Taxonomy: Homo sapiens

Fixed modifications: Carbamidomethyl (C)
Variable modifications: Oxidation (M)
Cleavage by Trypsin: cuts C-term side of KR unless next residue is P
Number of mass values searched: **29**
Number of mass values matched: **16**
Sequence Coverage: **65%**
Matched peptides shown in **Bold Red**

```
  1 EPKSSDKTHT CPPCPAPELL GGPSVFLFPP KPKDTLMISR TPEVTCVVVD
 51 VSHEDPEVKF NWYVDGVEVH NAKTKPREEQ YNSTYRVVSV LTVLHQDWLN
101 GKEYKCKVSN KALPAPIEKT ISKAKGQPRE PQVYTLPPSR EEMTKNQVSL
151 TCLVKGFYPS DIAVEWESNG QPENNYKTTP PVLDSDGSFF LYSKLTVDKS
201 RWQQGNVFSC SVMHEALHNH YTQKSLSLSP GK
```

Start - End	Observed	Mr(expt)	Mr(calc)	Delta	Miss	Sequence
34 - 40	636.1200	635.1126	634.9809	0.1318	0	K.DTLMISR.T
41 - 59	2140.4000	2139.3926	2139.3400	0.0526	0	R.TPEVTCVVVDVSHEDPEVK.F
60 - 73	1678.9900	1677.9826	1677.8131	0.1695	0	K.FNWYVDGVEVHNAK.T
74 - 77	501.9900	500.9826	500.5924	0.3902	0	K.TKPR.E
74 - 86	1673.6100	1672.6026	1671.7656	0.8370	1	K.TKPREEQYNSTYR.V
78 - 86	1191.2300	1190.2226	1189.1885	1.0341	0	R.EEQYNSTYR.V
112 - 119	839.3700	838.3626	838.0029	0.3597	0	K.ALPAPIEK.T
112 - 123	1268.1700	1267.1626	1267.3140	-0.1514	1	K.ALPAPIEKTISK.A
124 - 129	657.0800	656.0726	655.7469	0.3258	1	K.AKGQPR.E
130 - 140	1287.6100	1286.6026	1286.4330	0.1697	0	R.EPQVYTLPPSR.E
130 - 145	1905.9700	1904.9626	1905.1333	-0.1706	1	R.EPQVYTLPPSREEMTK.N
146 - 155	1162.6000	1161.5926	1161.3721	0.2205	0	K.NQVSLTCLVK.G
156 - 177	2546.7600	2545.7726	2544.6306	1.1341	0	K.GFYPSDIAVEWESNGQPENNYK.T
178 - 194	1874.9800	1873.9726	1874.0512	-0.0786	0	K.TTPPVLDSDGSFFLYSK.L
195 - 201	818.8500	817.8426	817.9306	-0.0879	1	K.LTVDKSR.W
225 - 232	788.1500	787.1426	787.9012	-0.7585	0	K.SLSLSPGK.-

No match to: 600.9900, 662.8000, 831.1100, 1086.2000, 1090.5300, 1184.1200, 1187.3500, 1311.2800, 1335.8400, 1883.1100, 2231.3700, 2239.5500

Fig. 5.37. Trastuzumab, heavy chain. Protein view section. CAC21795. Mascot/MSDB.

As shown in Figures 5.37 and 1.7, sequences of human protein CAC21795 (1-232), and heavy chain of trastuzumab (*humAb4D5-8*) (218-450), are identical with exception that Ser-5 in CAC21795 is replaced with Cys- 223 in trastuzumab heavy chain sequence. Actually, expect this Cys-Ser difference entire sequence of CAC21795 corresponds to trastuzumab hinge, C_H2 and C_H3 regions, which are fully human. Additionally, this protein and trastuzumab have the same allotype marker: $^{...359}$EEM$^{361...}$ sequence of trastuzumab, corresponds to $^{...141}$EEM$^{143...}$ of CAC21795. According protein view data (Fig. 5.37), 16 protein masses are matched and sequence coverage 65 % has been achieved.

Protein View

Match to: **1FVEB** Score: **85** Expect: **0.00051**
Fab fragment of humanized antibody 4d5, version 7, chain B - human

Nominal mass (M_r): **24008**; Calculated pI value: **8.91**
NCBI BLAST search of 1FVEB against nr
Unformatted sequence string for pasting into other applications

Taxonomy: Homo sapiens
Links to retrieve other entries containing this sequence from NCBI Entrez:
1FVED from Homo sapiens

Fixed modifications: Carbamidomethyl (C)
Variable modifications: Oxidation (M)
Cleavage by Trypsin: cuts C-term side of KR unless next residue is P
Number of mass values searched: **29**
Number of mass values matched: **12**
Sequence Coverage: **55%**

Matched peptides shown in **Bold Red**

```
     1 EVQLVESGGG LVQPGGSLRL SCAASGFNIK DTYIHWVRQA PGKGLEWVAR
    51 IYPTNGYTRY ADSVKGRFTI SADTSKNTAY LQMNSLRAED TAVYYCSRWG
   101 GDGFYAMDYW GQGTLVTVSS ASTKGPSVFP LAPSSKSTSG GTAALGCLVK
   151 DYFPEPVTVS WNSGALTSGV HTFPAVLQSS GLYSLSSVVT VPSSSLGTQT
   201 YICNVNHKPS NTKVDKKVEP KSC
```

Start - End	Observed	Mr(expt)	Mr(calc)	Delta	Miss	Sequence
1 - 19	1883.1100	1882.1026	1882.0797	0.0229	0	-.EVQLVESGGGLVQPGGSLR.L
20 - 30	2239.5500	2238.5426	2238.5233	0.0193	1	R.LSCAASGFNIKDTYIHWVR.Q
31 - 38	1090.5300	1089.5226	1089.2034	0.3192	0	K.DTYIHWVR.Q
44 - 50	831.1100	830.1026	829.9427	0.1599	0	K.GLEWVAR.I
51 - 59	1086.2000	1085.1926	1084.1820	1.0106	0	R.IYPTNGYTR.Y
60 - 65	682.8000	681.7926	681.7346	0.0581	0	R.YADSVK.G
66 - 76	1104.1200	1103.1126	1102.2030	0.9289	1	K.GRFTISADTSK.N
77 - 87	1311.2800	1310.2726	1310.4790	-0.2064	0	K.NTAYLQMNSLR.A
88 - 98	1335.6400	1334.6326	1334.4112	0.4214	0	R.AEDTAVYYCSR.W
125 - 136	1187.3500	1186.3426	1186.3569	-0.0143	0	K.GPSVFPLAPSSK.S
137 - 150	1322.6800	1321.6726	1321.5001	0.1725	0	K.STSGGTAALGCLVK.D
217 - 221	600.9900	599.9826	599.7202	0.2624	1	K.KVEPK.S

No match to: 501.9900, 657.0800, 788.1500, 818.8500, 836.1200, 839.3700, 1162.6000, 1191.2300, 1287.6100, 1673.6100, 1678.9900, 1874.9800, 1905.9700, 2140.4000, 2231.3700, 2546.7800

Fig. 5.38. Trastuzumab, heavy chain. Protein view section. 1FVEB. Mascot/MSDB.

Fab fragment of humanized antibody 4d5, chain B - human, **1FVEB,** was the second component of top score mixture (Fig. 5.38). In this instance there are 12 peptide matches, and sequence coverage is 55 %. Score value 85 indicates significant match. 1 **FVEB** corresponds to residues 1-223 of trastuzumab, including Fv and C_H1 domains.

Database output made possible the identification of the antigen binding domain of trastuzumab (humAb4D5-8). From the Table 1.6 and published data[165-168] is seen

that the sequences of trastuzumab heavy chain for both versions (humAb4D5-8 and humAb4D5-7) are identical. They differ in one amino acid in the light chain CDR2.

For mass tolerance (MT) parameter set to ±1, the same proteins were reported, with same ranking, provided that number of matched masses was lower, and consequently their sequence coverages: Total score of mixture was 231, and number of queries matched, 25. For CAC21795, reported score was 116, number of queries matched, 14, sequence coverage was 55 %; and for humAb4D5, reported score was 81, number of queries matched, 11, sequence coverage was 51 %.

By increasing MT value to ±1.5 and ±2, scores dropped slightly, provided that there were 17 queries matched for CAC21795.

Protein View

Match to: **1FVCB** Score: **77** Expect: **0.0029**
Fv fragment of humanized antibody 4d5, version 8, chain B - human

Nominal mass (M_r): **13279**; Calculated pI value: **8.03**
NCBI BLAST search of 1FVCB against nr
Unformatted sequence string for pasting into other applications

Taxonomy: Homo sapiens
Links to retrieve other entries containing this sequence from NCBI Entrez
1FVCD from Homo sapiens

Fixed modifications: Carbamidomethyl (C)
Variable modifications: Oxidation (M)
Cleavage by Trypsin: cuts C-term side of KR unless next residue is P
Number of mass values searched: **29**
Number of mass values matched: **10**
Sequence Coverage: **81%**

Matched peptides shown in **Bold Red**

```
     1 EVQLVESGGG LVQPGGSLRL SCAASGFNIK DTYIHWVRQA PGKGLEWVAR
    51 IYPTNGYTRY ADSVKGRFTI SADTSKNTAY LQMNSLRAED TAVYYCSRWG
   101 GDGFYAMDYW GQGTLVTVSS
```

Fig. 5.39. Trastuzumab, heavy chain.*1FVCB*. Protein view section. Mascot/MSDB

Interestingly, at MT ±1, 1,2 and 1.5, as second ranked result, variable fragment of humAb4D5-8 (**1 FVCB,** Fv fragment of humanized antibody 4d5, version 8, chain B - human), is reported, with score value 77, sequence coverage 81 % and 10 queries

matched. Variable fragment, 1 FVCB contains only 120 amino acids, and corresponds to sequence 1-120 of trastuzumab Fab fragment.
The section of protein view report for **1 FVCB,** (Fv fragment of humanized antibody 4d5, version 8, chain B - human) is presented in Fig. 5.39.
Results obtained in Figures 5.37, 5.38 and 5.39; provide confirmation of the sequence of trastuzumab heavy chain.

5.3.1.3. MASCOT/ NCBInr sequence database.

Second amino acid sequence database searched was NCBInr. As in previous instance search parameters were set at the same values.

For MT parameter set to ±1.2, **Protein Mixture 1** is reported as the highest ranking result, with total score value of 276.
The highest score mixture consisted of two identified proteins:

- *gi 226787, immunoglobulin gamma 1.*
- *gi 442924, Chain B, X-Ray Structures Of The Antigen-Binding Domains From Three Variants Of Humanized Anti-P185-Her2 Antibody 4d5 And Comparison With Molecular Modelling*. (Fig. 5.40.).

First reported protein, *gi 226787*, represents sequence of human recombinant immunoglobulin G polypeptide, more precisely its C_H2 and C_H3 regions, and its entire amino acid sequence (except Met-1, because it was produced in E. coli), corresponds to trastuzumab heavy chain sequence 228-450, (Fig. 5.41.).

Mascot Search Results

User : Dashnor Nebiu
Email : dashnornebiu@yahoo.com
Search title : Trastuzumab_HC
Database : NCBInr 20080826 (6937173 sequences; 2395285404 residues)
Taxonomy : Homo sapiens (human) (216737 sequences)
Timestamp : 3 Sep 2008 at 13:47:18 GMT
Top Score : 276 for Mixture 1, gi|226787 + gi|442924

Probability Based Mowse Score

Protein score is -10*Log(P), where P is the probability that the observed match is a random event.
Protein scores greater than 66 are significant (p<0.05).

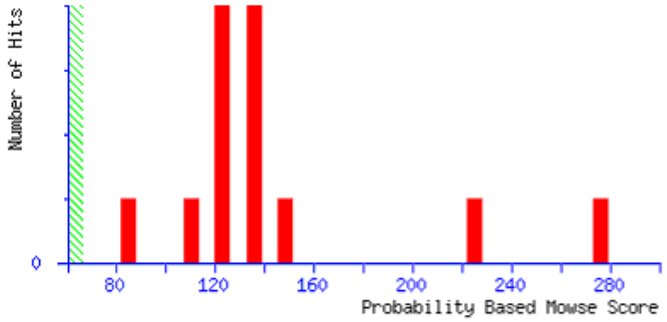

Concise Protein Summary Report

1. **Mixture 1** **Total score: 276** **Expect:** 5.4e-23 **Queries matched:** 28
Components (only one family member shown for each component):
gi|226787 **Mass:** 25572 **Score: 137** **Expect:** 4.3e-09 **Queries matched:** 16
Ig gamma1
gi|442924 **Mass:** 24008 **Score: 85** **Expect:** 0.00075 **Queries matched:** 12
Chain B, X-Ray Structures Of The Antigen-Binding Domains From Three Variants Of Humanized Anti-P185-Her2 Antibody 4d5 And Comparison With Molecular Modeling

2. **Mixture 2** **Total score: 227** **Expect:** 4.3e-18 **Queries matched:** 28
Components (only one family member shown for each component):
gi|49258108 **Mass:** 52842 **Score: 125** **Expect:** 6.9e-08 **Queries matched:** 19
IGHG1 protein [Homo sapiens]
gi|442924 **Mass:** 24008 **Score: 85** **Expect:** 0.00075 **Queries matched:** 12
Chain B, X-Ray Structures Of The Antigen-Binding Domains From Three Variants Of Humanized Anti-P185-Her2 Antibody 4d5 And Comparison With Molecular Modeling

Search Parameters

Type of search : Peptide Mass Fingerprint
Enzyme : Trypsin
Fixed modifications : Carbamidomethyl (C)
Variable modifications : Oxidation (M)
Mass values : Average
Protein Mass : Unrestricted
Peptide Mass Tolerance : ± 1.2 Da
Peptide Charge State : 1+
Max Missed Cleavages : 1
Number of queries : 29

Fig. 5.40. Trastuzumab, heavy chain. Mascot search results. Primary sequence database: NCBInr. Mas tolelrance set to ± 1.2 Da

There were reported 16 peptide masses to mach with masses obtained from *in silico* tryptic digest, score value was 137 and sequence coverage 67 %.

Fig. 5.41. shows that this protein and trastuzumab have the same allotype marker:$^{...359}$*EEM*$^{361...}$ residues of trastuzumab, corresponds to$^{...133}$EEM$^{135...}$ of *gi 226787.*

Protein View

Match to: **gi|226787** Score: **137** Expect: **4.3e-09**
Ig gamma1

Nominal mass (M_r): **25572**; Calculated pI value: **7.00**

NCBI BLAST search of gi|226787 against nr
Unformatted sequence string for pasting into other applications

Taxonomy: Homo sapiens

Fixed modifications: Carbamidomethyl (C)
Variable modifications: Oxidation (M)
Cleavage by Trypsin: cuts C-term side of KR unless next residue is P
Number of mass values searched: **29**
Number of mass values matched: **16**
Sequence Coverage: **67%**
Matched peptides shown in **Bold Red**

```
  1 MTCPPCPAPE LLGGPSVFLF PPKPKDTLMI SRTPEVTCVV VDVSHEDPEV
 51 KFNWYVDGVE VHNAKTKPRE EQYNSTYRVV SVLTVLHQDW LNGKEYKCKV
101 SNKALPAPIE KTISKAKGQP REPQVYTLPP SREEMTKNQV SLTCLVKGFY
151 PSDIAVEWES NGQPENNYKT TPPVLDSDGS FFLYSKLTVD KSRWQQGNVF
201 SCSVMHEALH NHYTQKSLSL SPGK
```

Start - End	Observed	Mr(expt)	Mr(calc)	Delta	Miss	Sequence
26 - 32	836.1200	835.1126	834.9809	0.1318	0	K.DTLMISR.T
33 - 51	2140.4000	2139.3926	2139.3400	0.0526	0	R.TPEVTCVVVDVSHEDPEVK.F
52 - 65	1678.9900	1677.9826	1677.8131	0.1695	0	K.FNWYVDGVEVHNAK.T
66 - 69	501.9900	500.9826	500.5924	0.3902	0	K.TKPR.E
66 - 78	1673.6100	1672.6026	1671.7656	0.8370	1	K.TKPREEQYNSTYR.V
70 - 78	1191.2300	1190.2226	1189.1885	1.0341	0	R.EEQYNSTYR.V
104 - 111	839.3700	838.3626	838.0029	0.3597	0	K.ALPAPIEK.T
104 - 115	1268.1700	1267.1626	1267.5140	-0.3514	1	K.ALPAPIEKTISK.A
116 - 121	657.0800	656.0726	655.7469	0.3258	1	K.AKGQPR.E
122 - 132	1287.6100	1286.6026	1286.4330	0.1697	0	R.EPQVYTLPPSR.E
122 - 137	1905.9700	1904.9626	1905.1333	-0.1706	1	R.EPQVYTLPPSREEMTK.N
138 - 147	1162.6000	1161.5926	1161.3721	0.2205	0	K.NQVSLTCLVK.G
148 - 169	2546.7800	2545.7726	2544.6386	1.1341	0	K.GFYPSDIAVEWESNGQPENNYK.T
170 - 186	1874.9000	1873.9726	1874.0512	-0.0786	0	K.TTPPVLDSDGSFFLYSK.L
187 - 193	818.8500	817.8426	817.9306	-0.0879	1	K.LTVDKSR.W
217 - 224	708.1500	707.1426	707.9012	-0.7585	0	K.SLSLSPGK.-

No match to: 600.9900, 682.8000, 831.1100, 1086.2000, 1090.5300, 1184.1200, 1187.3500, 1311.2800, 1322.6800, 1335.8400, 1883.1100, 2231.3700, 2239.5500

Fig. 5.41. Trastuzumab, heavy chain. Protein view section. gi226787.Mascot/NCBInr.

Second component of the reported Mixture 1 is *gi 442924* protein. This protein represents antigen binding domain of trastuzumab (anti p$^{185\text{-HER2}}$antibody 4D5, rhumAb4D5-8), heavy chain. It corresponds to trastuzumab sequence 1-223, therefore to its heavy chain variable and C_H1 domains. As observed from protein view report, in Fig. 5.42., amino acid sequences of the three complementarity determining regions (CDR1, 2 and 3 regions) are sequentially covered. From the

analytical perspective, this is very important issue; since these (murine) CDR regions were grafted into human heavy chain sequence, to obtain humanized antibody, and this fact make possible specific identification and its discrimination from antibodies of different origin, i.e. fully human, chimeric, murine and/or fusion proteins.

The score was significant (85), number of queries matched was 12 and sequence coverage 55 % (Fig. 5.42.)

Protein View

Match to: **gi|442924** Score: **85** Expect: **0.00075**
Chain B, X-Ray Structures Of The Antigen-Binding Domains From Three Variants Of Humanized Anti-P185-Her2 Antibody 4d5 And Comparison With Molecular Modeling

Nominal mass (M_r): **24008**; Calculated pI value: **8.91**
NCBI BLAST search of gi|442924 against nr
Unformatted sequence string for pasting into other applications

Taxonomy: Homo sapiens
Links to retrieve other entries containing this sequence from NCBI Entrez:
gi|442926 from Homo sapiens

Fixed modifications: Carbamidomethyl (C)
Variable modifications: Oxidation (M)
Cleavage by Trypsin: cuts C-term side of KR unless next residue is P
Number of mass values searched: **29**
Number of mass values matched: **12**
Sequence Coverage: **55%**
Matched peptides shown in **Bold Red**

```
  1 EVQLVESGGG LVQPGGSLRL SCAASGFNIK DTYIHWVRQA PGKGLEWVAR
 51 IYPTNGYTRY ADSVKGRFTI SADTSKNTAY LQMNSLRAED TAVYYCSRWG
101 GDGFYAMDYW GQGTLVTVSS ASTKGPSVFP LAPSSKSTSG GTAALGCLVK
151 DYFPEPVTVS WNSGALTSGV HTFPAVLQSS GLYSLSSVVT VPSSSLGTQT
201 YICNVNHKPS NTKVDKKVEP KSC
```

Start - End	Observed	Mr(expt)	Mr(calc)	Delta	Miss	Sequence
1 - 19	1083.1100	1082.1026	1082.0797	0.0229	0	-.EVQLVESGGGLVQPGGSLR.L
20 - 38	2239.5500	2238.5426	2238.5233	0.0193	1	R.LSCAASGFNIKDTYIHWVR.Q
31 - 38	1090.5300	1089.5226	1089.2034	0.3192	0	K.DTYIHWVR.Q
44 - 50	831.1100	830.1026	829.9427	0.1599	0	K.GLEWVAR.I
51 - 59	1086.2000	1085.1926	1084.1820	1.0106	0	R.IYPTNGYTR.Y
60 - 65	682.8000	681.7926	681.7346	0.0581	0	R.YADSVK.G
66 - 76	1184.1200	1183.1126	1182.2838	0.8289	1	K.GRFTISADTSK.N
77 - 87	1311.2800	1310.2726	1310.4790	-0.2064	0	K.NTAYLQMNSLR.A
88 - 98	1335.8400	1334.8326	1334.4112	0.4214	0	R.AEDTAVYYCSR.W
125 - 136	1167.3500	1166.3426	1166.3569	-0.0143	0	K.GPSVFPLAPSSK.S
137 - 150	1322.6800	1321.6726	1321.5001	0.1725	0	K.STSGGTAALGCLVK.D
217 - 221	600.9900	599.9826	599.7202	0.2624	1	K.KVEPK.S

No match to: 501.9900, 657.0800, 788.1500, 818.8500, 836.1200, 839.3700, 1162.6000, 1191.2300, 1268.1700, 1287.6100, 1673.6100, 1678.9900, 1874.9800, 1905.9700, 2140.4000, 2231.3700, 2546.7800

Fig. 5.42. Trastuzumab, heavy chain.*gi442924*. Protein view section. Mascot/NCBInr.

Similar results were obtained when MT set to ±1, provided that, the number of matched peptide masses (PM), score values (S) and sequence coverages (SEQ), for *gi 226787, immunoglobulin gamma 1* and *gi 442924, Humanized Anti-P185-Her2 Antibody 4d5,* were lower (PM -14, S -118, SEQ-57% and PM-11, S -81, SEQ-51% respectively). If MT is set to higher values, then score results for both proteins fall.
MASCOT/SwissProt sequence database outputted as a top score 137 with 18 matched peptides, human Ig gamma-1 chain C region protein.

Search results generated by PROFOUND Search engine were similar to those obtained by MASCOT (Fig. 5.43.)
At MT± 1.5 the highest rank protein candidates were:

- *gi 226787*, *Ig gamma1*, same protein as in case with MASCOT search engine (Figures 5.41. and 5.43.), corresponds to trastuzumab heavy chain sequence 228-450.
- *gi55669886*, *Fc fragment of Igg1*, identical with trastuzumab Fc fragment, its entire sequence corresponds to trastuzumab heavy chain sequence 227-450.

These results are generated searching after the removal of variable fragment matched masses.

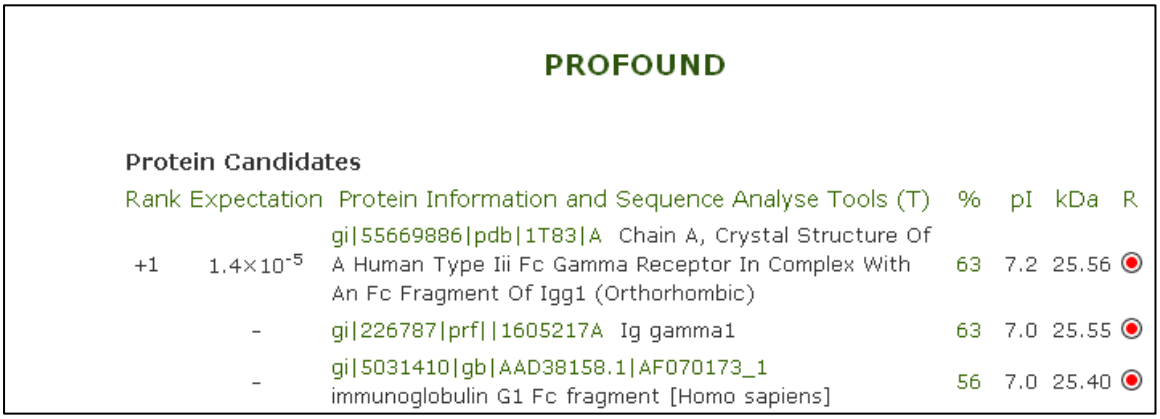

PROFOUND

Protein Candidates

Rank	Expectation	Protein Information and Sequence Analyse Tools (T)	%	pI	kDa	R
+1	1.4×10^{-5}	gi|55669886|pdb|1T83|A Chain A, Crystal Structure Of A Human Type Iii Fc Gamma Receptor In Complex With An Fc Fragment Of Igg1 (Orthorhombic)	63	7.2	25.56	
	-	gi|226787|prf||1605217A Ig gamma1	63	7.0	25.55	
	-	gi|5031410|gb|AAD38158.1|AF070173_1 immunoglobulin G1 Fc fragment [Homo sapiens]	56	7.0	25.40	

Fig. 5.43. Trastuzumab, heavy chain. PROFOUND/Prowl/NCBInr, section of protein information and sequence analysis tools. *1T83A*

Antigen binding domains of trastuzumab (rhumAb4D5-8, anti-$p^{185\text{-}HER2}$ antibody) were second protein candidates to be reported (Fig. 5.44). In this instance, sequence

coverages were 53 % and 73 %, depending on the reported fragment of antigen binding domain: only variable domain (1 FVCB, amino acid sequence 1-120) or variable domain and C_H1 domain (1 FVEB amino acid sequence 1-223; 1 N8ZB, amino acid sequence 1-220).

+2	2.8×10^{-3}	gi|442924|pdb|1FVE|B Chain B, X-Ray Structures Of The Antigen-Binding Domains From Three Variants Of Humanized Anti-P185-Her2 Antibody 4d5 And Comparison With Molecular Modeling	53	9.2	23.99
	-	gi|442920|pdb|1FVD|B Chain B, X-Ray Structures Of The Antigen-Binding Domains From Three Variants Of Humanized Anti-P185-Her2 Antibody 4d5 And Comparison With Molecular Modeling	53	9.2	23.97
	-	gi|28948773|pdb|1N8Z|B Chain B, Crystal Structure Of Extracellular Domain Of Human Her2 Complexed With Herceptin Fab	51	9.2	23.61
	-	gi|442916|pdb|1FVC|B Chain B, X-Ray Structures Of The Antigen-Binding Domains From Three Variants Of Humanized Anti-P185-Her2 Antibody 4d5 And Comparison With Molecular Modeling	73	8.2	13.26

Fig. 5.44. Trastuzumab, heavy chain. PROFOUND/Prowl/NCBInr, section of protein information and sequence analysis tools. *FVEB*.

MALDI-TOF analysis of trastuzumab has been performed measuring masses of peptides generated after tryptic digestion of Coomassie and silver stained gels. For both staining methods, MALDI-TOF analysis delivered qualitatively similar spectra. From Coomassie stained gels number of detected masses was higher (Fig. 5. 45.), which reflected on the increase of sequence coverage for identified trastuzumab.

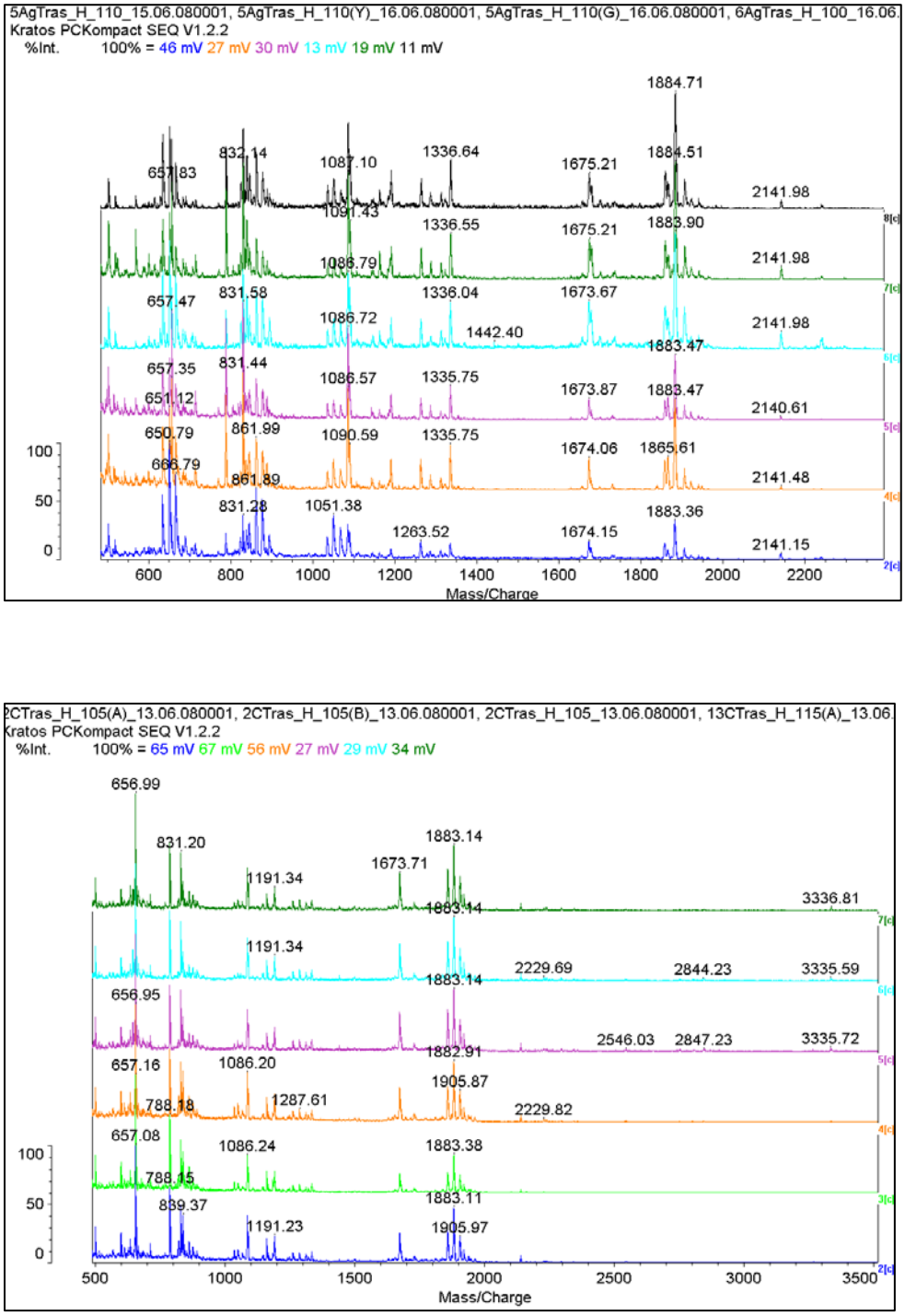

Fig. 5.45. MALDI_TOF Analysis of trastuzumab heavy chain. UP: MALDI -TOF Spectra of peptides generated from silver stained gels DOWN: MALDI -TOF Spectra of peptides generated from Coomassie stained gels.

5.3.1.4. Identification of light chain

For primary sequence confirmation and identification of the trastuzumab light chain, a list of 18 peptide masses (Fig. 5.46.) generated by MALDI-TOF MS of peptides obtained from corresponding positions of Coomassie and silver stained gels (Figures V and Fig 19), were searched with MASCOT and PROFOUND (Prowl) Search Engines using three sequence databases: MSDB, NCBInr and SwissProt.

523.59; 553.61; 560.80; 644.77; 749.79; 869.77; 891.61; 1773.57; 1798.93; 1877.51; 1897.88; 1947.62; 1992.36; 2103,51; 2142.17; 2289.33; 2611.00; 3623.68

Fig. 5.46. Trastuzumab light chain. List of entered peptide masses

During Database searching, taxonomy was restricted to *Homo sapiens*, selected enzyme was trypsin. Other search parameters were set to allow up to 1 missed cleavage, methionins in oxidized form (variable modification), cysteins in carbamidomethylated form (fixed modification), average mass, peptide ions in protonated $[M+H]^+$ form, mass tolerance was set ±1, ±1.2, ± 1.5 and ±2 Da. Protein molecular mass was not specified.
All databases searched in this study generated similar results concerning the identified protein and significance of obtained data.

In the Fig. 5. 47 MALDI-TOF spectrum obtained from peptides generated after tryptic digestion of light chain from Coomassie stained gel, is presented.

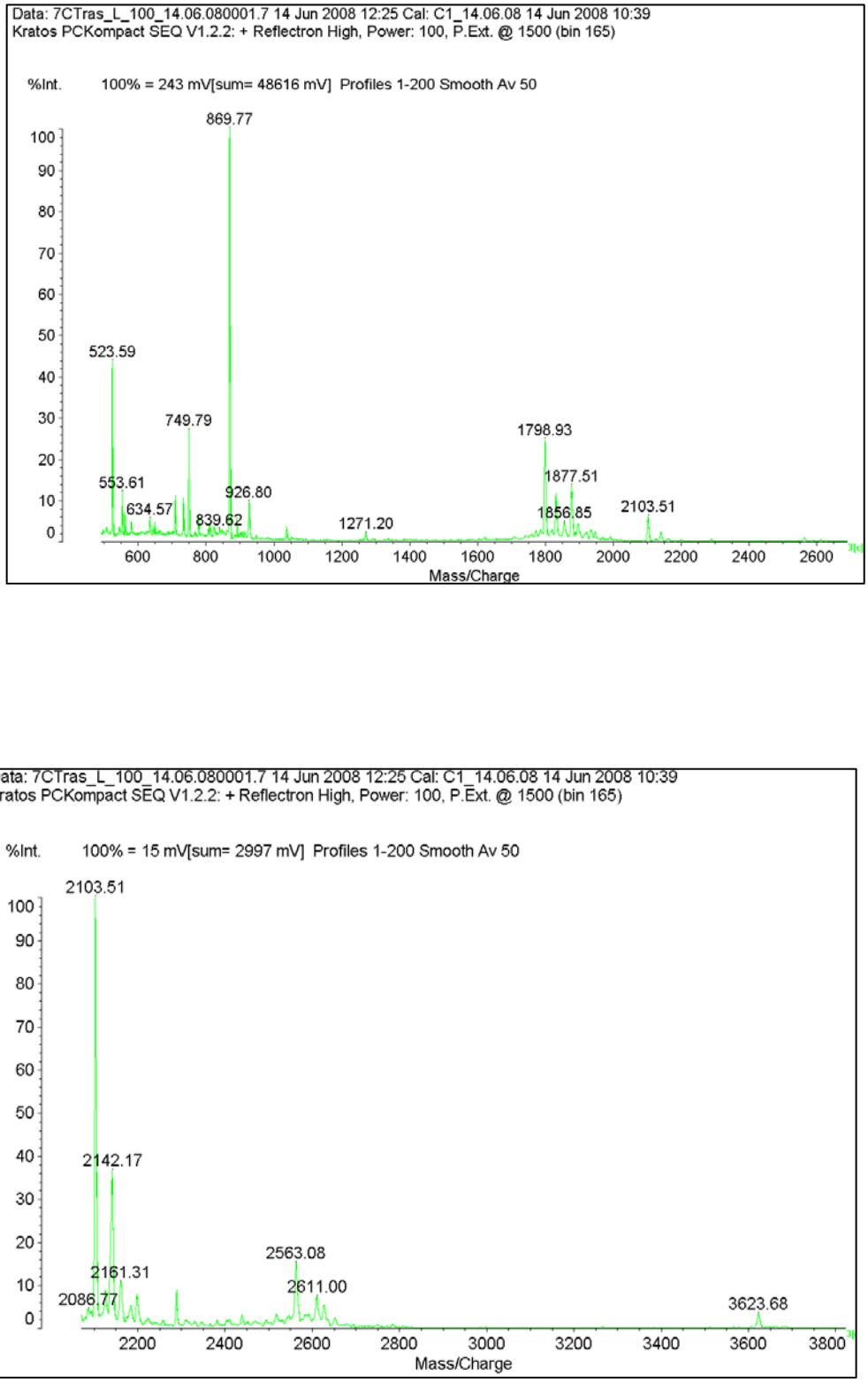

Fig. 5.47. MALDI-TOF Analysis of trastuzumab light chain. UP: Entire spectrum, DOWN: Detailed view of higher mass range.

MASCOT/NCBInr search engine (MT ±1), reported the highest ranking and scores for two proteins:

- The highest score had light chain of trastuzumab.
- Second highest score had light chain sequence variant of trastuzumab which differ from trastuzumab light chain in one amino acid residue, *Y55E* ,

As seen in protein view report (Fig. 5.48.) for Herceptin Fab (Herceptin is commercial name of trastuzumab, such as it was submitted to database[257], PDB ID. *1n8z*) the reported score was 212, there were 16 queries matched and the sequence coverage was 65 %.

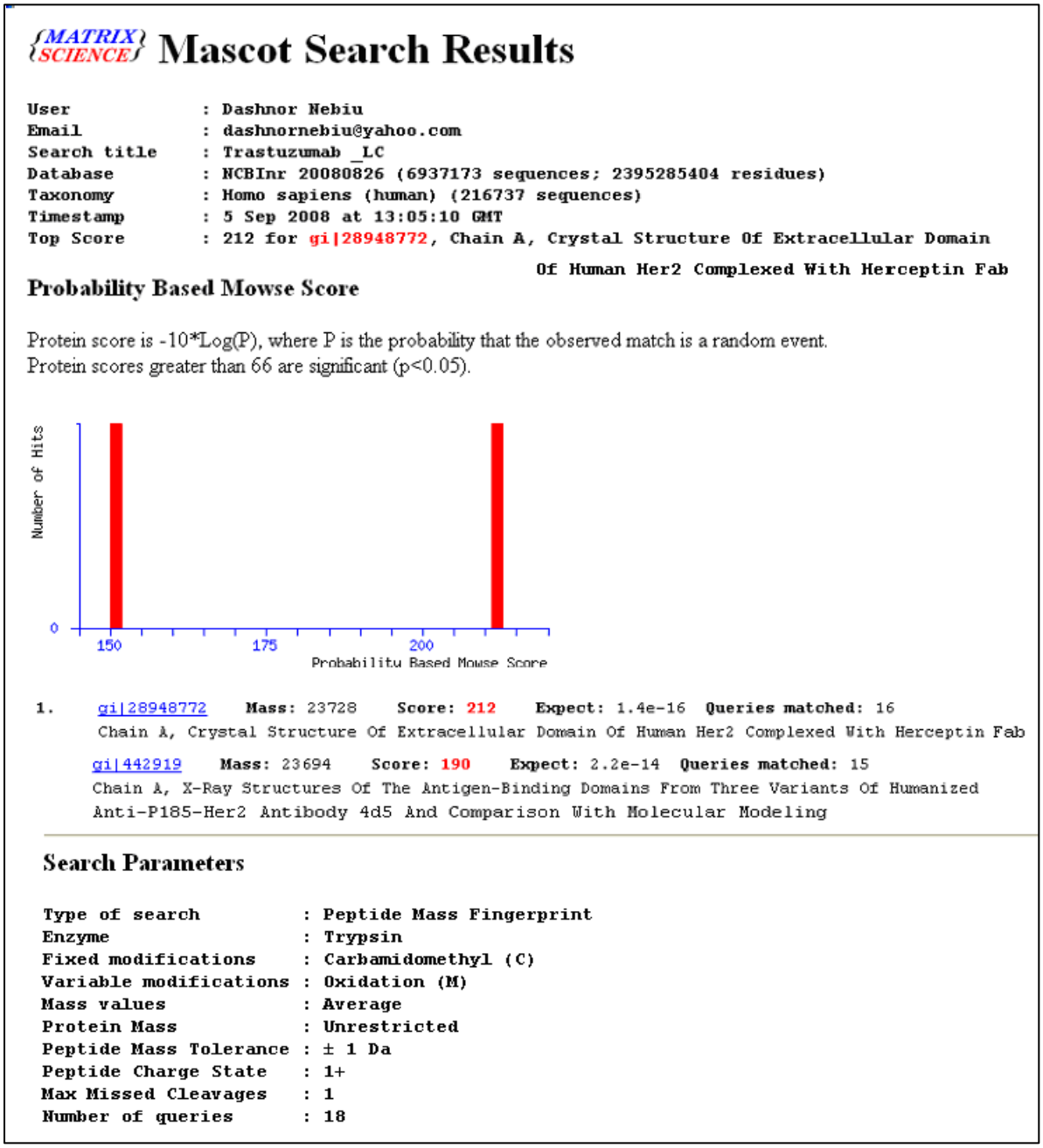

MATRIX SCIENCE **Mascot Search Results**

User : Dashnor Nebiu
Email : dashnornebiu@yahoo.com
Search title : Trastuzumab _LC
Database : NCBInr 20080826 (6937173 sequences; 2395285404 residues)
Taxonomy : Homo sapiens (human) (216737 sequences)
Timestamp : 5 Sep 2008 at 13:05:10 GMT
Top Score : 212 for gi|28948772, Chain A, Crystal Structure Of Extracellular Domain Of Human Her2 Complexed With Herceptin Fab

Probability Based Mowse Score

Protein score is -10*Log(P), where P is the probability that the observed match is a random event.
Protein scores greater than 66 are significant (p<0.05).

1. gi|28948772 Mass: 23728 Score: 212 Expect: 1.4e-16 Queries matched: 16
Chain A, Crystal Structure Of Extracellular Domain Of Human Her2 Complexed With Herceptin Fab

gi|442919 Mass: 23694 Score: 190 Expect: 2.2e-14 Queries matched: 15
Chain A, X-Ray Structures Of The Antigen-Binding Domains From Three Variants Of Humanized Anti-P185-Her2 Antibody 4d5 And Comparison With Molecular Modeling

Search Parameters

Type of search : Peptide Mass Fingerprint
Enzyme : Trypsin
Fixed modifications : Carbamidomethyl (C)
Variable modifications : Oxidation (M)
Mass values : Average
Protein Mass : Unrestricted
Peptide Mass Tolerance : ± 1 Da
Peptide Charge State : 1+
Max Missed Cleavages : 1
Number of queries : 18

Fig. 5.48. Trastuzumab, light chain. Mascot search results. Primary sequence database: NCBInr. Mas tolerance set to ± 1.0 Da

Increasing the MT parameter to ±2, the sequence coverage for light chain increased substantially, due to the match of the high mass, 3623.68 Da. Protein view data for light chain of trastuzumab (Herceptin Fab) are presented in Fig. 5.49. In this instance top score value obtained was 219, 18 masses matched and sequence coverage was 81 %.

Protein View

Match to: **gi|28948772** Score: **219** Expect: **2.7e-17**
Chain A, Crystal Structure Of Extracellular Domain Of Human Her2 Complexed With Herceptin Fab

Nominal mass (M_r): **23728**; Calculated pI value: **7.77**
NCBI BLAST search of gi|28948772 against nr
Unformatted sequence string for pasting into other applications

Taxonomy: Homo sapiens

Fixed modifications: Carbamidomethyl (C)
Variable modifications: Oxidation (M)
Cleavage by Trypsin: cuts C-term side of KR unless next residue is P
Number of mass values searched: **18**
Number of mass values matched: **18**
Sequence Coverage: **81%**

Matched peptides shown in **Bold Red**

```
     1 DIQMTQSPSS LSASVGDRVT ITCRASQDVN TAVAWYQQKP GKAPKLLIYS
    51 ASFLYSGVPS RFSGSRSGTD FTLTISSLQP EDFATYYCQQ HYTTPPTFGQ
   101 GTKVEIKRTV AAPSVFIFPP SDEQLKSGTA SVVCLLNNFY PREAKVQWKV
   151 DNALQSGNSQ ESVTEQDSKD STYSLSSTLT LSKADYEKHK VYACEVTHQG
   201 LSSPVTKSFN RGEC
```

Start - End	Observed	Mr(expt)	Mr(calc)	Delta	Miss	Sequence
1 - 18	1897.8800	1896.8726	1895.0108	1.8619	0	-.DIQMTQSPSSLSASVGDR.V Oxidation (M)
1 - 24	2611.0000	2609.9926	2609.8877	0.1049	1	-.DIQMTQSPSSLSASVGDRVTITCR.A
19 - 24	749.7900	748.7826	748.8916	-0.1090	0	R.VTITCR.A
25 - 42	1992.3600	1991.3526	1991.1642	0.1884	0	R.ASQDVNTAVAWYQQKPGK.A
25 - 45	2289.3300	2288.3226	2287.5296	0.7930	1	R.ASQDVNTAVAWYQQKPGKAPK.L
46 - 61	1773.5700	1772.5626	1773.0365	-0.4739	0	K.LLIYSASFLYSGVPSR.F
62 - 66	553.6100	552.6026	552.5808	0.0218	0	R.FSGSR.S
104 - 108	644.7700	643.7626	643.7760	-0.0133	1	K.VEIKR.T
108 - 126	2103.5100	2102.5026	2102.3890	0.1136	1	K.RTVAAPSVFIFPPSDEQLK.S
109 - 126	1947.6200	1946.6126	1946.2033	0.4093	0	R.TVAAPSVFIFPPSDEQLK.S
127 - 142	1798.9300	1797.9226	1798.0278	-0.1052	0	K.SGTASVVCLLNNFYPR.E
146 - 149	560.8000	559.7926	559.6578	0.1348	0	K.VQWK.V
150 - 183	3623.6800	3622.6726	3620.7492	1.9234	1	K.VDNALQSGNSQESVTEQDSKDSTYSLSSTLTLSK.A
184 - 190	891.6100	890.6026	889.9518	0.6509	1	K.ADYEKHK.V
189 - 207	2142.1700	2141.1626	2141.4068	-0.2442	1	K.HKVYACEVTHQGLSSPVTK.S
191 - 207	1877.5100	1876.5026	1876.0952	0.4074	0	K.VYACEVTHQGLSSPVTK.S
208 - 211	523.5900	522.5826	522.5548	0.0278	0	K.SFNR.G
208 - 214	869.7700	868.7626	868.9143	-0.1517	1	K.SFNRGEC.-

Fig. 5.49. Trastuzumab, light chain. Mascot search results. Primary sequence database: NCBInr. Protein view data/Section. Mas tolerance set to ± 2.0 Da.

As seen from the amino acid sequence in Fig. 5.49 amino acid residues Y-55 and R-66, both sequentially covered, are characteristic for trastuzumab (rhumAb4D5-8) light chain. Y-55 as part of CDR region, and R-66 as part of FR3 were imported from the

murine LC sequence into the human LC sequence (See Table 1.6). Therefore, they are determinants for humanised antibody. On the other hand, if the light chain sequence of trastuzumab is carefully observed (Fig. 5.49), between peptide fragments of positions 62-103 and 67-103 and 67-107 respectively there is no lysine, neither arginine, therefore their masses are very high to be extracted from the gel and subsequently detected by MALDI-TOF MS. Therefore that region of light chain sequence remained uncovered.

Second protein to be reported was variant of trastuzumab *humAb4D5-7* which contains *E* instead of *Y* at position 55. Score and sequence coverage for this protein was lower that for trastuzumab though.

For MT ±1.2 and ±1.5 obtained score results were 201 and 186, respectively. The number of queries matched was 16 in both cases.

MASCOT/MSDB search engine (MT± 2) reported as the highest rank *mixture 1* of two proteins,"separating" the sequence of trastuzumab light chain in two parts:

1. Protein *CAH68665,* Score: 106, Molecular mass: 11936, 10 matched queries, sequence coverage 97%. From Figures 5.49 and 5.50 is observed that the complete sequence of this protein is identical with trastuzumab sequence, corresponding to amino acid residues108-214, in other words to constant domain of its light chain.

Matched peptides shown in **Bold Red**

```
     1 RTVAAPSVFI FPPSDEQLKS GTASVVCLLN NFYPREAKVQ WKVDNALQSG
    51 NSQESVTEQD SKDSTYSLSS TLTLSKADYE KHKVYACEVT HQGLSSPVTK
   101 SFNRGEC
```

Fig. 5.50. Trastuzumab, light chain. Section of protein view from Macot/MSDB search results. Sequence of *CAH68665,* identical with trastuzumab light chain

2. Protein *1 FVCC* (*Fv fragment of humanised antibody 4D5, version 8, chain* C with scoring parameter 74, molecular mass 11966, queries matched 8, and sequence coverage 65 %, (Fig. 5.51).

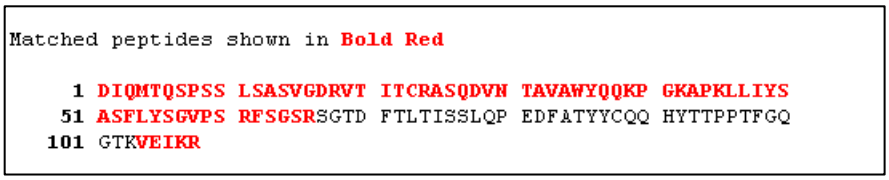

Fig. 5.51. Trastuzumab, light chain. Section of protein view from Macot/MSDB search results. *1 FVCC*.

This protein represents light chain variable domain of trastuzumab. It corresponds to light chain trastuzumab sequence 1-108 (Figures 1.7, 5.49 and 5.51).

Narrower mass tolerance parameters i.e. MT±1; MT±1.2 and MT±1.5, delivered same sequence coverage for *1 FVCC (*65 %), provided that for *CAH68665* coverage was reduced to 65 %.

In MASCOT/SwissProt the highest score (90) result was protein *IGKC_Human* (Ig kappa chain C region). There were 9 mass values matched with sequence coverage of 97 %. The sequence of *IGKC_Human* (Ig kappa chain C region) reported here is identical with trastuzumab sequence, 109-214.

Finally, PROFOUND/NCBInr generated same results as MASCOT/NCBInr.

As in the case of heavy chain analysis, for both staining methods, MALDI-TOF analysis delivered qualitatively similar spectra. From Coomassie stained gels number of detected masses was higher (Fig. 5.52), which reflected on the increase of sequence coverage for identified trastuzumab.

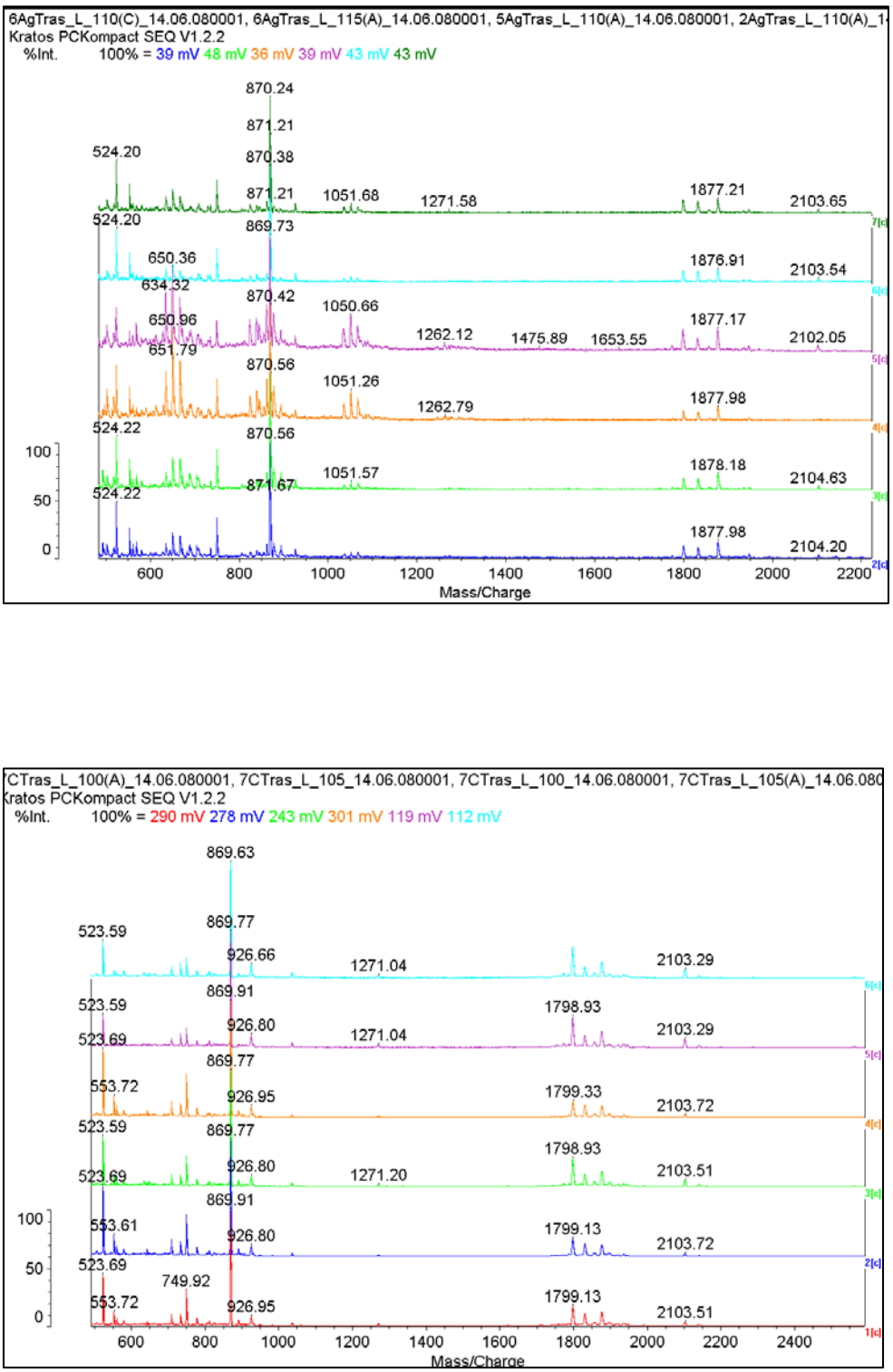

Fig. 5.52. MALDI_TOF Analysis of trastuzumab light chain. UP: MALDI -TOF Spectra of peptides generated from silver stained gels DOWN: MALDI -TOF Spectra of peptides generated from Coomassie stained gels.

5.4. Gel electrophoresis analysis of rituximab

In order to assess relevant quality parameters ncluding detection, molecular weight estimation and purity, one-dimensional sodium dodecylesulfate polyacrylamide gel electrophoresis analysis (1D-SDS PAGE) of rituximab has been performed under reducing and non-reducing conditions.
For the same purpose as above, and additionally for the estimation of the protein *pI*, study of the charge heterogeneity, and isoform pattern, two-dimensional gel electrophoresis analysis (2-DE) has been performed. Aiming the efficient resolution of protein spots two types of immobilized pI gradients (*IPG)* have been employed in the first dimension, IEF: *IPG* strips *3-11 NL* and *IPG* strips *6-9 L*.
Obtained 1-DE SDS PAGE and 2-DE gels have been stained with Coomassie and silver staining.

5.4.1. One dimensional (1D-SDS-PAGE) gel electrophoresis analysis of rituximab

5.4.1.1. Molecular weight estimation and sensitivity of staining

In Figures 5.53 and 5.54, 1D-SDS PAGE gels of rituximab under reducing and nonreducing conditions are presented. The electropherograms show typical gel patterns of IgG. Under reducing conditions, trastuzumab migrated as two sharp bands of heavy chain at located at ~ 50 kDa and light chain at ~23 kDa, respectively.
On the other hand under non-reducing conditions, single band of rituximab has been observed at molecular weight higher than 150 kDa, provided that lower molecular mass minor protein bands could be observed as well. The obtained molecular masses correspond to the masses of rituximab heavy and light chain. Since trastuzumab heavy chain is glycosilated observed mass corresponds to the glycosilated form which is approximately 3-5 % higher than the mass of heavy chain derived from its consensus sequence. Theoretical average molecular weight of rituximab heavy chain based on its amino acid sequence in reduced, non-glycosilated form is 49.214 kDa. On the other hand, the theoretical molecular weight

of the rituximab light chain is 23.057 kDa[252]. Therefore, the molecular weight of non-glycosilated rituximab is 144.542 kDa.

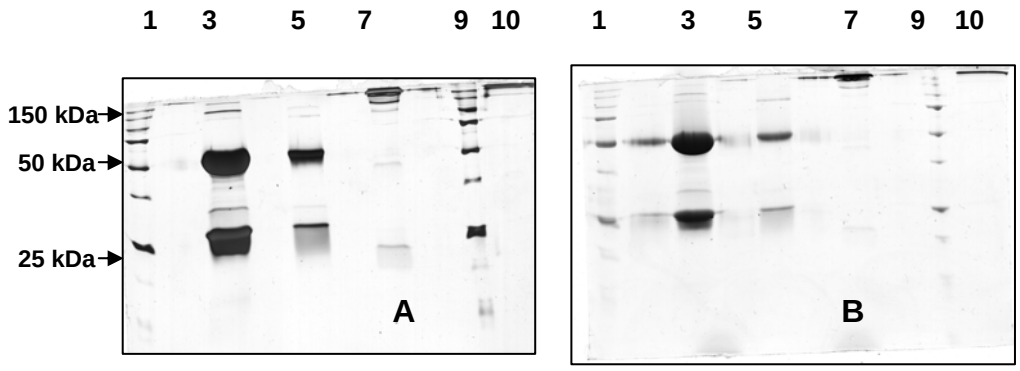

Fig. 5.53. 1-DE analysis of rituximab A) silver staining; B) Coomassie staining. Lanes **1** and **9**: MW standard; lanes **3** and **5**: rituximab, reducing conditions, 15 and 1.5 µg, respectively; lanes **7** and **10**: rituximab, non-reducing conditions, 15 and 1.5 µg respectively.

In order to assess, linearity and sensitivity of staining, 1D SDS PAGE analysis of rituximab under reducing conditions with the sample concentration ranging from (0.0067 µg/µl-0.33 µg/µl) was performed (Fig. 5.54.).

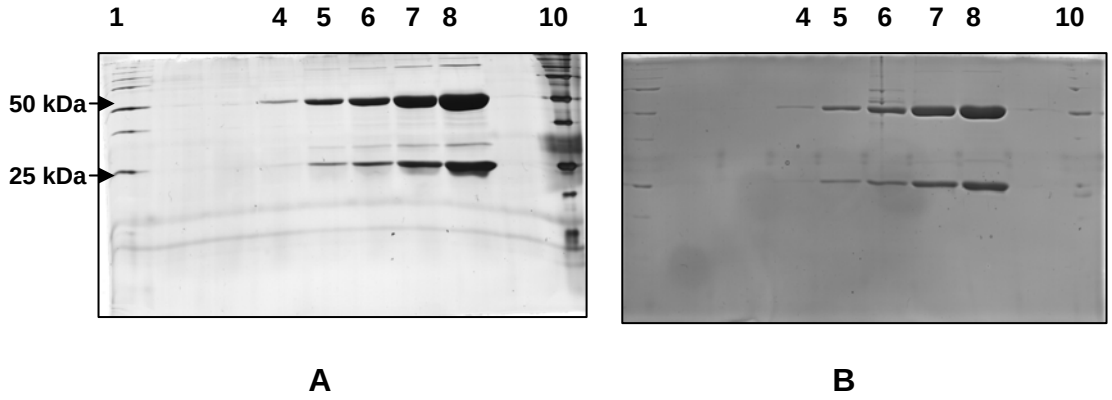

Fig. 5.54. 1-DE analysis of rituximab. Linearity/sensitivity A) silver staining. B) Coomassie staining. Lanes **1** and **10** MW standards. Lanes: **4,5, 6, 7** and **8**: rituximab in increasing amount: 0.1 µg, 0.5 µg, 1 µg, 2.5 µg, and 5 µg

The Gels in Fig. 5.54 showed that in this concentration range, both staining procedures enabled detection of rituximab bands, provided that for the lowest sample

concentration in silver stained gel band intensity. Additionally, upon silver staining procedure additional protein bands are detected as well i.e. at the aggregate region.

5.4.1.2.1-DE. Deglycosilation optimisation study. Preliminary experiments

In Fig. 5.55, 1-DE gels of rituximab treated with N-glycosidase F under different conditions are presented.

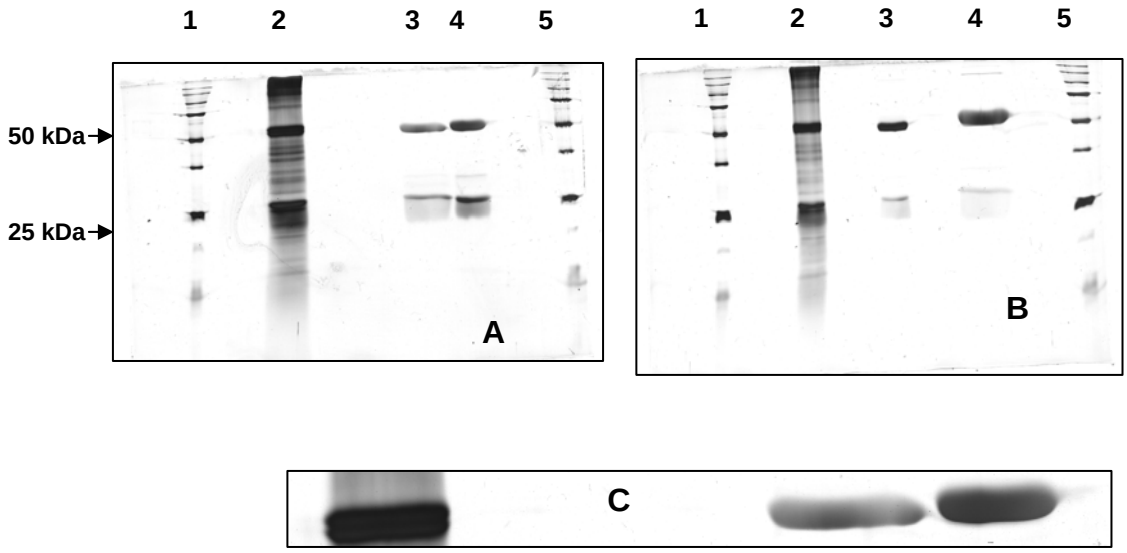

Fig. 5.55.1-DE analysis of rituximab. Deglycosilation monitorisation. Rituximab 2 µg. Silver staining
A) Digestion time 24 hour. B) Digestion time 48 hour. C) Section of gel **A**.
Lanes **1, 5**: MW standards, Lane **4**: glycosilated rituximab, Lane **2**: deglycosilated rituximab Method 1, Lane **3**: deglycosilated rituximab, Method 2.

Performed experiments for deglycosilation of rituximab and trastuzumab generated similar results. Gels bands from Fig. 5.55. show that deglycosilation performed under reducing and denaturing conditions (Method 1), brought about only partial deglycosilation. Heavy chain bands are split indicating non-efficient deglycosilation process (Fig. 5.55. lane 2 in both gels, Fig 5.55. C.)

On the other hand, lane 3 in both gels migrated at slightly lower molecular weight comparing to glycosilated band 4, and showed no splitting. On the basis of these observations was evident that deglycosilation Method 2, which employs surfactant Triton X-100, without reduction and denaturation is more efficient than the first

method. As discussed previously, upon denaturation, immunoglobulin heavy chains become insoluble consequently their deglycosilation process is hampered.

According results from Fig. 5.55.A and B, digestion times (24 and 48 hours) did not influence significantly the deglycosilation efficiency.

Monitorisation of deglycosilation efficiency for Methods 3 and 4 is depicted in the Fig. 5.56. Comparison of heavy chain bands of glycosilated trastuzumab (lane 2) with the lines of heavy chains of deglycosilated trastuzumab according Method 3 and 4 (lanes 3 and 4, respectively) revealed that the molecular weights of both deglycosilated samples were substantially lower. Furthermore 1-DE data from Fig. 5.55 and Fig. 5.56 indicate that deglycosilation Methods 3 and 4 result as more efficient than Method 2. The first method, results the one with the lowest deglycosilation efficiency.

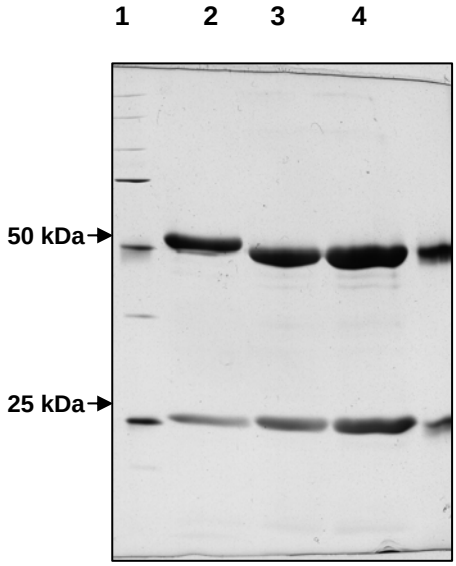

Fig. 5.56. 1-DE analysis of rituximab. Deglycosilation monitorization. Optimised conditions. Rituximab 2 µg. Silver staining. Digestion time 24 h. 10 I.U. NGF
Lane **1**: Molecular weight standards. Lane **2**: Nondeglycosilated sample/control, Lane **3**: deglycosilated, Method 3, Lane **4**: Deglycosilated, Method 4

5.4.2. Two-dimensional (2-DE) gel electrophoresis analysis of rituximab

5.4.2.1. Immobilized pH gradient IPG 3-11 NL

2-DE experiments of native, glycosilated rituximab revealed very complex two dimensional electrophoresis spot patterns characteristic for monoclonal antibodies: two sets of characteristic spots, one at ~50 kDa and other ~23 kDa.

Heavy chain spots appeared as a characteristic band forming spots located in the *pI* range from about 6.3 to 9 provided that the most intense spots are at the basic region above *pI* 8. According to the electrophoresis data, comparing to the heavy chain spots, rituximab light chin spots are slightly shifted to the lower *pI* range, from about 6 to about 8.5, the most intense spot(s) being around pI 8.1. Experimentally estimated isoelectric points were in accordance with the theoretical *pI* values derived from *cDNA* amino acid sequences of rituximab heavy and light chains: 8.67 and 8.26, respectivly[252]. According published data the *pI of* immunoglobulins of IgG class ranges from 6.4 to 9[258].

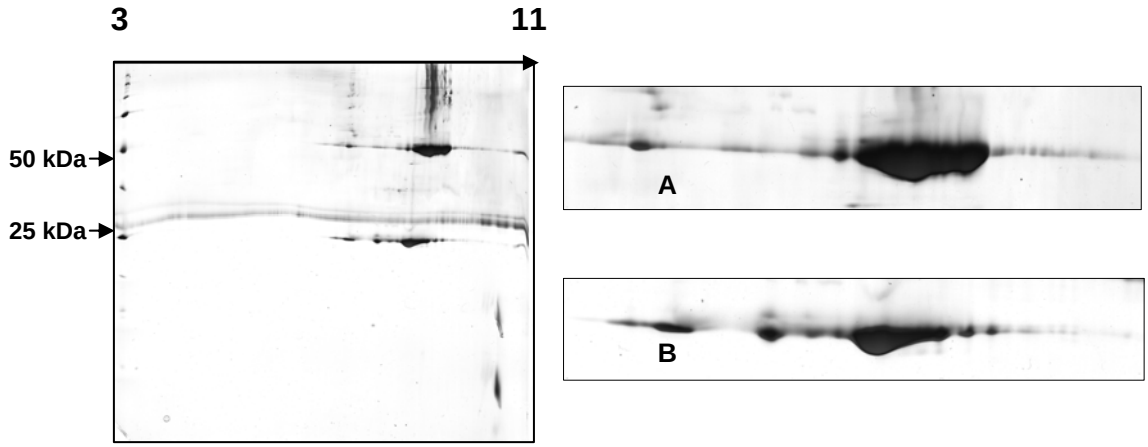

Fig. 5.57. 2-DE analysis of rituximab, glycosilated sample 10 µg. Silver staining
A) Heavy chain, detailed insight B) Light chain, detailed insight

Experimental data revealed that reduction of sample concentration generally delivered spot patterns of higher resolution. Furthermore it is confirmed superior sensitivity of silver staining comparing to Coomassie staining procedure. As observed in Fig. 5.58, Coomassie staining provided the characteristic spot pattern of rituximab,

of same *pI* range. However, as presented in Fig. 5.58A and B, spot intensities of silver and Coomassie stained gels are similar even at 10 fold higher sample amount loaded to Coomassie stained gel.

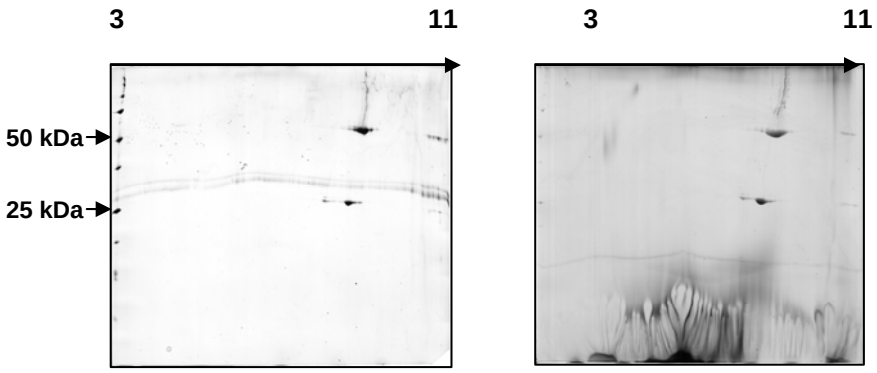

Fig. 5.58. 2-DE analysis of rituximab. Sample concentration.
A) Glycosilated, 1µg, Silver staining. B) Non-Glycosilated, 10 µg.
Coomassie staining

5.4.2.2. Immobilized pH gradient IPG 6-9 L

As observed in previous experiments, 2-DE gels of rituximab generated extremely complex spot pattern for both light and heavy chains and 2-DE gels as poorly resolved band forming spots, typical for all IgG are seen. Aiming to reduce spot overlapping and achieve better resolution, narrower immobiline pH gradient, 6 -9 *L* was used for the first dimension, isoelectric focusing. However, 2-DE data revealed no improvement in isoform resolution after application of narrow immobiline gradient (Fig. 5.59). Furthermore, comparing IPG 6-9 L with IPG 3-11 NL gels of rituximab and trastuzumab, isoform resolution obtained with IPG 6-9 L seems to be even worst than obtained from IPG 3-11 NL gels.

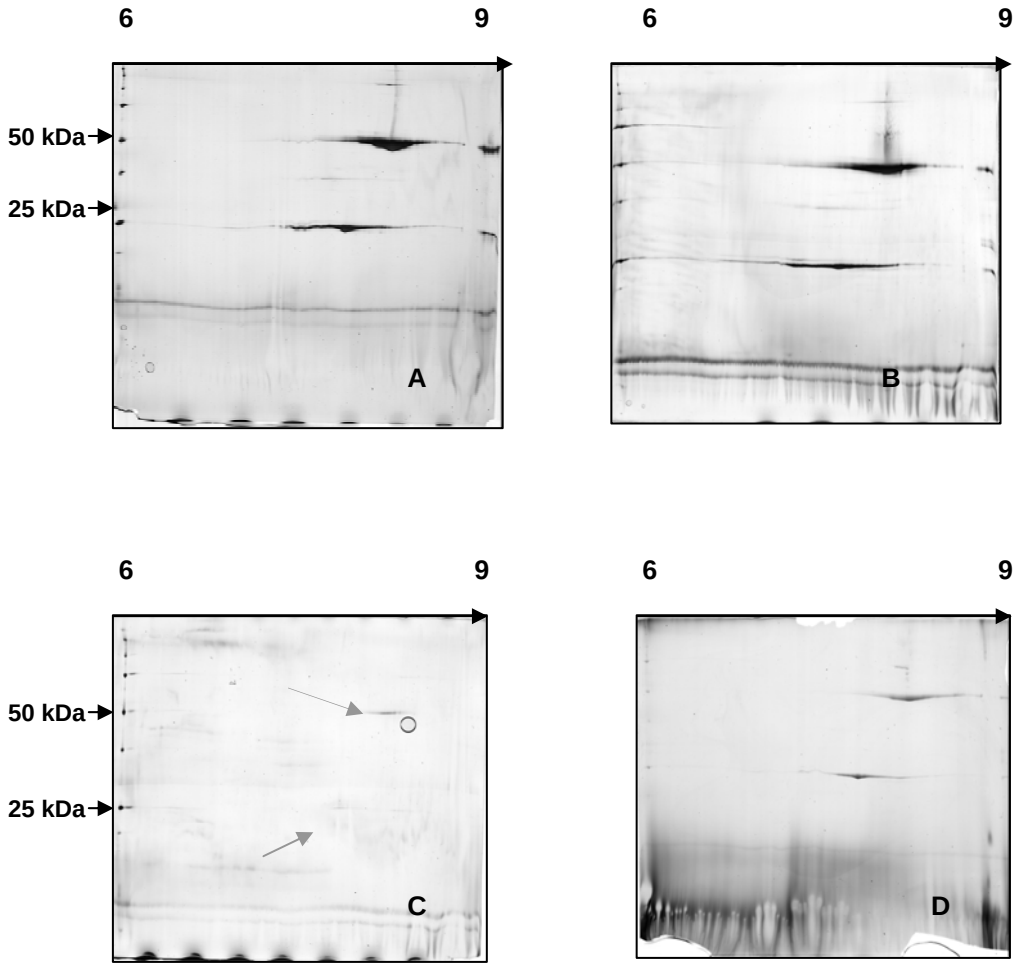

Fig. 5.59. 2-DE Analysis of glycosilated rituximab.
A) 10 µg rituximab, Silver staining. Control
B) 10 µg rituximab. 30 days, 4-8 °C
C) 0.1µg rituximab, Silver staining
D) 10 µg rituximab, Coomassie staining

Coomassie stained gels of rituximab afford typical gel electrophoresis pattern of rituximab, provided that the band streaking was not as intense as in the case of silver staining at the same sample concentration (Fig. 5.59.D). On the other hand the superior sensitivity of silver staining vs. Coomassie staining is demonstrated in Fig. 5.59.C., when 0.1µg sample is applied and both chain spots have been detected

In the Fig. 5.59.B 2-DE gel of rituximab aged sample is presented. No significant mass or *pI* changes were observed. For comparison 2-DE gel of control has been presented as well (Fig. 5.59.A).

5.4.2.3. Charge heterogeneity study of rituximab

After preliminary 1D SDS PAGE and 2-DE experiments, next step consisted in the study of the influence of glycosylation and lysine truncation on rituximab charge heterogeneity, aiming the reduction of sample complexity and/or optimization of deglycosilation as sample preparation procedure for the subsequent immunoglobulin identification with MALDI-TOF analysis.

For this study both immobiline pH gradients were applied: *IPG 3-11 NL* to assess changes at the broader *pI* range and *IPG 6-9 L* to eventually have a detailed insight in narrower range. Proteins were detected with silver staining.

Since deglycosilation study of rmAb trastuzumab indicated that no significant changes occurred in the *isomorf* pattern of this antibody after sialidase treatment the enzymatic desialination study of rituximab was omitted. Rituximab and trastuzumab oligosaccharides are mostly asialo neutral type of glycans, therefore desialination of sialo negatively charged glycans which are only minor component (less than 3 % in sugar content), could not be detected with 2-DE. In addition, according literature data rituximab contains no O-linked glycans , therefore, O-deglycosilation study was not performed, as well[253].
For the first dimension, *IEF*, immobiline *pH* gradients 3-11 *NL* and 6-9 *L* have been employed. Deglycosilation efficiency was monitored with 1-DE (Fig. 5.55 and Fig. 5.56).

5.4.2.4. N-linked glycans. N-glycosidase F

For the N-linked oligosaccharide removal enzyme N-glycosidase-F has been used.

This enzyme specifically hydrolyzes the aspartil glycosilamine bond between rituximab heavy chain Asn_{301} and the innermost N-acetylglucosamine of the oligosaccharide. Free carboxylate of aspartic acid, N-acetyl glucosamine which spontaneously hydrolizes to ammonia and free oligosaccharide are the reaction products. In rituximab (and trastuzumab) heavy chain there is only one oligosaccharide binding site Asn_{301} (Asn_{300}, respectively) therefore the release of only one free carboxylate occurs.

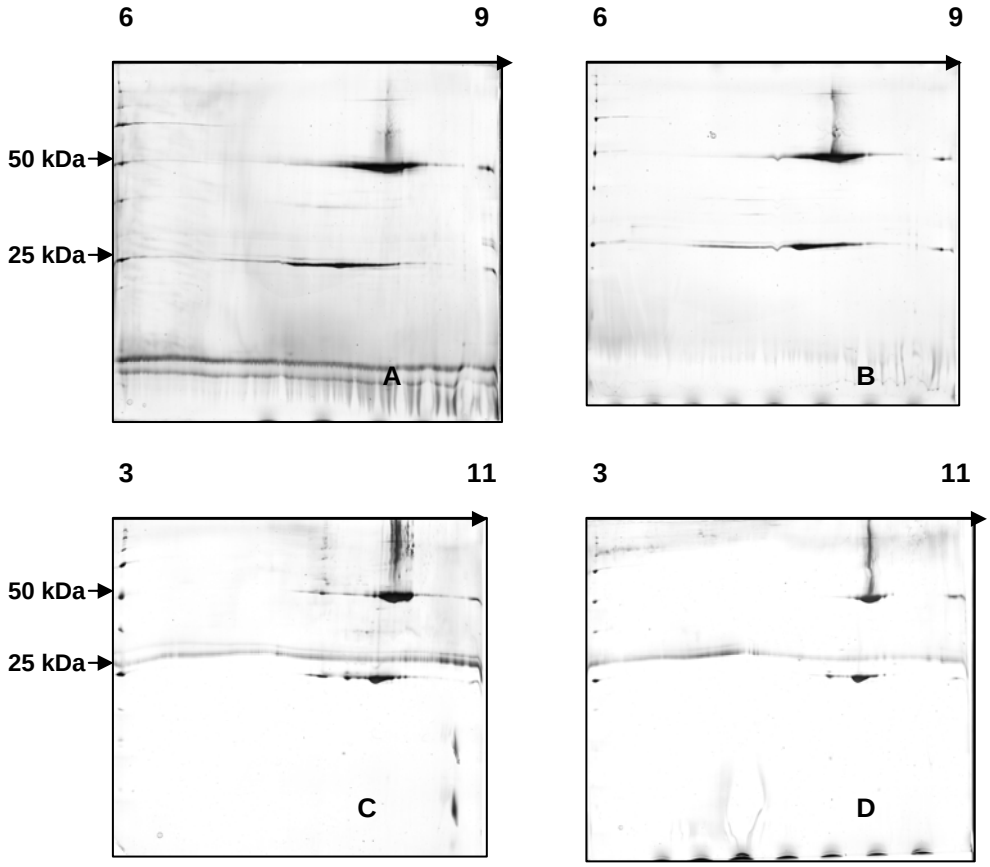

Fig. 5.60. 2-DE analysis of rituximab. Deglycosilation study. 10 µg rituximab. Silver staining
A) Glycosilated 6-9 L /Controle B) Deglycosilated, Method 2; 6-9 L
C) Glycosilated 3-11 NL /Controle D) Deglycosilated, Method 2, 3-11 NL

Data obtained by 2-DE experiments revealed that the influence of N-Glycosidase-F glycan release was very small and it could not be detected with this technique. After glycan release, expected heavy chain molecular mass decrease is only about 3-5 % and *pI* difference only 0.1 (8.67 N-301; 8.57 D-301) due to the fact that N-linked sugars are neutral. Therefore, 1-DE and not 2-DE was able to confirm heavy chain

molecular mass reduction, for studied rmAbs, trastuzumab and rituximab. Molecular mass of light chain anyway should remain unaffected.

After deglycosilation, charge heterogeneity remained the same, suggesting that other factor, as in case of trastuzumab, and not glycovariants might be relevant to determine charge heterogeneity pattern of rituximab.

In Fig. 5.60. 2-DE gels obtained from deglycosilated trastuzumab are presented. For N-linked glycan release, Method 2 employing nonionic surfactant, Triton X-100 was employed. Neither gels *IPG 3-11 NL* (Fig. 5.60. A, B) nor *IPG 6-9 L* (Fig. 5.60. C, D) were able to detect molecular weight and/or *pI* differences between deglycosilated and glycosilated (control) samples.

Deglycosilation employing Method 1 as in the case of trastuzumab brought about horizontal split up of spot bands, indicating incomplete degycosilation, (Fig. 5.61.)

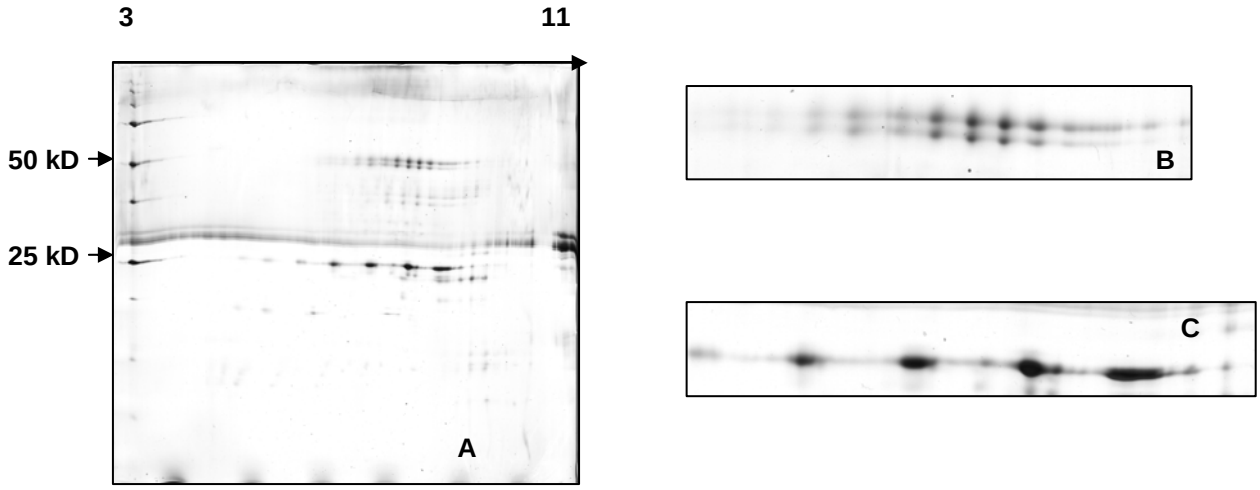

Fig. 5.61. 2-DE analysis of rituximab. Deglycosilation optimisation study. Silver staining. 10 µg rituximab
A) Deglycosilated, 3-11 NL, Method 1
B) Heavy chain spot band split suggesting incomplete/partial deglycosilation.
C) Light chain

Deglycosilation Methods 3 and 4, which on the basis of 1-DE data resulted as optimal, were used for trastuzumab N-linked glycan release for the preparation of sample for subsequent MALDI-TOF analysis (Fig. 5.62).

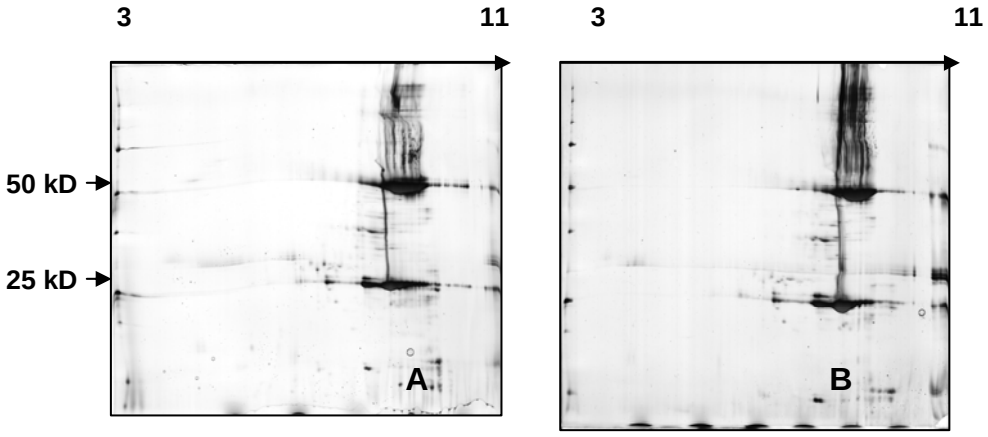

Fig. 5.62. 2-DE analysis of rituximab. Optimised deglycosilation conditions. 100 µg, 3-11NL, Silver staining Deglycosilated, N-Glycosidase F A) Method 3 B) Method 4

5.4.2.5. The study of lysine truncation. Carboxypeptidase B

For the study of lysine truncation, rituximab solution was digested with the enzyme carboxypeptidase B (CPB) which specifically cleaves the terminal lysines from the protein backbone. After 2-DE experiments no significant changes in the spot pattern of heavy chain upon carboxypeptidase B treatment were observed (Figures 5.63. and 5.64.).

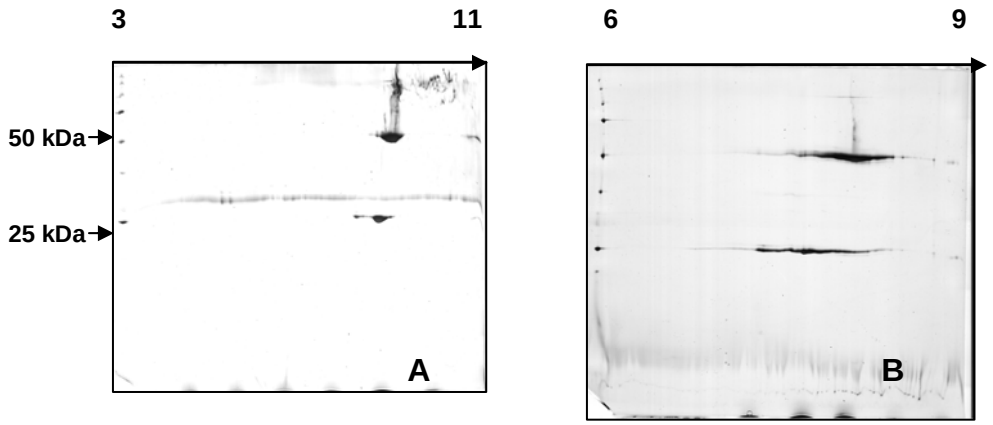

Fig. 5.63. 2-DE analysis of rituximab. Carboxypeptidase B. 10 µg, silver staining. A) 3-11 NL B) 6-9 L

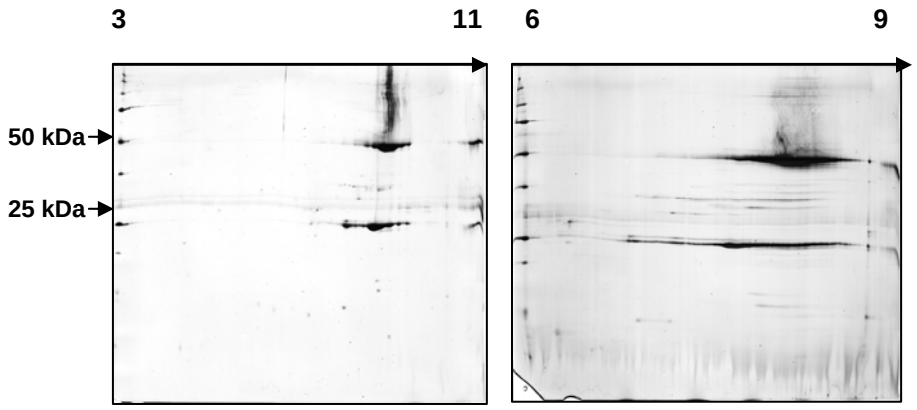

Fig. 5.64. 2-DE analysis of rituximab. Carboxypeptidase B plus N-Glycosidase F. 10µg rituximab. Silver staining. A) 3-11 NL B) 6-9 L

5.5. Matrix assisted laser desorption ionization time of flight mass spectrometric (MALDI-TOF MS) analysis of rituximab

5.5.1. Primary sequence confirmation. Peptide mass fingerprinting

In Fig. 5.65. MALDI-TOF spectrum of generated peptides from deglycosilated and in-gel tryptic digested rituximab heavy chain, is presented.

Rituximab is chimeric IgG1- κ antibody obtained by cloning murine light and heavy chain variable regions into the human framework.

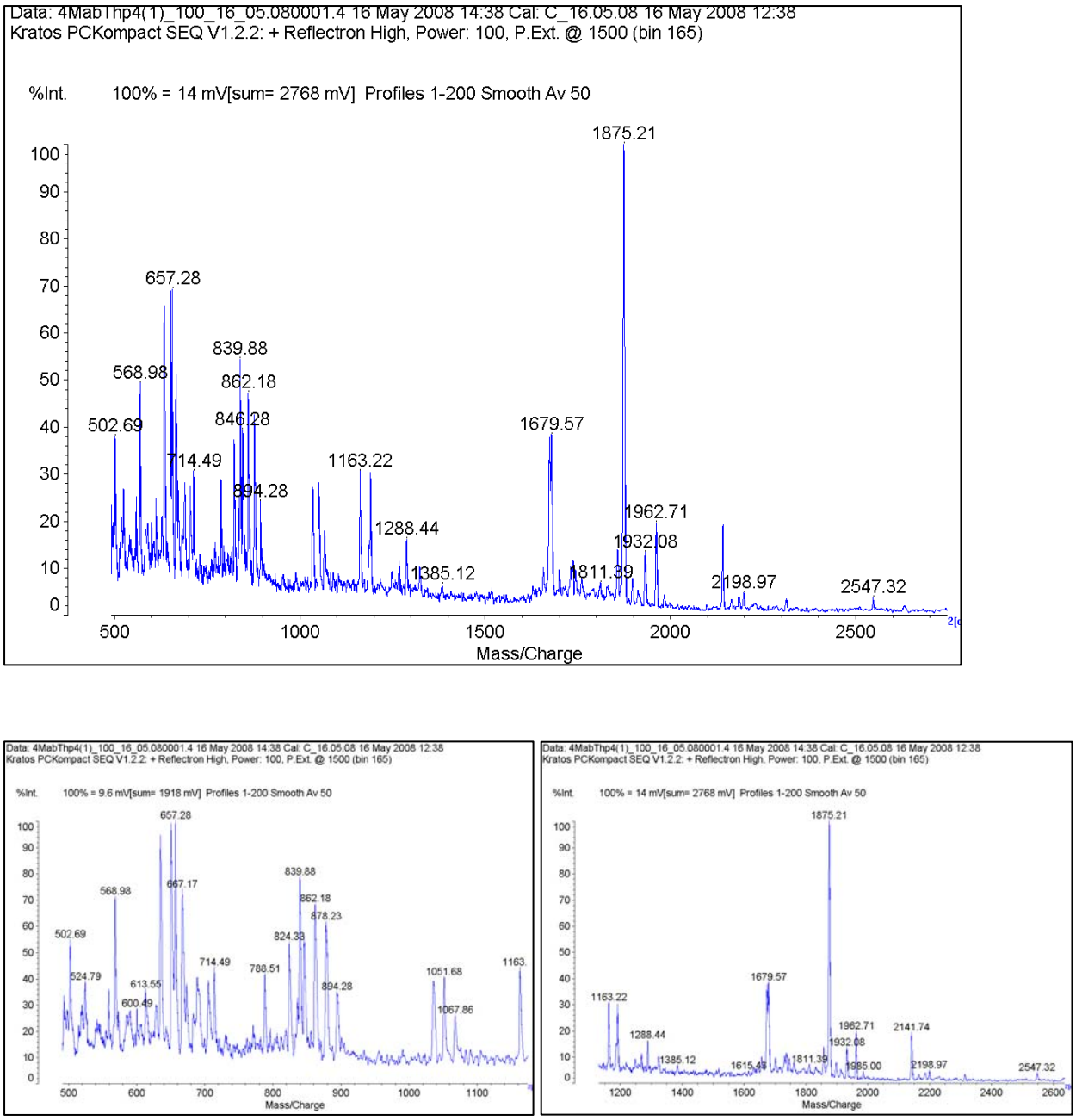

Fig. 5.65. MALDI-TOF spectra of deglycosilated rituximab heavy chain. Up: Entire spectrum; Down: Detailed spectra.

As discussed above, recombinant monoclonal antibody rituximab contains two heavy and two light chains linked via disulfide bridges. It is composed of 1,328 amino acids: heavy chain contains 451 and light chain 213, amino acids, respectively (Fig. 1.8).

5.5.1.1. Identification of heavy chain

For primary sequence confirmation and identification of the rituximab heavy chain, the list of 14 peptide masses (Fig. 5.66) generated by MALDI-TOF MS of peptides obtained from corresponding positions of silver stained gels (Fig. 5.62) were searched with MASCOT and PROFOUND (Prowl) search engines using three sequence databases: MSDB, NCBInr and SwissProt.

2547.32; 2141.74; 1875.21; 1679.57; 1674.77; 1288.44; 1191.86; 1163.22; 878.23; 839.88; 788.51; 657.28; 559.18; 502.69

Fig. 5.66. Rituximab heavy chain. List of entered peptide masses.

During Database searching, taxonomy was restricted to *Homo sapiens*, selected enzyme was trypsin. Other search parameters were set to allow up to 1 missed cleavage, methionins in oxidized form (variable modification), cysteins in carbamidomethylated form (fixed modification), average mass, peptide ions in protonated $[M+H]^+$ form, mass tolerance was set ±1, ±1.5 and ±2 Da. Protein molecular mass was not specified. The best results were obtained with MASCOT/NCBInr and PROFOUND (Prowl)/NCBInr databases.

5.5.1.2. MASCOT/NCBInr sequence database

List of searched peptides at MT±2 at MASCOT/NCBInr primary sequence database generated the top score values for human IgG1 constant region (score: 81- 119) and Fc fragment of rituximab (score 103) (Fig. 5.67).
As seen from search results, the highest score had an IgG1 Fc fragment. There were 12 masses matched and 60 % sequence coverage for this immunoglobulin fragment.
Chain A, Fc fragment of rituximab bound to minimized version of *protein A* (Z34c) had score 103, 11 matched masses and 57 % sequence coverage (Fig. 5.68).

Due to the fact that in database a version of Fc fragment lacking the last 4 amino acid residues at the C-terminus (448-SPGK-451) is registered, peptide mass 788.51 Da does not match. According *in silico* digest this peptide mass corresponds to heavy chain residue 444-SLSLSPGK-451 (Fig. 1.8.). Furthermore, in MALDI-TOF

spectrum peptide mass of 1962.71 Da has been observed. The difference of this peptide mass and the peptide mass of heavy chain fragment 1-19 (1978.29 Da) is 15.6 Da, suggesting possible glutamine (Q) to pyroglutamate conversion. The theoretical difference is between two masses is 17 kDa.

Decreasing Mass tolerance parameter to ±1.5, number of matched masses dropped to 9, sequence coverage was lower, however the score parameter although reduced, was still significant.

The observed peptide masses were searched in MSDB and SwissProt search engines. At the same search parameters, these two databases generated high score

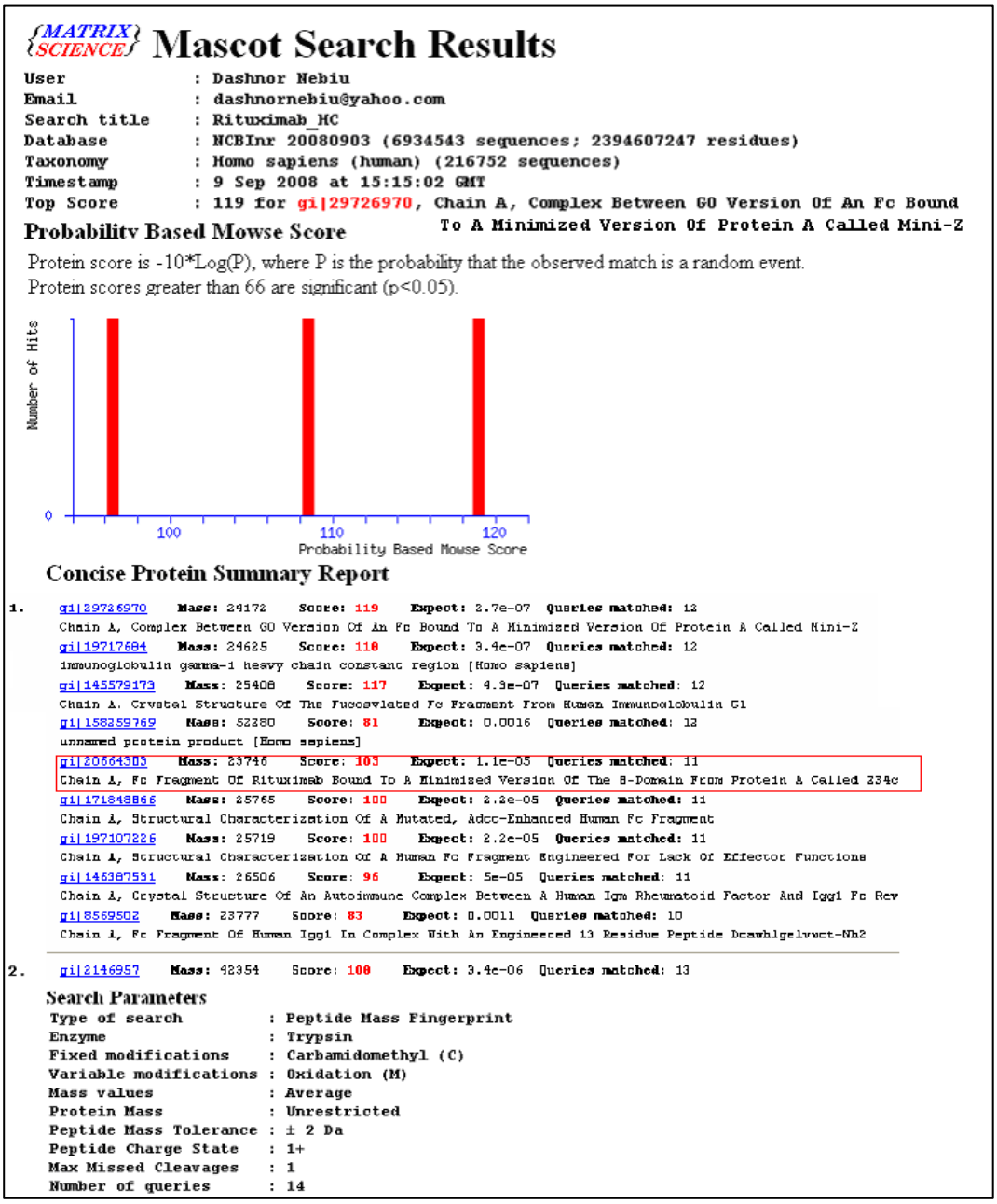

Fig. 5.67. Rituximab, heavy chain. Mascot search results. Primary sequence database: NCBInr. Mass tolerance was set to ± 2 Da

results for human IgG1 constant region and human IgG1 Fc fragment.

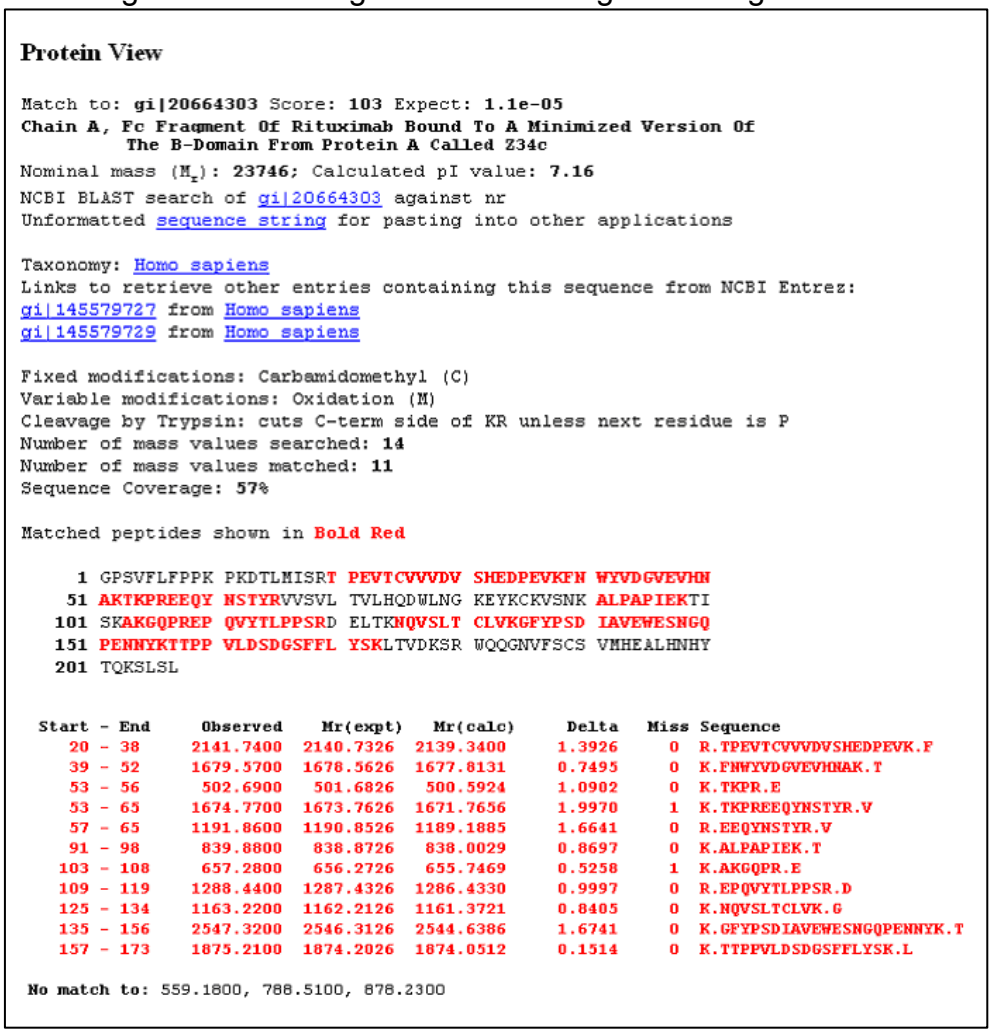

Protein View

Match to: **gi|20664303** Score: **103** Expect: **1.1e-05**
Chain A, Fc Fragment Of Rituximab Bound To A Minimized Version Of The B-Domain From Protein A Called Z34c
Nominal mass (M_r): **23746**; Calculated pI value: **7.16**
NCBI BLAST search of gi|20664303 against nr
Unformatted sequence string for pasting into other applications

Taxonomy: Homo sapiens
Links to retrieve other entries containing this sequence from NCBI Entrez:
gi|145579727 from Homo sapiens
gi|145579729 from Homo sapiens

Fixed modifications: Carbamidomethyl (C)
Variable modifications: Oxidation (M)
Cleavage by Trypsin: cuts C-term side of KR unless next residue is P
Number of mass values searched: **14**
Number of mass values matched: **11**
Sequence Coverage: **57%**

Matched peptides shown in **Bold Red**

```
     1 GPSVFLFPPK PKDTLMISRT PEVTCVVVDV SHEDPEVKFN WYVDGVEVHN
    51 AKTKPREEQY NSTYRVVSVL TVLHQDWLNG KEYKCKVSNK ALPAPIEKTI
   101 SKAKGQPREP QVYTLPPSRD ELTKNQVSLT CLVKGFYPSD IAVEWESNGQ
   151 PENNYKTTPP VLDSDGSFFL YSKLTVDKSR WQQGNVFSCS VMHEALHNHY
   201 TQKSLSL
```

Start - End	Observed	Mr(expt)	Mr(calc)	Delta	Miss	Sequence
20 - 38	2141.7400	2140.7326	2139.3400	1.3926	0	R.TPEVTCVVVDVSHEDPEVK.F
39 - 52	1679.5700	1678.5626	1677.8131	0.7495	0	K.FNWYVDGVEVHNAK.T
53 - 56	502.6900	501.6826	500.5924	1.0902	0	K.TKPR.E
53 - 65	1674.7700	1673.7626	1671.7656	1.9970	1	K.TKPREEQYNSTYR.V
57 - 65	1191.8600	1190.8526	1189.1885	1.6641	0	R.EEQYNSTYR.V
91 - 98	839.8800	838.8726	838.0029	0.8697	0	K.ALPAPIEK.T
103 - 108	657.2800	656.2726	655.7469	0.5258	1	K.AKGQPR.E
109 - 119	1288.4400	1287.4326	1286.4330	0.9997	0	R.EPQVYTLPPSR.D
125 - 134	1163.2200	1162.2126	1161.3721	0.8405	0	K.NQVSLTCLVK.G
135 - 156	2547.3200	2546.3126	2544.6386	1.6741	0	K.GFYPSDIAVEWESNGQPENNYK.T
157 - 173	1875.2100	1874.2026	1874.0512	0.1514	0	K.TTPPVLDSDGSFFLYSK.L

No match to: 559.1800, 788.5100, 878.2300

Fig. 5.68. Rituximab, heavy chain. Mascot/NCBInr. Protein view section.

PROFOUND (Prowl) search engine generated similar results as MASCOT/NCBInr for same peptide fragment masses searched (Fig. 5.69).

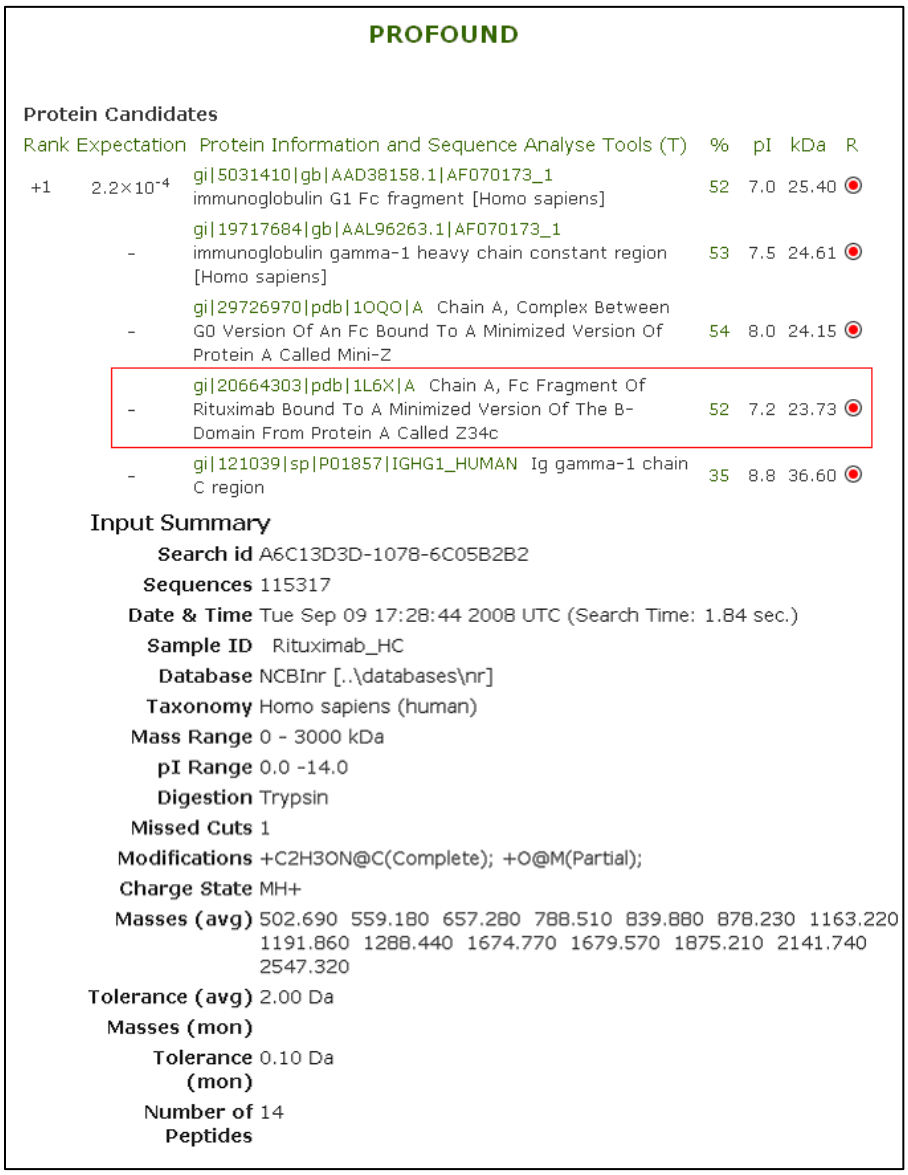

PROFOUND

Protein Candidates

Rank	Expectation	Protein Information and Sequence Analyse Tools (T)	%	pI	kDa	R
+1	2.2×10^{-4}	gi|5031410|gb|AAD38158.1|AF070173_1 immunoglobulin G1 Fc fragment [Homo sapiens]	52	7.0	25.40	
-		gi|19717684|gb|AAL96263.1|AF070173_1 immunoglobulin gamma-1 heavy chain constant region [Homo sapiens]	53	7.5	24.61	
-		gi|29726970|pdb|1OQO|A Chain A, Complex Between G0 Version Of An Fc Bound To A Minimized Version Of Protein A Called Mini-Z	54	8.0	24.15	
-		gi|20664303|pdb|1L6X|A Chain A, Fc Fragment Of Rituximab Bound To A Minimized Version Of The B-Domain From Protein A Called Z34c	52	7.2	23.73	
-		gi|121039|sp|P01857|IGHG1_HUMAN Ig gamma-1 chain C region	35	8.8	36.60	

Input Summary

Search id A6C13D3D-1078-6C05B2B2
Sequences 115317
Date & Time Tue Sep 09 17:28:44 2008 UTC (Search Time: 1.84 sec.)
Sample ID Rituximab_HC
Database NCBInr [..\databases\nr]
Taxonomy Homo sapiens (human)
Mass Range 0 - 3000 kDa
pI Range 0.0 -14.0
Digestion Trypsin
Missed Cuts 1
Modifications +C2H3ON@C(Complete); +O@M(Partial);
Charge State MH+
Masses (avg) 502.690 559.180 657.280 788.510 839.880 878.230 1163.220 1191.860 1288.440 1674.770 1679.570 1875.210 2141.740 2547.320
Tolerance (avg) 2.00 Da
Masses (mon)
Tolerance (mon) 0.10 Da
Number of Peptides 14

Fig. 5.69. Rituximab, heavy chain. Profound (Prowl)/NCBInr search results. Protein view section.

On the basis of heavy chain PMF results it is demonstrated that only rituximab Fc fragment including C_H2 and C_H3 domains was identified with sequence coverage of 57 % and 52 % respectively.

In the Fig. 5.70 MALDI TOFF Spectra generated from peptide fragments of heavy chain of rituximab are presented.

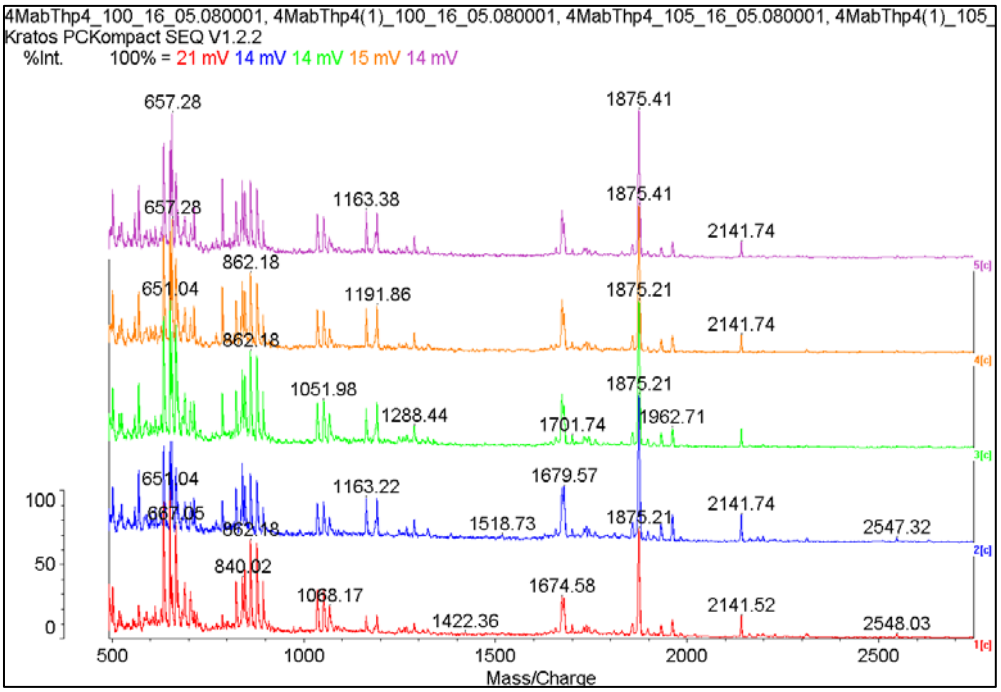

Fig. 5.70 MALDI-TOF Analysis of rituximab heavy chain.

5.5.1.3. Identification of light chain

For primary sequence confirmation and identification of the rituximab light chain, a list of 18 peptide masses (Fig. 5.71) generated by MALDI-TOF MS of peptides obtained from corresponding positions of silver stained gels (Fig. 5.62, Gel A), were searched with MASCOT and PROFOUND (Prowl) Search Engines using three sequence databases: MSDB, NCBInr and SwissProt.

For primary sequence confirmation and identification of the rituximab light chain, the list of 13 peptide masses (Fig. 5.71) generated by MALDI-TOF MS of peptides obtained from corresponding positions of silver stained gels (Fig. 5.72), were searched with MASCOT and PROFOUND (Prowl) search engines using three sequence databases: MSDB, NCBInr and SwissProt.

2142.81 2104.16 1948.50 1878.19 1800.02 1608.56 892.60 870.62 768.44 660.29
561.46 524.34 503.09

Fig. 5.71. Rituximab, light chain. List of entered peptide masses

During Database searching, taxonomy parameter was not specified, selected enzyme was trypsin. Other search parameters were set to allow up to 1 missed cleavage, methionins in oxidized form (variable modification), cysteins in carbamidomethylated form (fixed modification), average mass, peptide ions in protonated $[M+H]^+$ form, mass tolerance was set ±1- ±2 Da. Protein molecular mass was not specified. The best results were obtained with MASCOT/NCBInr at mass tolerance parameter set to ± 1.7 (Fig. 5.73).

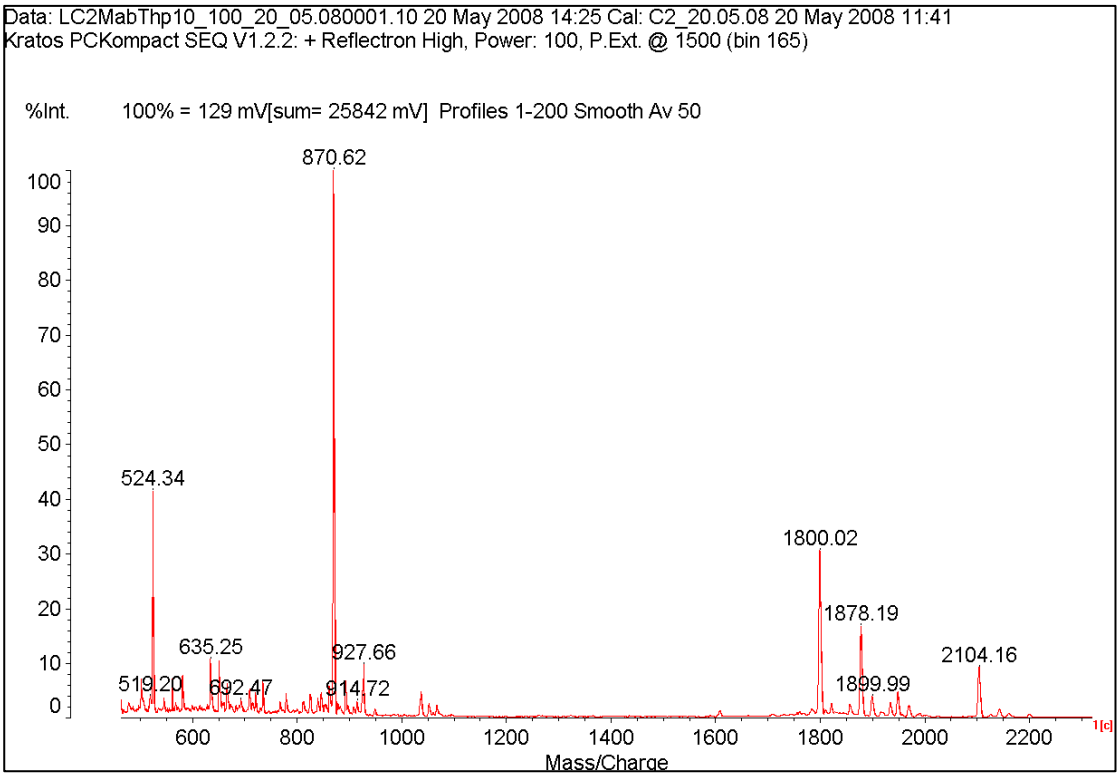

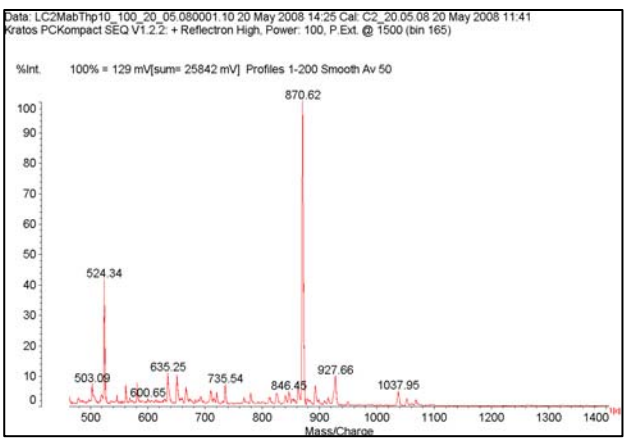

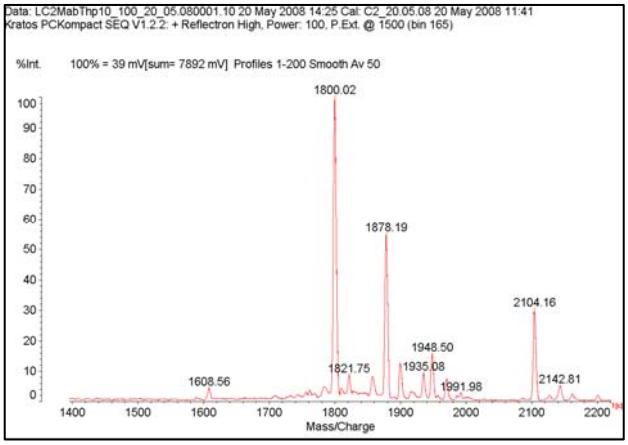

Fig. 5.72. MALDI-TOF spectrum of rituximab light chain. Up: Entire spectrum up, Down: Detailed spectra

Mascot Search Results

User : Dashnor Nebiu
Email : dashnornebiu@yahoo.com
Search title : Rituximab_LC
Database : NCBInr 20080903 (6934543 sequences; 2394607247 residues)
Timestamp : 10 Sep 2008 at 10:59:56 GMT
Top Score : 157 for gi|146387638, Chain L, Crystal Structure Of Rituximab Fab In Complex With An Epitope Peptide

Probability Based Mowse Score

Protein score is -10*Log(P), where P is the probability that the observed match is a random event.
Protein scores greater than 81 are significant (p<0.05).

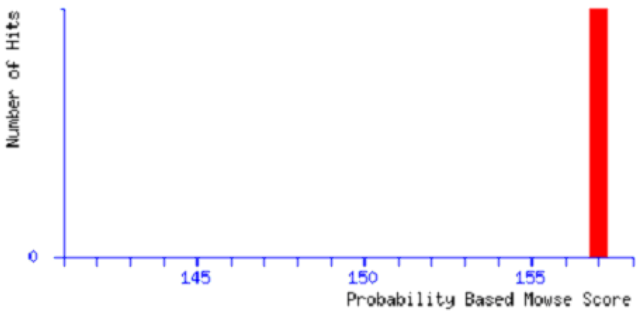

Concise Protein Summary Report

gi|146387638 **Mass:** 23342 **Score:** 157 **Expect:** 1.4e-09 **Queries matched:** 13
Chain L, Crystal Structure Of Rituximab Fab In Complex With An Epitope Peptide
gi|186972968 **Mass:** 23404 **Score:** 157 **Expect:** 1.4e-09 **Queries matched:** 13
Chain L, Crystal Structure Of Chimeric Antibody C2h7 Fab In Complex With A Cd20 Peptide
gi|62988814 **Mass:** 13303 **Score:** 141 **Expect:** 5.5e-08 **Queries matched:** 11

Search Parameters

Type of search : Peptide Mass Fingerprint
Enzyme : Trypsin
Fixed modifications : Carbamidomethyl (C)
Variable modifications : Oxidation (M)
Mass values : Average
Protein Mass : Unrestricted
Peptide Mass Tolerance : ± 1.7 Da
Peptide Charge State : 1+
Max Missed Cleavages : 1
Number of queries : 13

Fig. 5.73. Rituximab, light chain. Mascot search results. Primary sequence database: NCBInr. Mass tolerance was set to ± 1.7 Da

As shown in Fig. 5.73, peptide masses searched at MASCOT/NCBInr, MT±1.7 Da, as the highest score results generated two proteins:

- Rituximab Fab
- Antibody C2H7 Fab

Score parameter for both proteins was 157. For Rituximab Fab, there were 13 queries matched, and sequence coverage, 45 % (Fig. 5.74.).

Protein View

Match to: **gi|146387638** Score: **157** Expect: **1.4e-09**
Chain L, Crystal Structure Of Rituximab Fab In Complex With An Epitope Peptide

Nominal mass (M_r): **23342**; Calculated pI value: **8.26**
NCBI BLAST search of gi|146387638 against nr
Unformatted sequence string for pasting into other applications
Links to retrieve other entries containing this sequence from NCBI Entrez:
gi|146387640 (no taxonomy information for this entry)

Fixed modifications: Carbamidomethyl (C)
Variable modifications: Oxidation (M)
Cleavage by Trypsin: cuts C-term side of KR unless next residue is P
Number of mass values searched: **13**
Number of mass values matched: **13**
Sequence Coverage: **45%**

Matched peptides shown in **Bold Red**

```
     1 QIVLSQSPAI LSASPGEKVT MTCRASSSVS YIHWFQQKPG SSPKPWIYAT
    51 SNLASGVPVR FSGSGSGTSY SLTISRVEAE DAATYYCQQW TSNPPTFGGG
   101 TKLEIKRTVA APSVFIFPPS DEQLKSGTAS VVCLLNNFYP REAKVQWKVD
   151 NALQSGNSQE SVTEQDSKDS TYSLSSTLTL SKADYEKHKV YACEVTHQGL
   201 SSPVTKSFNR GEC
```

Start - End	Observed	Mr(expt)	Mr(calc)	Delta	Miss	Sequence
19 - 24	768.4400	767.4326	766.9302	0.5024	0	K.VTMTCR.A
61 - 76	1608.5600	1607.5526	1606.6888	0.8638	0	R.FSGSGSGTSYSLTISR.V
103 - 106	503.0900	502.0826	501.6167	0.4659	0	K.LEIK.R
103 - 107	660.2900	659.2826	657.8024	1.4802	1	K.LEIKR.T
107 - 125	2104.1600	2103.1526	2102.3890	0.7636	1	K.RTVAAPSVFIFPPSDEQLK.S
108 - 125	1948.5000	1947.4926	1946.2033	1.2893	0	R.TVAAPSVFIFPPSDEQLK.S
126 - 141	1800.0200	1799.0126	1798.0278	0.9848	0	K.SGTASVVCLLNNFYPR.E
145 - 148	561.4600	560.4526	559.6578	0.7948	0	K.VQWK.V
183 - 189	892.6000	891.5926	889.9518	1.6409	1	K.ADYEKHK.V
188 - 206	2142.8100	2141.8026	2141.4068	0.3958	1	K.HKVYACEVTHQGLSSPVTK.S
190 - 206	1878.1900	1877.1826	1876.0952	1.0874	0	K.VYACEVTHQGLSSPVTK.S
207 - 210	524.3400	523.3326	522.5548	0.7778	0	K.SFNR.G
207 - 213	870.6200	869.6126	868.9143	0.6983	1	K.SFNRGEC.-

Fig. 5.74. Rituximab, light chain. Mascot/NCBInr. Protein view section.

The highest score result of NCBInr database, reported here, Fab fragment of rituximab, represents the full sequence of its light chain (murine variable region, residues 1-106 and human constant region, residues 107-213).

As shown in Fig 80, murine variable domain of light chain was sequentially less covered as human constant domain counterpart. An explanation would be that lysines at position 38 and 44 are followed by proline, therefore not amenable to trypsine cleavage. Therefore the majority of other variable region peptide fragments generated from *in silico* tryptic digest have masses higher than 3300 Da and consequently, are more difficult to be extracted from gels and eventually to be detected by MALDI-TOF MS.

This search engine generated the highest score results for rituximab Fab (light chain) for all MT parameters, provided that for more stringent MT values the sequence coverage was reduced *e.g.* (MT± 1, Score: 100, 9 matched queries; MT±1.5, Score 141, 12 matched queries). However, if MT parameter is set to ± 2, then score slightly dropped (149) due to the fact that the number of matched masses remained constant.

Other sequence databases, MASCOT/MSDB, and SwissProt, generated the highest score results for Ig kappa light chain, and fragments of other monoclonal antibodies suggesting that in this databases rituximab light chain is not included.

MALDI-TOF spectra obtained from peptides generated after in gel trypsin digestion of rituximab light chain spots (Fig. 5.62, Gel A), are presented in Fig. 5.75.

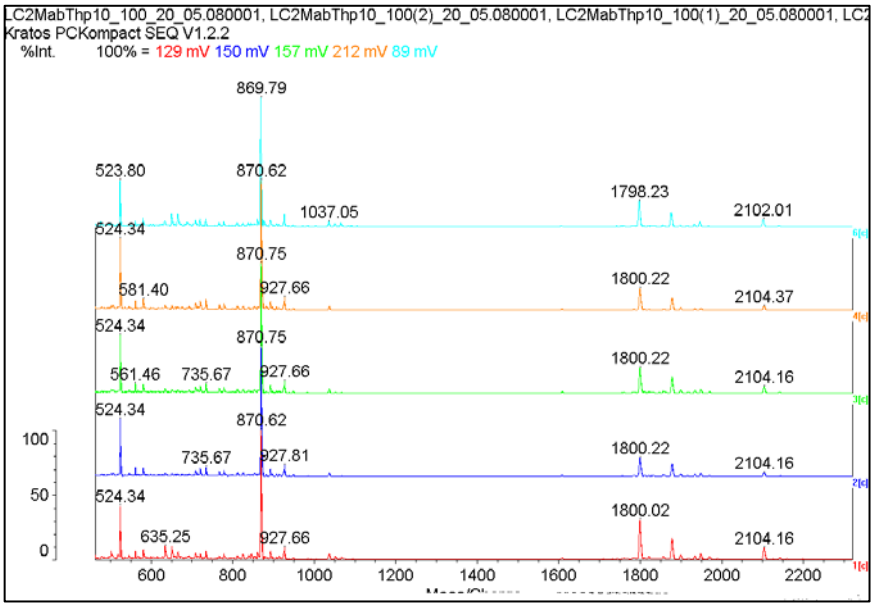

Fig. 5.75 MALDI-TOF Analysis of rituximab light chain

5.6. Gel electrophoresis analysis of abatacept

One- dimensional sodium dodecylsulfate polyacrilamid gel electrophoresis (1D-SDS-PAGE) under reducing and nonreducing conditions, and two-dimensional gel electrophoresis (2-DE) pattern of abatacept have been studied, focusing on the examination of different factors influencing electrophoretic behavior of this complex molecule. Aiming the estimation of molecular weight and *pI* range, examination of charge heterogeneity and the influence of the posttranslational modifications in isoform distribution, 1-SDS-PAGE and 2-DE experiments were run under different conditions. Optimization of deglycosilation procedure for the study of charge heterogeneity and sample preparation for the subsequent MALDI-TOF analysis have been addressed as well.

5.6.1. One dimensional (1D-SDS-PAGE) gel electrophoresis analysis of abatacept

5.6.1.1. Molecular weight estimation and sensitivity of staining

In the Fig. 5.76 silver stained and Coomassie stained gels of abatacept under non-reducing and reducing conditions are presented. The amount of applied sample was increased from 0.05 μg-5 μg in both gels under reducing conditions and 1 and 5 μg in non-reducing conditions, respectively. For both staining procedures, gels show that reduced form of abatacept migrated as a sharp band at around 50 kDa. Under nonreducing conditions abatacept migrated at about 100 kDa, provided that for the highest sample amount shading toward lower molecular weight is observed (Fig. 5.76 , Lane 8 in Gel A and B).

In the gel A the band of the smallest amount of abatacept (0.05μg) is clearly noted (Lane 6). On the other hand for the Coomassie stained gel Fig. 5.76B protein band is barely noticeable. This observation proves the higher sensitivity of silver staining toward Coomassie staining procedure.

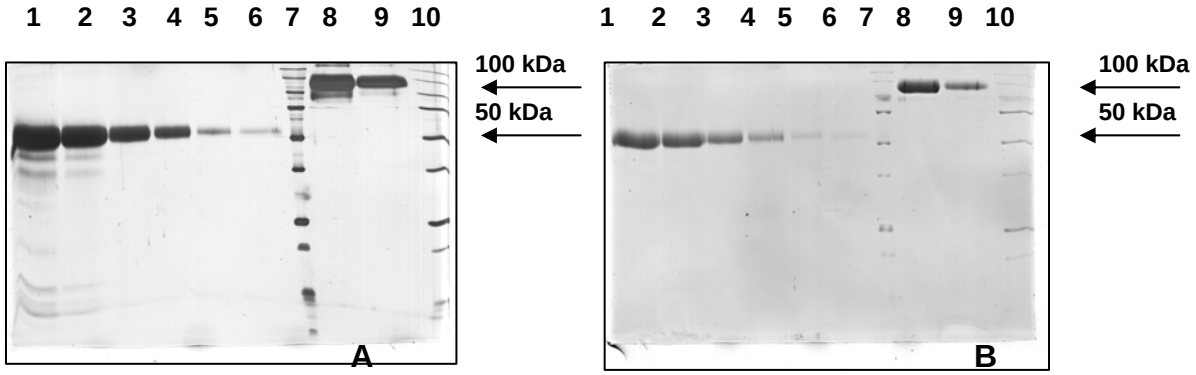

Fig. 5.76. 1-DE Analysis of abatacept: A) Silver stained gel B) Coomassie stained gel.
Lanes 1-6: Abatacept 5 µg-0.05 µg, reducing conditions.
Lanes 8 and 9: Abatacept 5 and 1 µg, respectively, nonreducing conditions.
Lanes 7 and 10: MW Standards

5.6.1.2. Deglycosilation optimisation study

1D-SDS-PAGE analysis of abatacept was used for the study of deglycosilation efficiency, following the application of different enzymes for the cleavage of N-and O linked glycans.

The N-deglycosilation is performed in the similar way as for the rmAbs trastuzumab and rituximab. While for trastuzumab and rituximab the preferred deglycosilation conditions comprised no-denaturation of the sample prior to the reduction and deglycosilation, experimental results from 1D-SDS-PAGE and 2-DE experiments of abatacept demonstrated that sample reduction prior the deglycosilation does not hamper the deglycosilation process. It is even preferred step for efficient N-deglycosilation process. The optimal methods resulted methods which employ no solubilizator or surfactant (Methods 3 and 4).

As for trastuzumab and rituximab, for methods of deglycosilation have been studied:

1. Deglycosilation under reducing and denaturated conditions
2. Deglycosilation under nonreducing conditions. Nonionic surfactant
3. Deglycosilation under reducing conditions, with no surfactants and no previous boiling
4. Deglycosilation under non-reducing conditions, no surfactants and no previous boiling

For detailed information see Experimental section.

Literature data indicates that abatacept molecule apart from N-linked oligosaccharides contains O- linked glycans of different degree of terminal sialidation[245]. Therefore, in contrast to trastuzumab and rituximab, the deglycosilation optimization study of abatacept involved the O-deglycosilation and desialination, as well.

5.6.1.3. Preliminary deglycosilation experiments

In the Fig. 5.77, 1-DE gels of abatacept deglycosilated and control sample under reducing and nonreducing conditions have been presented.

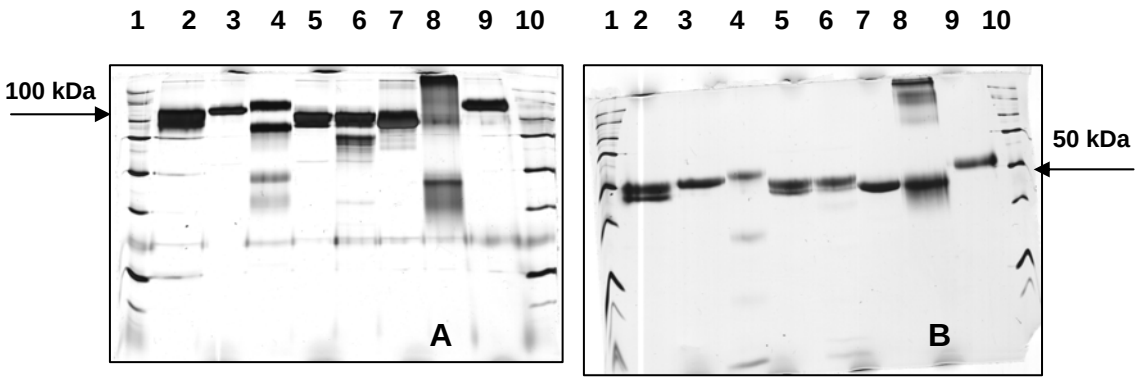

Fig. 5.77. Abatacept (1µg). Deglycosilation optimisation, silver stained gels: A) Non-reducing B) Reducing conditions. Lane 2: NGF-Method 2M, Lane 3: Sialidase, Lane 4: CPB, Lane 5: NGF, sialidase, Lane 6: NGF, Sialidase, CPB, Lane 7: NGF, Method 2; Lane 8: NGF, Method 1, Lane 9: Control, Lanes 1 and10: MW Standards

For the preliminary experiments abatacept sample was digested with required enzymes according Method 2 (Non-reducing/non-denaturing conditions Triton X-100 0.5 %) and its modification, where Triton X-100 was replaced with CHAPS 0.5 % and SDS 0.1 % (Method 2 M). Abatacept samples were in reduced and nonreduced forms (Fig 5.77 A and B, respectively). Method 1 has been studied as well.

Fig. 5.77 indicates no change in the MW for abatacept sample treated with carboxypeptidase B (CPB) under reducing (Fig. 5.77A, lane 4) and non-reducing conditions (Fig. 5.77B lane 4). This is normal due to the expected small MW difference (146.2 Da) between abatacept and its corresponding truncated 0-Lys or 2-Lys form.

N-deglycosilation employing Method 1 (denaturation/reduction) under non-reducing conditions (Fig. 5.77A Lane 8) was not optimal. Under reducing conditions the molecular weight of abatacept has considerably decreased, comparing with non-deglycosilated sample (Fig. 5.77B Lanes 8 and 9, respectively) however the abatacept band is not sharp.

On the other hand, molecular weight difference of bands 7 and 9 under non-reducing conditions (Fig. 5.77A) is evident. This difference is better noted comparing bands 7 and 9 under reducing conditions (Fig. 5.77B): the MW of glycosilated abatacept band is estimated ~ 50 kDa whereas MW of deglycosilated sample is much lower (~ 42-44 kDa). These data suggest that the N-deglycosilation employing Method 2 is more efficient than the one which employs Method 1.

As indicated above, modification of the Method 2 consisted on the replacement of Triton X-100 with CHAPS 0.5 % and SDS 0.1 %. With this method experiments involving sialidase and carboxypeptidase B digestion were performed.

From the Fig 5.77A and 5.77B, no significant difference in the molecular weight of deglycosilated abatacept employing Method 2M an Method 2 was noted (Lanes 2 and 7 respectively in both gels), provided that, Method 2 provided sharper bands than Method 2M.

Fig. 5.77A and 5.77B shows that abatacept samples treated with N-glycosidase F, Sialidase (Lane 5) and N-glicosidase F, Sialidase and carboxypeptidase B (Lane 6) employing Method 2M, exhibit no significant differences in the molecular weight neither with sample treated with N-glycosidase F Method 2, nor with sample treated with N-glycosidase F Method 2M (Lanes 2 and 7), indicating small contribution of terminal silaic acids and lysine in the abatacept MW.

Interestingly, in gels of abatacept digested only with sialidase (Method 2M) small difference in MW between sialidase treated abatacept and control has been observed (Lanes 3 and 9 in both gels) suggesting small contribution of terminal N-Acetylneuraminic acid residues (MW 309.27) from O-linked sugars in the MW of abatacept. The presence of terminal silaic acid resuidues in abatacept was confirmed with 2-DE analysis (see the next section).

Preliminary deglycosilation experiments confirmed that N-deglycosilation and desialination give rise to the abatacept species with lower molecular weght.

The deglycosilation procedure hovewer was further optimised.

5.6.1.4. Optimized experimental conditions

Fig. 5.78 shows that the optimal conditions for deglycosilation of abatacept consist of the application of the Method 3 (deglycosilation under reducing conditions, employing no surfactant).

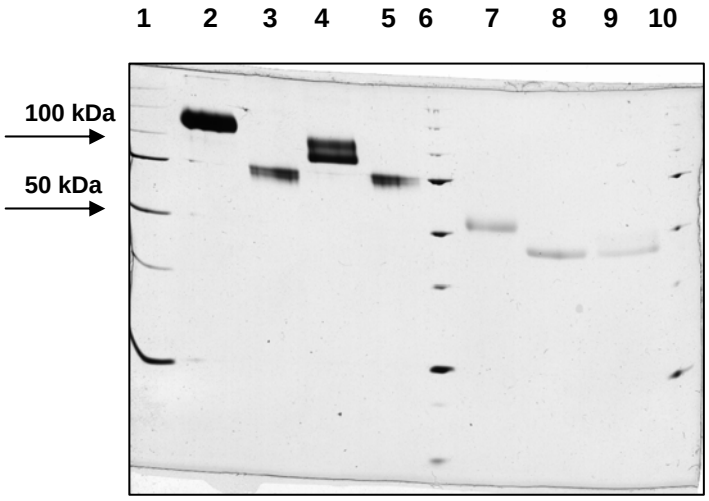

Fig. 5.78. Abatacept (2 μg) optimised deglycosilation conditions. Silver staining. Lanes **1, 6** and **10**, MW Standards, lane **2** Nonreducing/glycosilated, lane **3** and **5** Deglycosilated, Method 3, lane **4** Deglycosilated Method 4. Lane **7** Reducing/glycosilated, lane **8** Deglycosilated, Method 3, lane **9** Deglycosilated, Method 4.

In the Fig. 5.78 substantial decrease in molecular weight under reduced and non-reduced conditions is observed upon deglycosilation according Method 3 (Lanes 3, 5 and 8).

Molecular weight of glycosilated native sample (Lane 2), estimated ~ 100 kDa after N-Glycosidase digestion changed to ~ 75 kDa. At the same time, molecular weight of glycosilated reduced sample (Lane 7) decreased to ~ 40 kDa provided that 1-DE does not make possible exact measurement of molecular difference. Nevertheless, significant molecular weight difference after N-deglycosilation suggests that N-linked sugars are predominant glycans of abatacept molecule.

Lanes 4 and 9, show that for abatacept deglycosilation procedure employing Method 4 did not perform as efficiently as Method 3.

5.6.1.5. Optimized electrophoresis conditions. Comparison of biological medicinal substances

In order to compare relative extent of glycosylation in two classical rmAbs trastuzumab and rituximab with fusion protein abatacept, three substances have been run in one SDS-PAGE gel, under reducing and non-reducing conditions (Fig. 5.79).

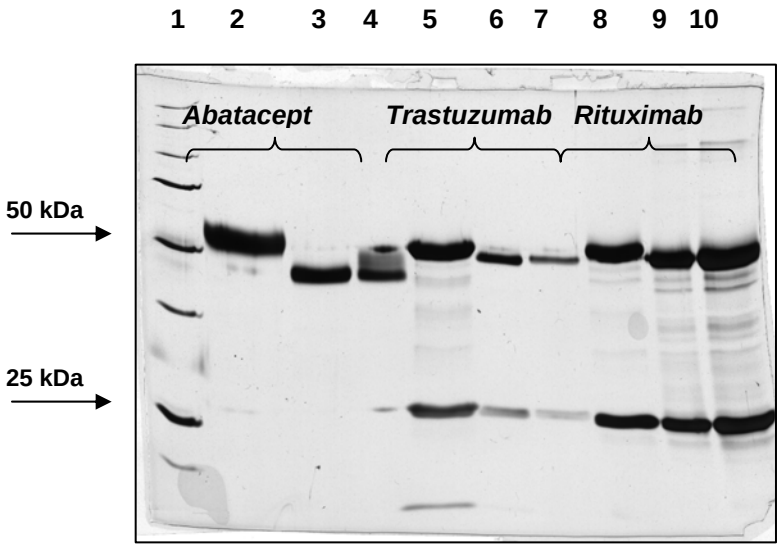

Fig. 5.79. Deglycosilation efficiency. Abatacept, trastuzumab and rituximab, 2 µg each. silver staining. Lane 1: MW Standard, Lanes 2,3,4: abatacept; Lanes 5,6, 7 trastuzumab; Lanes 8,9,10 rituximab.

Two sets of heavy and light chain bands, ~ 50 kDa and ~ 23 kDa respectively, are observed for trastuzumab and rituximab. The difference in molecular weight between deglycosilated (lanes 6, 7 and 9, 10 for trastuzumab and rituximab respectively) and non-deglycosilated samples (lanes 5 and 8 for trastuzumab and rituximab respectively) is not large. This difference is noted only in the bands of heavy chains since they are glycosilated. Position of light chain bands remains the same.

On the other hand, glycosilated abatacept which has about the same molecular weight as trastuzumab and rituximab heavy chains (~ 50 kDa), after deglycosilation provides band with considerably lower MW, ~40 kDa. Therefore one the basis of these experiments one can conclude that the extent of glycosylation in the fusion protein abatacept is substantially higher than in rmAbs trastuzumab and rituximab.

5.6.2. Two-dimensional (2-DE) gel electrophoresis analysis of abatacept

Biologics produced by recombinant DNA technology are complex heterogeneous mixtures of posttranslational anticipated forms, i.e. glycoforms or other variants produced during manufacture and/or storage, like deamidation, isomerisation etc. The characterisation of the degree and profile of the heterogeneity is of the great importance from the regulatory point of view since the heterogeneity of these products defines their quality[161].

Abatacept is a biological product derived from rDNA technology and produced in CHO cells. Therefore it is expected, that like other biological products, to have certain degree of heterogeneity and isoforms.

This study addresses 2-DE electrophoresis behaviour of abatacept aiming to analyse its charge heterogeneity, and subsequently with MALDI-TOF analysis to identify and characterise the drug substance, its purity and stability.

For the 2-DE optimisation, electrophoresis experiments are performed using different immobiline *pH gradients* (*IPG strips*: 3-11 NL, 6-9 L; 4-7 L and 3-6 L). In order to have a view on the broader *pI* range the preliminary experiments are performed with *IPG gradient* 3-11 *NL. IPG* gradient 4-7 *L* results the most suitable for charge heterogeneity study.

The influence of glycosylation pattern in the charge heterogeneity of abatacept was studied using enzyme N-glycosidase F for the release of N-linked glycans, O-glycosidase for O-linked glycans and the sialidase for the release of terminal sialic acids. In addition carboxypeptidase B was used for the study of lysine truncation.

Gels were stained with Coomassie Blue and silver staining procedure.

5.6.2.1. Preliminary 2-DE experiments. IPG strips 3-11 NL

As expected, 2-DE analysis revealed that abatacept is very complex mixture of different isoforms. In the Fig. 5.80 two gels of abatacept developed under different conditions with detailed section of gel A are presented.

The estimated *pI* of this acidic glycoprotein ranged from 4.5-5.5, and there are observed 13-14 spots. Molecular weight is estimated to be higher than 50 kDa. There are obvious differences in the 2-DE spot pattern of abatacept and heavy chains of classic rmAb studied so far, rituximab and trastuzumab. First, the abatacept's *pI* is substantially lower. This is in agreement with the difference of sugar composition of these two classes of biologics. Namely, abatacept contains acidic O-linked glycans which do not occur in molecules of rmAbs.

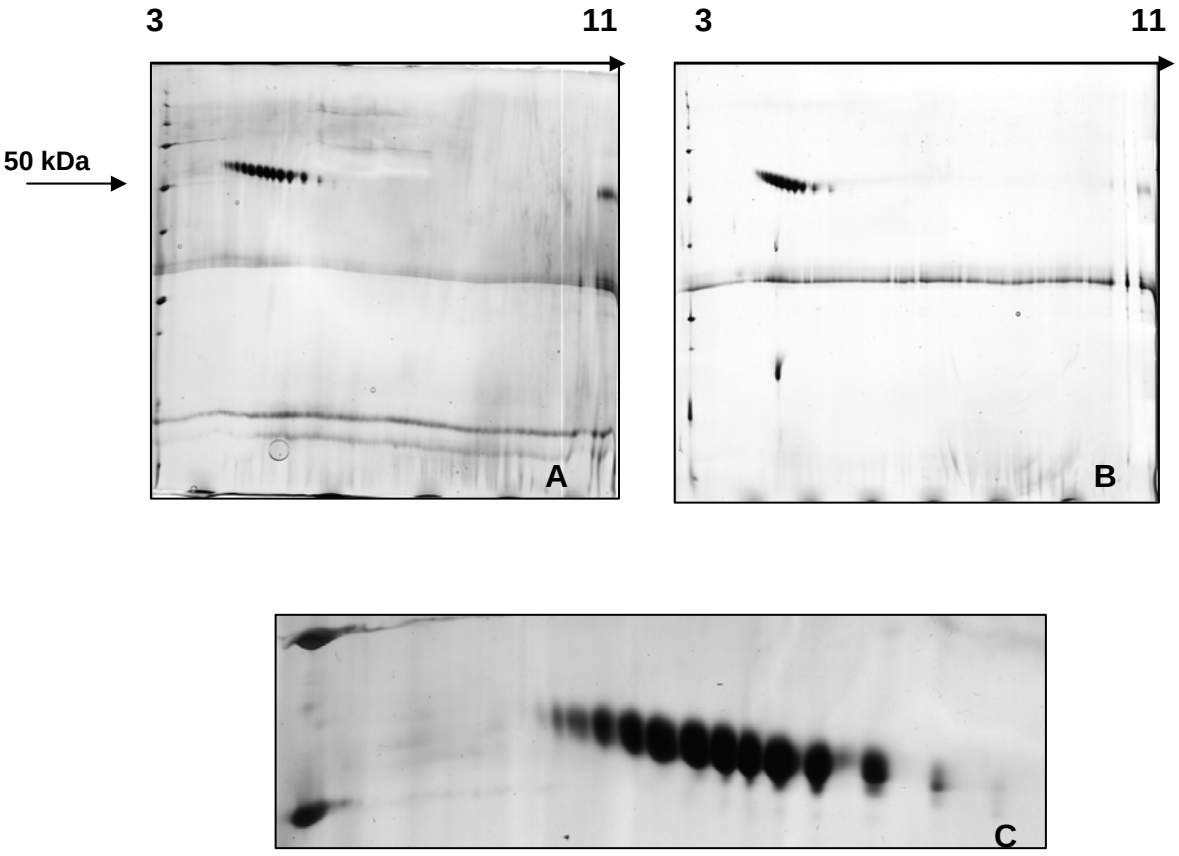

Fig. 5.80. 2-DE analysis of abatacept (10 µg). Silver staining A) Development time 5 min, B) Development time 2.5 min, C) Detailed section of A.

Second, as seen in the gels from Fig. 5.80, abatacept spots extend in an oblique direction, which proves the presence not only of charged but mass variants, as well, suggesting that its not only the type but the quantity of particular attached glycan and/or other factor(s) which will determine the mass and charge heterogeneity.

Third, resolution of abatacept spots was better to resolution of rmAb therapeutics, rituximab and trastuzumab.

In Fig. 5.80 the influence of the time of development phase in gel transparency and spot intensity has been depicted. The development time of 2.5 minutes has been selected as optimal.

Aiming to compare the staining sensitivity, 1 μg of abatacept is applied into the gels and they are stained with silver staining and Coomassie staining procedure.

Gel spots could be visualized in both cases however with the large difference in their intensities (Fig. 5.81).

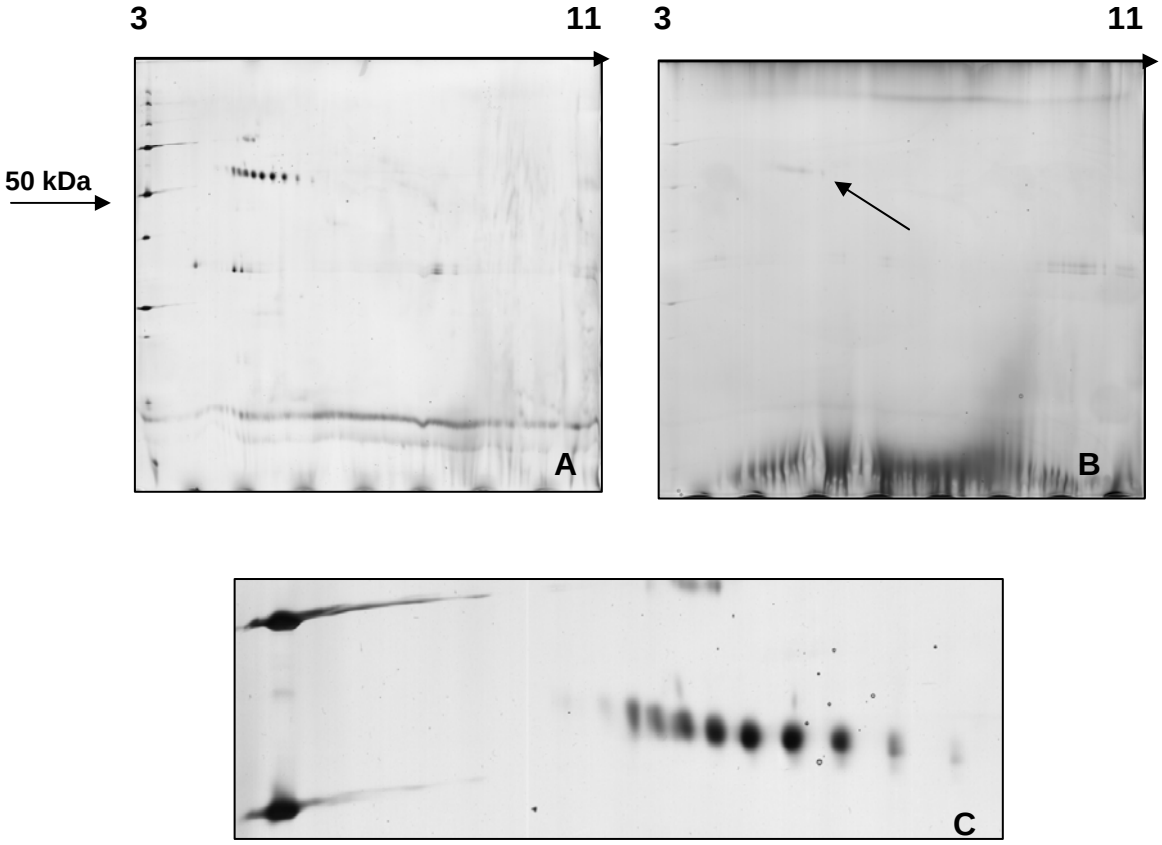

Fig. 5.81. 2-DE analysis of abatacept (1 μg). Silver versus Coomassie staining. A) Silver staining A)Coomassie staining C) detailed section of A. Arrow indicates abatacept spots in gel B.

Experimental data revealed that the reduction of sample concentration generally brought about enhancement in the spot resolution. For illustration, detailed section of silver stained gel with 1 µg abatacept applied is presented in Fig. 5.81.

Improvement in the spot resolution was observed when immobiline pH gradient was narrower, as well. In this study *IPG* gradients of 3-6 L, 4-7 L and 6-9 L have been employed.

Comparing to IPG 3-11 NL, IPG gradients 3-6 L and 4-7 L, afforded better spot resolution at the same sample amount, 10 µg abatacept (Fig. 5.82).

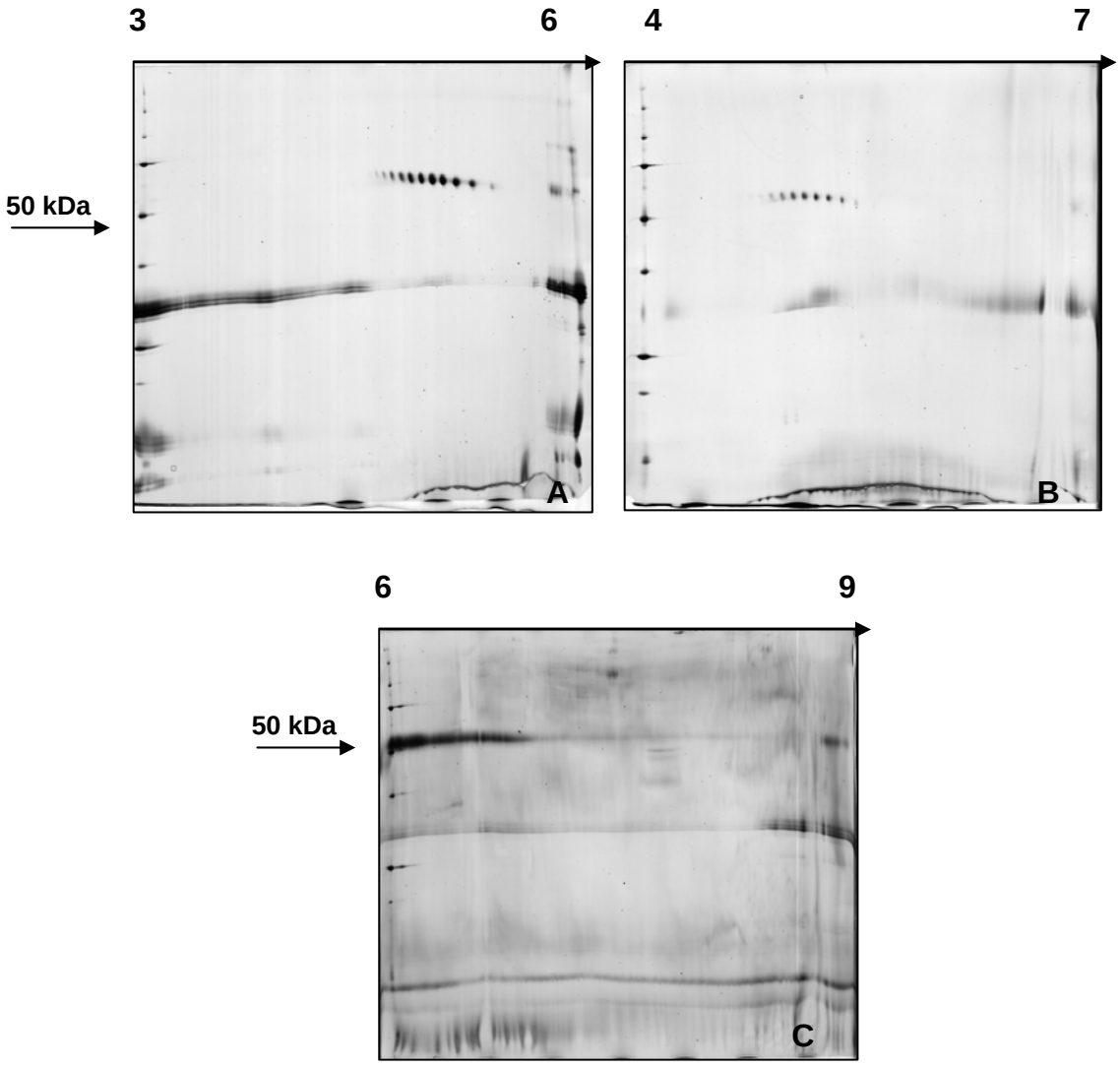

Fig. 5.82. 2-DE analysis of abatacept (10 µg).Optimisation of pH gradient. Silver staining A) IPG 3-6 L, B) IPG 4-7 L C) IPG 6-9 L

In contrary, immobiline gradient IPG 6-9 L brought about poorly resolved band around pI 6, most likely only minor component of the abatacept protein, consequently studies with this IPG gradient were not pursued further.

5.6.2.2. The study of charge heterogeneity

From previous 2-DE experiments performed under different IPG gradients it was documented that abatacept is very complex molecule, containing 13-14 spots. Consequently the charge heterogeneity study should employ the conditions which must permit obtaining of the maximal information for the spot pattern complexity of abatacept sample. In other words, IPG strips which provide maximally resolved spots should be selected for the study. Previous experiments indicated that strips 3-6 L and 4-7 L might fulfill these requirements.

Therefore, for the study of the influence of terminal sialic acids in charge variant complexity, the first immobiline pH gradient employed was IPG 3-6 L.

Experimental data revealed that after sialidase digestion due to the cleavage of terminal N-acetylneuraminic acid residues, spot complexity was substantially reduced, however since pI of resulting variants shifted toward more basic values, approaching pI 6, and this pI is the upper pH limit for the strips (3-6 L), the number of spots and their position could not be precisely determined Fig. 5.83.

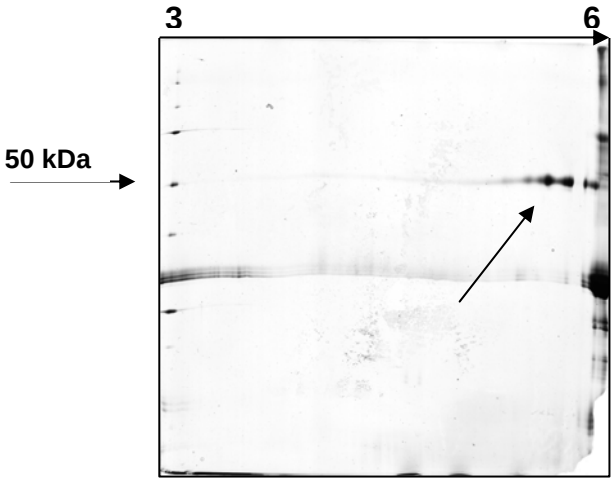

Fig. 5.83. 2-DE analysis of abatacept (10µg) 3-6 L. Sialidase. Silver staining. Arrow indicates the position of abatacept spots

Nevertheless, from the Fig. 5.83 important information is obtained. The pI of resulting spots is more basic comparing to native sample, their number and complexity is reduced, and their molecular weight seems to be lower, as well.

The next step was to study more suitable pI gradient conditions (broader pI range) with additional examination of the influence of other factors such are N-linked glycans and O-linked glycans on the charge heterogeneity. (In)complete terminal lysine processing should be addressed, as well.

5.6.2.3. Immobiline pH gradient 4-7 L

The study involving IPG 4-7 L tends to answer very important questions related to posttranslational modification of abatacept, primarily to test which is the contribution of N-linked and O-linked glycans on its charge heterogeneity, what is their relative content in abatacept molecule, which oligosaccharides contain terminal sialic acid residues: N-linked, O-linked or both of them? This information, supplemented with 1-DE and 2-DE experiments of native sample and in conjunction with subsequent MALDI-TOF analysis, could represent an important step not only for the elucidation and confirmation of isomorf pattern, but for the identity and purity assessment of this biological product as well.

In the Figures 5.84 and 5.85 Gels of abatacept under different digestion conditions using N-glycosidase F, O-glycosidase, and Sialidase are presented.

For the comparison purpose, in both Figures gel obtained from nontreated, control sample has been included.

In the Table 5.12 a list of corresponding pI values is presented.

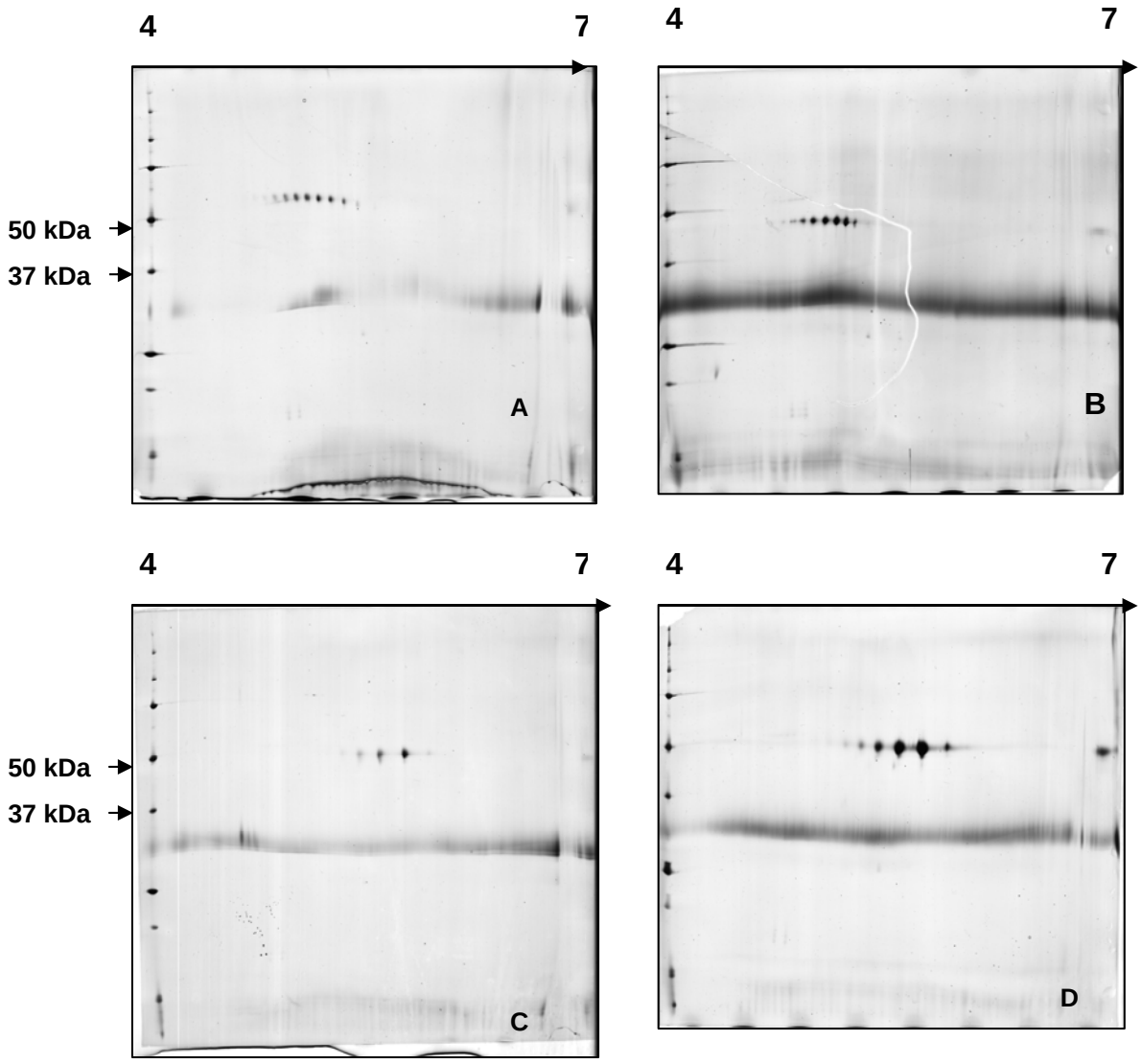

Fig. 5.84. 2-DE analysis of abatacept. Charge heterogeneity study I. *4-7 L*. Abatacept (10µg) Silver staning. A) Glycosilated sample, control; **B.** N-glycosidase F; **C.** Sialidase; **D.** Sialidase and O-glycosidase

Fig 5.84. shows that in comparison with the spots of control gel A (non-deglycosilated sample), spots of abatacept digested with N-glycosidase F in gel B of the same Fig. are displayed as spot pattern of lower molecular weight than control spots. Their pI range shifted toward lower pI range although not in greater extent (Table 5.12.). A considerable difference in molecular weight confirms that abatacept is extensively N-glycosilated molecule containing predominantly N-linked glycans.

On the other hand, pI shift toward lower pI range after N-oligosaccharide release, suggests that N-linked glycans of abatacept are neutral molecules containing no

sialic acid residues at their non-reducing termini. After the hydrolysis of glycoside bond with the release of oligosaccharide and ammonia, for each N-glycosylation site one free carboxylate of aspartic acid is released, hence the pI of molecule is lower.

Larger difference in abatacept spot pattern is observed upon the digestion of sample with sialidase (Fig. 5.84C) and with both enzymes together, sialidase and O-glycosidase (Fig. 5.84D). In these instances, the molecular weight change is not so much pronounced as after digestion with N-glycosidase F, but there is a considerable change in the abatacept pI and its spot complexity.

Namely, after sialidase digestion (Fig. 5.84 C) pI range increased in order of magnitude 0.5 suggesting that O-linked abatacept glycans contain terminal N-Acetylneuraminic acid residues which are responsible for acidic nature of abatacept. However after sialidase cleavage, they are released, with concomitant release of neutral serine residues from protein backbone therefore pI of asialo abatacept is shifted toward higher values. In contrast to non-deglycosilated abatacept the spot complexity is substantially reduced, as well suggesting that the different degree of sialidation and/or different structures of O-linked glycans, are major contributors to abatacept charge heterogeneity.

In order to examine the influence of O-linked glycans in the charge variant distribution abatacept was first digested with sialidase followed by O-glycosidase (Fig 5.84 D). The previous desialination was needed due to the fact that in contrast to N-glycosidase F, O-glycosidase can not cleave modified (i.e. sialinated) O-linked glycans.

The experimental results show that O-deglycosilated (and desialinated) abatacept has lower molecular weight comparing to control and desialinated sample although still considerably higher than of N-deglycosilated abatacept form. This observation suggests that the size of O-glycans and/or their abundance is lower than of N-linked glycans in molecule of abatacept. Fig 5.84 D shows as well that the pI range of resulting abatacept has moved toward higher pI values, as in the case when only sialidase is employed (Fig 5.84 A, C, D, Table 5.12).

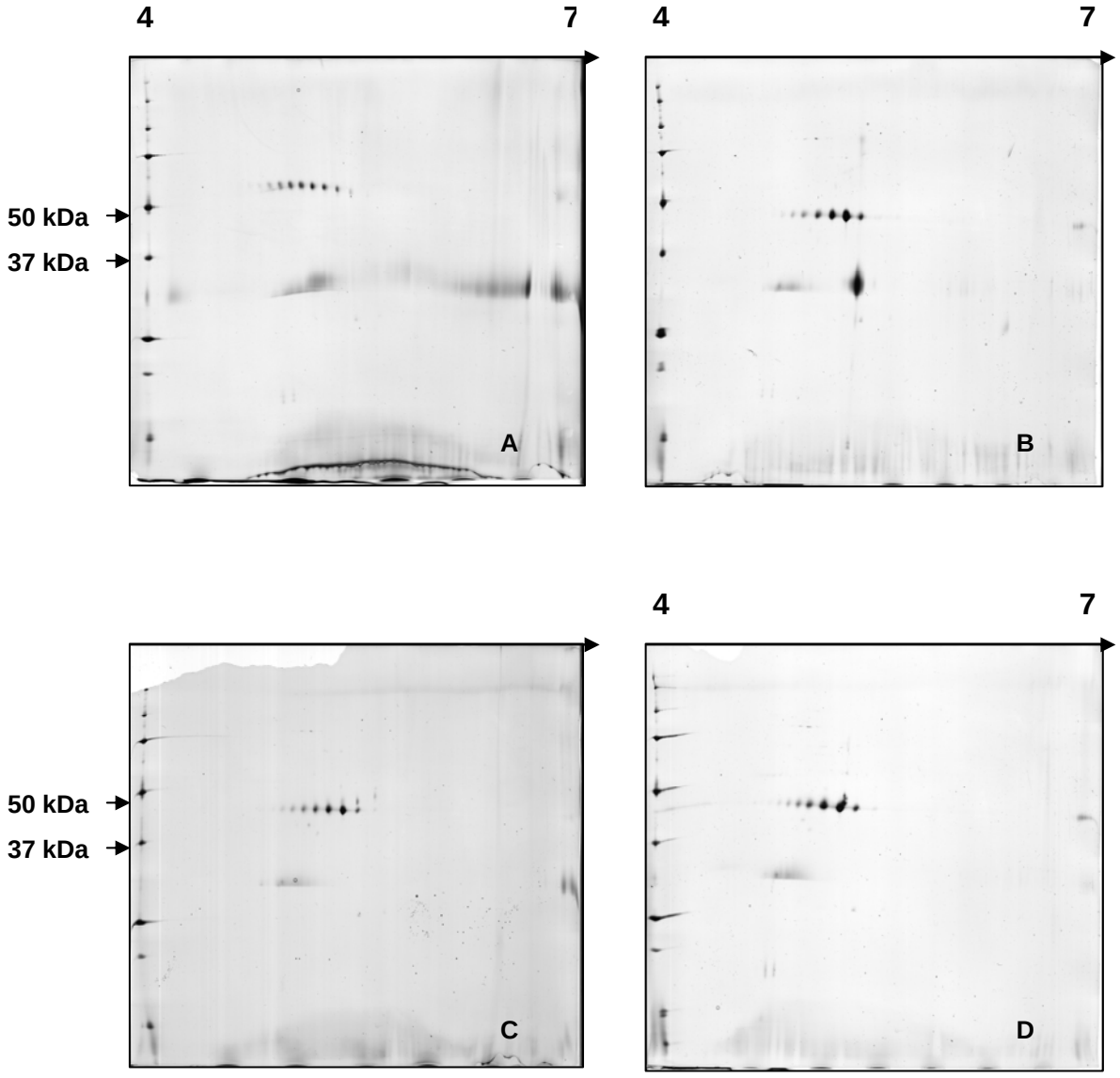

Fig. 5.85. 2-DE analysis of abatacept. Charge heterogeneity study.II *4-7 L* .Abatacept (10µg). Silver staning. A) Glycosilated sample, control; B) N-glycosidase F and sialidase; C) N-glycosidase F, Sialidase and O-glycosidase, Triton X-100; D) N-glycosidase F, Sialidase and O-glycosidase.

In order to cleave both, N-linked glycans and N-Acetyl neuraminic acid termini from abatacept molecule N-glycosidase F and sialidase were used simultaneously (Fig .5.85B). For the removal of N-linked and O-linked glycans, abatacept sample was initially desialinated and subsequently N and O-deglycosilated using slightly different deglycosilation procedures which gave similar results (Fig. 5.85C and D).

Fig 5.85A and B show that asialo and N-deglycosilated abatacept has lower molecular weight that control sample with additional reduction in charge

heterogeneity pattern. Its pI range however is similar to control provided that spots begin at higher pI values, but end at the approximately same pI values as control. Very small difference in pI might be consequence of two opposite processes during the N-deglycosilation and desialination. In the first instance pI is decreased due to aspartic acid release, and in the second, pI increases due to removal of negatively charged sialic acid species (Table 5.11). On the basis of experimental data desialination resulted preponderant.

In the last experiments with IPG 4-7 abatacept was digested with three enzymes simultaneously N-glycosidase F, O-glycosidase and sialidase (Fig. 5.85C) and initially digested with sialidase and N-glycosdidase F followed by the O-glycosidase digestion (Fig. 5.85D).

Both gels provided similar results. Larger difference in molecular weight between resulting abatacept form and control sample has been observed, invoking the additive effect in the molecular weight reduction of three enzymes. Charge heterogeneity is reduced, provided that the pI range is similar to the one in Fig.5.85B.

Deglycosilation status	Glycosilated	N-Glycosidase F (NGF)	Sialidase (S)	O-glycosidase (OG), sialidase	S, NGF	S,NGF, OG
pI range	4.6-5.5	4.3-5.3	5.4-5.9	5.3-5.9	4.9-5.3	5.0-5.6

Table 5.12. Charge heterogeneity study of abatacept

5.6.2.4. Immobiline pH gradient 3-11NL

After application of immobiline pH gradient IPG 3-11 NL similar results were obtained as in previous cases with IPGs 3-6 L and 4-7 L. Corresponding gels are presented in Fig. 5.86.

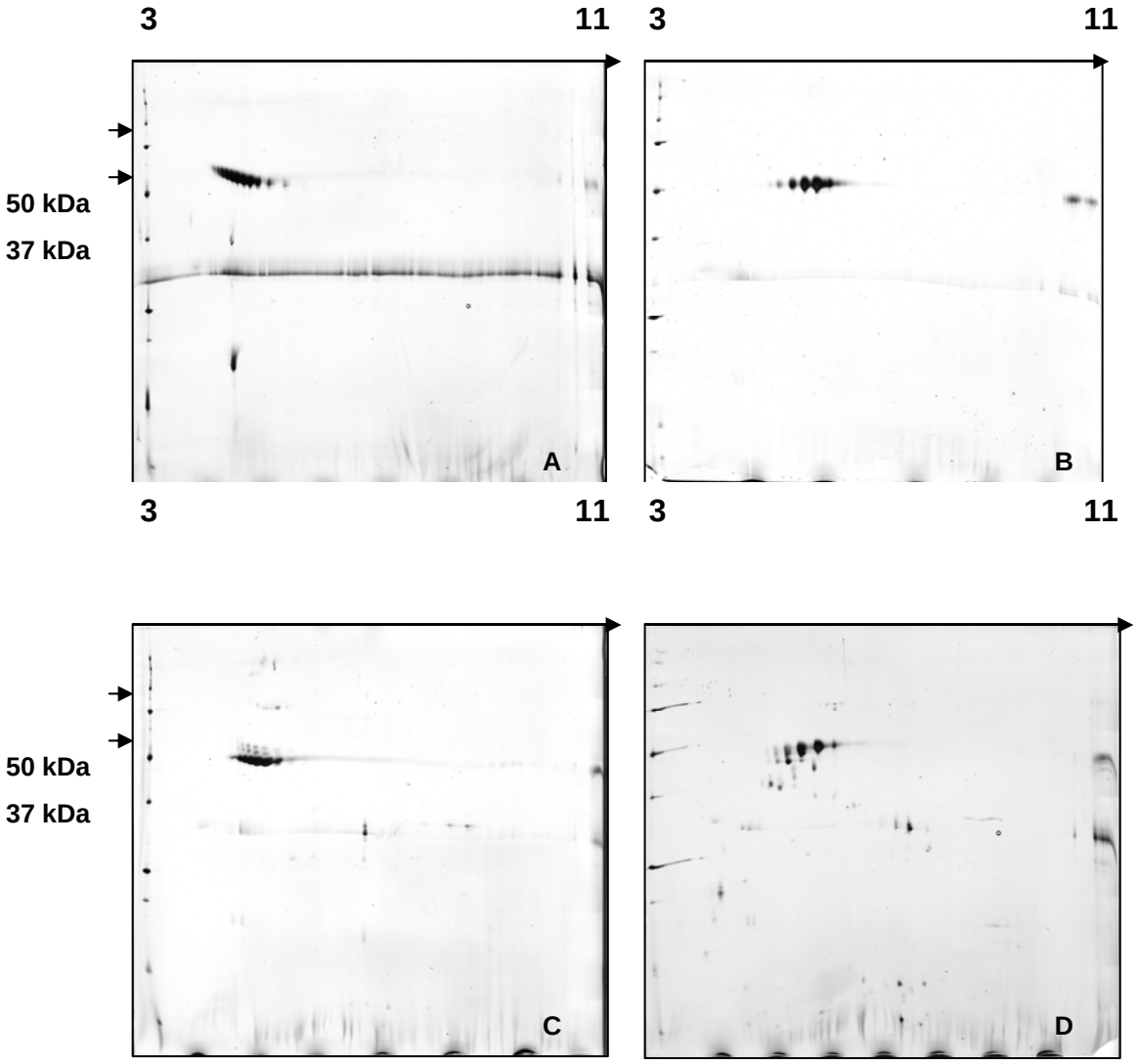

Fig. 5.86. 2-DE analysis of abatacept. Charge heterogeneity study. *3-11 NL*. Abatacept (10µg). Silver staning. A) Non-deglycosilated, control; B) Sialidase; C) N-glycosidase F, Triton X-100; D) N-glycosidase F, Sialidase.

2-DE study of abatacept charge heterogeneity, presented in Fig. 5.86 is possible with broader pI gradient 3-11 which in this instance is non-linear. As in previous cases (3-6 L and 4-7 L) N-deglycosilated abatacept displayed the similar charge complexity as non-treated sample. Additionally, its pI range shifted to lower values and molecular weight substantially decreased in comparison with control (Fig. 5.86A and C).

Desialinated abatacept resulted less acidic, and displayed reduced complexity comparing to control sample. Molecular weight decrease was small (Fig 5.86B).

Finally, abatacept sample digested simultaneously with N-glycosidase F and sialidase displayed difference in pI range with considerable molecular weigh and spot complexity reduction (Fig. 5.86D).

The lysine truncation study of abatacept with 2-DE provided no conclusive data. Fig. 5.87 shows the gel of abatacept treated with enzyme carboxypeptidase B for illustration purpose.

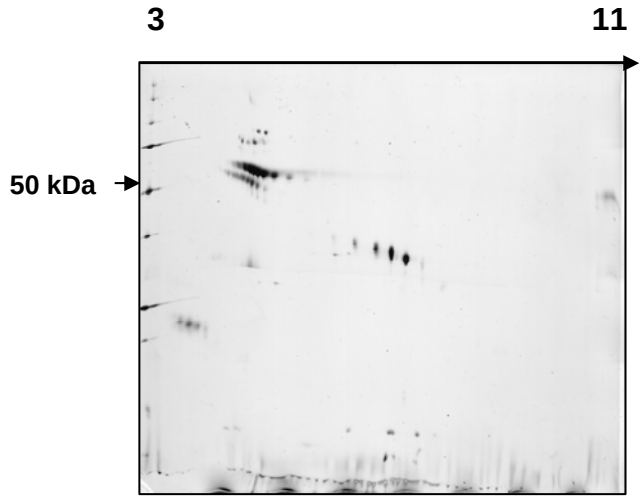

Fig. 5.87. 2-DE analysis of abatacept. Charge heterogeneity study. Carboxypeptidase B. *3-11 NL*. Silver staning. Abatacept 10 µg.

On the basis of experimental data obtained employing three types of IPG gradients it can be concluded that 1-DE and 2-DE are suitable methods to detect, estimate molecular weight and monitor the charge heterogeneity pattern of abatacept.

Since the enzymatic deglycosilation is nondestructive technique the resulting abatacept peptides could be further analyzed with MALDI-TOF MS in order to confirm its identity.

On the other hand, for the full characterization of abatacept glycoforms, i.e. glycan sequencing, a supplementary method is required.

In summary, as indicated above, charge variants and other variants of this drug substance define its quality, the establishment of suitable methods to monitor the heterogeneity of this rDNA derived medicinal product would be of great importance for its overall quality assessment.

5.7. Matrix assisted laser desorption ionization time of flight mass spectrometric (MALDI-TOF MS) analysis of abatacept.

Identification of abatacept was the primary goal of MALDO-TOF mass spectrometric analysis which followed the in-gel tryptic digestion of the molecule.
For analysis, two silver stained gel spots of deglycosilated abatacept (indicated with arrows in the Fig. 5.85 gel D) have been selected and with the use of clean scalpel excised in pieces of approximately 1 mm^3 size. A piece of gel is excised from blank region and processed parallel with the sample to serve as control. After destaining[131], proteins were in-gel reduced (DTT, 45 min. 56°C) and acetamidated (iodoacetamide, 30 min in the dark). In- gel tryptic digestion is performed according published procedures[129, 130] (For details see experimental section). Digestion buffer consisted of 12.5 ng/µl modified trypsin in 50 mM ammoniumhydrogene carbonate, pH 8.5.
After extraction (formic acid 5 %, acetonitrile 1:1) and vacuum evaporation, pellet of resulting peptides was dissolved in 3-5 µl of 0.1 % trifluoroacetic acid.

5.7.1. MALDI-TOF sample presentation

Application of sample onto MALDI target is performed according the method which eliminates the mixing of sample with matrix prior to application to the MALDI target[259]. 0.5 µl of saturated matrix solution (8mg α-Cyano- 4-hydroxycinnamic acid dissolved in 1 ml mixture of 70 % ACN and 30% of the 0.1% TFA solution) was applied onto the well of the MALDI target. After 1-2 seconds excess matrix was removed and target surface allowed to dry. After drying, 0.5 µl of sample solution was applied to the sample deposit area. While sample deposit was still wet, further 0.5µl of matrix solution were added and allowed to dry passively. In the same way were applied solutions of molecular mass standards.
All mass spectra were acquired on Compaq SEQ, Kratos Analytical, Manchester, UK) MS instrument operated in positive reflectron mode, peptides were observed as $[M+H]^+$ ions.
For external calibration were used bradykinin fragment 1-7, angiotensin II, ACTH fragment 18-39 and insulin oxidized beta chain.
The identity of abatacept could be confirmed by MALDI-TOF MS by matching the measures molecular weights of resulting peptides to a sequence database.

5.7.2. Peptide mass fingerprint analysis of abatacept

Experimental peptide masses obtained from MALDI-TOF- MS analysis of *in gel* trypsin digested abatacept, are compared with calculated peptide masses by applying the enzyme cleavage rules from three primary sequence databases: MSDB, NCBInr and SwissProt using MASCOT search engine. The closest matches have been identified by using the scoring algorithm.

PeptideMass (http://www.expasy.ch/tools/peptide-mass.html) program was used to *in silico* cleave entered abatacept sequence with trypsine and to compute generated peptide masses with their specified modifications[252].

Only peptide masses bigger than 500 Da have been displayed since in mass region below 500 Da MALDI-TOF spectrum is obscured by the presence of matrix peaks.

For the sequence confirmation, list of peptide masses from MALDI-TOF spectrum (Fig. 5.88) of deglycosilated abatacept is entered to Mascot search engine and corresponding primary sequence database is selected.

MALDI-TOF spectrum of generated peptides from deglycosilated and in-gel tryptic digested abatacept is presented in Fig. 5.88.

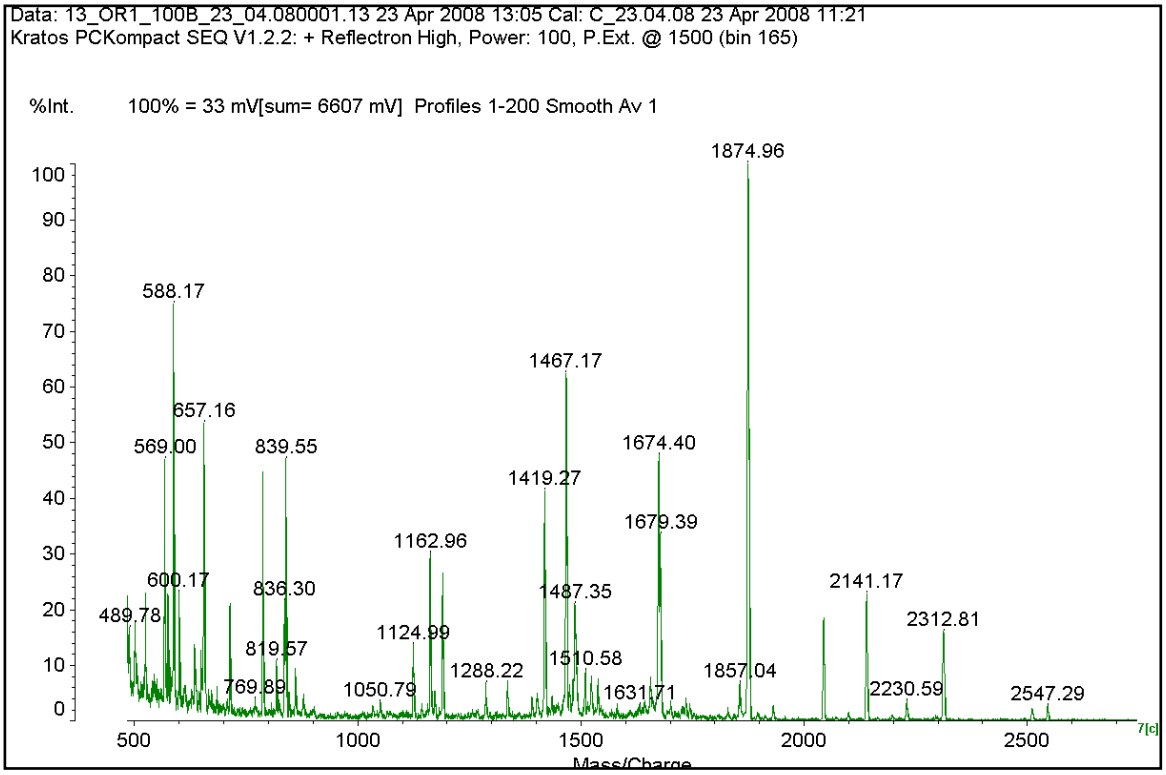

Fig. 5.88. MALDI-TOF spectrum of deglycosilated abatacept.

5.7.3. Primary sequence confirmation. Peptide mass fingerprinting.

For primary sequence confirmation and identification of abatacept, the list of 22 peptide masses (Fig. 5.89) obtained by MALDI-TOF MS were searched with MASCOT and Profound (Prowl) search engines using three sequence databases: MSDB, NCBInr and SwissProt.

Taxonomy was restricted to *Homo sapiens*, selected enzyme was trypsin. Other search parameters were set to allowed up to 1 missed cleavages, methionins in oxidized form (variable modification), cysteins in carbamidomethylated form (fixed modification), average mass, peptide ions in protonated $[M+H]^+$form, mass tolerance was set 1, 1.5 and 2 Da. Protein molecular mass was not specified.

2547.29 2230.59 2141.17 2044.04 1874.96 1674.40 1679.39 1467.17 1487.35 1288.22 1191.35 1172.98 1162.96 1145.21 839.55 836.30 819.57 788.34 657.16 588.17 576.18 501.89

Fig. 5.89. Abatacept. List of entered peptide masses

All databases searched for given peptide masses generated similar results. Entered masses matched with high scores with two components of CTLA4-Ig (abatacept):

1. ***AAL96263*** **Fragment of human immunoglobulin gamma-1 heavy chain constant region IgG_1.**
2. ***Q9BZK2_HUMAN*** **Fragment of human CTLA-4 V domain region.**

For human IgG_1 fragment sequence coverage and score values were dependent on the entered mass tolerance (MT) parameter. On the other hand, for CTLA-4 V domain region, only score values were affected by the MT change. For example, for MT ± 1 Da Mascot search results (MSDB sequence database), reported top score ***180*** for mixture of ***AAL96263,*** **human IgG_1 fragment** and ***Q9BZK2_HUMAN*** **Fragment of human CTLA-4 V domain region**. From 22 entered queries, matched 18(12 for IgG_1Fc fragment and for 7 CTLA-4 V domain). Sequence coverages were 51 % and 41 % for heavy chain IgG_1 fragment and CTLA-4 V domain region,

respectively. With the increase of MT to ±1.5 Da, sequence coverage of IgG_1 fragment was higher i.e. corresponding sequence coverages were 64 % and 41 %. From 22 queries matched 20 (14 queries matched for IgG_1 fragment and 7 queries for CTLA-4 V domain). For MT ± 2 Da the highest sequence coverage was achieved for IgG_1 fragment (74 %). In the same time this was the maximal number of queries matched (16 matched). The sequence coverage of CTLA-4 V domain and matched queries remained the same, 41 % and 7 queries matched, respectively.

Increasing the MT the total score (TS) of mixture increased. For MT ± 1, TS was 180; for MT ± 1.5, TS 186 and for MT ± 2, TS was 210. Individual protein reported scores were affected inversely: Scores for IgG_1fragment increased and those of CTLA-4 V domain decreased because if the number of matched mass values is constant the score in a peptide mass fingerprint will be inversely related to the mass tolerance as in the case of CTLA-4 V domain.

In the Fig. 5.90 Mascot search results using MSDB sequence database with MT parameter set to ±1 Da are presented. Apart from protein summary report this database output contains probability Mowse score histogram and search parameters with specified modifications. As seen from Fig. 5.90 the Mixture 1 is the result with the highest score, lowest expectation value and with 18 queries matched.

Mascot Search Results

User : dashnor nebiu
Email : dashnornebiu@yahoo.com
Search title : Abatacept
Database : MSDB 20060831 (3239079 sequences; 1079394700 residues)
Taxonomy : Homo sapiens (human) (148148 sequences)
Timestamp : 23 Aug 2006 at 17:05:10 GMT
Top Score : 180 for Mixture 1, AAL96263 + Q9BZK2_HUMAN

Probability Based Mowse Score

Protein score is -10*Log(P), where P is the probability that the observed match is a random event.
Protein scores greater than 64 are significant (p<0.05).

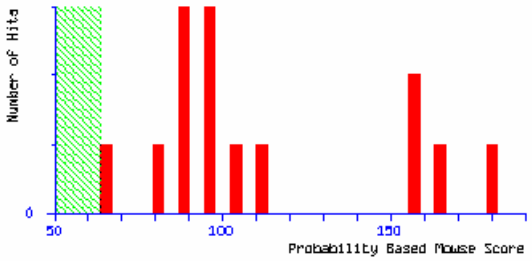

Concise Protein Summary Report

Format As | Protein Summary | Help
Significance threshold p< 0.05 | Max. number of hits AUTO
Re-Search All | Search Unmatched

1. **Mixture 1** **Total score: 180** **Expect:** 1.5e-13 **Queries matched:** 16
Components (only one family member shown for each component):
AAL96263 **Mass:** 24625 **Score: 110** **Expect:** 1.5e-06 **Queries matched:** 12
Immunoglobulin gamma-1 heavy chain constant region (Fragment).- Homo sapiens (Human)
Q9BZK2_HUMAN **Mass:** 12575 **Score: 66** **Expect:** 0.041 **Queries matched:** 7
CTLA-4 V domain region (Fragment).- Homo sapiens (Human).

2. **Mixture 2** **Total score: 165** **Expect:** 4.7e-12 **Queries matched:** 19
Components (only one family member shown for each component):
BAC85237 **Mass:** 44729 **Score: 93** **Expect:** 7.8e-05 **Queries matched:** 13
AK129809 NID: - Homo sapiens
Q9BZK2_HUMAN **Mass:** 12575 **Score: 66** **Expect:** 0.041 **Queries matched:** 7
CTLA-4 V domain region (Fragment).- Homo sapiens (Human).

3. **Mixture 3** **Total score: 159** **Expect:** 1.9e-11 **Queries matched:** 19
Components (only one family member shown for each component):
BAC86226 **Mass:** 49973 **Score: 87** **Expect:** 0.00029 **Queries matched:** 13
AK125633 NID: - Homo sapiens
Q9BZK2_HUMAN **Mass:** 12575 **Score: 66** **Expect:** 0.041 **Queries matched:** 7
CTLA-4 V domain region (Fragment).- Homo sapiens (Human).

14. Q9BZK2_HUMAN **Mass:** 12575 **Score: 66** **Expect:** 0.041 **Queries matched:** 7
CTLA-4 V domain region (Fragment).- Homo sapiens (Human).

Search Parameters

Type of search : Peptide Mass Fingerprint
Enzyme : Trypsin
Fixed modifications : Carbamidomethyl (C)
Variable modifications : Oxidation (M)
Mass values : Average
Protein Mass : Unrestricted
Peptide Mass Tolerance : ± 1 Da
Peptide Charge State : 1+
Max Missed Cleavages : 1
Number of queries : 22

Fig. 5.90. Abatacept (CTLA4-Ig). Mascot search results, section. Mas tolerance ± 1 Da

From the histogram of score distribution (Fig. 5.90) is seen that scores grater then 64 are significant.

In Fig. 5.91 for mass tolerance parameter MT± 2 histogram of probability based mowse score with part of concise protein summary report is presented.

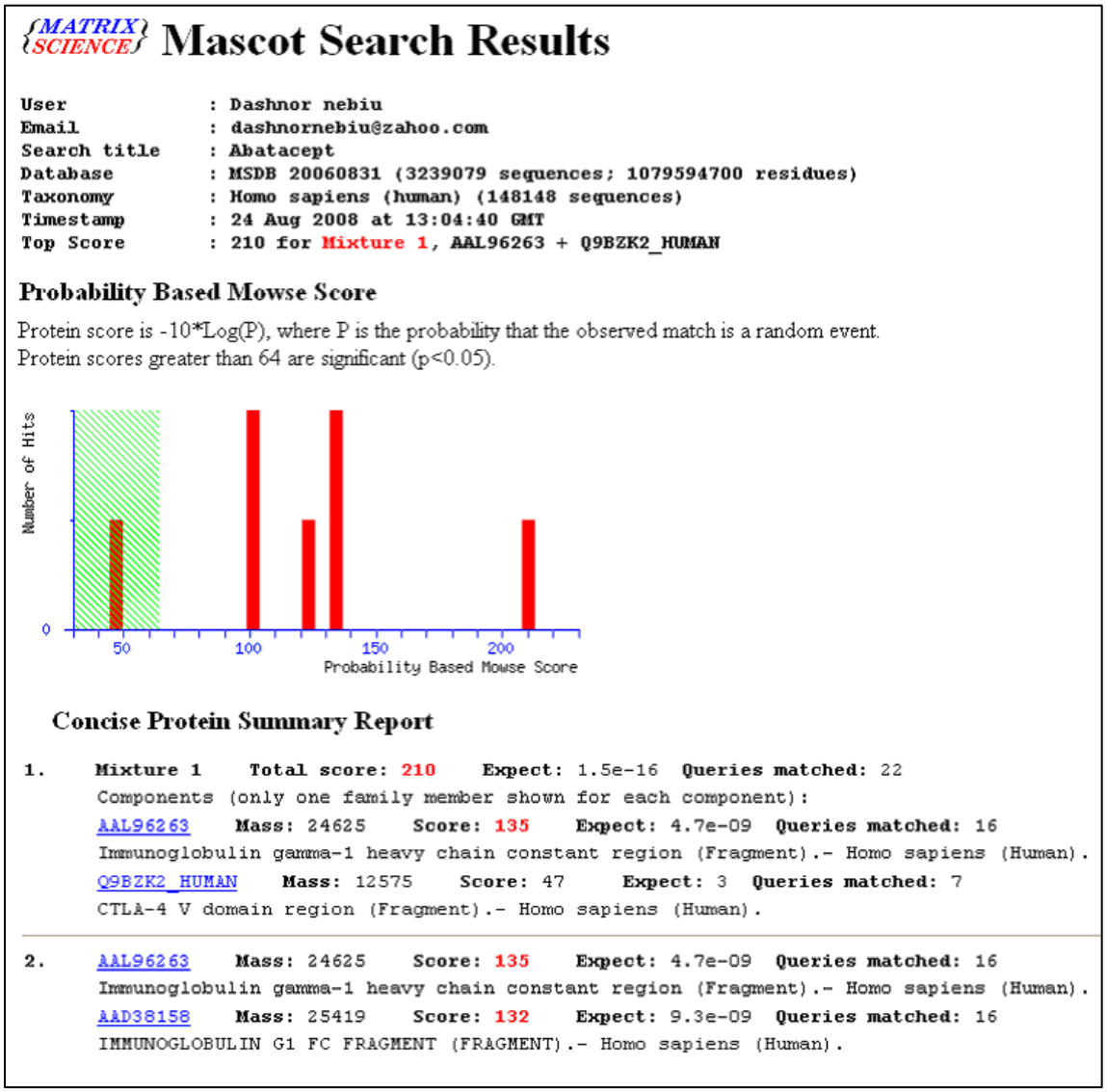

MATRIX SCIENCE **Mascot Search Results**

User : Dashnor nebiu
Email : dashnornebiu@zahoo.com
Search title : Abatacept
Database : MSDB 20060831 (3239079 sequences; 1079594700 residues)
Taxonomy : Homo sapiens (human) (148148 sequences)
Timestamp : 24 Aug 2008 at 13:04:40 GMT
Top Score : 210 for Mixture 1, AAL96263 + Q9BZK2_HUMAN

Probability Based Mowse Score

Protein score is -10*Log(P), where P is the probability that the observed match is a random event.
Protein scores greater than 64 are significant (p<0.05).

Concise Protein Summary Report

1. **Mixture 1** **Total score: 210** **Expect:** 1.5e-16 **Queries matched:** 22
Components (only one family member shown for each component):
AAL96263 **Mass:** 24625 **Score:** 135 **Expect:** 4.7e-09 **Queries matched:** 16
Immunoglobulin gamma-1 heavy chain constant region (Fragment).- Homo sapiens (Human).
Q9BZK2_HUMAN **Mass:** 12575 **Score:** 47 **Expect:** 3 **Queries matched:** 7
CTLA-4 V domain region (Fragment).- Homo sapiens (Human).

2. AAL96263 **Mass:** 24625 **Score:** 135 **Expect:** 4.7e-09 **Queries matched:** 16
Immunoglobulin gamma-1 heavy chain constant region (Fragment).- Homo sapiens (Human).
AAD38158 **Mass:** 25419 **Score:** 132 **Expect:** 9.3e-09 **Queries matched:** 16
IMMUNOGLOBULIN G1 FC FRAGMENT (FRAGMENT).- Homo sapiens (Human).

Fig. 5.91. Abatacept (CTLA4-Ig). Mascot search results, section. Mas tolerance ± 2 Da.

The total score is the absolute probability that the observed match is a random event and it is reported as $-10 \times \log_{10}(P)$, where P is the absolute probability.

Expectation is the number of matches with equal or better scores that are expected to occur by chance alone. The lower the expectation value, the more significant the

score. For a score that is exactly on the default significance threshold, ($p<0.05$), the expectation value is also 0.05.

As indicated above, and documented in Fig. 5.91, at the MT parameter set to ± 2 total score for Mixture 1 and AAL96263 increased to 210 and 135 respectively, and for Q9BZK2 decreased at the value 47.

In Figures 5.92 and 5.93, proton view reports for identified proteins are presented.

MATRIX SCIENCE **Mascot Search Results**

Protein View

Match to: **AAL96263** Score: **135** Expect: **4.7e-09**
Immunoglobulin gamma-1 heavy chain constant region (Fragment).- Homo sapiens (Human).

Nominal mass (M_r): **24625**; Calculated pI value: **7.38**
NCBI BLAST search of AAL96263 against nr
Unformatted sequence string for pasting into other applications

Taxonomy: Homo sapiens

Fixed modifications: Carbamidomethyl (C)
Variable modifications: Oxidation (M)
Cleavage by Trypsin: cuts C-term side of KR unless next residue is P
Number of mass values searched: **22**
Number of mass values matched: **16**
Sequence Coverage: **74%**

Matched peptides shown in **Bold Red**

```
     1 PELLGGPSVF LFPPKPKDTL MISRTPEVTC VVVDVSHEDP EVKFNWYVDG
    51 VEVHNAKTKP REEQYNSTYR VVSVLTVLHQ DWLNGKEYKC KVSNKALPAP
   101 IEKTISKAKG QPREPQVYTL PPSRDELTKN QVSLTCLVKG FYPSDIAVEW
   151 ESNGQPENNY KTTPPVLDSD GSFFLYSKLT VDKSRWQQGN VFSCSVMHEA
   201 LHNHYTQKSL SLSPGK
```

Start - End	Observed	Mr(expt)	Mr(calc)	Delta	Miss	Sequence
18 - 24	836.3000	835.2926	834.9809	0.3118	0	K.DTLMISR.T
25 - 43	2141.1700	2140.1626	2139.3400	0.8226	0	R.TPEVTCVVVDVSHEDPEVK.F
44 - 57	1679.3900	1678.3826	1677.8131	0.5695	0	K.FNWYVDGVEVHNAK.T
58 - 61	501.8900	500.8826	500.5924	0.2902	0	K.TKPR.E
58 - 70	1674.4000	1673.3926	1671.7656	1.6270	1	K.TKPREEQYNSTYR.V
62 - 70	1191.3500	1190.3426	1189.1885	1.1541	0	R.EEQYNSTYR.V
71 - 89	2230.5900	2229.5826	2228.5452	1.0374	1	R.VVSVLTVLHQDWLNGKEYK.C
96 - 103	839.5500	838.5426	838.0029	0.5397	0	K.ALPAPIEK.T
108 - 113	657.1600	656.1526	655.7469	0.4058	1	K.AKGQPR.E
114 - 124	1288.2200	1287.2126	1286.4330	0.7797	0	R.EPQVYTLPPSR.D
130 - 139	1162.9600	1161.9526	1161.3721	0.5805	0	K.NQVSLTCLVK.G
140 - 161	2547.2900	2546.2826	2544.6386	1.6441	0	K.GFYPSDIAVEWESNGQPENNYK.T
162 - 178	1874.9600	1873.9526	1874.0512	-0.0986	0	K.TTPPVLDSDGSFFLYSK.L
179 - 183	576.1800	575.1726	574.6676	0.5051	0	K.LTVDK.S
179 - 185	819.5700	818.5626	817.9306	0.6321	1	K.LTVDKSR.W
209 - 216	788.3400	787.3326	787.9012	-0.5685	0	K.SLSLSPGK.-

No match to: 588.1700, 1145.2100, 1172.9800, 1467.1700, 1487.3500, 2044.0400

Fig. 5.92. Abatacept (CTLA4-Ig). Macot Protein view report, section. *AAL96263.*

In the AAL96263, amino acids sequence 1-109 correspond to the C_H2 domain, and sequence 110-216 to C_3H domain of immunoglobulin heavy chain fragment. This part of CTLA4-Ig (abatacept) molecule sequence is identified with high score and high

sequence coverage of 74 %. It corresponds to CTLA4-Ig (Fig. 1.9) sequence 142-357.The rest of the abatacept sequence, 1-141, contains sequences of CTLA-4 extracellular domain (1-124) and modified hinge region.

In the Fig. 5.93 sequence of identified CTLA-4 part of molecule is presented. Amino acid sequences 1-38 and 84-93 are covered (total 41 % sequence coverage). If remaining non-covered amino acid sequences of CTLA-4 and modified hinge region are carefully observed, it is noted that from position 39 there are neither arginines (R) nor lysines (K) until positions 83, 93 and 128 respectively. Trypsin specifically cleaves peptide chains at the carboxyl side of the amino acids K and R, therefore the resulting masses are to high, peptide sizes to large to efficiently diffuse out of gel, extracted and eventually measured by MALDI-TOF. Referring the *in silico* calculated masses, peptide masses of sequences 39-93 is 5877.71 Da; 34-83, 5350.57 Da, 84-128, 5033.36; 39-83 is 4782.20; 94-132, 4355.04. A good mass range for trypsin is 1000-3500 Da[260]

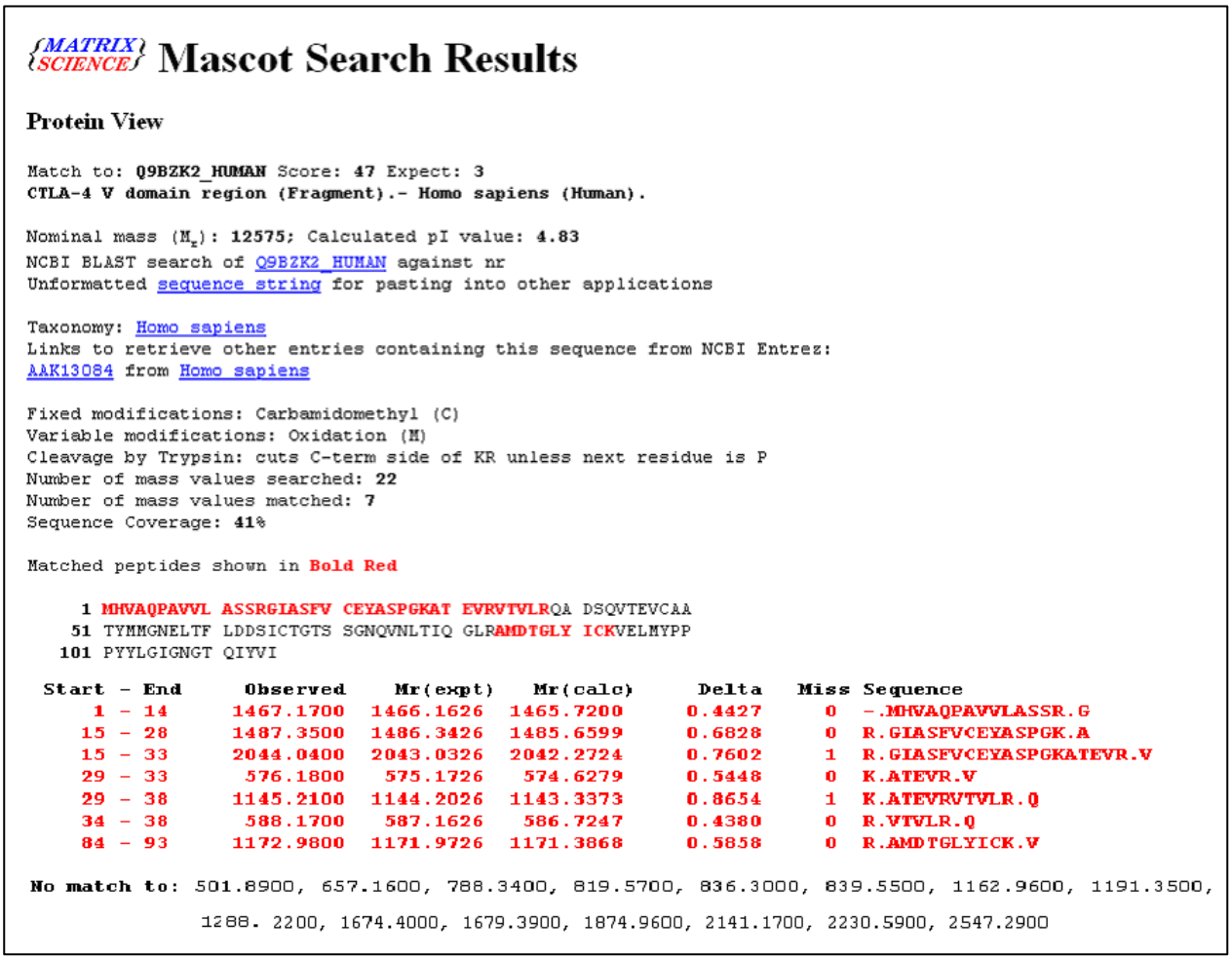

{MATRIX SCIENCE} **Mascot Search Results**

Protein View

Match to: **Q9BZK2_HUMAN** Score: **47** Expect: **3**
CTLA-4 V domain region (Fragment).- Homo sapiens (Human).

Nominal mass (M_r): **12575**; Calculated pI value: **4.83**
NCBI BLAST search of Q9BZK2_HUMAN against nr
Unformatted sequence string for pasting into other applications

Taxonomy: Homo sapiens
Links to retrieve other entries containing this sequence from NCBI Entrez:
AAK13084 from Homo sapiens

Fixed modifications: Carbamidomethyl (C)
Variable modifications: Oxidation (M)
Cleavage by Trypsin: cuts C-term side of KR unless next residue is P
Number of mass values searched: **22**
Number of mass values matched: **7**
Sequence Coverage: **41%**

Matched peptides shown in **Bold Red**

```
     1 MHVAQPAVVL ASSRGIASFV CEYASPGKAT EVRVTVLRQA DSQVTEVCAA
    51 TYMMGNELTF LDDSICTGTS SGNQVNLTIQ GLRAMDTGLY ICKVELMYPP
   101 PYYLGIGNGT QIYVI
```

Start - End	Observed	Mr(expt)	Mr(calc)	Delta	Miss	Sequence
1 - 14	1467.1700	1466.1626	1465.7200	0.4427	0	-.MHVAQPAVVLASSR.G
15 - 28	1487.3500	1486.3426	1485.6599	0.6828	0	R.GIASFVCEYASPGK.A
15 - 33	2044.0400	2043.0326	2042.2724	0.7602	1	R.GIASFVCEYASPGKATEVR.V
29 - 33	576.1800	575.1726	574.6279	0.5448	0	K.ATEVR.V
29 - 38	1145.2100	1144.2026	1143.3373	0.8654	1	K.ATEVRVTVLR.Q
34 - 38	588.1700	587.1626	586.7247	0.4380	0	R.VTVLR.Q
84 - 93	1172.9800	1171.9726	1171.3868	0.5858	0	R.AMDTGLYICK.V

No match to: 501.8900, 657.1600, 788.3400, 819.5700, 836.3000, 839.5500, 1162.9600, 1191.3500, 1288.2200, 1674.4000, 1679.3900, 1874.9600, 2141.1700, 2230.5900, 2547.2900

Fig. 5.93. Abatacept (CTLA4-Ig). Mascot Protein view report, section. *Q9BZK2_HUMAN.*

In summary results obtained from MASCOT/MSDB sequence data base specifically made possible identification of abatacept through identification, with high score, low expectation and relatively high sequence coverage of the mixture of its extracellular CTLA-4 domain and highly conserved C_H2 and C_H3 domains of human IgG.

The list of peptide masses searched in sequence database MSDB was submitted to second sequence database, NCBInr, and the search results provided similar scores and sequence coverages as with the MSDB for both identified abatacept sequence fragments.
The search results from the third database, SwissProt reported top scores for: IGHG1_HUMAN (Ig gamma-1 chain C region Homo sapiens MASS 36628 Da).

- Top score 84. Expectation $8.4e^{-05}$. Queries matched 12 for MT ±1
- Top score 90. Expectation $2e^{-05}$. Queries matched 14 for MT ±1.5
- Top score 103. Expectation $1e^{-06}$. 14 queries matched, MT ± 2

IGHG1_HUMAN (Ig gamma-1 chain C region Homo sapiens with molecular mass of 36628 Da) is actually the complete sequence of human heavy chain constant region (Fig 100) and not of the heavy chain IgG1 fragment which contains 114 amino acids less (Protein view Fig. 5.92). Therefore SwissProt reported less sequence coverage (48 %).

```
  1 ASTKGPSVFP LAPSSKSTSG GTAALGCLVK DYFPEPVTVS WNSGALTSGV
 51 HTFPAVLQSS GLYSLSSVVT VPSSSLGTQT YICNVNHKPS NTKVDKKVEP
101 KSCDKTHTCP PCPAPELLGG PSVFLFPPKP KDTLMISRTP EVTCVVVDVS
151 HEDPEVKFNW YVDGVEVHNA KTKPREEQYN STYRVVSVLT VLHQDWLNGK
201 EYKCKVSNKA LPAPIEKTIS KAKGQPREPQ VYTLPPSRDE LTKNQVSLTC
251 LVKGFYPSDI AVEWESNGQP ENNYKTTPPV LDSDGSFFLY SKLTVDKSRW
301 QQGNVFSCSV MHEALHNHYT QKSLSLSPGK
```

Fig. 5.94. Amino acid sequence of human IgG1 heavy chain constant region. Mached sequences are highlighted.

Abatacept, however, contains only modified sequence of the human IgG1 Fc region, hinge, CH2 and CH3 domain (Fig. 1.9).

When only the following MALDI peptide masses: 575.172; 587.162; 1144.202; 1172.292; 1466.162; 1486.522; and 2042.822, which correspond to *in silico* calculated masses (Peptide mass Expassy) for CTLA-4 variable domain of abatacept

are searched, top scores higher than 100, with low expectations values, were obtained. This significant protein identification results were reported from both MSDB and NCBInr sequence databases which provided same results with MT set to ± 1 (Fig. 5.95)

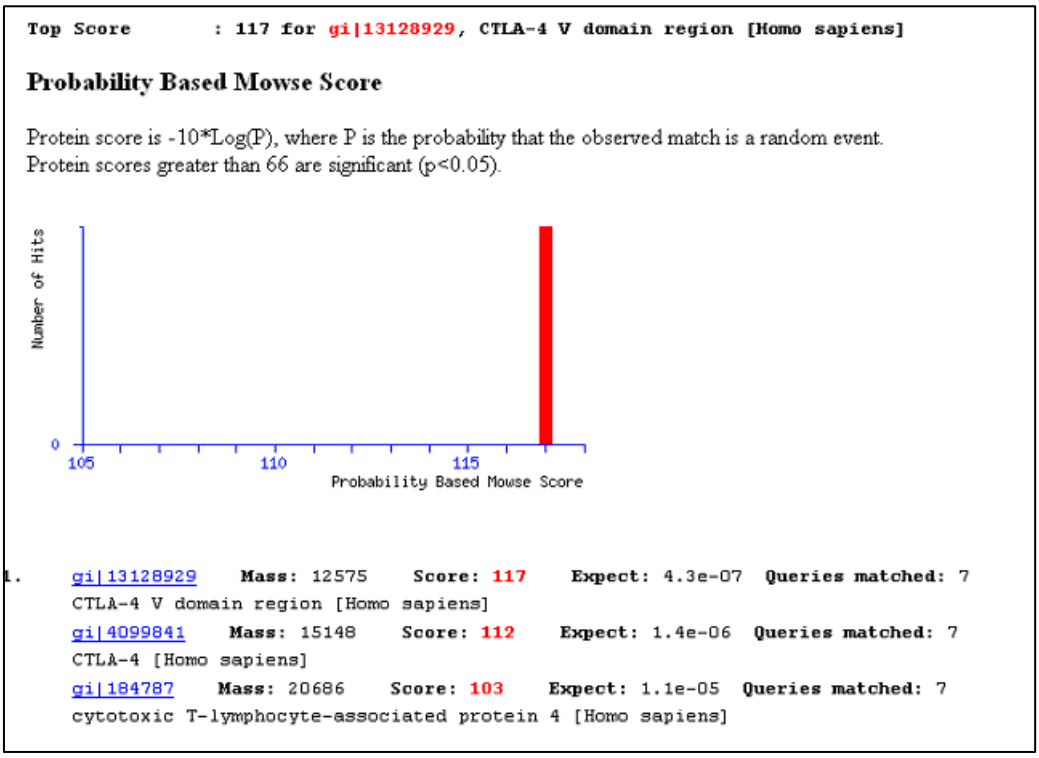

Fig. 5.95 . Abatacept (CTLA4-Ig). Mascot search results, section. MSDB/NCBInr

The top score (117) protein *gi 13128929* has the same sequence as *Q9BZK2_HUMAN* fragment of human CTLA-4 V domain region (Figures 5.91, 5.93 and 5.95, Mol. mass 12575 Da).

Two next two proteins reported are longer sequence variants of CTLA-4 protein. *gi 184787* is complete amino acid sequence of human CTLA-4 (186 amino acids). As indicated in Fig 1 only extracellular domain of CTLA-4 is part of abatacept molecule. Additional 62 amino acids of full CTLA-4 sequence compose its transmemrane and intracellular domains.

Interestingly, protein with top score obtained from SwissProt database is a variant of human CTLA-4 (precursor), with 223 amino acids therefore 99 amino acids more than CTLA-4 ECD. These additional amino acids compose signal peptide 1-35;

transdermal domain 162-182, and 183-223 cytoplasmatic domain of human CTLA-4 precursor.

In this case score is 75, and there are only 6 queries matched. MALDI peptide mass 1466.16 does not much in contrast to 7 matches seen in Figures 5.90 and 5.91. Peptide mass 1466.16 covers the sequence of CTLA-4 V region from position 1-14 (M_1 to R_{14}). In the human CTLA-4 precursor, searched in SwissProt database this position is occupied with the rest of signal peptide therefore there is no matching.

Measured peptide masses were submitted to the second search engine, Profound (Prowl).The proteins of the highest rank were human immunoglobulin G_1 Fc fragment and human CTLA-4 V domain region. Rank +1, expectation 5.0×10^{-5}, sequence coverage 57 %, pI 7 and molecular weight 25.40 kDa are reported for the first and Rank +2, expectation 2.8×10^{-3}, sequence coverage 42 %, pI 4.8 and molecular weight 12.56 kDa for the latter, respectively. Mass tolerance parameter was set to ±1.2 Da. While human CTLA-4 V domain protein is identical with the protein *Q9BZK2_HUMAN,* reported from MASCOT search engine (NCBInr, MSDB and Swiss Prot), human immunoglobulin G_1 Fc fragment reported in this sequence database is identical as well with the one reported from MASCOT, provided that the amino terminus here has been extended for additional 7 amino acids, which are part of F_C fragment (3 amino acids from C_H2 and 4 amino acids from hinge region respectively).

In the Fig. 5.96 as illustration, amino acid sequences human immunoglobulin-G fragments reported in both search engines are presented.

```
  1 PELLGGPSVF LFPPKPKDTL MISRTPEVTC VVVDVSHEDP EVKFNWYVDG
 51 VEVHNAKTKP REEQYNSTYR VVSVLTVLHQ DWLNGKEYKC KVSNKALPAP
101 IEKTISKAKG QPREPQVYTL PPSRDELTKN QVSLTCLVKG FYPSDIAVEW
151 ESNGQPENNY KTTPPVLDSD GSFFLYSKLT VDKSRWQQGN VFSCSVMHEA
201 LHNHYTQKSL SLSPGK


  1 TCPPCPAPEL LGGPSVFLFP PKPKDTLMIS RTPEVTCVVV DVSHEDPEVK
 51 FNWYVDGVEV HNAKTKPREE QYNSTYRVVS VLTVLHQDWL NGKEYKCKVS
101 NKALPAPIEK TISKAKGQPR EPQVYTLPPS RDELTKNQVS LTCLVKGFYP
151 SDIAVEWESN GQPENNYKTT PPVLDSDGSF FLYSKLTVDK SRWQQGNVFS
201 CSVMHEALHN HYTQKSLSLS PGK
```

Fig. 5.96 Identified human IgG_1 fragment :
Up: MASCOT: Immunoglobulin gamma-1 heavy chain constant region (Fragment).- Homo sapiens Accession: AAL96263 Down: Profound**:** Immunoglobulin G_1 F_C fragment.-Homo sapiens. Accession: AAD38158 Amino acid difference is highlighted.

In Summary, peptide mass fingerprinting results as a suitable method for the identification of abatacept. It is also confirmed that this method is successful when amino and /or cDNA sequence of searched protein is known and present in sequence databases. To document the reproducibility, MALDI-TOF spectra, acquired from the abatacept excised from two different 2-DE gel spots are presented in Fig. 5.97.

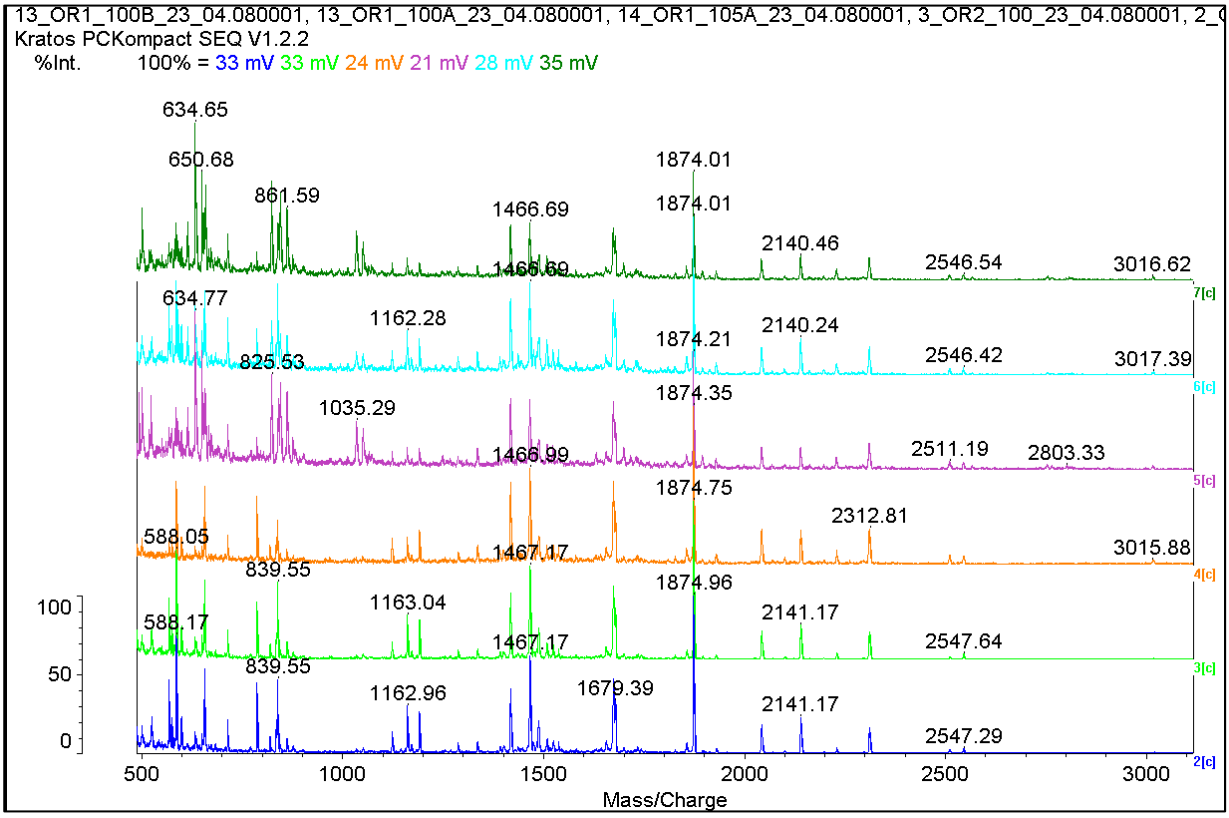

Fig. 5.97. MALDI-TOF Analysis of abatacept (CTLA4-Ig). Spectra generated from different 2-DE spots.

6. Conclusions

The main objective of this work was to evaluate the suitability of 1-DE, 2-DE and MALDI-TOF analysis for the demostration of identity, structural integrity and purity of therapeutically relevant *rmAbs* (trastuzumab, rituximab) and *fusion protein*, abatacept. In addition, in order to assess the stability indicating power of 2-DE, forced degradation studies of trastuzumab were undertaken.

Experimental results confirmed that SDS-PAGE analysis can be used as a simple, fast and reliable method for the quality assessment of studied biological products. This technique enables the estimation of molecular weights and purity of biological medicinal products studied, however only limited information regarding the heterogeneity of these products could be obtained.

Recombinant monoclonal antibodies trastuzumab and rituximab, under non-reducing SDS-PAGE migrated as single bands at ~150 kDa, while under reducing conditions two distinct molecular weight species, corresponding their light and heavy chains, migrated at ~23 and ~50 kDa respectively. *Fusion protein* abatacept migrated at ~100 kDa under non-reducing conditions, while upon reduction of its disulfide bridges, single sharp band was observed at ~ 50 kDa.

SDS-PAGE deglycosilation experiments confirmed that the contribution of posttranslational glycosilation in abatacept molecular weight is considerably higher (~15%) comparing to trastuzumab and rituximab (3-5%).

Higher sensitivity of Silver staining over Coomassie staining, restricted linear dynamic range and problematic gel-to-gel reproducibility of band intensities, especially for silver staining were documented as well. In all cases, reducing SDS-PAGE delivered sharper bands comparing to non-reducing conditions.

This study documented that in contrast to SDS-PAGE, 2-DE analysis delivered more comprehensive information regarding identity and structural integrity of studied medicinal products. Apart from the estimation of molecular weight and *pI*, additional information related to the charge heterogeneity and posttranslational modifications of studied substances has been obtained and on the basis of obtained results it was shown that 2-DE is suitable method for the monitoring of charge heterogeneity and isomorf patterns of recombinant monoclonal antibodies and fusion proteins.

2-DE analysis of *rmAbs* trastuzumab and rituximab using IPG strips 6-9 L and 3-11 NL for the first dimension, demonstrated typical antibody glycoprotein complex spot pattern consisting on numerous poorly resolved trains of spots tending to spread as a bands, for both chains. On the other hand, acidic glycoprotein abatacept migrated as a single set of sloping spots with estimated *pI* ranging from 4.5-5.5.

Experimentally estimated isoelectric points were in agreement with literature data and their theoretical *pI* values calculated from respective *cDNA* derived amino acid sequences in case of their deglycosilated forms.

In all cases, an improved resolution was observed upon the reduction of sample amount. Optimized 2-DE electrophoresis conditions for deglycosilation experiments and subsequent MALDI-TOF MS analysis included *IPG* strips 3-11 *NL* (for rituximab and trastruzumab) and 4-7 *L* for abatacept. Linear 12. 5 *% polyacrylamide gels* (30.8 *%T* and *2.6 %* C) were run and more sensitive silver staining procedure was applied for gel visualization.

For the monitorization of trastuzumab, rituximab and abatacept N-deglycosilation SDS-PAGE and 2-DE were used. 1-DE experiments comparing native ande N-deglycosilated samples proved the presence of N-linked glycan molecules and delivered straightforward information concerning deglycosilation efficiency. On the otherhand, 2-DE could be used only for deglycosilation monitorization of abatacept, while for trastuzumab and rituximab due to the small charge difference between their N-deglycosilated and glycosilated forms, results were equivocal.

The contribution of N- linked sugars, terminal sialic acids and C-terminal lysine truncation in 2-DE spot pattern of trastuzumab, rituximab and abatacept, was studied using *N-glycosilade F*, *sialidase* and *Caroxypeptidase B* . *O- glycosidase* was used for the removal of abatacept O-linked glycans.

No significant differences were observed in the 2-DE patterns of N-deglycosilated, desialynated, and Carboxypeptidase B treated *rmAbs* and native samples. These results were in accordance with published data: since in *rmAbs* molecules there is only one N-glycosilation site containing predominantly neutral oligosaccharides, the expected *pI* and *MW* differences after N-linked glycan release are very small to be unambiguously detected with 2-DE.

On the other hand, enzymatic deglycosilation experiments of abatacept resulted in completely different behavior comparing to *rmAbs*. After PNGase, silaidase and O-glicosidase treatment significant changes in molecular weight and isoelectric point

with additional reduction in the complexity of spot pattern were observed. Apart from neutral N-linked glycans, 2-DE experiments confirmed the significant presence of acidic O-linked sialo-glycans.

Forced degradation study of trastuzumab was used for the assessment of stability indicating power of SDS-PAGE and 2-DE. Experimental data demonstrated stability indicating capability for both methods, provided that for 2-DE results were less straightforward.

Peptide mass fingerprinting (PMF) analysis was used for the identification of trastuzumab, rituximab and abatacept.

PMF analysis resulted as a fast and reliable method for the identification of trastuzumab. Confirmation of humanized origin and allotype marker *(...^{359}EEM^{361}...)* of this antibody was possible, as well. For the identification of trastuzumab heavy chain, list of entered peptides matched with highest scores with the mixture of two peptides: *gi 226787, immunoglobulin gamma 1*, which corresponds to trastuzumab heavy chain residues 228-450, Fc fragment (sequence coverage 67 %) and *gi 442924*, *Antigen-binding domains of humanized Anti-P$^{185\text{-}Her2}$ Antibody 4d5*- trastuzumab, which corresponds to trastuzumab heavy chain residues 1-223, trastuzumab Fab (sequence coverage 55 %).

For trastuzumab light chain, the highest rank protein reported after the entering of the list of peptide masses was *gi28948772* (trastuzumab light chain, sequence coverage 81 %). Since the sequence coverage included amino acid residues, parts of light chain CDR regions and FR3 which are imported from the murine light chain sequence into the human sequence, this method is capable to specifically discriminate the humanized antibody from the antibodies of other origin.

The identification of the light chain of chimeric antibody rituximab was possible using PMF analysis. The highest rank protein reported after the entering of the list of peptide masses was *gi146387638 (Rituximab Fab fragment,* light chain entire sequence, residues 1-213*)* with the sequence coverage 45 %. Concerning rituximab heavy chain identification, list of entered peptide masses into MASCOT/NCBInr database generated top score values for *gi 20664303* (*Fc fragment of rituximab*), with sequence coverage 57 % and other *IgG1 Fc fragments*.

With PMF analysis it was possible identification of both fusion partners of fusion protein abatacept, CTLA4-Ig. List of entered abatacept masses matched with high scores with two components of *CTLA4-Ig* (abatacept): *AAL96263* (Fragment of

human immunoglobulin gamma-1 heavy chain constant region IgG_1) and *9BZK2_HUMAN* (Fragment of human *CTLA-4 V* domain region). Sequence coverage for human IgG1 part of molecule was 74 % while for variable domain of *CTLA4* 41 %.

Presented results suggest that PMF analysis is a suitable method for the fast identity confirmation of recombinant monoclonal antibodies and antibody related substances such are fusion proteins. In our opinion, apart from its use for in-process control purposes, the simplicity, speed and specificity of this method make it suitable for regulatory environment as well.

Other advantage of this method is that previous separation of peptides with HPLC or CE like in *peptide mapping* is not required, and rapid demonstration of molecular identity of the product before committing it to protein sequence analysis is possible.

Furthermore, protein samples subjected to MALDI-TOF analysis are previously separated with 2-DE, therefore sample complexity is greatly reduced. On the other hand, additional sample information can be obtained during the 2-DE analysis *i.e.* molecular weight, charge heterogeneity, information about the oligosaccharide content and posttranslational modifications, before the *in gel* tryptic digestion.

Since 2-DE, MALDI-TOF MS and peptide mass fingerprinting analysis have already matured, necessary equipment is commercially available and no special personnel requirements are needed, this method might be used as routine technique in quality control laboratories.

In addition, *PMF* analysis might enable the discrimination of rmAbs of different origin (murine, chimeric, humanized and human), and the identification of structurally related antibody fusion proteins could be possible, as well. This could be of great importance for in process control during the production of different products in same production platform.

As seen above, for all studied substances the basic requirement for the success of peptide mass fingerprinting strategy is that the searched peptide sequence must be present at opened access databases. For instance abatacept was identified as a mixture of its constituent fragments and not as an entire sequence. The same holds for rituximab and trastuzumab heavy chains. In given databases Fv, Fab, and Fc fragments are stored and not entire sequences of their heavy chains.

Other tasks to be fulfilled in the future remain more detailed optimization of 2-DE-MALDI-TOF MS with subsequent PMF analysis for identification purposes, *i.e.* in

order to increase the sequence coverage for the *PMF* analysis of studied biological medicinal products, the application of enzymes of different specificity, *i.e.* chymotrypsin, should be studied and a suitable method for the full characterization of abatacept glycoforms should be development as well.

7. Literature

1. Anand, B. et al. Monoclonal antibodies: From Structure to Therapeutic Application. In *Pharmaceutical Biotechnology* 3rd Ed. pp. 309-337. Edited by: Daan J.A. Crommelin, Robert D. Sindelar and Bernd Meibohm. Informa Healthcare USA, Inc. 2008. ISBN-13: 978-1-4200-6752-1 ,
2. D. Brown: Overview of Sources of New Drugs. In *Comprehensive Medicinal Chemistry II*, Vol.1 Global Perspective. Peter Kennwell (Ed), Elsevier Ltd. pp. 321-353,1st Ed. (2007). ISBN-13: 978-0-08-044513-7
3. U.S. Food and Drug Administration. Center for Biologics Evaluation and Research. FAQ: http://www.fda.gov/cber/faq.htm#3. Accessed: 15.09.08
4. European Medicines Agency. http://www.emea.europa.eu/. Accessed: 15.09.08
5. Rader, A.R. What is a Biopharmaceutical? Part 1: (Bio) Technology-Based Definitions. *BioExecutive International (*March 2005), pp. 60-65
6. Cichutek, K. Gene and Cell Therapy in Germany and the EU. *Journal für Verbraucherschutz und Lebensmittelsicherheit*. **3** (2008) Supplement 1, pp. 73 – 76
7. Walsh, G. Biopharmaceutical Benchmarks 2003. *Nature Biotechnology*. **21** (2003), pp. 865-870
8. Robinson, K. An Industry comes of age. *Biopharm. Int.***15** (2002), pp. 20-24.
9. IMS Health Reports. News release: *Global Biotech sales grew 12.5 percent in 2007, exceeding $75 Billion*. http://www.imshealth.com/portal/site/imshealth. Accessed: 10.09.08
10. Peng, Z. et al: The application of gene therapy in China. *IDrugs*. **11(5)**(2008), pp. 346-350
11. Danna, K et al.Specific cleavage of simian virus 40 DNA by restriction endonuclease of *Hemophilus influenzae Pro. Nat. Acad. Sci.* **68(12)** (1971) pp. 2913-2917
12. Smith, H.O. et al. A restriction enzyme from *Hemophilus influenzae*. I. Purification and general properties. *J. Mol. Biol*. **51** (1970), 379–391
13. Cohen et al. Construction of Biologically Functional Bacterial Plasmids In Vitro. *Proc. Nat. Acad. Sci. USA*. **70 (11)**, (1973), pp. 3240-3244

14. Johnson, I.S. Human insulin from recombinant DNA technology. Science, **219**, Issue 4585 (1983) pp. 632-637
15. http://www.gene.com/gene/about/corporate/history/timeline.html. Accessed: 10.09.08
16. Gary Walsh. Current Status of Biopharmaxceuticals: Approved Products and Trends in Approvals. Modern Biopharmaceuticals. Ed. Jörg Knäblein Vol 1. Design, Development Optimization, pp. 1-34 (2005). Wiley VHC Verlag GmbH Weinheim ISBN: 978352731184-2
17. Soumitra Basu, Adegboyega K. Oyelere: Application of Recombinant DNA Technology in Medicinal Chemistry and Drug Discovery. In *Burgers Medicinal chemistry and Drug Discovery,* Vol.2. Drug Development, Donald J. Abraham (Ed), John Willey & Sons Inc. pp. 81-106, 6th Ed (1996) ISBN: 0-471-37038-2
18. Fineberg, S.E. et al. Immunogenicity of Recombinant DNA Human Insulin. *Diabetologia*. **25** (1983) pp. 465-469
19. Cabolco, L.O.et al. Iatrogenic Creutzfeldt-Jakob disease following human growth hormone therapy: case report. *Arquivos de neuro-psiquiatria*. **60(2-B)** (2002), pp. 458-61
20. Lundberg, P.O. Still a small problem with the mad cow disease? Creutzfeldt-Jakob disease and other prion diseases: current status. *Läkartidningen*. **98(1-2)** (2001), pp.19-24
21. Pipe, S.W. The promise and challenges of bioengineered recombinant clotting factors. *Journal of Thrombosis and Haemostatsis*. **3** (2005), pp.1692-1701.
22. Walsh, G. Biopharmaceutical benchmarks 2006. *Nature Biotechnology*. **24**, (2006), pp. 769-776,
23. Schreiber, I. Treatment of acromegaly with the GH receptor antagonist pegvisomant in clinical practice: safety and efficacy evaluation from the German Pegvisomant Observational Study. *European Journal of Endocrinology* **156 (1)** (2007), pp. 75–82
24. Pfizer/Aventis. Exubera European Public Assessment Report. http://www.emea.eu.int/humandocs/PDFs/ EPAR/exubera/058806en1.pdf (2006). Accessed: 10.09.08
25. Wang, W. Antibody Structure, Instability, and Formulation. *Journal of Pharmaceutical Sciences*. **96(1)** (2007), pp. 1-26

26. Adair, J.R: Antibody Engineering and Expression. http://www.wiley-vch.de/books/biotech/pdf/v05a_ant.pdf. Accessed: 17.09.2008
27. Angelika Vollmar, Theodor Dingermann. Immunologie. Grundlagen und Wirkstoffe. 1-45. Dingermann, T. Wissenschaftliche Verlagsgesellschft mBH Stuttgart, 2005. ISBN 3-8047-2189-3
28. A.J. Meulenbroek and W.P. Zeijlemaker. Human Immunoglobulin subclasses. Useful diagnostic markers for immunocompetence. Published by CLB, Plesmanlaan 125, 1066 CX Amsterdam, The Netherlands. CLB, 1996. ISBN 90-5267-011-0 Published online. http://www.researchd.com/rdikits/rdisubbk.htm. Accessed: 17.09.2008
29. Sandlie, I. et al. C1q binding to chimeric monoclonal IgG3 antibodies consisting of mouse variable regions and human constant regions with shortened hinge containing 15 to 47 amino acids. *European Journal of Immunology*. **19 (9)** (2005), pp.1599-1603
30. *E*xPASy. UniProtKB/Swiss-Prot. Entries: P01857 (IGHG1_HUMAN); P01859 (IGHG2_HUMAN); P01860 IGHG3_HUMAN; P01861 (IGHG4_HUMAN). http://ca.expasy.org/. Accessed: 17.09.2008.
31. Roux, K.H. Flexibility of human IgG subclasses. The Journal of Immunology. **159(7)** (1997) pp. 3372-3382
32. De Lange G.G. Polymorphisms of human immunoglobulins: Gm, Am, Em and Km allotypes. *Exp. Clin. Immunogenet.* **6** (1989), pp. 7-17
33. Greenwood et al. *Effector functions of human IgG*. M. Clark (1998). Published on-line; http://www.path.cam.ac.uk/~mrc7/iggfunctions/index.html. Accessed: 19.09.2008
34. Zhang, W. free sulfhydril in recombinant monoclonal antibodies. *Biotechnology Progress.* **18(3)** (2002) pp. 509-13
35. Wright, A. et al. Effect of glycosylation on antibody function: implications for genetic engineering. *Trends in Biotechnology*. **15 (1)** (1997) pp. 26-32
36. Kilgore, B.R. et al. Comparability and Monitoring Immunogenic N-linked Oligosaccharides from Recombinant Monoclonal Antibodies from two different cell lines using HPLC with fluorescence detection and Mass spectrometry. *Methods in Molecular Biology.* **446** (2008), pp. 333-346. DOI: 10.1007/978-1-60327-084-7_23.

37. Jefferis, R. et al., IgG-Fc Mediated Effector Functions: Molecular definition of Interaction Sites for Effector Ligands and the Role of Glycosylation. *Immunol. Rev.* **163** (1998), pp. 50-76
38. Chirino, A.J. Characterising Biological products and assessing comparability following manufacture changes. *Nature Biotechnology* **22(11)** (2004), pp. 1383-1391
39. Wright A. et al. *In vivo* trafficking and catabolism of IgG1 antibodies with Fc-associated carbohydrates of differing structure.*Glycobiology* **10** (2000), pp.1347-1355.
40. Wan, H.Z. Rapid method for monitoring galactosylation levels during recombinant antibody production by electrospray mass spectrometry with selective-ion monitoring. *Journal of Chromatography A.* **913** (2001), pp. 437-446
41. Hodoniczky, J. Control of Recombinant Monoclonal Antibody Effector Functions by Fc *N*-Glycan Remodeling in Vitro. *Biotechnol. Prog.* **21** (2005), pp.1644-1652
42. Almagro, J.C. Humanization of Antibodies. *Frontiers in Bioscience*. **13** (2008), pp.1619-1633
43. Carter et al. Genetech Inc. Humanized antibodies and methods for making them. United States Patent (2000),Nr. 6054297
44. Lowman, H. B. Polypeptide variants with altered effector function. International Publication Number: WO 2006/031370; International Application Number: PTC/US2005/029511
45. Woof, J.M. Localisation of the monocyte-binding region on human immunoglobulin G. *Molecular immunology*. **23(3)** (1986), pp. 319-330
46. Burton, D.R. Immunoglobulin G: Functional sites. *Molecular immunology*. **22(3)** (1985), pp.161-349
47. Ghetie, V. et al. Multiple roles for the major histocompatibility complex class I-related receptor FcRn. *Annual Reviews of Immunology*. **18** (2000), pp. 739-66
48. Newcombe, C. et al. Antibody production: Polyclonal-derived biotherapeutics. *Journal of Chromatography B*, **848** (2007), pp. 2–7.
49. Haurum, J.S. Recombinant polyclonal antibodies: the next generation of antibody therapeutics? *Drug Discovery today*. (2006), pp: 655-660

50. Brekke, O.H. Therapeutic antibodies for human diseases at the dawn of the twenty-first century. *Nature Reviews Drug Discovery* **2**, (2003) pp. 52-62
51. Kohler, G. et al. Continuous cultures of fused cells secreting antibody of predefined specificity. *Nature* **256** (1975), pp. 495–497.
52. Douglas F. Lake et al. Future strategies in Immunotherapy. Chapter Six. In : Burger's Medicinal Chemistry and Drug Discovery. 6th Ed. Vol 5: pp: 223-247. Chemotherapeutic Agents. Ed. by Donald J. Abraham ISBN 0-471-37031-2 2003 John Wiley &Sons. Inc.
53. Stoll, T.et al. Production of immunoglobulin A in different reactor configurations. *Cytotechnology* **17**(1995), pp. 53-63
54. Presta, L.G. Engineering of therapeutic antibodies to minimize immunogenicity and optimize function. *Advanced drug delivery reviews*. **58(5-6)**,(2006), pp.640-656
55. Morrison, S.L. Chimeric human antibody molecules: mouse antigen-binding domains with human constant region domains. *Proc. Natl. Acad. Sci. U.S.A.* **81** (1984), pp. 6851-55
56. Reff, M.E. et al. Depletion of B cells in vivo by a chimeric mouse human monoclonal antibody. *Blood*. **83** (1994), p. 435
57. Reff et al. Future of monoclonal antibodies in the treatment of hematologic malignancies. *Cancer control*, **9**(2002), p. 152
58. Riechmann, L. et al.. Reshaping human antibodies for therapy. *Nature*. **332**, (1988), pp. 323-327
59. Quin et al. A humanised antibody that binds to the interleukin-2 receptor. *Proc. Nat. Acad. Sci. USA.* **86** (1991), pp.10029-33
60. Chapman P.A. PEGylated antibodies and antibody fragments for improved therapy: a review. *Advanced Drug Delivery Reviews.* **54(4)** (2002), pp. 531-545
61. Hwang, W.Y.K. et al. Immunogenicity of engineered antibodies, *Methods* **36** (2005), pp. 3–10
62. Rau, R. Adalimumab (a fully human anti tumour-necrosis factor α monoclonal antibody) in the treatment of active rheumatoid arthritis: the initial results of five trials. *Ann.Rheum. Dis.* **61(70)**, (2002)
63. Hoogenboom, H.R. Selecting and screening recombinant antibody libraries.*Nat. Biotechnology*. **23** (2005) pp. 1105-1116

64. Reichert, J.M. Monoclonal antibodies in the clinic. *Nat. Biotechnology*. **19** (2001), pp. 819-822,
65. Wu, A.M. et al. Arming antibodies: prospects and challenges for immunoconjugates. *Nature Biotechnology* **23** (2005), pp. 1137 - 1146
66. Holliger, et al. Engineered antibody fragments and the rise of single domains. *Nature Biotechnology* **23** (2005), pp. 1126 - 1136
67. Ashkenazi, A. et al. Immunoadhesins: An Alternative to Human Monoclonal Antibodies. *METHODS*: A Companion to Methods in Enzymology **8** (1995), pp. 104–115
68. US Patent 6870034 - Protein purification. Breece,T. N. et al. March 22. 2005.
69. EMEA, EPARs Human Medicines. Orencia http://www.emea.europa.eu/humandocs/Humans/EPAR/orencia/orencia.htm. Accessed 19.09.2008
70. EMEA, EPARs, Human Medicines. Enbrel. http://www.emea.europa.eu/humandocs/Humans/EPAR/enbrel/enbrel.htm. Accessed 19.09.2008
71. FDA. CDER. Acralyst. Chemistry Review http://www.fda.gov/cder/foi/nda/2008/125249s000TOC.htm. Accessed: 19.09.08
72. Dübel, S. Recombinant therapeutic antibodies. *Appl Microbiol Biotechnol* **74** (2007), pp. 723–729
73. U.S. Food and Drug Administration. Center for Drug Evaluation and Research. http://www.accessdata.fda.gov/Scripts/cder/DrugsatFDA/. Accessed: 20.07.2008
74. European Medicines Agency (EMEA), EPARs for medicinal products for human use. http://www.emea.europa.eu/htms/human/epar/eparintro.htm Accessed: 27.08.2007
75. The International Immunogenetics Informational System. Immunogenetics Repertoire (IG and TR). Monoclonal antobodies with clinical indications. http://imgt.cines.fr/textes/IMGTrepertoire/ Accessed. 20.07.2008
76. American Medical Association. United States Adopted Names. Monoclonal antibodies. http://www.ama-assn.org/ama/pub/category/13280.html. Accessed: 17.07.2008

77. Guidelines on the use of International nonproprietary names (INNs) for pharmaceutical substances. Programme on International nonproprietary names (INN). Division of Drug management & policies. WHO, Geneva © World Health Organisation (1997) http://www.who.int/medicines/services/inn/en/index.html Accessed:17.07.2008
78. World Health Organisation, 2007. International Nonproprietary Names (INN) for Biological and Biotechnological Substances. Available on the INN programme Website at: http://www.who.int/medicines/services/inn/en/. Accessed: 17.07.2008
79. Pavlovic, M.et al: Similar Biological Medicinal Products Containing Recombinant Human Growth Hormone: European Regulation. *Hormone Research*. **69** (2008), pp. 14-21
80. Garnick et al. The Role of Quality control in Biotechnology: An Analytical Perspective. *Analytical Chemistry*. 1988, 60, 2546-2557
81. ICH. Specifications: *Test Procedures and Acceptance Criteria for Biotechnological/Biological Products. Q6B.* http://www.ich.org/LOB/media/MEDIA432.pdf. Accessed: 1 September 2008
82. ICH. *Quality of Biotechnological Products: Stability Testing of Biotechnological/Biological Products.Q5C.* http://www.ich.org/LOB/media/Media427.org. Accessed: 2 September 2008
83. The United States Pharmacopeia 2008 (USP 31, NF 26). The United States Pharmacopeial Convention 2007. Rockville MD USA ISBN: 1-889788-53-8
84. Küster et al. Sequencing of N-linked oligosaccharides ddirectly from protein gels: in gel deglycosilation followed by matrix-assissted laser desorption/ionization mass spectrometry and normal-phase high-performance liquid chromatography. *Analytical Biochemistry*. **250** (1997), pp.82-101
85. Masuko, T. et al. Carbohydrate analysis by a phenol-sulfuric acid method in microplate format. *Analytical Biochemistry*. **339(1)** (2005), pp.69-72
86. Warren, L. The Thiobarbituric Assay of Sialic Acids. *The Journal of Biological Chemistry*. **234** (1959), pp. 1971-75
87. Gates, R. et Al. Glycoprotein analysis manual. 1st ed. Sigma-Aldrich, Inc. http://www.sigmaaldrich.com/etc/medialib/docs/Sigma/Instructions/glycoprotein_web_pdf_linked_pdf. Accessed: 07.September 2008.

88. Gennaro, L.A. et al. On-line CE-LIF-MS Technology for the direct characterisation of N-linked glycans from therapeutic antibodies. *Analytical Chemistry* **80** (2008), pp. 3838-3845
89. Europäisches Arzneibuch 6 Ausgabe, Grundwerk 2008. Monoklonale Antikörper für Menschen*(Anticorpora monoclonalia ad usum humanum)* Monograph 6.0/2031. Strasbourg (2008). Verlag Österreich GmbH ISBN 978-3-7046-5215-7
90. Roda, A et al: Combined Approach to the Analysis of Recombinant Protein Drugs Using Hollow-Fiber Flow Field-Flow Fractionation, Mass Spectrometry, and Chemiluminescence Detection. *Anal. Chem.* **78 (4)** (2006), pp.1085 -1092
91. Anonymus. USP Guideline for Submitting Requests for Revision to USP-NF (2007). Chapter 2. Biologics and biotechnology drug substances or products. http://www.usp.org/USPNF/submitMonograph/subGuide.html Accessed: 29.09.2008
92. Fountoulakis, M. et al. Comparison of the Coomassie brilliant blue, bicinchoninic acid and Lowry quantitation assays, using non-glycosylated and glycosylated proteins. *J. Biochem. Biophys. Methods*. **24(3-4)** (1992), pp. 265-74
93. ICH. *Quality of Biotechnological Products: Stability Testing of Biotechnological/Biological Products.Q5C.* http://www.ich.org/LOB/media/Media427.org. Accessed: 2 September 2008
94. EMEA/CHMP/BWP/157653/2007. *Guideline on Production and Quality Control of Monoclonal Antibodies and Related Substances*. London 5 April 2007. http://www.europa.eu/htms/human/humanguidelines/biologicals.htm Accessed: 3 September 2008
95. Mellstedt, H. The challenge of biosimilars. *Annals of Oncology*. (2007), pp: 1-9
96. Pavlovic, M. et al: Similar Biological Medicinal Products Containing Recombinant Human Growth Hormone: European Regulation. *Hormone Research*. **69** (2008),pp.14–21
97. EMEA/ CHMP/437/04. *Guideline on Similar Biological Medicinal Products*. London, October 2005, 043704en.pdf from www.emea.europa.eu Accessed: 02. September 2007
98. Covic, A. et al. Biosimilars: recent developments. *Int Urol Nephrol* **39** (2007), pp. 261–266.

99. Anonymus. Biosimilars: How similar are they? *The International Journal of Artificial Organs*. **28 (6)** (2005), pp. 552-553
100. Kuhlmann et al.: The protein science of biosimilars. *Nephrol Dial Transplant* **21(5)** (2006), pp.4-8
101. Hesse F et al. Developments and improvements in the manufacturing human therapeutics with mammalian cell cultures. *Trends Biotechnol* **18** (2000), pp. 73-180
102. Dingermann T. Recombinant therapeutic proteins: Production platforms and challenges. *Biotechnology Journal*. **3** (2008),pp. 90–97
103. European Medicines Agency. Guideline on similar biological medicinal products containing biotechnology-derived proteins as active substance: quality issues. (2006). http://www.emea.eu.int/pdfs/human/biosimilar/ 4934805en.pdf Accessed: 1 September 2008
104. European Medicines Agency. Guideline on similar biological medicinal products containing biotechnology-derived proteins as active substance: non-clinical and clinical issues. (2006). http://www.emea.eu.int/pdfs/human/ biosimilar/4283205en.pdf Accessed:1 September 2008
105. Boven, K.et al.The increased incidence of pure red cell aplasia with an Eprex formulation in uncoated rubber stopper syringes. *Kidney Int.* **67(6)** (2005), pp. 2346-53
106. Nowicki, M: What do nephrologists need to know about biosimilars. *Port J Nephrol Hypert* **21(3)** (2007), pp. 201-207
107. Anonymus. EBE - EFPIA Position Paper. Naming of biosimilar medicinal products: options for addressing unique safety concerns (2006) pp: 1-5. http://www.ebe-biopharma.org/ Accessed: 2 September 2008
108. EMEA. EPARs for authorized medicinal products for human use http://www.emea.europa.eu/humandocs/Humans/EPAR/omnitrope/omnitrope. htm. Accessed: 31.September 2008
109. Teare, I. Biosimilar warfare: The arrival of generic biopharmaceuticals – the Omnitrope decision. *Bio-science Law Review*. (2005/2006), pp. 9-13.
110. Schneider, C.K. et al: Toward biosimilar monoclonal antibodies. *Nature Biotechnology*. **26(9)** (2008), pp. 985-990
111. Görg, A. et al: Two-Dimensional Electrophoresis of Proteins using Immobilized pH Gradients. Technical University of Munich.

http://www.weihenstephan.de/blm/deg/manual/manualwork2html02test.htm Accessed: 01. October 2008

112. Anonymus. 2-D Electrophoresis. Pinciples and Methods. Handbooks from GE Healthcare (Handbook 80-6429-60AC). http://www4.gelifesciences.com/aptrix/upp01077.nsf/Content/2d_electrophoresis~2delectrophoresis_handbook Accessed: 01. October 2008
113. O'Farrel, F.H. High Resolution Two-dimansional Electrophoresis of Proteins. *The Journal of Biological Chemistry*. **250(10)** (1976), pp. 4007-21
114. Bjellqvist, B et al. Isoelectric focusing in immobilized pH gradients: Principle, methodology and some applications. *J.Biochem. Biophys. Methods* **6** (1982), pp. 317-339
115. Görg, A. et al. The current state of two-dimensional electrophoresis with immobilized pH gradients. *Electrophoresis* **9** (1988) pp. 531-546
116. Van der Bergh, G. et al: Recent advances in 2D electrophoresis: an array of possibilities. *Expert review of proteomics*. **2(2)** (2005), pp. 243-252
117. Schlags, W. et al: Two-dimensional electrophoresis of recombinant human erythropoietin: A future method for the European Pharmacopoeia. *Proteomics* **2** (2002), pp. 679-682
118. Caldini, A. et al: Epoetin alpha, epoetin beta and darbepoetin alfa:Two-dimensional gel electrophoresis isoforms characterization and mass spectrometry analysis. *Proteomics*. **3** (2003), pp. 937-941
119. Europäisches Arzneibuch 6 Ausgabe, Grundwerk 2008. Methoden der Physik und physikalischen Chemie *6.0/2.02.31.00 Elektrophorese)*. Strasbourg (2008). Verlag Österreich GmbH ISBN 978-3-7046-5215-7
120. GE Healthcare. 2-D Electrophoresis. http://www5.gelifesciences.com/aptrix/upp01077.nsf/Content/2d_electrophoresis Accessed: 03.10.2008
121. Sigma-Aldrich®. http://www.sigmaaldrich.com/Area_of_Interest/Life_Science/Proteomics_and_Protein_Expr_.html Accessed: 03.10.2008
122. Ibel, K. et al: Protein-decorated micelle structure of sodium-dodecyl-sulfate–protein complexes as determined by neutron scattering. *Eur. J. Biochem.* **190**, (1990), pp. 311–318

123. Laemmli, U.K. Cleavage of Structural Proteins during the Assembly of the Head of Bacteriophage T4. *Nature* **227** (1970), pp. 680 - 685
124. Anonymus.University of Wisconsin-Madison. Denaturing SDS-PAGE http://www.biochem.wisc.edu/courses/biochem651/labs/ing.aspx Accessed: 03.10.08
125. G.L. Corthals et al. Identification of Proteins by Mass Spectrometry, pp. 198-231. In: Principles and Practice. Proteome Research: Two-Dimesional Gel Electrophoresis and Identification Methods. Ed. by. T. Rabilloud. Springer Verlag Berlin, Heidelberg (2000). ISBN 3-540-65792-4
126. Patton, W.F. Detection technologies in proteome analysis. *J. Chromatogr. B* **771** (2002), pp. 3–31
127. Chevallet et al: Silver staining of proteins in polyacrylamide gels. *Nature Protocols.* (2006), **1(4)**, pp. 1852-1858
128. Angela Koller, Hermann Wätzig. Precision and variance components in quantitative gel electrophoresis. *Electrophoresis* **26** (2005), pp. 2470-2475
129. I. Gromova and J.E. Celis. Protein Detection in Gels by Silver Staining: A Procedure Compatible with Mass-Spectrometry. *Cell Biology, Four-volume set*, 1-4. A Laboratory Handbook. 3 Edition Volume 4. Editors: Celis, J.E., Carter N., Hunter T., Simons K., Small J.V. and Shotton D. (2006), Academic Press. ISBN-13: 978-0-12-164730-8
130. Shevchenko, A. et al: Mass Spectrometric Sequencing of Proteins from Silver-Stained Polyacrylamide Gels. *Anal. Chem*. **68** (1996), pp. 850-858
131. Garahdaghi et al. Mass spectrometric identification of proteins from silver-stained polyacrylamide gel: A method for the removal of silver ions to enhance sensitivity. *Electrophoresis* **20** (1999), pp. 601-605
132. Fernandez-Patron, C. *et al.* Understanding the mechanism of the zinc-ion stains of biomacromolecules in electrophoresis gels: generalization of the reverse-staining technique. *Electrophoresis* **19** (1998), pp. 2398–2406
133. Berggren, K. et al. Background-free, high sensitivity staining of proteins in one- and two-dimensional sodium dodecyl sulfate-polyacrylamide gels using a luminescent ruthenium complex. *Electrophoresis*. **21(12)**(2000),pp. 2509-21
134. Gygi, S. P. et al. Mass spectrometry and proteomics. Current Opinion in Chemical Biology **4(5)** (2000), pp. 489-494

135. A. Loo, A. et al. High sensitivity mass spectrometric methods for obtaining intact molecular weights from gel-separated proteins. *Electrophoresis* **20** (1999), pp. 743–748
136. Mazatti et al. SELDI-TOF-MS ProteinChip array profiling of T-cell clones propagated in long-term culture identifies human profilin-1 as a potential bio-marker of immunosenescence. *Proteomic Science* **5(7)** (2007), pp.1-13
137. Marouga, R. et al: The development of the DIGE system: 2D fluorescence difference gel analysis technology. *Anal Bioanal Chem* **382** (2005), pp. 669-678
138. Unlu, M. et al. Difference gel electrophoresis:a single gel method for detecting changes in cell extracts. *Electrophoresis* **18** (1997), pp. 2071-2077
139. Gygi, S.P. et al: Quantitative analysis of complex protein mixtures using isotope-coded affinity tags. *Nat. Biotechnol.* **17** (1999), pp. 994–999
140. Lee, M.S. Spectrometric Methods of Analysis-Mass spectrometry. *Encyclopedia of Pharmaceutical Technology ENCL* 100200012-8/10/2001-00012. Marcel Dekker, Inc. (2002), pp: 2545-62
141. K. Tanaka, et al., *Rapid Commun. Mass Spectrom.* **2** (1988), pp. 151-153
142. M. Karas, F. Hillenkamp, *Anal. Chem.* **60** (1988), pp. 2299-2301
143. Anonymus. King's College London. Instrumentation and tutorials. Matrix-Assisted Laser Desorption/Ionisation Time-Of-Flight Mass Spectrometry. http://www.umds.ac.uk/schools/health/resfac/mspec/instr/maldi-tof-intro.html Accessed: 08.10.08
144. F. Lottspeich, J. Engels: Bioanalytik. 2. Auflage. Elsevier GmbH, Muenchen, (2006), pp. 329-372. ISBN-13: 978-3-8274-1520-9
145. Van Bramer, S.E. An Introduction to Mass Spectrometry (1997). pp:13-22. science.widener.edu/svb/massspec/massspec.pdf, Accessed: 07.10.2008)
146. Hillenkamp, F. et al. The Maldi Process and Method, pp. 1-50. In: MALDI MS A Practical Guide to Instrumentation, Methods and Applications. Edited by: Hellenkamp, P. and Peter-Katalinic, J.; WILEY-VHC Verlag GmbH & Co. KGaA, Weinheim (2007). ISBN: 978-3-527-31440-9
147. Vestal, M.L et al. Delayed extraction matrix-assisted laser desorption time-of-flight mass spectrometry. *Rapid communications in Mass Spectrometry* **9 (11)** (1995), pp. 1044-1050.

148. Pappin, D.J. et al. Rapid identification of proteins by peptide-mass fingerprinting. *Curr Biol.* **3(6)**(1993), pp.327-32
149. James, P. Protein identification by mass profile fingerprinting. *Biochem Biophys Res Commun*. **195(1)** (1993), pp. 58-64
150. Yates, J.R. Peptide mass maps: a highly informative approach to protein identification. *Anal Biochem*. **214(2)** (1993), pp. 397-408
151. Jansen, O.N. Identification of the components of simple protein mixtures by high-accuracy peptide mass mapping and database searching. *Anal Chem*. **69(23)** (1997), pp. 4741-50
152. Henzel, W.J. Protein identification: the origins of peptide mass fingerprinting. *J Am Soc Mass Spectrom*. **14(9)** (2003), pp. 931-42
153. Anonymus. Trypsin Gold Mass Spectrometry Grade. Technical buletin http://www.promega.com/tbs/. Accessed: 10.10.08
154. Nguyen, N.D. et al. Protein mass spectrometry: applications to analytical biotechnology. *J. Chrornatogr. A* **705** (1995), pp. 21-45
155. Perkins et al. Probability-based protein identification by searching databases using mass spectrometry data. *Electrophoresis* **20** (1999), pp. 3551-3567
156. Cotrel, J. Database searching for protein identification and characterization. http://www.matrixscience.com/pdf/asms_tutorial_2005.pdf Accessed:10.10.08)
157. European Medicines Agency/EMEA. Guideline on Production and Quality Control of Monoclonal Antibodies and Related Substances www.emea.europa.eu/pdfs/human/bwp/15765307en.pdf Accessed 10.11.08
158. U.S.Food and Drug Administration /CBER. Points to consider in the Manufacture and Testing of Monoclonal antibody Products for Human Use www.fda.gov/cber/gdlns/ptc mab.pdf Accessed 10.11.08
159. European Pharmacopoeia 6.0. *Monoclonal Antibodies for Human Use (Anticorpora monoclonalia ad usum humanum)*, Monograph 2031, Strasbourg (2008)
160. Europäisches Arzneibuch, 6 Ausgabe, Grundwerk 2008. *DNA-rekombinations-technisch hergestellte Produkte (Producta ab arte ADN recombinandorum)*, Monograph 6.0/0784 Strasbourg (2008). Verlag Österreich ISBN 978-3-7046-5215-7

161. European Medicines Agency/EMEA. Specifications: test procedures and acceptance criteria for biotechnological/biological products Q6B. www.emea.europa.eu/pdfs/human/ich/036596en.pdf Accessed:10.11.08
162. U.S. FDA. Biotechnology inspection guide reference materials and training aids http://www.fda.gov/ora/inspect_ref/igs/biotech.html#TESTING Accessed 10.11.08
163. DJ Slamon, et al, Studies of the HER-2/neu proto-oncogene in human breast and ovarian cancer. *Science*. **244 (4905)** (1989), pp. 707-712
164. HERCEPTIN® Product information ROCHE PRODUCT PTY LIMITED, 21, (2006)
165. R.J. Harris et al. Identification of multiple sources of charge heterogeneity in a recombinant antibody. *Journal of Chromatography B,* **752** (2001), pp. 233-245
166. Carter, P.J. and Presta, L.G Method for making humanized antibodies. United States Patent. October 28.2003. PNr. 6,639,055
167. Carter et al. Humanisation of an anti-p185^{HER2} antibody for human cancer therapy. *Proc. Natl. Acad. Sci. USA*, *Immunology*. **89** (1992), pp. 4285-428
168. Eigenbrot, C. et al: X-ray structures of the antigen binding domain from three variants of humanised anti$^{-p-185HER2}$ antibody 4D5 and comparison with molecular modeling. European Bioinformatics Institute (MSD Atlas: PDB entry *1fvd*).
169. Carter et al. Immunoglobulin variants. United States Patent. October 13.1998 PNr. 5,821,337
170. Hudziak et al. Monoclonal antibodies directed to the HER2 receptor. United States Patent. October 14.1997 PNr. 5,677,171
171. EMEA. EPARs for authorised medicinal products for human use. Herceptin. Scientific discussion. http://www.emea.europa.eu/humandocs/Humans/EPAR/herceptin/herceptin.htm Accessed: 06. July 2007
172. Ellison, W.J. The nucleotide sequence of human immunoglobulin Cγ1gene. *Nucleic Acids Research*. **10(13)** (1982), pp. 4071-4079
173. http://ca.expasy.org/uniprot/P01857. Protein entry P01857 ,IGHG1. Accessed 30.07.2008

174. Kamoda, S. profiling analysis of oligosaccharides in antibody pharmaceuticals by capillary electrophoresis. *Journal of Chromatography A*. **1050** (2004), pp. 211-216
175. Raju, T.S: Terminal sugars of Fc glycans influence antibody effector functions of IgGs. *Current Opinion in Immunology*, **20 (4)** (2008) pp. 471-78
176. Zhang, W. et al. Free Sulfhydryl in Recombinant Monoclonal Antibodies. *Biotechnol. Prog.* **18** (2002), pp. 509-513
177. Olver, I.N Trastuzumab as the Lead Monoclonal Antibody in Advanced Breast Cancer: Choosing Which Patient and When. *Future Oncol*. **4(1)** (2008), pp. 125-131
178. Emens, L.A.Trastuzumab: targeted therapy for the management of HER-2/neu-overexpressing metastatic breast cancer. American Journal of Therapeutics. **12(3)** (2005), pp. 243-53
179. Konecny G.E. et al: Activity of the dual kinase inhibitor lapatinib (GW572016) against HER-2-overexpresssing and trastuzumab treated breast cancer cells. Cancer Res. **66**(2006), pp. 1630-1639
180. Brockhoff, G. et al. Differential impact of Cetuximab, Pertuzumab and Trastuzumab on BT474 and SK-BR-3 breast cancer cell proliferation.Cell proliferation. **40 (4)** (2007), pp. 488-507
181. http://www.cancer.gov/clinicaltrials/digespage/ALTTO, Accessed: 31.07.08
182. Mandler, R *et al*. Herceptin-Geldanamycin Immunoconjugates. Pharmacokinetics, Biodistribution, and Enhanced Antitumor Activity. *Cancer Research* **64** (2004), pp.1460-1467
183. EMEA. EPARs for authorised medicinal products for human use. Herceptin. Summary of Product Characteristics http://www.emea.europa.eu/humandocs/Humans/EPAR/herceptin/herceptin.htm Accessed: 06. July 2007
184. U.S. Food and Drug Administration. Center for Drug Evaluation and Research. Herceptin. Drug details. http://www.accessdata.fda.gov/scripts/cder/drugsatfda/index.cfm?fuseaction=Search.DrugDetails Accessed: 07. July 2007
185. Clemens, M. et al. Trastuzumab plus anastrozole may prolong overall survival in postmenopausal women with HER2-positive, hormone-dependent metastatic breast cancer: Results of a post-hoc analysis from the TANDEM

study. American Society of Clinical Oncology Symposium. Breast Cancer Symposium (2007). Abstract 231

186. Wolf A.C. et al. American Society of Clinical Oncology/College of American Pathologists guideline recommendations for human epidermial growth factor receptor 2 testing in breast cancer. *J. Clin. Oncol.* **25** (2007), pp. 118-45
187. Yarden.Y al. Untangling the erb B signaling network. Nature reviews. Molecular cell biology. **2 (186)** (2001), pp. 127-137
188. Herceptin official web site. Possible Benefits of Herceptin and Metastatic Breast Cancer. Herceptin: http://www.herceptin.com/metastatic/what-is/benefits.jsp, Accessed: 31.07.08
189. Valabrega, G. et al. Trastuzumab: mechanism of action, resistance and future perspectives in HER2-overexpressing breast cancer. *Annals of Oncology* **18** (2007), pp. 977–984
190. Arnould, L et al. Trastuzumab-based treatment of HER2-positive breast cancer:an antibody-dependent cellular cytotoxicity mechanism? British Journal of Cancer **94** (2006), pp. 259 – 267
191. Reff ME et al. Depletion of B cells in vivo by a chimeric mouse human monoclonal antibody to CD20*. Blood.* **83 (2)** (1994), pp. 435-445
192. European Medicines Agency, EMEA. European public assessment report. http://www.emea.europa.eu/humandocs/Humans/EPAR/mabthera/mabthera.htm MabThera. Accessed 06.09.08
193. J.Du et al. Crystal structure of chimeric antibody C2H7 Fab in complex with a CD20 peptide. *Molecular immunology*. **45** (2008), pp. 2861-2868
194. Drug Bank. http://www.drugbank.ca/search/search?query=rituximab. Accessed 06.09.2008
195. European Medicines Agency, EMEA. Mabthera. Scientific discussion. http://www.emea.europa.eu/humandocs/Humans/EPAR/mabthera/mabtheraM2.htm. Accessed 06.09.08
196. Roche Investigator's Brochure 11th Version December 2006 RO45-2294 - Page 21
197. Expasy Proteomic serverhttp://www.expasy.ch/cgi-bin/peptide-mass.pl. Accessed 06.09.2008
198. Food and Drug Administration. Center for Drug Evaluation and Research. Rituxan. Overview.

http://www.accessdata.fda.gov/scripts/cder/drugsatfda/index.cfm?fuseaction=Search.Overview&DrugName=RITUXAN. Accessed: 07.09.2008

199. http://www.zevalin.com/HealthCarePro/description.htm. Official Product website. Accessed 06.09.2008.
200. DAVID R. C. et al: Off-label uses of rituximab in dermatology. *Dermatologic Therapy*. **20** (2007), pp. 277–287
201. Jiamu D. et al. Structural Basis for Recognition of CD20 by Therapeutic Antibody Rituximab. *The Journal of Biological Chemistry* **282 (20)** (2007), pp. 5073-5080
202. Pedersen I.M et al: The dimeric anti CD-20 antibody induces apoptosis in B-cell chronic lymphocytic leukemia cells through a *p38* mitogen activated protein-kinase-dependent mechanism. *Blood* **99(4)**, (2002), pp. 1314-1319
203. Vega, M.I. et al: Rituximab induced inhibition of *YY1* and *Bcl-xl* expression in Ramos non Hodgkin's lymphoma cell via inhibition of NF-kappa B activity: role of *YY1* and *Bcl-xl* in *Fas* resistance and chemioresistence, respectively. *J. Immunol.* **175(4)** (2005), pp. 2174-83
204. Jazirehi, A. R., and Bonavida, B. *Oncogene* **24** (2005), 2121–2143
205. Pestovitz, M.D. Rituximab, an Anti-CD20 Monoclonal Antibody: History and Mechanism of Action. *American Journal of Transplantation* **6** (2006), pp. 859-866
206. FDA ALERT [12/18/2006] P06-206 December 18, 2006. On-line. http://www.fda.gov/bbs/topics/NEWS/2006/NEW01532.html. Accessed 30.08.2008
207. Genentech Inc. Development pipeline http://www.gene.com/gene/pipeline/status/immunology/anti-cd20/. Accessed 07.10.2007
208. The international immunogenetics information system, IMGT Repertoire http://imgt.cines.fr/textes/IMGTrepertoire/GenesClinical/monoclonalantibodies/#Human_monoclonal_antibodies, Accessed: 07.09.2008
209. Anonymus. *Jurnal Okologie* 2000-2008, Beginn von Studien zu Ofatumumab bei CLL und NHL. 26.08.2008. On-line, http://www.journalonko.de/newsview.php?id=2736, Accessed: 07.09.2008.

210. INNEXUS Biotechnology Inc. R&D Pipeline. http://www.ixsbio.com/products.html, Accessed 09.08.2008.
211. EMEA. EPARs for authorised medicinal products for human use. Orencia. Summary of Product Characteristics. http://www.emea.europa.eu/humandocs/Humans/EPAR/orencia/orencia.htm Accessed: 26.08.08
212. EMEA: EPARs for authorised medicinal products for human use. Orencia. Scientific Discussion. http://www.emea.europa.eu/humandocs/Humans/EPAR/orencia/orencia.htm Accessed: 26.08.08
213. Duncan, AR; Winter, G. The binding site for C1q on IgG. *Nature*. **332(6166)** (1988), pp. 738–740
214. Chappel, M.S. et al: Identification of the Fc gamma receptor class I binding site in human IgG. through the use of recombinant IgG1/IgG2 hybrid and point-mutated antibodies. *Proc. Natl. Acad. Sci.* USA. **88** (1991), pp. 9036-9040
215. Emery et al: Selective Co-stimulation Modulators: Addressing unmet needs in Rheumathoid Arthritis Management. 2005, *Medscape General Medicine*^{TM}, Published Online, Section 1-13. http://www.medscape.com/viewarticle/496108 Accessed: 26.11.2008
216. Linsley et al. CTLA4 Is a Second Receptor for the B Cell Activation Antigen B7.*J.Exp. Med.***174** (1991) pp. 561-569
217. Linsley et al. *CTLA4Ig fusion proteins*. Unated States Patent. Nr. 5844095. December 1998
218. Stamper, C.C. et al. Crystal structure of the B7-1/CTLA-4 complex that inhibits human immune responses. *Nature*. **410** (2001), pp. 608-611
219. Isaacs, J.D: Immunoadhesins for immunomodulation of autoimmune and rheumatic disease *Rheumatology* **36** (1997), pp. 305-307
220. Breece, T. N: *Protein purification.* Unated States Patent. Nr. 6870034. March 2005
221. U.S. Food and Drug Administration. Center for Drug Evaluation and Research. Orencia. Drug details. http://www.accessdata.fda.gov/Scripts/cder/DrugsatFDA/index.cfm?fuseaction=Search.DrugDetails Accessed. 17.05.08

222. Health Canada. Summary Basis of Decision (SBD). Orencia. http://www.hc-sc.gc.ca/dhp-mps/prodpharma/sbd-smd/phase1-decision/drug-med/sbd_smd_2007_orencia_098531-eng.php. Accessed: 17.11.2008
223. Biopharma: Biopharmacuetical Products in the US and European Markets.7 Edition, 2008. *CTLA4-Ig, rDNA*. Online:http://www.biopharma.com. Accessed: 17.11.2008
224. US. FDA/CBER: Orencia: Label and Application History. Online: http://www.accessdata.fda.gov/scripts/cder/drugsatfda/index.cfm?fuseaction=Search.Drug Details. Accessed: 17.11.2008
225. Bristol-Mayers Squibb. Orencia: Product monograph. 4 January 2008. pp.1-35 www.bmscanada.ca/upload/File/pdf/products/ORENCIA_E_PM_29%20June%2006_APP.pdf Accessed: 17.11.2008
226. US.FDA/CBER: Orencia Chemistry Review http://www.fda.gov/cder/foi/nda/2005/125118_s0000_OrenciaTOC.htm. Accessed 18.11.08
227. US. FDA. Herceptin Drug Details. http://www.accessdata.fda.gov/scripts/cder/drugsatfda/index.cfm?fuseaction=Search.DrugDetails. Accessed 18.11.08
228. Hunt, G et al. Capillary isolelctric focusing and sodium dodecyle sulfate capillary gel electrophoresis of recombinant humanized monoclonal antibody HER2. *Journal of Chromatography A*. **744** (1996), pp. 295-301
229. Nigel Jenkins. Modifications of therapeutic proteins: challenges and prospects. *Cytotechnology*. **53** (2007), pp. 121-125
230. Harris, R.J.et al. Processing of C-terminal lysine and arginine residues of proteins isolated from mammalian cell culture. *Journal of Chromatography A,* **705** (1995), pp. 129-134
231. Lam, X.M. et al. Antioxidants for prevention of methionine oxidation in recombinant monoclonal antibody HER2. *Journal of Pharmaceutical Sciences*. **86(11)** (1997), pp. 1250-1255
232. Kamoda, S et al. Capillary electrophoresis with laser-induced fotodetection for detailed studies on N-linked oligosaccharide profile of therapeutic recombinant monoclonal antibodies. *Journal of Chromatography A.* **1133** (2006), pp. 332-339

233. Harris, R.J. et al. Assessing genetic heterogeneity in production of cell lines: detection by peptide mapping of a low level Tyr to Gln Sequence variant in a recombinant antibody. *Biotechnology*. **11** (1993), pp.1293-97
234. Cleland, J.L et al. A specific molar ratio of stabilizer to protein is required for storage stability of a lyophylised monoclonal antibody. *Journal of Pharmaceutical Sciences*. **90(3)** (2001) pp. 310-321
235. Sigma-Aldrich. New Glycoprotein Analysis Manual, 2nd ed. http://www.sigmaaldrich.com/life-science/proteomics/learning-center/literature/the-new-glycobiology.html Accessed: 20.11.2008
236. Nose, M et al. Biological significance of carbohydrate chains on monoclonal antibodies. *Proc. Natl. Acad. Sci.* **80(21)** (1983), pp.6632–6636
237. Rothman, R.J. et al. Clonal analysis of the glycosylation of immunoglobulin G secreted from by murine hybridomas. *Biochemistry* **28** (1989), pp.1377-1384
238. Stadlmann et al. Analysis of immunoglobulin glycosylation by LC-ESI-MS of glycopeptide oligosaccharides. *Proteomics*. **8** (2008), pp. 2858-2871
239. Kelly, J.A. et al: On-line post-capillary affinity detection of immunoglobulin G subclasses and monoclonal antibody variants for capillary electrophoresis. *Journal of Chromatography A*. **790 (1-2)** 28 (1997), pp. 207-214
240. Moorhoudse, K.G. Validation of an HPLC method for the analysis of the charge heterogeneity of the recombinant monoclonal antibody IDEC-C2B8 after papain digestion. *Journal of Pharmaceutical and Biomedical Analysis*. **16** (1997), pp. 593-603
241. EMEA. EPARs for authorised medicinal products for human use. MabThera. Scientific discussion. http://www.emea.europa.eu/humandocs/Humans/EPAR/mabthera/mabthera.htm. Accesses: 16.08 2008
242. McLaughlin et al. Rituximab chimeric anti-CD20 monoclonal antibody therapy for relapsed indolent lymphoma: half of patients respond to a four-dose treatment program. *J. Clin. Oncol.* **16** (1998), p. 2825
243. Beum, P.V. et al. Three new assays for rituximab based on its immunological activity or antigenic properties: analyses of sera and plasmas of RTX-treated patients with chronic lymphocytic leukemia and other B cell lymphomas. *Journal of Immunological Methods*. **289(1-2)** (2004), pp 97-109

244. US FDA, CDER: Rituxan, Product review. Accessed 10.09.08 http://www.fda.gov/cder/biologics/products/ritugen112697.htm
245. US.FDA.CDER. Orencia. Chemistry review. http://www.accessdata.fda.gov/scripts/cder/drugsatfda/index.cfm?fuseaction=Search. DrugDetails. Accessed. 18.11.2008
246. Greve et al. Liquid chromatographic and capillary electrophoretic examination of intact and degraded fusion protein CTLA4Ig and kinetics of conformational transition. *Journal of chromatography A* **723** (1996), pp. 273-284.
247. Flesher, A. R.et al: Fluorophore-labeled carbohydrate analysis of immunoglobulin fusion proteins: Correlation of oligosaccharide content with in vivo clearance profile. *Biotechnology and bioengineering,* **46(5)** (1994), pp. 399-407
248. Hyoung et al: The Glycosylation and Pharmacokinetics of CTLA4Ig Produced in Rice Cells. *Biol.Pharm.Bull.* **30(10)** (2007), pp. 1913-1917
249. Greve, K. et al: Capillary electrophoretic examination of underivatized oligosaccharide mixtures released from immunoglobulin G antibodies and CTLA4Ig fusion proteins. *J. Chromatogr A* **749 (1-2)** (1996), pp.237-45
250. Blum, H et al. Improved silver staining of plant proteins, RNA and DNA in polyacrylamide gels. *Electrophoresis* **8** (1987), pp. 93-99
251. ProZyme Inc. FAQ. http://www.prozyme.com/faqs/gk0002.pdf. Accessed 20.11.2008
252. Swiss Institute of Bioinformatics (SIB) Sequence analysis tools. Expasy. http://us.expasy.org/tools/peptide-mass.html. Accessed: 20.10.2008
253. Irazoqui et al: Agaricus bisporus lectin binds mainly O-glycans but also N-glycans of human IgA subclasses. *Glycoconjugate Journal,* **14(3)** (1997), pp. 313-319
254. Scwartz, D. et al: Integrity and stability studies of precipitated rhBMP-2 microparticles with a focus on ATR-FTIR measurements. European Journal of Pharmaceutics and Biopharmaceutics. **63(3)** (2006) pp. 241-248
255. ICH. Q5C: Quality of Biotechnological Products: Stability Testing of Biotechnological/Biological Products, November 1995. www.emea.europa.eu/pdfs/human/bwp/3ab5aen.pdf and www.ich.org. Accessed: 20.11.2008

256. Chu, G.C. et al: Protein formulation of an IGG1 antibody with atypical glycosylation: A study on the stability of its glycoforms. *Abstr Pap Am Chem Soc.* **229** (2005), pp. 210-211.
257. Cho.S.H.et al: Structure of the extracellular region of HER2 alone and in complex with the Herceptin Fab. *Nature* **421** (2003), pp. 756-760
258. IDEON Science Park: Human IgG-Purified Immunoglobulin. Product Information, P100, Version A. www.euris.org/Product_information_P100.pdf . Accessed: 20.11.2008
259. Sigma-Aldrich® ProteoMass Protein MALDI-MS Calibration Kit (MSCAL3) Technical Bulletin www.sigmaaldrich.com/sigma/bulletin/mscal3bul.pdf Accessed: 20.11.2008.
260. http://www.matrixscience.com/help/search_field_help.html Accessed : 20.11.2008

8. Attachment

Table 8.13. Reagents used for sample preparation

		Concentration		Amount
Solution A1	*Rehydration Stock solution*			
	Urea	8M		48.05 g
	Thiourea	2M		15.22 g
	Chaps	4 %		4.00 g
	TritonX100	0.5 %		0.50 ml
	Bromphenol blue (Sol 1 %)	0.005 %		0.50 ml
	Milli-Q water		ad	100.00 ml
	1ml Aliquots stored at -20°C			
Solution A2	*Prepared rehydration solution*			
	Dithiothreitol	0.5 %		5 mg
	IPG Buffer	0.5 %		5 µl
	Rehydration solution (freshly prepared)		1.00 ml	

Table 8.14. Reagents used for preparation of the gels

		Concentration		Amount
Solution B1	*Acrylamide Stock Solution (%T 30.8 %, % C 2.6 %)*			
	Acrylamide 2X	30 %		150 g
	N,N'-Methylene bisacrylamide	0.8 %		4.00 g
	Milli-Q water		ad	500.0 ml
	Stored at 4°C			
Solution B2	*Resolving gel Buffer*			
	Tris(hydroxymethyl)aminomethane	1.5 M		90.80 g
	Sodium dodecyl sulfate	0.4 %		2.00 g
	6 M Hydrochloric acid			pH 8.8
	Milli-Q water		ad	500.00 ml
Solution B3	*Stacking gel Buffer*			
	Tris(hydroxymethyl)aminomethane	0.5 M		6.06 g
	Sodium dodecyl sulfate	0.4 %		0.40 g
	6 M Hydrochloric acid			pH 6.8
	Milli-Q water		ad	100.00 ml
	Solutions B2 and *B3* stored at room temperature.			

Solution B4	*Ammonium persulfate 10 %*			
	Ammonium persulfate	10 %	5.0 g	
	Milli-Q water		ad	50.0 ml
	1 ml Aliquots stored at -20°C			

Table 8.15. Reagents used for 1-D and 2-D electrophoresis experiments

		Concentration		**Amount**
Solution C1	*Equilibration Buffer*			
	Tris(hydroxymethyl)aminomethane	0.05 M		4.84 g
	Urea	6M		288.28 g
	Glycerol	30 %		240.00 ml
	Sodium dodecyl sulfate	2 %		16.00
	Bromphenol blue (Sol 1 %)	0.005 %		4.00 ml
	Milli-Q water		ad	800.00 ml
	20 ml Aliquots stored at -20°C			
Solution C1a	*Equilibration Buffer with DTT*			
	Dithiothreitol	1 %		100 mg
	Equilibration Buffer		ad	10 ml
	Freshly prepared			
Solution C1b	*Equilibration Buffer with IAM*			
	Iodoacetamide	2.5 %		250 mg
	Equilibration Buffer		ad	10 ml
	Freshly prepared			
Solution C2	*Agarose sealing solution*			
	Agarose	0.5 %		100 mg
	Diluted cathode buffer		ad	20 ml
Solution C3	*10 X Anode Buffer*			
	Tris(hydroxymethyl)aminomethane	0.25 M		30.2 g
	Sodium dodecyl sulfate	1 %		10.0 g
	Milli-Q water		ad	1000.0 ml
Solution C3a	*Diluted Anode Buffer*			
	10 X Anode Buffer			100.0 ml
	Milli-Q water		ad	1000.0 ml
Solution C4	*10 X Cathode Buffer*			

	Tris(hydroxymethyl)aminomethane	0.25 M		30.2 g
	Sodium dodecyl sulfate	1 %		10.0 g
	Glycine	14.42 %		144.2 g
	Milli-Q water		ad	1000.0 ml
Solution C4a	*Diluted Cathode Buffer*			
	10 X Cathode Buffer			100.0 ml
	Milli-Q water		ad	1000.0 ml
Solution C5	*Laemmli Buffer*			
	Tris(hydroxymethyl)aminomethane	0.25 M		3.03 g
	Glycerol	20 %		20.0 ml
	Sodium dodecyl sulfate	8 %		8.0
	Bromphenol blue (Sol 1 %)	0.02 %		20 µl
	Milli-Q water		ad	100.00 ml
	1 ml Aliquots stored at -20°C			
	Prior to use 6.2 mg/ml DTT are added.			

Table 8.16. Reagents used for silver staining procedure

		Concentration		**Amount**
Solution D1	*Fixing reagent*			
	Acetic acid conc. 99%	10 %		100.0 ml
	Methanol	40 %		400.0 ml
	Milli-Q water		ad	1000.0 ml
Solution D2	*Wash-solution*			
	Ethanol conc.	30%		300.0 ml
	Milli-Q water		ad	1000.0 ml
Solution D3	*Thiosulfate reagent*			
	Sodium thiosulfate	0.02 %	200.0 mg	
	Milli-Q water		ad	1000.0 ml
Solution D4	*Silver nitrate reagent*			
	Silver nitrate	0.2 %		2.0 g
	Formaldehyde (37 %)	0.002		200 µl
	Milli-Q water		ad	1000.0 ml
Solution D5	*Developer reagent*			
	Sodium carbonate	3 %		30.0 g
	Formaldehyde (37 %)	0.05 %		500 µl
	Sodium thiosulfate	0.0005 %		5 mg

	Milli-Q water		ad	1000.0 ml
Solution D6	*Glycine stop reagent*			
	Glycine	0.5 %		5.0 g
	Milli-Q water		ad	1000.0 ml

Table 8.17. Reagents used for Coomassie staining procedure

		Concentration		**Amount**
Solution E1	*Fixing reagent*			
	Methanol	45 %		450.0 ml
	Acetic acid conc. 99 %	5 %		50.0 ml
	Milli-Q water		ad	1000.0 ml
Solution E2	*Coomassie staining reagent*			
	Coomassie R250	0.025 %		0.25 g
	Methanol	40 %		400.0 ml
	Acetic acid conc. 99 %	7 %		70.0 ml
	Milli-Q water		ad	1000.0 ml
Solution E3	*Destaining reagent I*			
	Methanol	40 %		400.0 ml
	Acetic acid conc. 99 %	7 %		70.0 ml
	Milli-Q water		ad	1000.0 ml
Solution E4	*Destaining reagent II*			
	Methanol	5 %		50.0 ml
	Acetic acid conc. 99 %	7 %		70.0 ml
	Milli-Q water		ad	1000.0 ml

Table 8.18. Reagents used for gel tryptic digestion procedure and MALDI-TOF sample preparation and presentation

		Concentration		**Amount**
Solution F1	*Potassium ferricianyde solution*			
	Potassium ferricianyde	30 mM		0.494 g
	Milli-Q water		ad	50.0 ml
Solution F2	*Sodium thiosulfate solution*			
	Potassium ferricianyde	100 mM		0.791 g
	Milli-Q water		ad	50.0 ml
Solution F3	*Ammonium bicarbonate Buffer*			

	Ammonium bicarbonate	50 mM		0.395 g
	Ammonium hydroxide 10 %			pH 8.5
	Milli-Q water		ad	100.0 ml
Solution F4	*Digestion Buffer,*			
	Trypsine (modified, sequence grade)	12.5 ng/µl		25 µg
	Hydrochloric acid 1 mM		ad	2.0 ml
	Aliquots 100 µl after speed drying were stored at -20°C. Just prior to use Aliquots were reconstituted with 100 µl *Ammonium bicarbonate Buffer pH 8.5*.			
Solution F5	*Formic acid solution*			
	Formic acid	5 %		50.0 µl
	Milli-Q water		ad	950.0 µl
Solution F6	*Trifluoroacetic acid solution*			
	Trifluoroacetic acid solution, 1 % 0.1 %			10.0 µl
	Milli-Q water		ad	100.0 µl
Solution F7	*Saturated matrix solution*			
	α-Cyano- 4-hydroxycinnamic acid	0.8 %		8.0 µg
	Solution F6: Acetonitrile (70:30 *v/v)*		ad	1.0 ml

Table 8.19. Reagents used for deglycosilation experiments

		Concentration		**Amount**
Solution G1	*Phosphate Buffer*			
	Sodium phosphate monobasic, monohydrate	25 mM		0.345 g
	Sodium hydroxide 2M			pH 7.5
	Milli-Q		ad	100 ml
Solution G2	*CHAPS in 0.1 % SDS*			
	CHAPS	10 %		10.0 g
	Sodium dodecyl sulfate 0.1 %			0.1 g
	Milli-Q water		ad	100.0 ml
Solution G3	*0.5 % Triton X 100*			
	Triton X 100	0.5 %		0.5 ml
	Sodium hydroxyde			pH 7.2
	Milli-Q water		ad	100.0ml

PERSÖNLICHE DATEN:

Name:	Mag. Pharm. Dashnor Nebija
Anschrift:	Denisgasse 19/28 A-1020, Wien
Telefon:	+ 43 676 9037669
E-mail:	dashnornebiu@yahoo.com
Geburtsdatum und-ort:	20.01.1970. Prizren, FRY
Familienstand:	Verheiratet, 2 Kinder, 22 und 46 Monate

BERUFSTÄTIGKEIT:

2008- :	MarienApotheke 1160, Wien. Aspirantenausbildung.
1998-2005:	Universität Prishtina, Pharmazeutische Fakultät. Assistent für Pharmazeutische Chemie
2002-2003:	Universität Wien. Fakultät für Lebenswissenschaften, Department für Medizinische Chemie. Forschungsprojekt: Impurity profile studies of IND(R,R)-Glycopyrronium bromide.
2000-2002:	Pharmazeutischer Grosshandel “Aris Trade”, Prishtina
1999-2000:	Institut für Pharmakoepidemiologie. Universität Valladolid. Forschungsprojekt: Rational Drug Utilisation.
1999-2000:	Institut für Analytische Chemie. Universität Valladolid. Forschungsprojekt: Cleaning Validation. Validation of a HPLC Method for determination of valacyclovire hydrochloride in different surfaces.
1995-1999:	Apotheke “Belladonna”, Prishtina.
1992-1995:	Apotheke “Aesculap”, Prishtina.

BERUFLICHE WEITERBILDUNG:

2000:	Universität Salamanca. VI Simposio interactivo de diseño de farmacós.

AUSBILDUNG:

2005- :	Doktoratsstudium. Universität Wien. Fakultät für Lebenswissenschaften, Department für Medizinische Chemie. Mentor: Prof. Dr. Christian Noe.
2006-2007:	Studium zu Erlangung der Nostrifizierung. Universität Wien. Fakultät für Lebenswissenschaften: Studienrichtung Pharmazie. Akademischer Grad: Magister der Pharmazie.

2001-2004:	Masterstudium. Universität Skopje. Pharmazeutische Fakultät. Department für Pharmazeutische Chemie und Pharmakoinformatik. Akademischer Grad: Master der Pharmazeutischen Wissenschaften.
1987-1992:	Pharmaziestudium. Universität Belgrad. Pharmazeutische Fakultät. Akademischer Grad: Diplompharmazeut.

SPRACHKURSE:

2006:	Sprachzentrum Universität Wien. Wiener Internationale Hochschulkurse Mittelstufe 1.
2001:	The International Benedict School of Languages, Prishtina. Advanced Course of English Language.
2000:	Universität Valladolid. Curso de estudios hispanicos, 2000.
1998:	Centre for Foreign Languages, Oxford Studio, Prishtina. Advanced Course of English Language.

PUBLIKATIONEN UND KONFERENZBEITRÄGE:

Nebiu D, Kopelent H, Noe C.R, Lachmann B: Two-dimensional gel electrophoresis (2-DE) and MALDI-TOF Analysis of therapeutic recombinant monoclonal antibodies. Poster Präsentation. 2nd EUFEPS and EAPB workshop on Monoclonal Antibodies: Cutting-edge Science of New Medicines. June 3-5, 2008. Heidelberg, Germany.

Nebiu D, Walter M, Lachmann B, Kopelent H, Noe C.R: Determination of (R,R)-Glycopyrronium bromide and its related impurities by ion-pair HPLC, *Pharmazie* 2007, 62(6); 406-10.

Nebiu D: Selected Chapters of Pharmaceutical Analysis. Laboratory manual. Universität Prishtina, 2005.

Limit testing of certain drug substances with TLC: Congress of Macedonian Pharmaceutical Association with International Participation. Poster Presentation. Ohrid, Mazedonien, Juni 2003.

WEITERE PROJEKTE:

2005:	Course Development Program. *Selected topics of Pharmaceutical Analysis.* Project coordinated by WUS Austria,

Prishtina Office, implemented at the University of Prishtina and financed by the Austrian Development Agency.

SPRACHKENNTNISSE:

Albanisch: Muttersprache.
English, Serbo-Kroatisch, Spanisch: Verhandlungssicher in Wort und Schrift.
Deutsch: fließend.

EDV-KENNTNISSE:

Microsoft-Standardapplikationen (MS-Windows 2000, MS Windows XP, MS-Word, MS-Exel, MS-Powerpoint ständig in Anwendung). Verschiedene chemisch-pharmazeutische Datenbanksysteme, wie z.B.SciFinder, Beilstein-Crossfire, Medline, Esp@cenet